10-31-2007

Dependency of Loosening Parameters on Secondary Locking Features of Threaded Inserts

Carlos Felipe Acosta
University of South Florida

Dependency of Loosening Parameters on Secondary Locking Features of Threaded Inserts

by

Carlos Felipe Acosta

A thesis submitted in partial fulfillment
of the requirements for the degree of
Master of Science in Mechanical Engineering
Department of Mechanical Engineering
College of Engineering
University of South Florida

Major Professor: Daniel P. Hess, Ph.D.
Craig Lusk, Ph.D.
Nathan Crane, Ph.D.

Date of Approval:
October 31, 2007

Keywords: Heli-Coil, bolt, transverse vibration, prevailing torque, Loctite

Dedication

To my mother, who taught me the fundamentals of ethics, morals and love helping me to grow professionally and spiritually. She has been a supportive mother, a best friend, and a great life mentor. To my late father who evoked in me the principles of honor, loyalty and discipline. Your love accompanies me in every phase of my life.

Acknowledgments

I would like to express my deepest gratitude to my major professor Dr. Daniel Hess for his expert guidance in this journey. His undeniable patience and extensive knowledge were critical factors in the completion of this work.

I would like to extend this gratitude to Dr. Craig Lusk and Dr. Nathan Crane for taking the time to be in my committee as well as sharing their knowledge of engineering.

Table of Contents

List of Tables iv

List of Figures vi

Abstract xix

Chapter 1 Introduction 1

1.1 Introduction 1

1.2 Background 3

1.3 Overview 8

Chapter 2 Raw Data 9

2.1 Introduction 9

2.2 Apparatus 9

2.3 Test specimens 10

2.4 Installation 11

2.5 Test specifications 12

2.6 Test data 12

Chapter 3 Extraction of Loosening Parameters 33

3.1 Introduction 33

3.2 Percentage loss of initial preload parameter 34

3.2.1 Data extraction 34

3.2.2 Statistical analysis 38
3.3 Initial rate of preload loss parameter 44
3.3.1 Data extraction 44
3.3.2 Statistical analysis 48
3.4 Secondary rate of preload loss parameter 55
3.4.1 Data extraction 55
3.4.2 Statistical analysis 59
3.5 Steady-state value parameter 64
3.5.1 Data extraction 64
3.5.2 Statistical analysis 68
3.6 Final preload value parameter 68
3.6.1 Data extraction 68
3.6.2 Statistical analysis 71
Chapter 4 Interpretation of Results 78
4.1 Introduction 78
4.2 Percentage loss of initial preload parameter 80
4.3 Initial rate of preload loss parameter 83
4.4 Secondary rate of preload loss parameter 84
4.5 Steady-state / final preload value parameter 85
Chapter 5 Conclusions 87
References 91
Appendices 93
Appendix A: Data extracted for all locking levels 94

Appendix B: Zoomed data plots for the percentage loss of initial preload parameter.....101

Appendix C: Zoomed data plots for the initial rate of preload loss parameter.....120

Appendix D: Zoomed data plots for the secondary rate of preload loss parameter.....139

Appendix E: Zoomed data plots for the steady-state and the final preload value parameter.....152

List of Tables

Table 2.1 Torque test data 32

Table 3.1 Data extracted for all locking levels 36

Table 3.2 Percentage loss of initial preload 37

Table 3.3 ANOVA table for the percentage loss of initial preload 40

Table 3.4 LSD method table for the percentage loss of initial preload 43

Table 3.5 95 percent confidence intervals for the percentage loss of initial preload 43

Table 3.6 Initial rate of preload loss for all locking levels (lb/cycle) 46

Table 3.7 ANOVA table for the initial rate of preload loss 51

Table 3.8 LSD method table for the initial rate of preload loss 54

Table 3.9 95 percent confidence intervals for the initial rate of preload loss 54

Table 3.10 Secondary rate of preload loss for all locking levels (lb/cycle) 58

Table 3.11 ANOVA table for the secondary rate of preload loss 61

Table 3.12 95 percent confidence intervals for the secondary rate of preload loss 63

Table 3.13 Steady-state values for all locking levels (lb), (nr: never reached) 66

Table 3.14 Final preload values for all locking levels (lb), (**bolt broke) 70

Table 3.15 t-test statistic table for the final preload value 74

Table 3.16 95 percent confidence intervals for the final preload value 76

Table 4.1 Minimum, mean and maximum angle of twist 81

Table 4.2 Preload due to angle of twist 83

Table 5.1 Dependency of loosening parameters on secondary locking features 89

Table A.1 Extracted data from "Standard Heli-Coil with Braycote" 94

Table A.2 Extracted data from "Locking Heli-Coil with Braycote" 95

Table A.3 Extracted data from "Standard Heli-Coil with Loctite" 96

Table A.4 Refined data points from "Standard Heli-Coil with Braycote" 97

Table A.5 Refined data points from "Locking Heli-Coil with Braycote" 98

Table A.6 Refined data points from "Standard Heli-Coil with Loctite" 99

Table A.7 Extracted data from "Standard Heli-Coil with Braycote" and "Locking Heli-Coil with Braycote" 100

List of Figures

Figure 1.1 Block on incline plane 4

Figure 1.2 Effect of prevailing torque in reducing loosening [11]....6

Figure 1.3 Locking Heli-Coil's grip coil [14] 6

Figure 2.1 Schematic of test machine 10

Figure 2.2 Preload vs. cycles for "Standard Heli-Coil with Braycote" run number 1 13

Figure 2.3 Preload vs. cycles for "Standard Heli-Coil with Braycote" run number 2 13

Figure 2.4 Preload vs. cycles for "Standard Heli-Coil with Braycote" run number 3 14

Figure 2.5 Preload vs. cycles for "Standard Heli-Coil with Braycote" run number 4 14

Figure 2.6 Preload vs. cycles for "Standard Heli-Coil with Braycote" run number 5 15

Figure 2.7 Preload vs. cycles for "Standard Heli-Coil with Braycote" run number 6 15

Figure 2.8 Preload vs. cycles for "Standard Heli-Coil with Braycote" run number 7 16

Figure 2.9 Preload vs. cycles for "Standard Heli-Coil with Braycote" run number 8 16

Figure 2.10 Preload vs. cycles for "Standard Heli-Coil with Braycote" run number 9 17

Figure 2.11 Preload vs. cycles for "Standard Heli-Coil with Braycote" run number 10 17

Figure 2.12 Preload vs. cycles for "Standard Heli-Coil with Braycote" run number 11 18

Figure 2.13 Preload vs. cycles for "Standard Heli-Coil with Braycote" run number 12 18

Figure 2.14 Preload vs. cycles for "Locking Heli-Coil with Braycote" run number 13 19

Figure 2.15 Preload vs. cycles for "Locking Heli-Coil with Braycote" run number 14 19

Figure 2.16 Preload vs. cycles for "Locking Heli-Coil with Braycote" run number 15 20

Figure 2.17 Preload vs. cycles for "Locking Heli-Coil with Braycote" run number 16 20

Figure 2.18 Preload vs. cycles for "Locking Heli-Coil with Braycote" run number 17 21

Figure 2.19 Preload vs. cycles for "Locking Heli-Coil with Braycote" run number 18 21

Figure 2.20 Preload vs. cycles for "Locking Heli-Coil with Braycote" run number 19 22

Figure 2.21 Preload vs. cycles for "Locking Heli-Coil with Braycote" run number 20 22

Figure 2.22 Preload vs. cycles for "Locking Heli-Coil with Braycote" run number 21 23

Figure 2.23 Preload vs. cycles for "Locking Heli-Coil with Braycote" run number 22 23

Figure 2.24 Preload vs. cycles for "Locking Heli-Coil with Braycote" run number 23 24

Figure 2.25 Preload vs. cycles for "Locking Heli-Coil with Braycote" run number 24 24

Figure 2.26 Preload vs. cycles for "Standard Heli-Coil with Loctite" run number 25 25

Figure 2.27 Preload vs. cycles for "Standard Heli-Coil with Loctite" run number 26 25

Figure 2.28 Preload vs. cycles for "Standard Heli-Coil with Loctite" run number 27 26

Figure 2.29 Preload vs. cycles for "Standard Heli-Coil with Loctite" run number 28 26

Figure 2.30 Preload vs. cycles for "Standard Heli-Coil with Loctite" run number 29 27

Figure 2.31 Preload vs. cycles for "Standard Heli-Coil with Loctite" run number 30 27

Figure 2.32 Preload vs. cycles for "Standard Heli-Coil with Loctite" run number 31 28

Figure 2.33 Preload vs. cycles for "Standard Heli-Coil with Loctite" run number 32 28

Figure 2.34 Preload vs. cycles for "Standard Heli-Coil with Loctite" run number 33 29

Figure 2.35 Preload vs. cycles for "Standard Heli-Coil with Loctite" run number 34 29

Figure 2.36 Preload vs. cycles for "Standard Heli-Coil with Loctite" run number 35 30

Figure 2.37 Preload vs. cycles for "Standard Heli-Coil with Loctite" run number 36 30

Figure 3.1 Representation of loosening parameters (run number 18) 33

Figure 3.2 Loosening curve for "Locking Heli-Coil with Braycote" run number 18 35

Figure 3.3 Zoomed loosening curve for "Locking Heli-Coil with Braycote" run number 18 35

Figure 3.4 Box plot for the percentage loss of initial preload 38

Figure 3.5 Normal probability plot of residuals for the percentage loss of initial preload 40

Figure 3.6 Multiple comparisons of means for the percentage loss of initial preload 42

Figure 3.7 Loosening curve for "Standard Heli-Coil with Braycote" run number 11 45

Figure 3.8 Zoomed loosening curve for "Standard Heli-Coil with Braycote" run number 11 46

Figure 3.9 Composite tangent lines for "Standard Heli-Coil with Braycote" 47

Figure 3.10 Composite tangent lines for "Locking Heli-Coil with Braycote" 47

Figure 3.11 Composite tangent lines for "Standard Heli-Coil with Loctite" 48

Figure 3.12 Box plot for the initial rate of preload loss 49

Figure 3.13 Normal probability plot of residuals for the initial rate of preload loss 51

Figure 3.14 Multiple comparisons of means for the initial rate of preload loss 53

Figure 3.15 Loosening curve for "Locking Heli-Coil with Braycote" run number 3 57

Figure 3.16 Zoomed loosening curve for "Locking Heli-Coil with Braycote" run number 3 57

Figure 3.17 Box plot for the secondary rate of preload loss 59

Figure 3.18 Normal probability plot for the secondary rate of preload loss 61

Figure 3.19 Multiple comparisons of means for the secondary rate of preload loss 63

Figure 3.20 Loosening curve for "Locking Heli-Coil with Braycote" run number 22 65

Figure 3.21 Zoomed loosening curve for "Locking Heli-Coil with Braycote" run number 22 66

Figure 3.22 All steady-state value plots for "Locking Heli-Coil with Braycote" 67

Figure 3.23 All steady-state value plots for "Standard Heli-Coil with Loctite" 67

Figure 3.24 Loosening curve for "Standard Heli-Coil with Loctite" run number 33 69

Figure 3.25 Zoomed loosening curve for "Standard Heli-Coil with Loctite" run number 33 70

Figure 3.26 Box plot for the final preload value 72

Figure 3.27 Normal probability plot of residuals for the final preload value 74

Figure 3.28 Multiple comparisons of means for the final preload value 76

Figure 4.1 Reaction forces on bolts 79

Figure B.1 Loss of initial preload for "Standard Heli-Coil with Braycote" run number 1 101

Figure B.2 Loss of initial preload for "Standard Heli-Coil with Braycote" run number 2 102

Figure B.3 Loss of initial preload for "Standard Heli-Coil with Braycote" run number 3 102

Figure B.4 Loss of initial preload for "Standard Heli-Coil with Braycote" run number 4 103

Figure B.5 Loss of initial preload for "Standard Heli-Coil with Braycote" run number 5 103

Figure B.6 Loss of initial preload for "Standard Heli-Coil with Braycote" run number 6 104

Figure B.7 Loss of initial preload for "Standard Heli-Coil with Braycote" run number 7 104

Figure B.8 Loss of initial preload for "Standard Heli-Coil with Braycote" run number 8 105

Figure B.9 Loss of initial preload for "Standard Heli-Coil with Braycote" run number 9 105

Figure B.10 Loss of initial preload for "Standard Heli-Coil with Braycote" run number 10 106

Figure B.11 Loss of initial preload for "Standard Heli-Coil with Braycote" run number 11 106

Figure B.12 Loss of initial preload for "Standard Heli-Coil with Braycote" run number 12 107

Figure B.13 Loss of initial preload for "Locking Heli-Coil with Braycote" run number 13 107

Figure B.14 Loss of initial preload for "Locking Heli-Coil with Braycote" run number 14 108

Figure B.15 Loss of initial preload for "Locking Heli-Coil with Braycote" run number 15 108

Figure B.16 Loss of initial preload for "Locking Heli-Coil with Braycote" run number 16 109

Figure B.17 Loss of initial preload for "Locking Heli-Coil with Braycote" run number 17 109

Figure B.18 Loss of initial preload for "Standard Heli-Coil with Braycote" run number 18 110

Figure B.19 Loss of initial preload for "Locking Heli-Coil with Braycote" run number 19 110

Figure B.20 Loss of initial preload for "Locking Heli-Coil with Braycote" run number 20 111

Figure B.21 Loss of initial preload for "Locking Heli-Coil with Braycote" run number 21 111

Figure B.22 Loss of initial preload for "Locking Heli-Coil with Braycote" run number 22 112

Figure B.23 Loss of initial preload for "Locking Heli-Coil with Braycote" run number 23 112

Figure B.24 Loss of initial preload for "Locking Heli-Coil with Braycote" run number 24 113

Figure B.25 Loss of initial preload for "Standard Heli-Coil with Loctite" run number 25 113

Figure B.26 Loss of initial preload for "Standard Heli-Coil with Loctite" run number 26 114

Figure B.27 Loss of initial preload for "Standard Heli-Coil with Loctite" run number 27 114

Figure B.28 Loss of initial preload for "Standard Heli-Coil with Loctite" run number 28 115

Figure B.29 Loss of initial preload for "Standard Heli-Coil with Loctite" run number 29 115

Figure B.30 Loss of initial preload for "Standard Heli-Coil with Loctite" run number 30 116

Figure B.31 Loss of initial preload for "Standard Heli-Coil with Loctite" run number 31 116

Figure B.32 Loss of initial preload for "Standard Heli-Coil with Loctite" run number 32 117

Figure B.33 Loss of initial preload for "Standard Heli-Coil with Loctite" run number 33 117

Figure B.34 Loss of initial preload for "Standard Heli-Coil with Loctite" run number 34 118

Figure B.35 Loss of initial preload for "Standard Heli-Coil with Loctite" run number 35 118

Figure B.36 Loss of initial preload for "Standard Heli-Coil with Loctite" run number 36 119

Figure C.1 Initial rate of preload loss for "Standard Heli-Coil with Braycote" run number 1 120

Figure C.2 Initial rate of preload loss for "Standard Heli-Coil with Braycote" run number 2 121

Figure C.3 Initial rate of preload loss for "Standard Heli-Coil with Braycote" run number 3 121

Figure C.4 Initial rate of preload loss for "Standard Heli-Coil with Braycote" run number 4 122

Figure C.5 Initial rate of preload loss for "Standard Heli-Coil with Braycote" run number 5 122

Figure C.6 Initial rate of preload loss for "Standard Heli-Coil with Braycote" run number 6 123

Figure C.7 Initial rate of preload loss for "Standard Heli-Coil with Braycote" run number 7 123

Figure C.8 Initial rate of preload loss for "Standard Heli-Coil with Braycote" run number 8 124

Figure C.9 Initial rate of preload loss for "Standard Heli-Coil with Braycote" run number 9 124

Figure C.10 Initial rate of preload loss for "Standard Heli-Coil with Braycote" run number 10 125

Figure C.11 Initial rate of preload loss for "Standard Heli-Coil with Braycote" run number 11 125

Figure C.12 Initial rate of preload loss for "Standard Heli-Coil with Braycote" run number 12 126

Figure C.13 Initial rate of preload loss for "Locking Heli-Coil with Braycote" run number 13 126

Figure C.14 Initial rate of preload loss for "Locking Heli-Coil with Braycote" run number 14 127

Figure C.15 Initial rate of preload loss for "Locking Heli-Coil with Braycote" run number 15 127

Figure C.16 Initial rate of preload loss for "Locking Heli-Coil with Braycote" run number 16 128

Figure C.17 Initial rate of preload loss for "Locking Heli-Coil with Braycote" run number 17 128

Figure C.18 Initial rate of preload loss for "Standard Heli-Coil with Braycote" run number 18 129

Figure C.19 Initial rate of preload loss for "Locking Heli-Coil with Braycote" run number 19 129

Figure C.20 Initial rate of preload loss for "Locking Heli-Coil with Braycote" run number 20 130

Figure C.21 Initial rate of preload loss for "Locking Heli-Coil with Braycote" run number 21 130

Figure C.22 Initial rate of preload loss for "Locking Heli-Coil with Braycote" run number 22 131

Figure C.23 Initial rate of preload loss for "Locking Heli-Coil with Braycote" run number 23 131

Figure C.24 Initial rate of preload loss for "Locking Heli-Coil with Braycote" run number 24 132

Figure C.25 Initial rate of preload loss for "Standard Heli-Coil with Loctite" run number 25 132

Figure C.26 Initial rate of preload loss for "Standard Heli-Coil with Loctite" run number 26 133

Figure C.27 Initial rate of preload loss for "Standard Heli-Coil with Loctite" run number 27 133

Figure C.28 Initial rate of preload loss for "Standard Heli-Coil with Loctite" run number 28 134

Figure C.29 Initial rate of preload loss for "Standard Heli-Coil with Loctite" run number 29 134

Figure C.30 Initial rate of preload loss for "Standard Heli-Coil with Loctite" run number 30 135

Figure C.31 Initial rate of preload loss for "Standard Heli-Coil with Loctite" run number 31 135

Figure C.32 Initial rate of preload loss for "Standard Heli-Coil with Loctite" run number 32 136

Figure C.33 Initial rate of preload loss for "Standard Heli-Coil with Loctite" run number 33 136

Figure C.34 Initial rate of preload loss for "Standard Heli-Coil with Loctite" run number 34 137

Figure C.35 Initial rate of preload loss for "Standard Heli-Coil with Loctite" run number 35 137

Figure C.36 Initial rate of preload loss for "Standard Heli-Coil with Loctite" run number 36 138

Figure D.1 Secondary rate of preload loss for "Standard Heli-Coil with Braycote" run number 1 139

Figure D.2 Secondary rate of preload loss for "Standard Heli-Coil with Braycote" run number 2 140

Figure D.3 Secondary rate of preload loss for "Standard Heli-Coil with Braycote" run number 3 140

Figure D.4 Secondary rate of preload loss for "Standard Heli-Coil with Braycote" run number 4 141

Figure D.5 Secondary rate of preload loss for "Standard Heli-Coil with Braycote" run number 5 141

Figure D.6 Secondary rate of preload loss for "Standard Heli-Coil with Braycote" run number 6 142

Figure D.7 Secondary rate of preload loss for "Standard Heli-Coil with Braycote" run number 7 142

Figure D.8 Secondary rate of preload loss for "Standard Heli-Coil with Braycote" run number 8 143

Figure D.9 Secondary rate of preload loss for "Standard Heli-Coil with Braycote" run number 9 143

Figure D.10 Secondary rate of preload loss for "Standard Heli-Coil with Braycote" run number 10 144

Figure D.11 Secondary rate of preload loss for "Standard Heli-Coil with Braycote" run number 11 144

Figure D.12 Secondary rate of preload loss for "Standard Heli-Coil with Braycote" run number 12 145

Figure D.13 Secondary rate of preload loss for "Locking Heli-Coil with Braycote" run number 13 145

Figure D.14 Secondary rate of preload loss for "Locking Heli-Coil with Braycote" run number 14 146

Figure D.15 Secondary rate of preload loss for "Locking Heli-Coil with Braycote" run number 15 146

Figure D.16 Secondary rate of preload loss for "Locking Heli-Coil with Braycote" run number 16 147

Figure D.17 Secondary rate of preload loss for "Locking Heli-Coil with Braycote" run number 17 147

Figure D.18 Secondary rate of preload loss for "Locking Heli-Coil with Braycote" run number 18 148

Figure D.19 Secondary rate of preload loss for "Locking Heli-Coil with Braycote" run number 19 148

Figure D.20 Secondary rate of preload loss for "Locking Heli-Coil with Braycote" run number 20 149

Figure D.21 Secondary rate of preload loss for "Locking Heli-Coil with Braycote" run number 21 149

Figure D.22 Secondary rate of preload loss for "Locking Heli-Coil with Braycote" run number 22 150

Figure D.23 Secondary rate of preload loss for "Locking Heli-Coil with Braycote" run number 23 150

Figure D.24 Secondary rate of preload loss for "Locking Heli-Coil with Braycote" run number 24 151

Figure E.1 Steady-state value for "Locking Heli-Coil with Braycote" run number 13 152

Figure E.2 Steady-state value for "Locking Heli-Coil with Braycote" run number 14 153

Figure E.3 Steady-state value for "Locking Heli-Coil with Braycote" run number 15 153

Figure E.4 Steady-state value for "Locking Heli-Coil with Braycote" run number 16 154

Figure E.5 Final preload value for "Locking Heli-Coil with Braycote" run number 17 154

Figure E.6 Steady-state value for "Locking Heli-Coil with Braycote" run number 18 155

Figure E.7 Steady-state value for "Locking Heli-Coil with Braycote" run number 19 155

Figure E.8 Final preload value for "Locking Heli-Coil with Braycote" run number 20 156

Figure E.9 Steady-state value for "Locking Heli-Coil with Braycote" run number 21 156

Figure E.10 Steady-state value for "Locking Heli-Coil with Braycote" run number 22 157

Figure E.11 Steady-state value for "Locking Heli-Coil with Braycote" run number 23 157

Figure E.12 Steady-state value for "Locking Heli-Coil with Braycote" run number 24 158

Figure E.13 Final preload value for "Standard Heli-Coil with Loctite" run number 25 158

Figure E.14 Steady-state value for "Standard Heli-Coil with Loctite" run number 26 159

Figure E.15 Final preload value for "Standard Heli-Coil with Loctite" run number 27 159

Figure E.16 Final preload value for "Standard Heli-Coil with Loctite" run number 28 160

Figure E.17 Final preload value for "Standard Heli-Coil with Loctite" run number 30 160

Figure E.18 Final preload value for "Standard Heli-Coil with Loctite" run number 31 161

Figure E.19 Steady-state value for "Standard Heli-Coil with Loctite" run number 32 161

Figure E.20 Final preload value for "Standard Heli-Coil with Loctite" run number 33 162

Figure E.21 Final preload value for "Standard Heli-Coil with Loctite" run number 34 162

Figure E.22 Final preload value for "Standard Heli-Coil with Loctite" run number 35 163

Figure E.23 Final preload value for "Standard Heli-Coil with Loctite" run number 36 163

Dependency of Loosening Parameters on Secondary Locking Features of Threaded Inserts

Carlos Felipe Acosta

ABSTRACT

This thesis presents a study of the dependency of loosening parameters on secondary locking features of threaded inserts subjected to dynamic shear loads. Secondary locking is used to assist and/or provide redundancy to the primary locking feature (threads) in preventing preload loss in almost any mechanical applications. Two different secondary locking features are studied: the Locking Heli-Coil insert and the Loctite Threadlocker® applied before assembly to a Standard Heli-Coil insert. Five parameters are studied in this thesis: percentage loss of initial preload, initial rate of preload loss, secondary rate of preload loss, steady-state value, and the final preload value.

Statistical analysis was used to quantify the dependencies between locking levels. Results show that the loss of initial preload is dependent on secondary locking features, the initial and secondary rate of preload loss are dependent on secondary locking features, the steady-state value and the final preload value are dependent on secondary locking features. Also, due to secondary locking features, 83% of the "Locking Heli-Coil with Braycote" tests reached steady-state while only 16% of the "Standard Heli-Coil with

Loctite" tests reached steady-state even though the final preload value were higher for "Standard Heli-Coil with Loctite".

Chapter 1

Introduction

1.1 Introduction

Threaded fasteners are a very important element in nonpermanent joints. They are widely used because of their many benefits. One of the main advantages of threaded fasteners is that they allow the maintenance (inspection, cleaning and repair) of components in machines. Another main advantage is the ability to develop a clamping force in which the threads of the bolt or the primary locking mechanism are engaged against the clamped elements by the threads of either nuts, tapped holes or threaded inserts causing elongation of the bolts. Loosening of threaded fasteners due to dynamic shear loading is an ongoing problem that not only threatens the lifespan of the machine but can also threaten the life of human beings in catastrophic failures. Thus, the use of secondary locking mechanisms is often used to increase the resistance against loosening and provide redundancy.

Nonetheless, there are still catastrophic failures such as the bolt related failure that took the life of Milena Del Valle, a facility maintenance worker at a restaurant in Boston. She was driving with her husband to pick up her brother in law from the Logan International Airport when a faulty bolt fixture that supported a concrete panel from the I-90 tunnel ceiling fell on top of her car. Investigators found that bolt loosened completely

even though high-strength epoxy was utilized. They concluded that the epoxy failed to bond properly. Furthermore, studies on secondary locking features are needed to better understand their loosening resistance in order to prevent accidents such as the ceiling failure on Interstate 90.

Specifically, this thesis will focus on identifying the dependency of loosening parameters on secondary locking features of thread inserts that are subjected to dynamic shear loads. This information can then be used to provide better insight for engineers in understanding, selecting or designing secondary locking mechanisms. In this thesis, the loosening parameters studied include: the percentage loss of initial preload, the initial rate of preload loss, the secondary rate of preload loss, the steady-state and the final preload value. The dependencies of the loosening parameters for each secondary locking feature are determined statistically.

1.2 Background

In a bolt, the threads are considered one of the most important elements because of their helical nature which not only leads to the ability to be assembled and disassembled, but also they are responsible for the performance of the bolt. The loosening of threaded fasteners due to transverse vibration has been a subject of study since the mid 1960's, so there are several references about loosening that were reviewed and that are cited in this thesis.

Early research on loosening due to transverse vibration was performed by Junker. He explains how, under transverse vibration (shear loading), the incline plane and friction forces in the bolt play a major role in the loosening process. Junker [1] explains his theory of loosening by the analogy of a block on top of an incline plane, as shown in Figure 1.1 where part a shows the friction forces between the block and the incline in equilibrium (no motion). However, when subjected to a transverse vibration strong enough to overcome the frictional force between the block and the incline, the bolt would slip in the direction of the transverse vibration as well as down the incline shown in part b of Figure 1.1.

Junker showed that loosening due to severe shear loadings results from a slippage of the head and the threads when bending forces overcome frictional forces between the engaged threads as well as the head of the bolt [1]. Hess [2] has analyzed the problem of self-loosening for several years and explains that the main mechanism of self-loosening is relative thread slip and component slip, caused by static and dynamic forces, moments, and/or reduced friction, manifesting themselves in joints through bending, pressure fluctuations, shocks, impacts, thermal expansion, and axial force fluctuations.

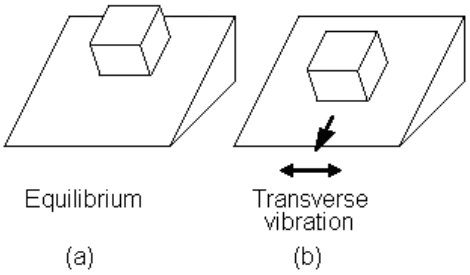

Figure 1.1 Block on incline plane.

Pai and Hess [3, 4] developed Junker's theory further by showing that in addition to complete slip, loosening can also result from the accumulation of localized slip. Bolt Science [5] lists that the common causes of the relative motion in bolted joints threads are; 1. Component bending that results in forces being induced at the friction surface. If slip occurs, the head and threads will slip, which can cause loosening. 2. Differential thermal effect caused by either differences in temperature or differences in clamped materials. 3. Applied forces on the joint that lead to shifting of the joint surfaces can induce bolt loosening.

Sanclemente and Hess [6] focused on the parameters influencing loosening in which it was shown that preload and fastener material are the most significant. These studies have been excellent sources in providing a clearer understanding of loosening in bolts. However, these studies are only focused on loosening of bolted joints without any secondary locking feature.

Bickford [7] documents other sources of preload loss such as bolt relaxation. He cites a report by Fisher and Struik [8] that tested bolt tension and found a preload loss of 2% to 11% immediately after tightening and 3.6% after the next 21 days and concludes that the bolt does undergo relaxation. Bickford [7] also comments on an experiment he

performed on bolts and found that a torsional relaxation of 50% occurred when the wrench was removed. He concluded that embedment (plastic deformation that occurs in the area of clamped component and the fastener [7]) allows the relaxation, not only axially but also torsionally, to occur. Nonetheless, it is unclear whether in these experiments secondary locking features were used. According to Ibrahim [9], relaxation effects cause time-dependent boundary conditions and depend on the level of structural vibration. During operation, the non-linear random response can usually change the joint mechanical properties, which creates new self-induced uncertainties.

Bickford [7] refers to the Motosh [10] equation where the input torque is resisted by three reaction forces produced by the stretch of the bolt, the friction between the engaged threads and the friction between the face of the nut and the washer or joint (prevailing torque is added when present). In addition, he comments on the effect of prevailing torque on preload loss under vibratory motion as a means to prevent loosening of the bolt. He also lists and describes on a variety of secondary locking mechanisms that help to reduce loosening. Hess [2] comments on ways to improve loosening resistance by the increase of preload, finer thread pitch, higher thread and head friction, tighter tolerances, higher excitation frequency, and lower excitation amplitude.

Finkelston [11] shows that the prevailing torque (the distortion or modification of metal threads, bolts or nuts to provide some inference with the matting part that is not dependant entirely on friction forces [7]) reduces the rate of preload loss when the effective prevailing torque counteracts the loosening torque as shown in Figure 1.2. He claims that the prevailing torque could stop the rate of preload loss. However, Figure 1.2

is only for one test sample which prevents him from drawing any meaningful statistical conclusions.

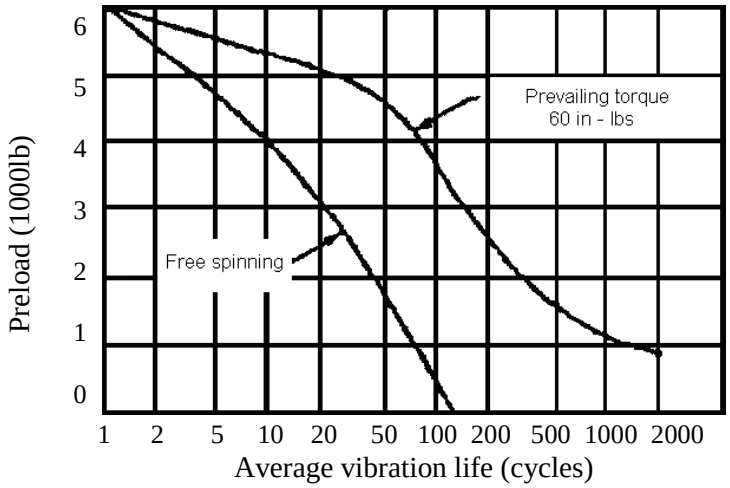

Figure 1.2 Effect of prevailing torque in reducing loosening [11].

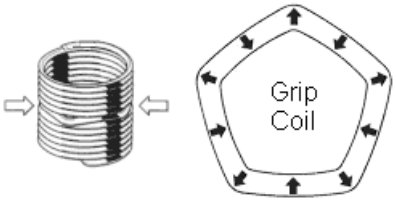

Figure 1.3 Locking Heli-Coil's grip coil [14].

Generally, in order to prevent loosening, safety-wire, coatings and inserts, thread-locking adhesives and spring washers are used [12]. However, these secondary locking mechanisms have their limitations and do not necessarily prevent relaxation. Wolfe [13] focuses on the advantages of thread inserts over conventional methods (i.e. nuts). Hillclif tools [14] provides an overview of the free running thread insert as well as an explanation

on the Locking Heli-Coil system as a alternative secondary locking mechanism consisting of a grip coil, shown in Figure (1.3), that when bent outward creates high pressure on the bolt which secures it against loosening.

Henkel Corp [15] explains that Loctite Threadlocker fills microscopic gaps between the interfacing threads and when it comes in contact with metal, in the absence of air, it polymerize to a tough solid. Bardon [16] documents on thread lockers as an effective and inexpensive way to ensure reliable performance in machinery. Liquid anaerobic adhesives such as Loctite Threadlocker help against vibrations as well as leakage and corrosion.

In short, there is a lack of literature where the dependency of loosening parameters on secondary locking features is statistically analyzed. The literature does show the overall advantage of secondary locking features. However, it is important to quantify, statistically, the dependencies of the loosening parameters on secondary locking features in order to better understand their behavior since it would help engineers to better design and maintain equipment or even improve secondary locking mechanism technology.

1.3 Overview

This thesis focuses on the dependency of loosening parameters on secondary locking mechanisms. Chapter 2 describes the test data and apparatus, test specimens and experimental procedures. It also provides plots of the raw data (loosening plots) which are used in this study. Chapter 3 focuses on the extraction of the loosening parameters used in this thesis. Also, in this chapter, statistical analysis is performed on the extracted data in order to quantify the results. Chapter 4 gives meaning to the statistical results obtained in Chapter 3. Finally, Chapter 5 states the conclusions.

Chapter 2

Raw Data

2.1 Introduction

This chapter presents the preload versus cycle data used in this thesis. The data is from an experiment performed on testing the loosening of threaded fasteners subjected to dynamic shear with different locking levels. The data was obtained using a DIN 65151 or Junker type [1] test machine which provides transverse vibration.

2.2 Apparatus

The test apparatus used to obtain the data is shown in Figure 2.1. It consists of a top plate clamped to a rigid fixed base through a threaded insert using a test screw. In order to minimize sliding friction and galling, roller bearings are used between the top plate and the fixed base. Cyclic shear loads are applied to the top plate by an arm linked to an adjustable eccentric. The apparatus is driven by a 5 HP AC motor through an adjustable pulley arrangement while load cells measure screw preload and the shear force acting on the top plate. An LVDT transducer (linear variable differential transformer), located at the end of the plate, was used to measure the transverse displacement of the plate.

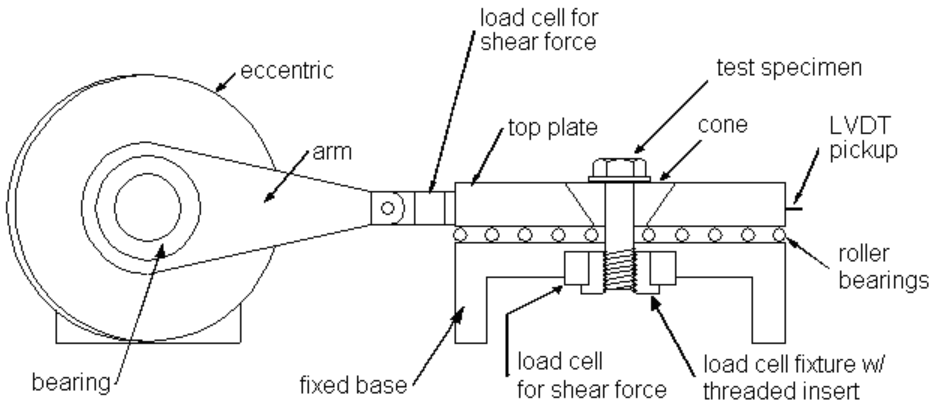

Figure 2.1 Schematic of test machine.

2.3 Test specimens

The test specimens were NAS 1004 1/4-28 UNJF-3A hex head screws [17] with:

1. Standard free-running Heli-Coil inserts with Braycote 601 EF high vacuum grease.
2. Locking Heli-Coil with Braycote 601 EF high vacuum grease.
3. Standard free-running Heli-Coil inserts with Loctite 242 Threadlocker.

Twelve tests were run for each configuration or locking level for a total of thirty-six runs. The specifications for the screws, washers and Heli-Coils inserts used in these test are the following:

1. Thirty-six NAS1004-29A, ¼-28 UNJF-3A, 2.356 inch long, hex head screws, made of A286 stainless steel [17].
2. Thirty-six NAS 1149-C0463R washers for ¼ inch screw made of corrosion resistant steel with passivated finish [18].

3. Twenty-four MS124696, 0.375 inch long, standard, free-running Heli-Coil inserts, made of 304 stainless steel [19].
4. Twelve MS21209-F4-15, 0.375 inch long, Heli-Coil inserts, made of 304 stainless steel [19].

New screws, washers and Heli-Coils were used for each test. In the test machine, a test screw secured the top plate to the fixed base by a cone and load fixture as shown in Figure 2.1. A test Heli-Coil insert is installed into the load cell fixture. The cone was placed in the top plate and the load fixture sets in the preload load cell. The cone and load fixtures are made of 15-5 stainless steel and heat treated to RC35 and the surfaces grounded to 32µin. The load cell fixture has tapped holes ready for Heli-Coil installation and the cone has thru-holes.

2.4 Installation

All test specimens parts (screws, washers, cones and load fixtures with installed Heli-Coil) were pre-cleaned in ultrasonic bath cleaner with MEK as the solvent for 3 minutes. The Standard free running and Locking Heli-Coil inserts were installed in the load cell fixtures following manufacturer's instructions [19]. Braycote 601 EF grease was applied under screw head and washer to all thirty-six test specimens. Also, Braycote 601 EF grease was applied to cover screw threads and Heli-Coil threads to twenty-four test runs. The remaining twelve test specimens were sprayed with Loctite 7471 activator (primer T) five minutes prior to the application (two to three drops) of Loctite 242 Threadlocker, the bolts were tightened to specified preload and allowed to cure for 24 hours.

2.5 Test specifications

The experiment was conducted with Braycote lubricant applied under the screw head and washer, the Junker test machine is set at 15Hz with a 0.12 inch (3mm) eccentric, the preload at 2,400 lbs or 66% yield, and a record length of 160 seconds or 2,400 cycles. The data was collected at 51.2 samples/second for a total of 8,192 data points for each measured variable for each test. The preload of 2,400 lbs was calculated by multiplying the 0.2% yield strength (100,000 psi) by the 66% of the thread stress area which is 0.0364 in^2.

2.6 Test data

All preload versus cycles plots are shown below for all three locking levels These plots illustrates test runs with the “Standard Heli-Coil with Braycote”, “Locking Heli-Coil with Braycote” as well as “Standard Heli-Coil with Loctite”.

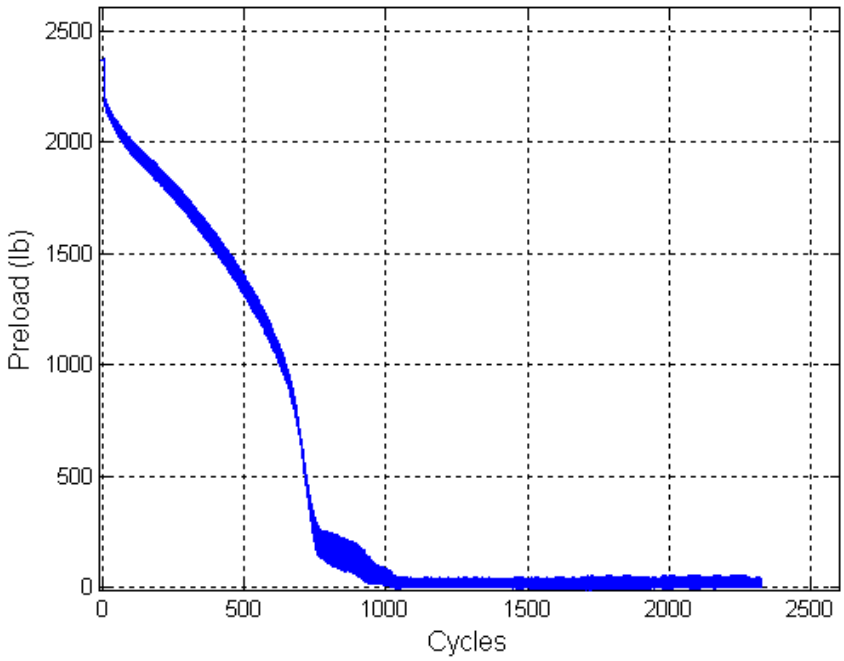

Figure 2.2 Preload vs. cycles for "Standard Heli-Coil with Braycote" run number 1.

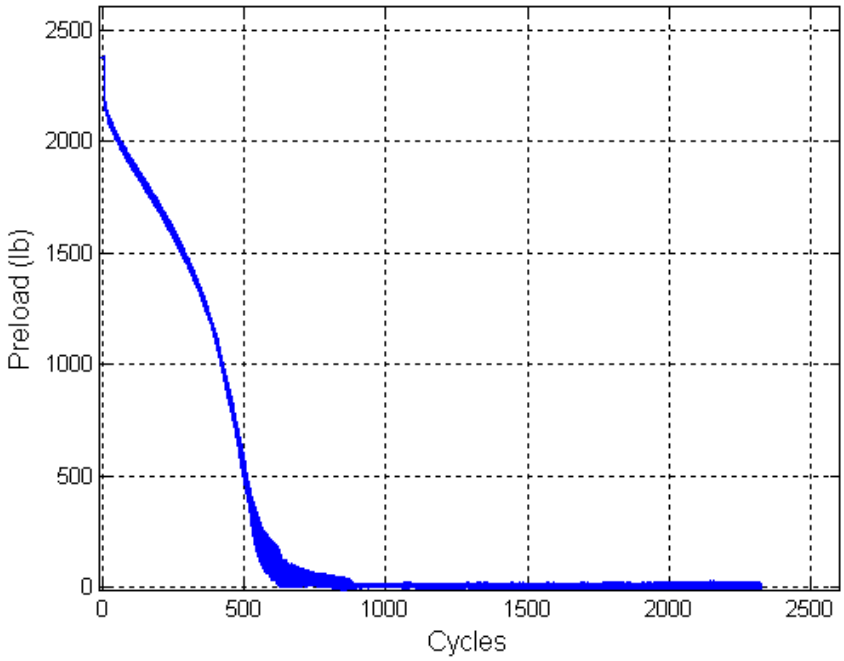

Figure 2.3 Preload vs. cycles for "Standard Heli-Coil with Braycote" run number 2.

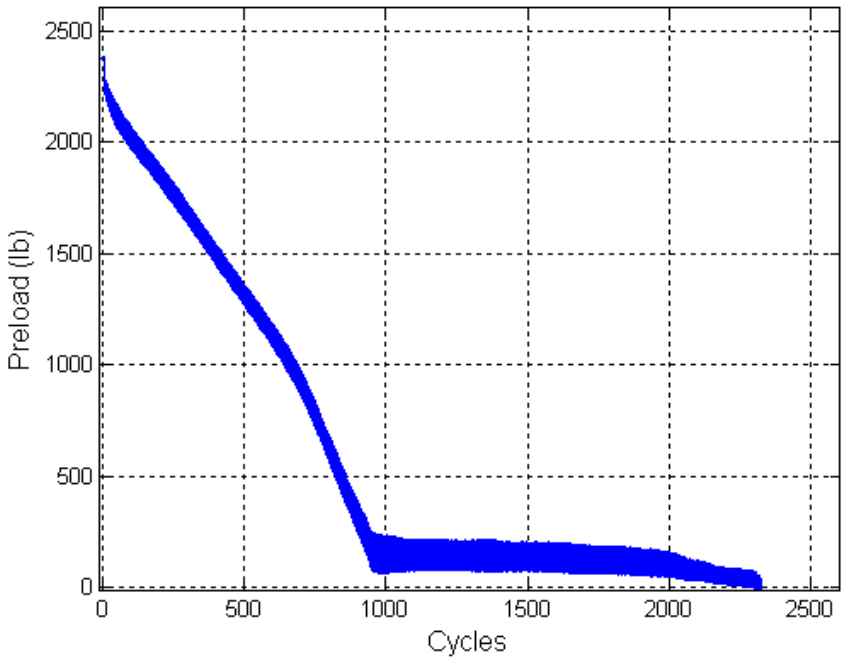

Figure 2.4 Preload vs. cycles for "Standard Heli-Coil with Braycote" run number 3.

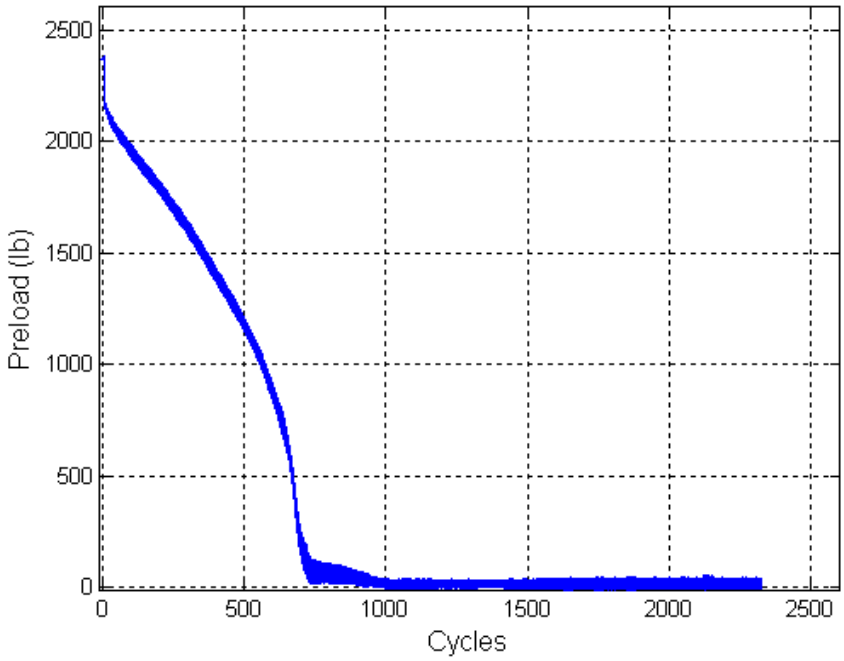

Figure 2.5 Preload vs. cycles for "Standard Heli-Coil with Braycote" run number 4.

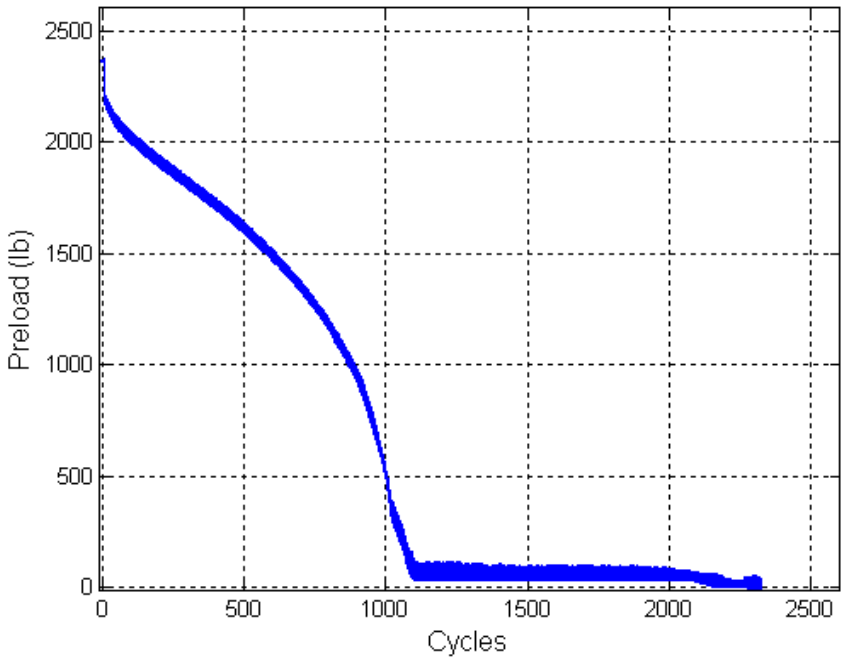

Figure 2.6 Preload vs. cycles for "Standard Heli-Coil with Braycote" run number 5.

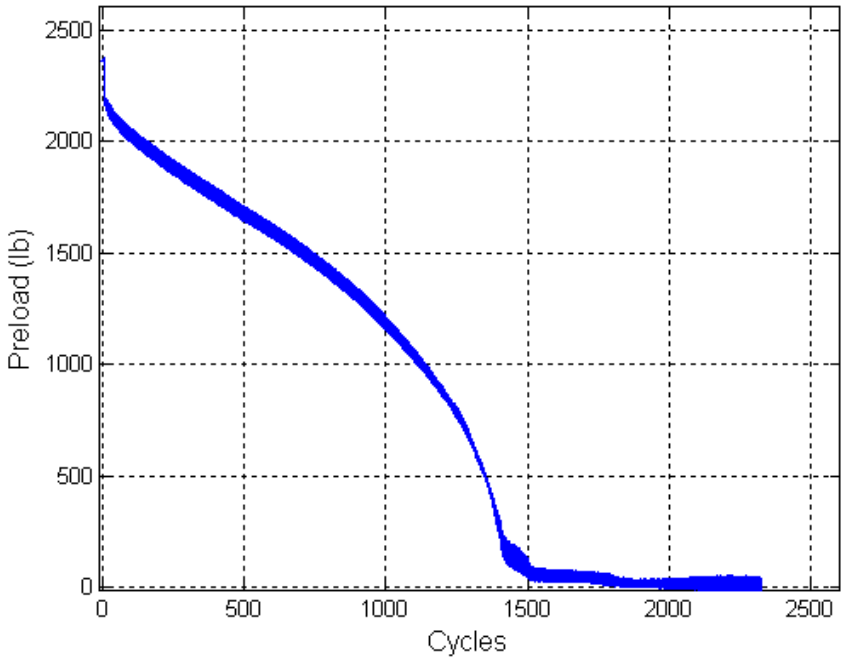

Figure 2.7 Preload vs. cycles for "Standard Heli-Coil with Braycote" run number 6.

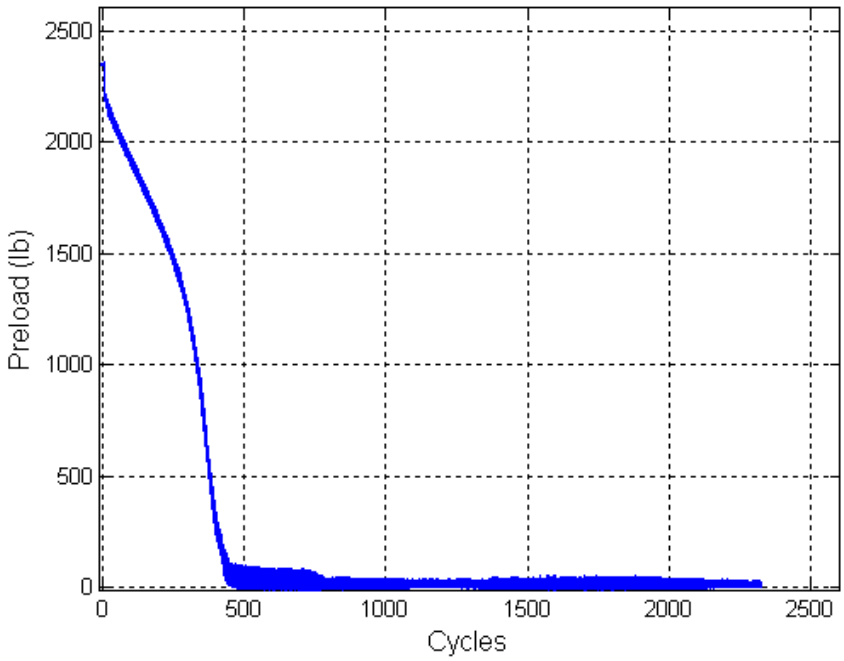

Figure 2.8 Preload vs. cycles for "Standard Heli-Coil with Braycote" run number 7.

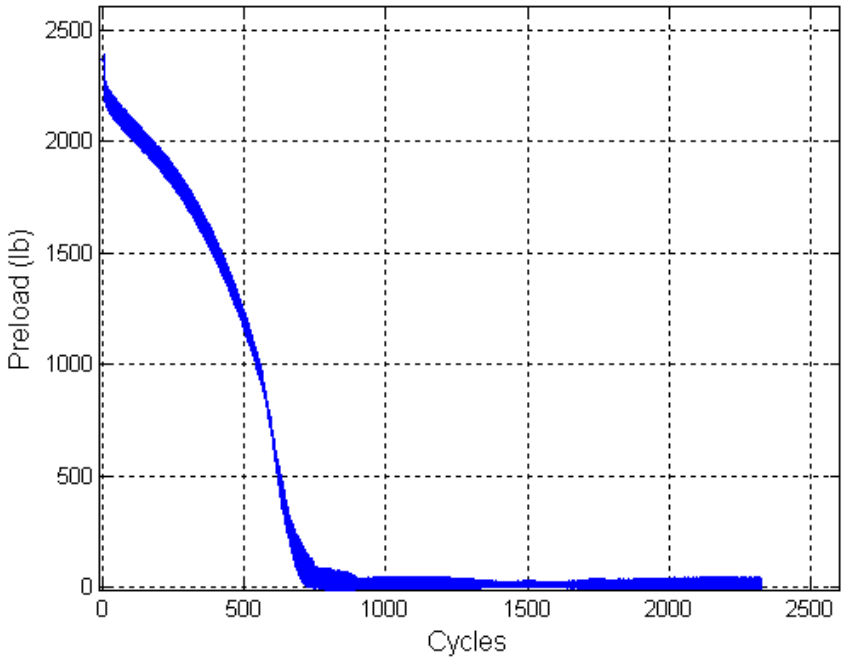

Figure 2.9 Preload vs. cycles for "Standard Heli-Coil with Braycote" run number 8.

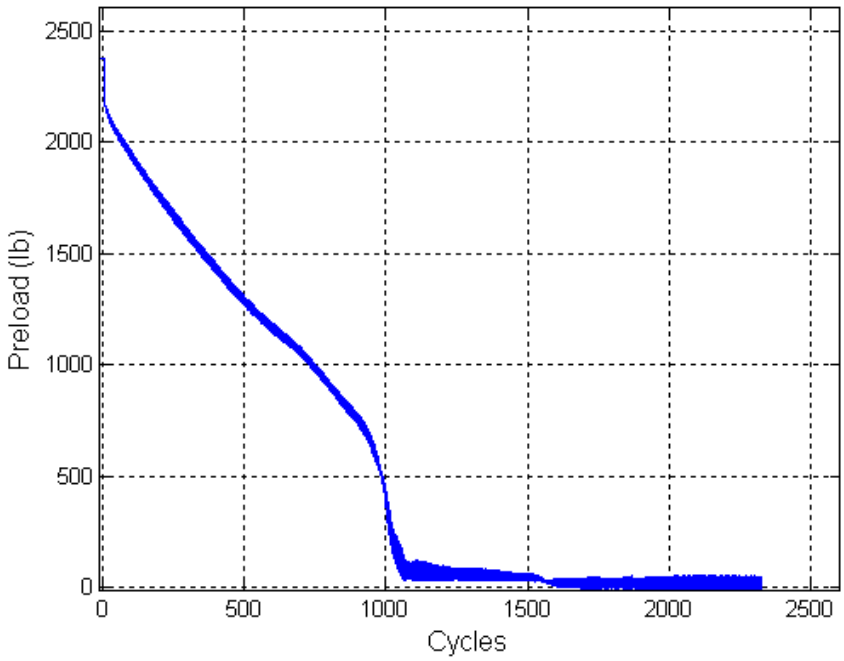

Figure 2.10 Preload vs. cycles for "Standard Heli-Coil with Braycote" run number 9.

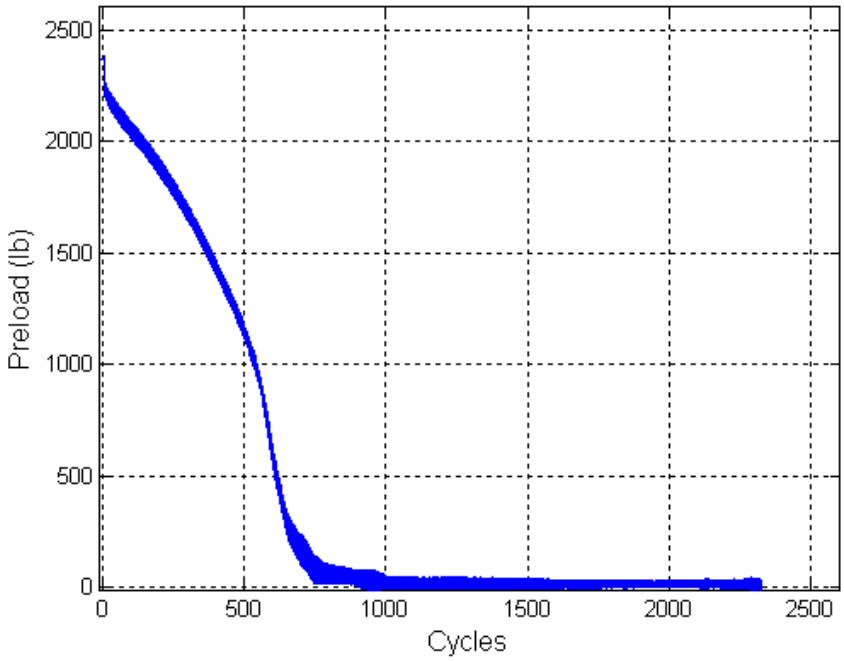

Figure 2.11 Preload vs. cycles for "Standard Heli-Coil with Braycote" run number 10.

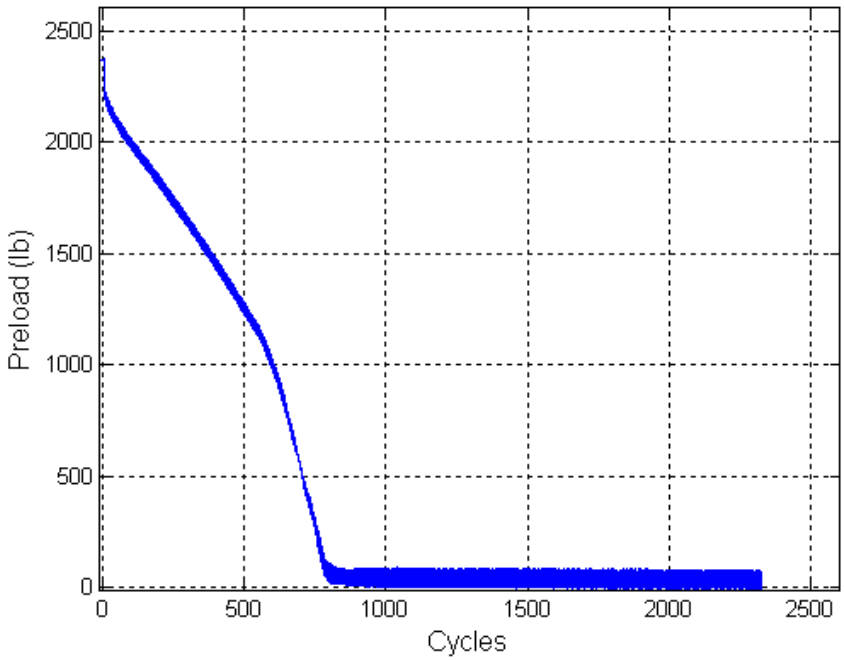

Figure 2.12 Preload vs. cycles for "Standard Heli-Coil with Braycote" run number 11.

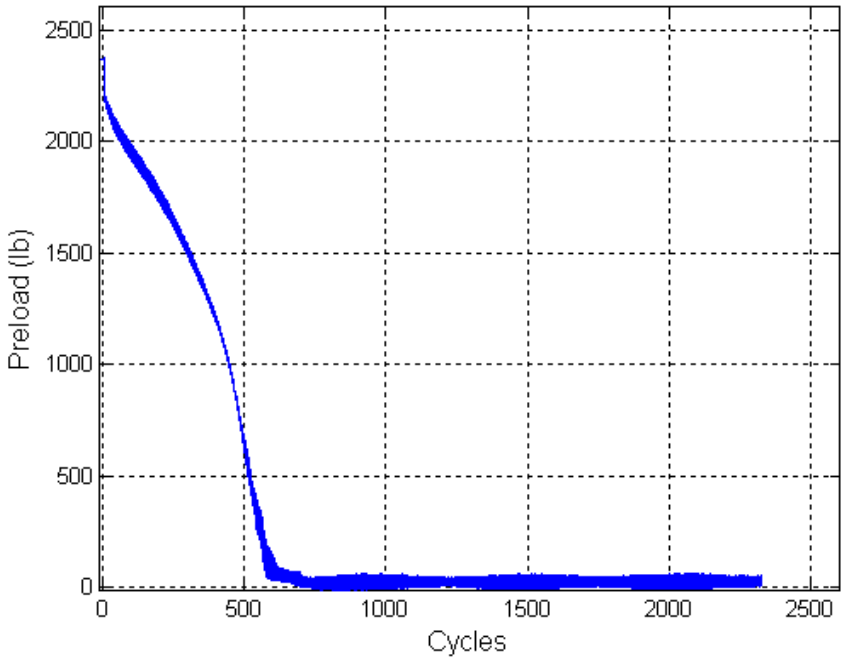

Figure 2.13 Preload vs. cycles for "Standard Heli-Coil with Braycote" run number 12.

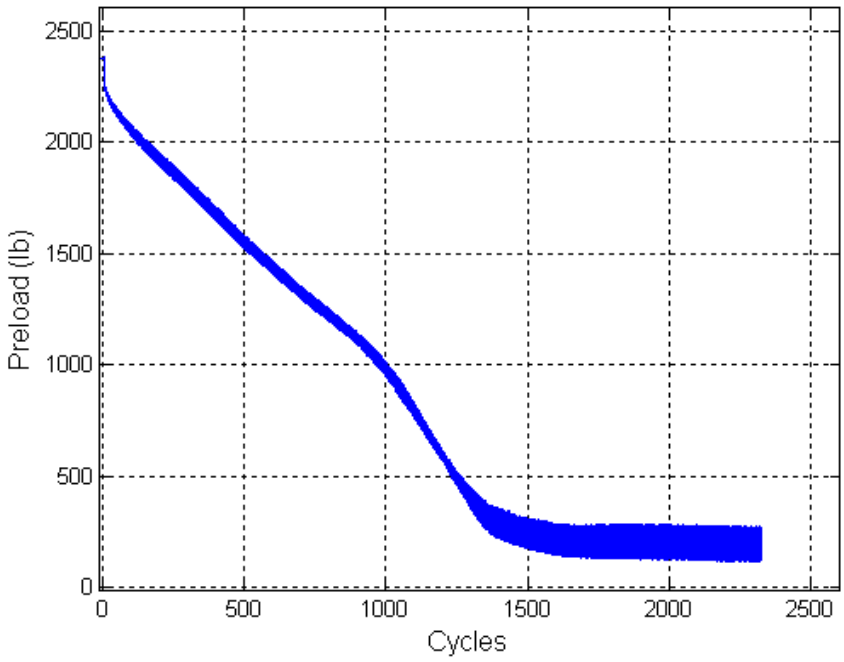

Figure 2.14 Preload vs. cycles for "Locking Heli-Coil with Braycote" run number 13.

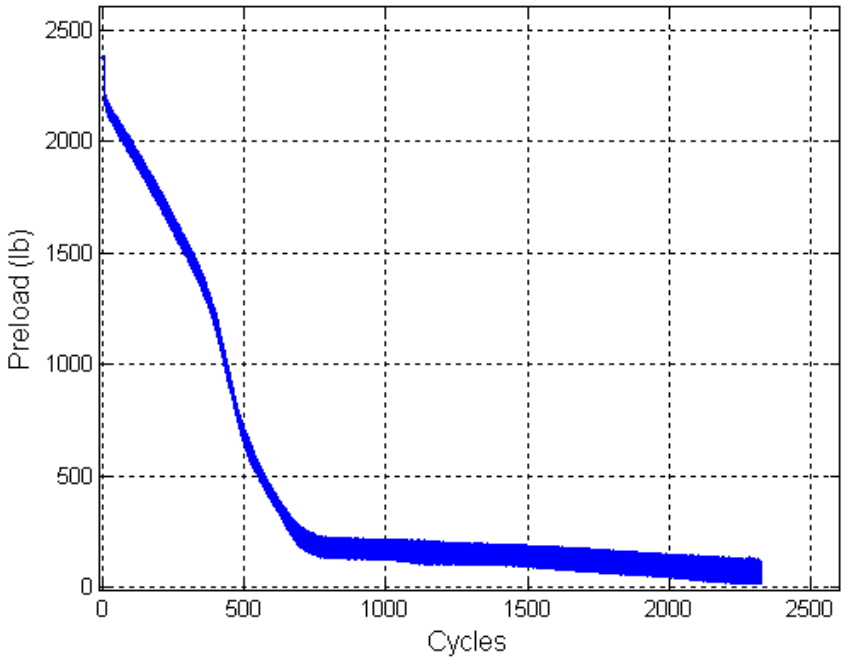

Figure 2.15 Preload vs. cycles for "Locking Heli-Coil with Braycote" run number 14.

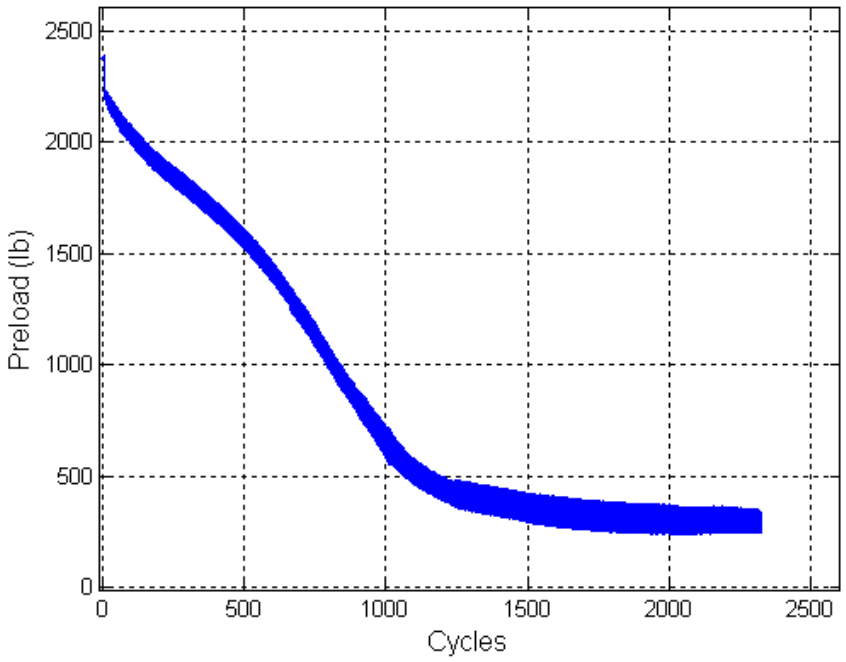

Figure 2.16 Preload vs. cycles for "Locking Heli-Coil with Braycote" run number 15.

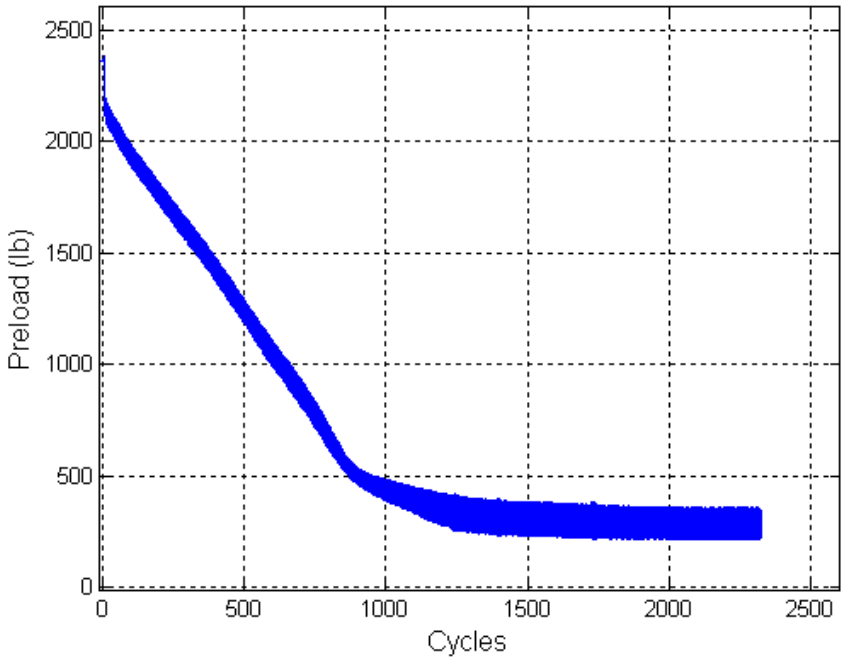

Figure 2.17 Preload vs. cycles for "Locking Heli-Coil with Braycote" run number 16.

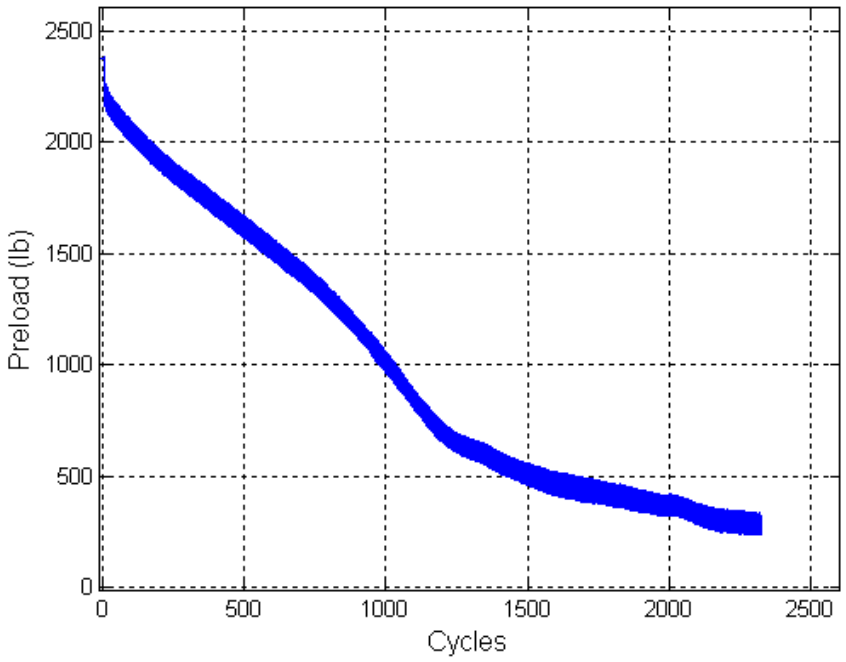

Figure 2.18 Preload vs. cycles for "Locking Heli-Coil with Braycote" run number 17.

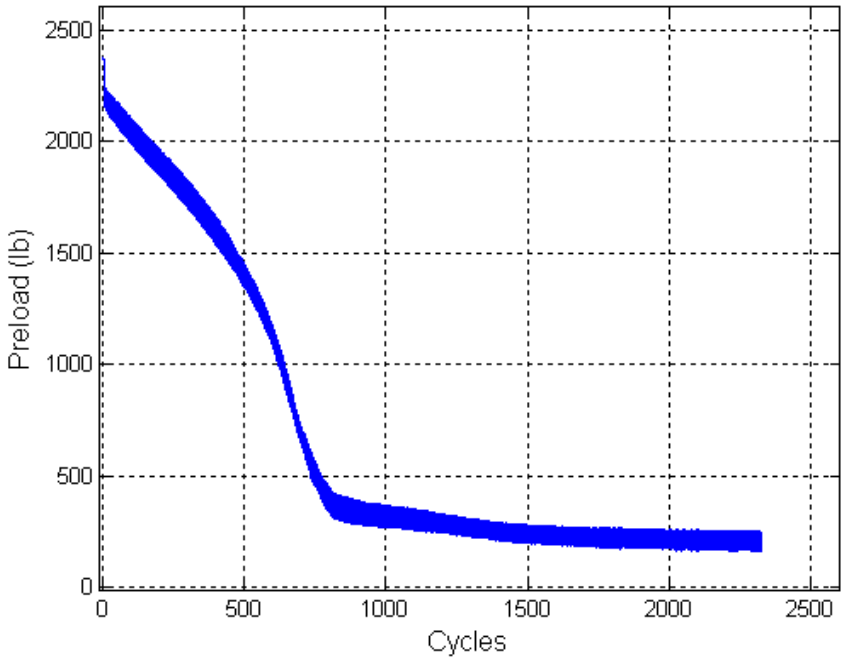

Figure 2.19 Preload vs. cycles for "Locking Heli-Coil with Braycote" run number 18.

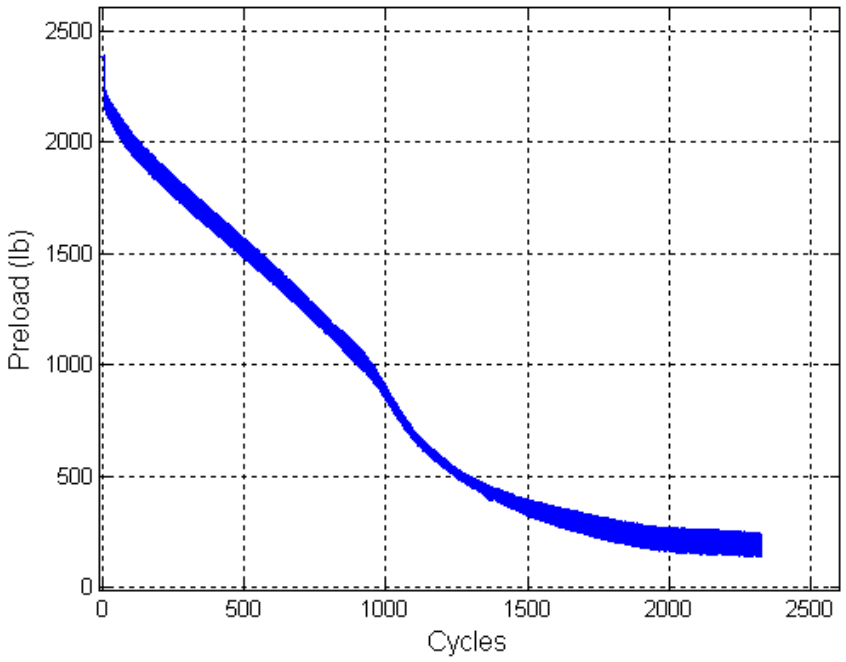

Figure 2.20 Preload vs. cycles for "Locking Heli-Coil with Braycote" run number 19.

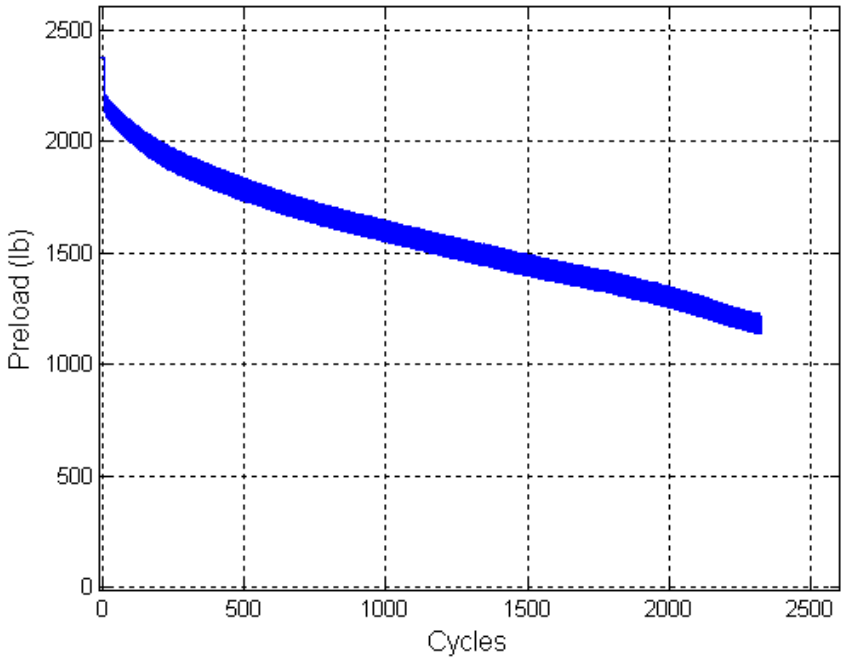

Figure 2.21 Preload vs. cycles for "Locking Heli-Coil with Braycote" run number 20.

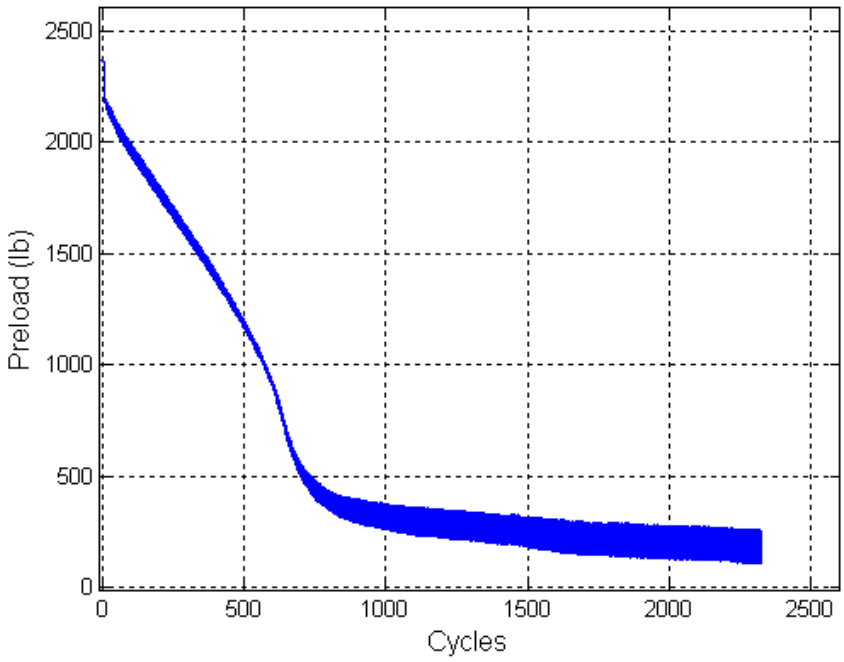

Figure 2.22 Preload vs. cycles for "Locking Heli-Coil with Braycote" run number 21.

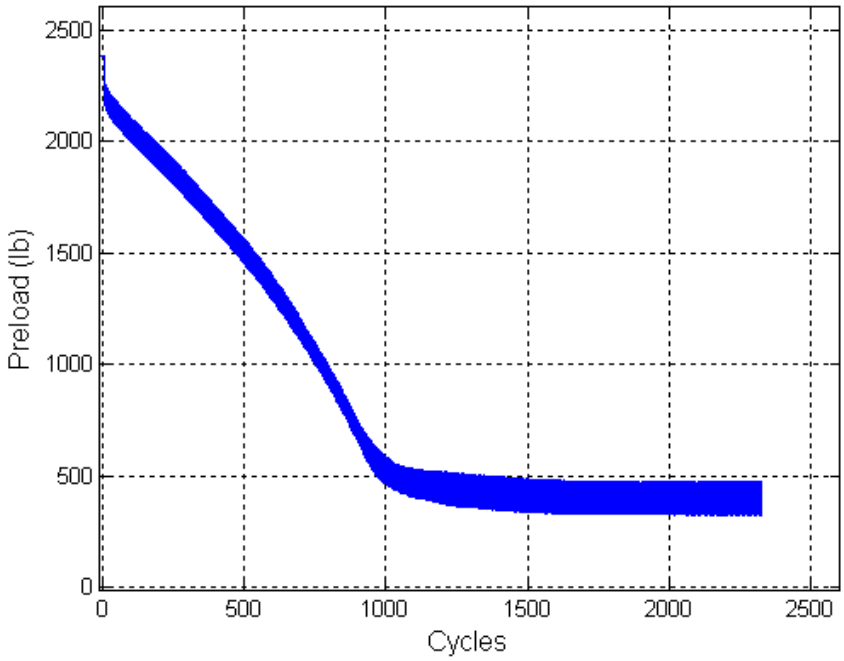

Figure 2.23 Preload vs. cycles for "Locking Heli-Coil with Braycote" run number 22.

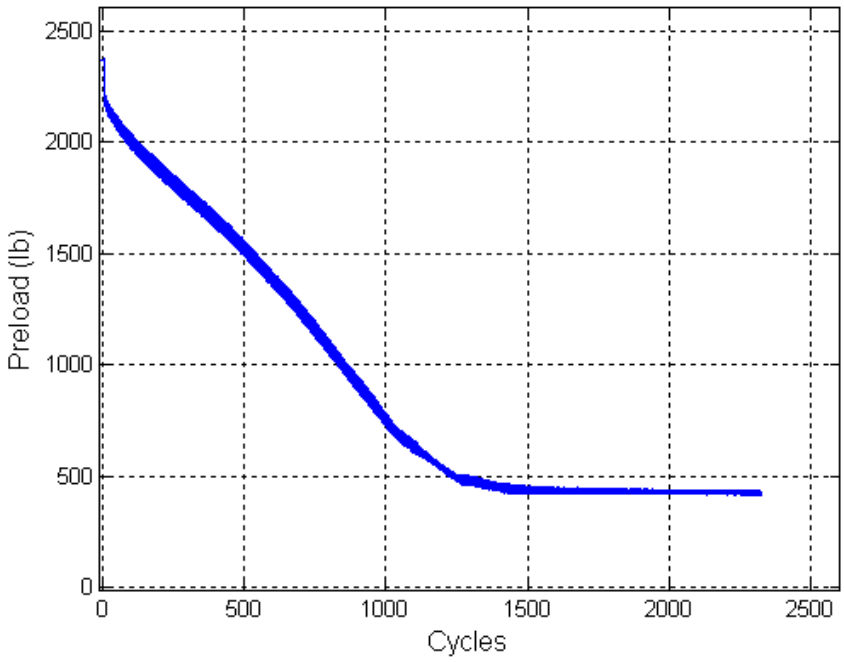

Figure 2.24 Preload vs. cycles for "Locking Heli-Coil with Braycote" run number 23.

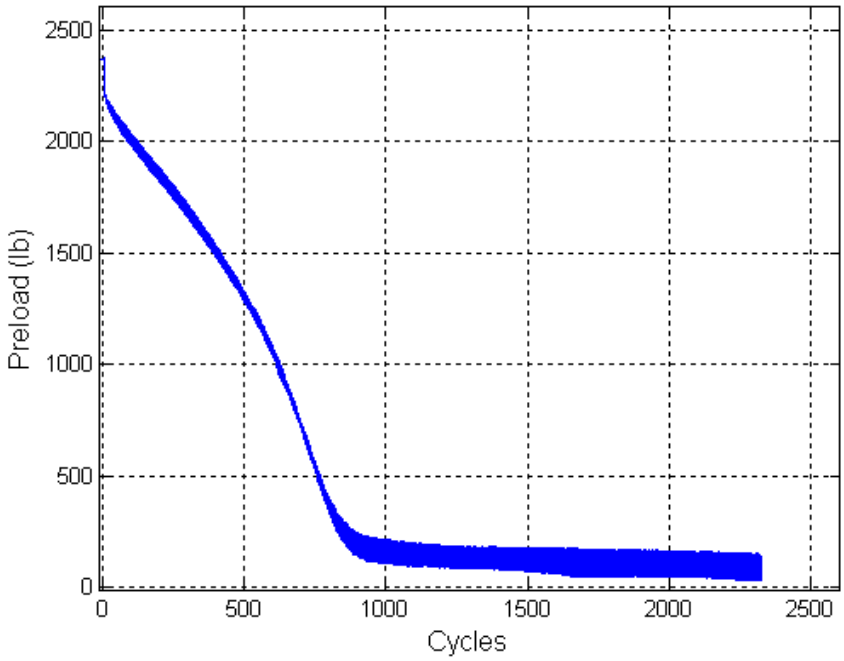

Figure 2.25 Preload vs. cycles for "Locking Heli-Coil with Braycote" run number 24.

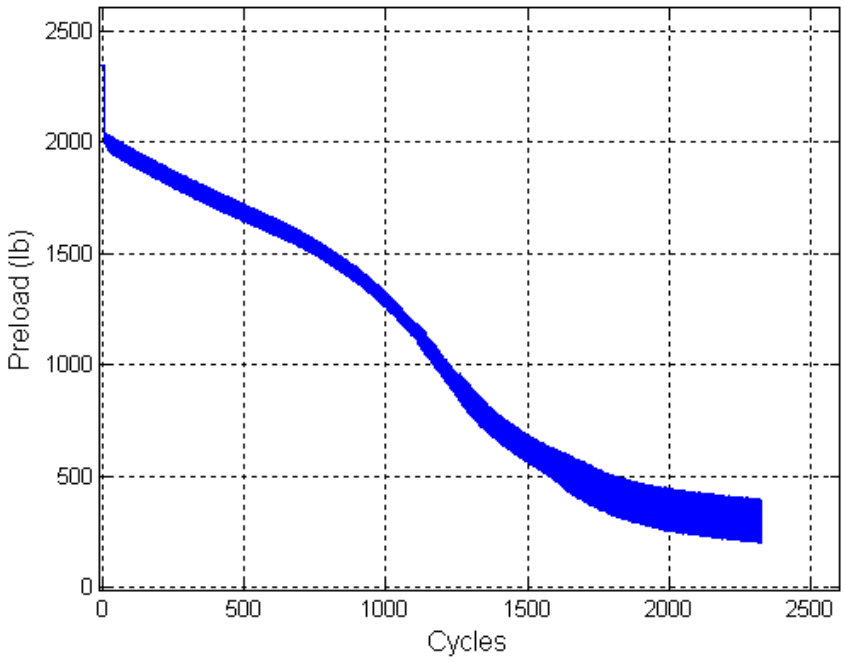

Figure 2.26 Preload vs. cycles for "Standard Heli-Coil with Loctite" run number 25.

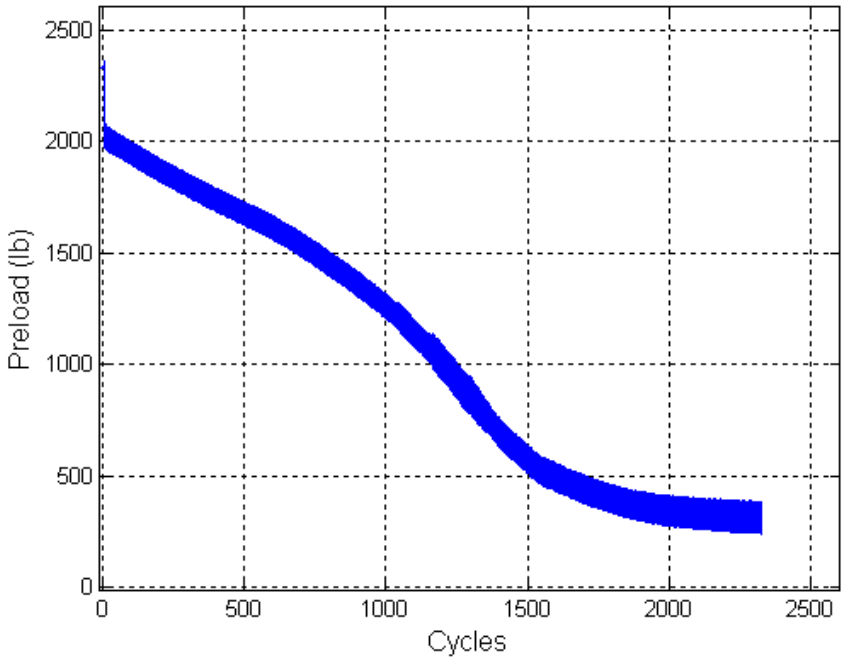

Figure 2.27 Preload vs. cycles for "Standard Heli-Coil with Loctite" run number 26.

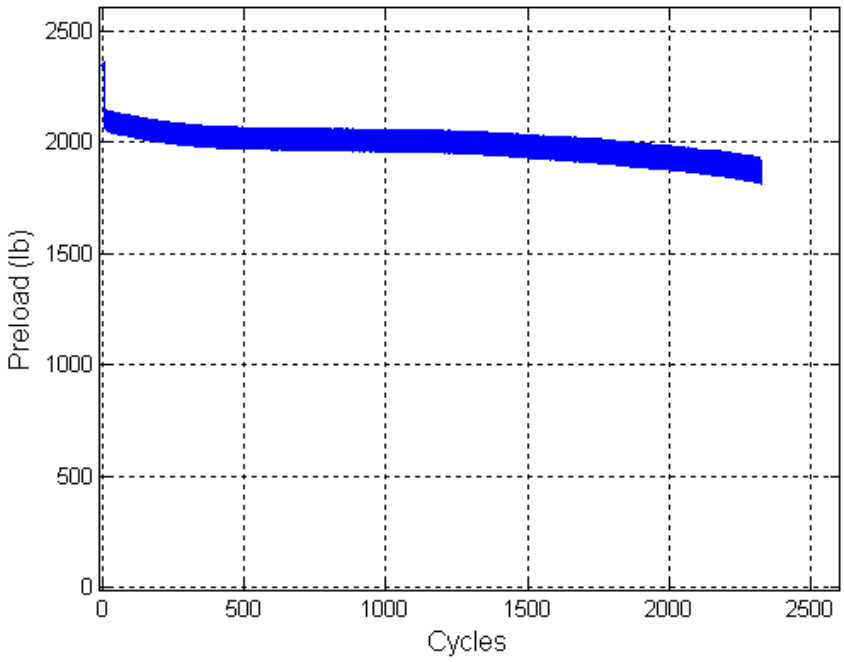

Figure 2.28 Preload vs. cycles for "Standard Heli-Coil with Loctite" run number 27.

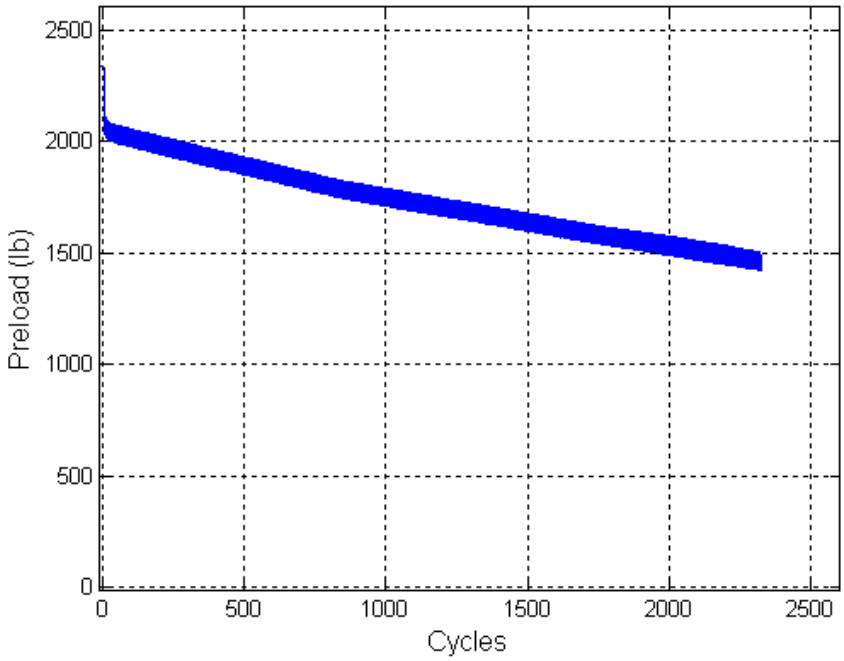

Figure 2.29 Preload vs. cycles for "Standard Heli-Coil with Loctite" run number 28.

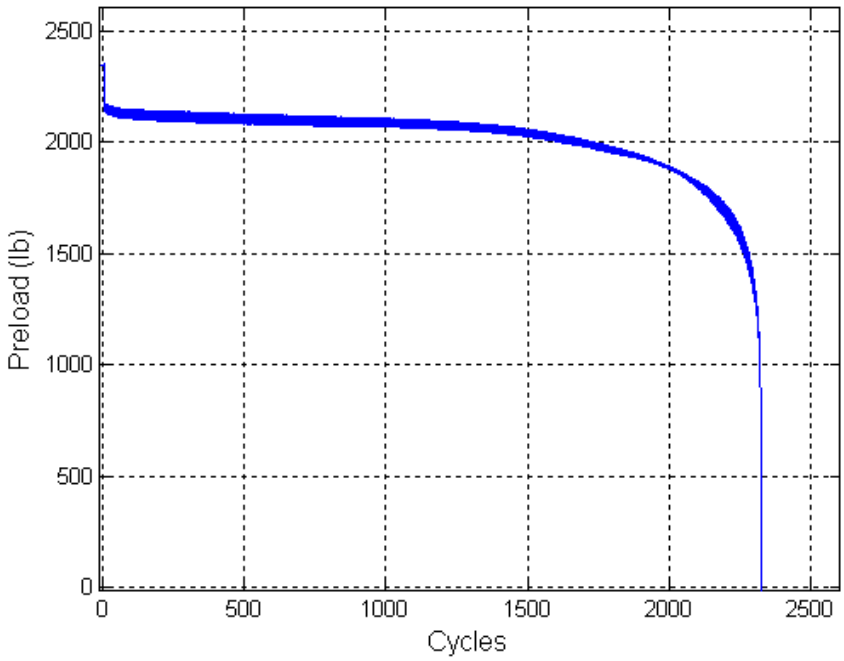

Figure 2.30 Preload vs. cycles for "Standard Heli-Coil with Loctite" run number 29.

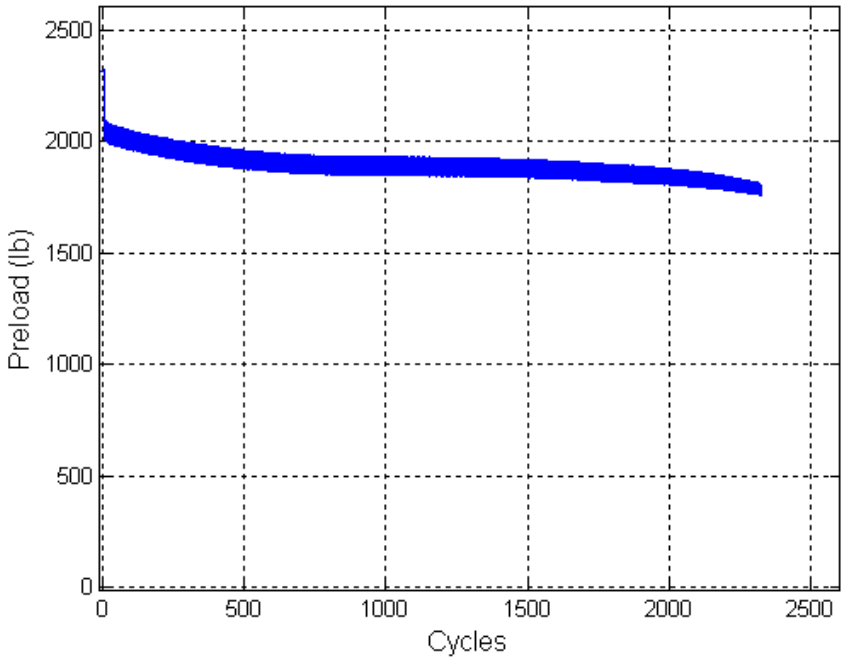

Figure 2.31 Preload vs. cycles for "Standard Heli-Coil with Loctite" run number 30.

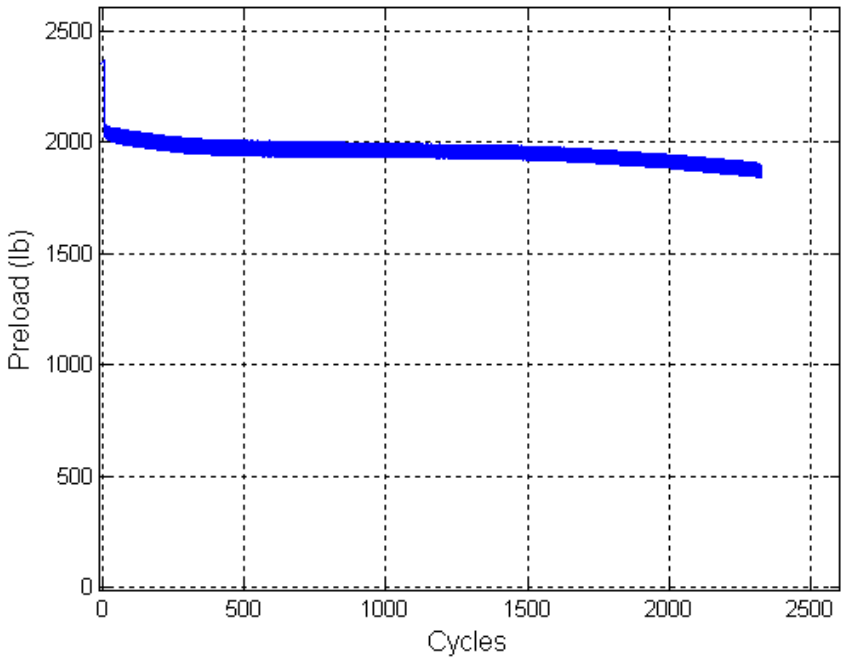

Figure 2.32 Preload vs. cycles for "Standard Heli-Coil with Loctite" run number 31.

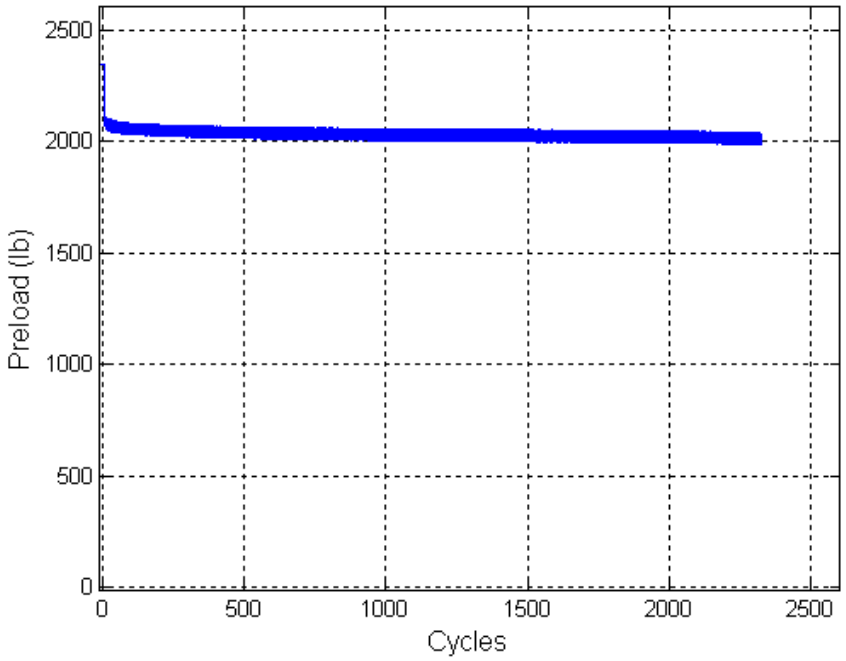

Figure 2.33 Preload vs. cycles for "Standard Heli-Coil with Loctite" run number 32.

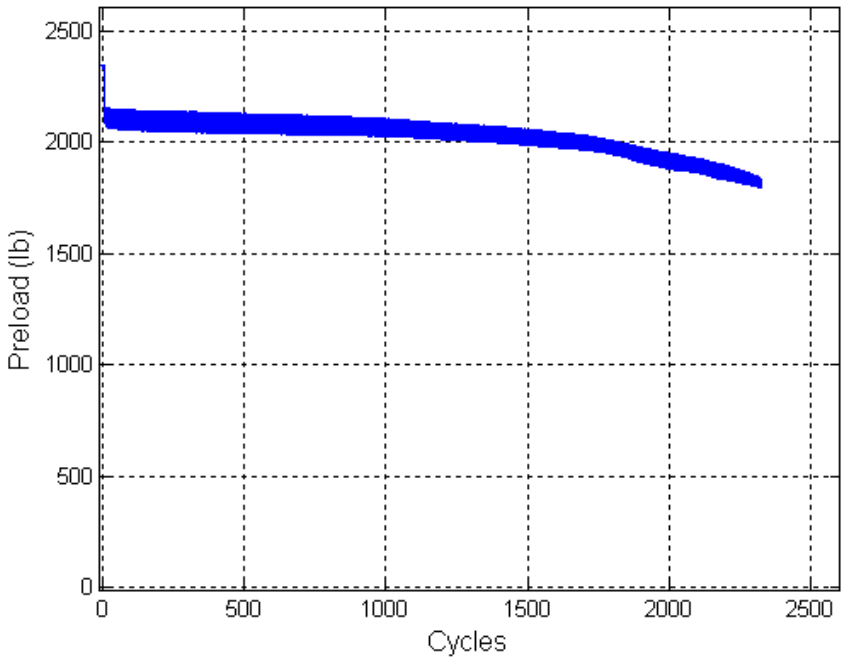

Figure 2.34 Preload vs. cycles for "Standard Heli-Coil with Loctite" run number 33.

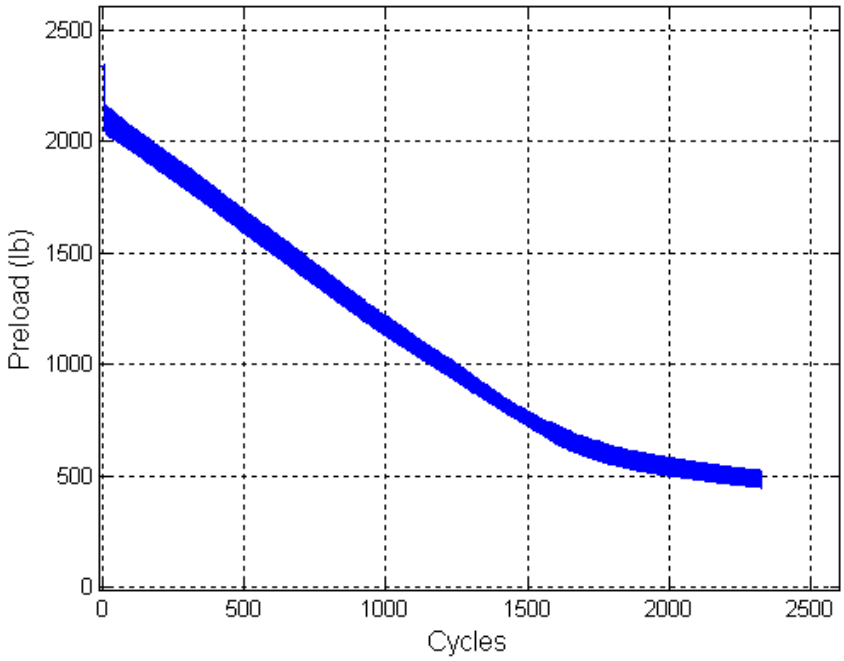

Figure 2.35 Preload vs. cycles for "Standard Heli-Coil with Loctite" run number 34.

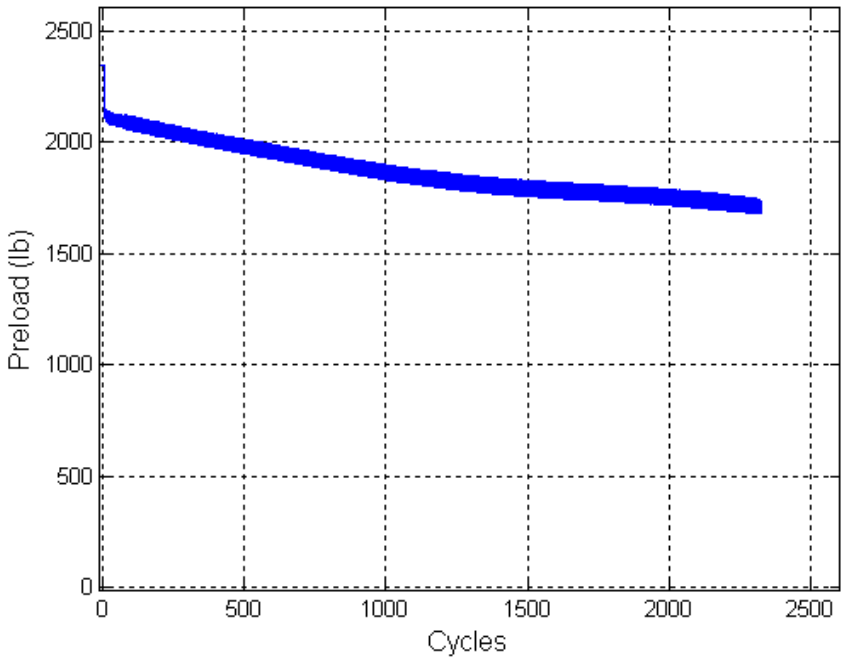

Figure 2.36 Preload vs. cycles for "Standard Heli-Coil with Loctite" run number 35.

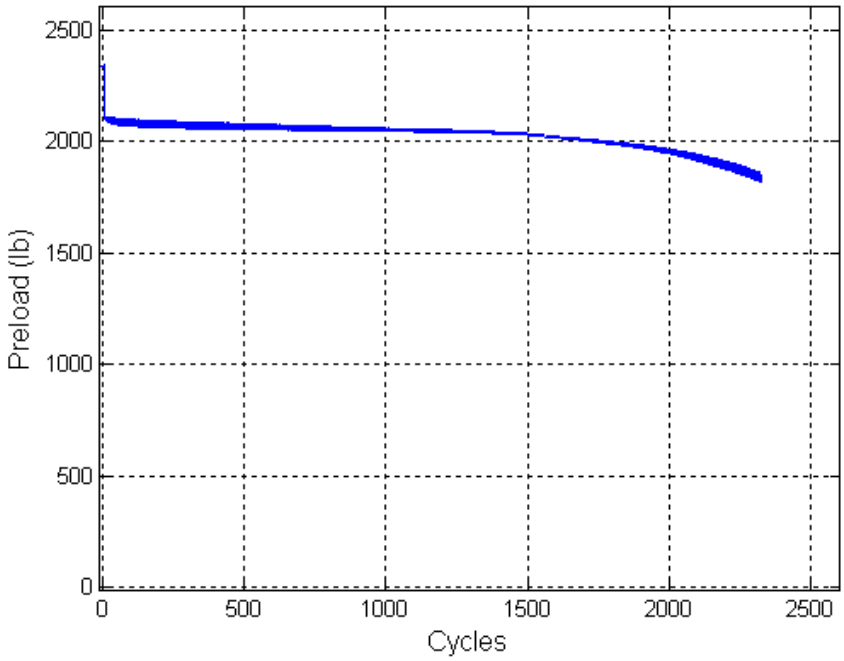

Figure 2.37 Preload vs. cycles for "Standard Heli-Coil with Loctite" run number 36.

Note that for run number 29 ("Standard Heli-Coil with Loctite"), the screw broke at 2,324 cycles. The corresponding preload versus cycle plot, Figure 2.30, reveals this rapid failure suggesting that the tests operate close to the lower bound of the screw fatigue life when the majority of the preload is maintained for close to the duration of the test.

The initial and residual preload values were recorded, documented and provided from the preload measurements for all thirty-six runs in Table 2.1 which shows the initial preload and torque; breakaway or removal torques; the assembly as well as the removal prevailing torques are also included in this table. The initial preload varies from 2,315 to 2,385 lbs caused by joint embedment and assembly variation. Because of the Loctite's 24 hour cure time period from tightening to testing, data runs from 25 to 36 ("Standard Heli-Coil with Loctite"), have lower initial preload than the other levels of locking. Thus, some preload loss may be expected due to asperity relaxation (the deformation on the surface protuberances). Whereas the time period between tightening and testing for the other runs are about one minute where little to no asperity relaxation occurs.

The tightening torque for the data shown in Table 2.1 required to achieve the desired 2,400 lbs of preload for the "Standard Heli-Coil with Braycote" ranges from 100 to 105 lbs while for "Locking Heli-Coil with Braycote" shows to be higher because of the assembly prevailing torque of 20 lbs. The higher required tightening torque values for "Standard Heli-Coil with Loctite" is due to the higher friction caused by Loctite Threadlocker compared with Braycote grease.

The removal prevailing torque for the "Locking Heli-Coil with Braycote" and "Standard Heli-Coil with Loctite" runs were found to be similar. In addition, The

discrepancies between the assembly prevailing torque and the removal prevailing torque of "Locking Heli-Coil with Braycote" are due to wear caused by assembly and testing.

Table 2.1 Torque test data

Run Number	Initial Preload (lbs)	Maximum tightening torque (lb-in)	Breakaway Torque (lbs-in)	Assembly prevailing Torque (lbs-in)	Removal Prevailing torque (lbs-in)
1	2365	100	0	-	-
2	2375	100	0	-	-
3	2375	100	0	-	-
4	2370	100	0	-	-
5	2360	100	0	-	-
6	2360	105	0	-	-
7	2350	100	0	-	-
8	2365	100	0	-	-
9	2370	100	0	-	-
10	2365	105	0	-	-
11	2370	100	0	-	-
12	2370	105	0	-	-
13	2370	120	20	20	15
14	2375	120	10	20	10
15	2375	115	20	20	15
16	2360	120	25	20	15
17	2370	125	20	20	15
18	2370	115	20	20	15
19	2385	120	20	20	15
20	2370	115	60	20	15
21	2365	120	15	20	10
22	2380	120	25	20	15
23	2365	115	30	20	15
24	2365	120	15	20	15
25	2350	115	25	-	10
26	2330	110	25	-	15
27	2345	115	100	-	20
28	2335	115	80	-	20
29	2345	115	screw broke	-	**
30	2315	110	85	-	20
31	2355	115	95	-	20
32	2345	110	105	-	20
33	2340	110	105	-	20
34	2340	110	40	-	15
35	2340	115	85	-	20
36	2340	110	110	-	15

Chapter 3

Extraction of Loosening Parameters

3.1 Introduction

In order to asses the dependency of loosening parameters on secondary locking features, it is necessary to split each preload vs. cycles plot mentioned in Chapter 2 by stages. These sections represent different loosening parameters experienced by the bolt; thus, facilitating the study of the effect of the secondary locking features during dynamic shear loadings. Figure 3.1 is a representation of the states aforementioned illustrating the purpose of this chapter. Note that any transition area will not be studied in this thesis.

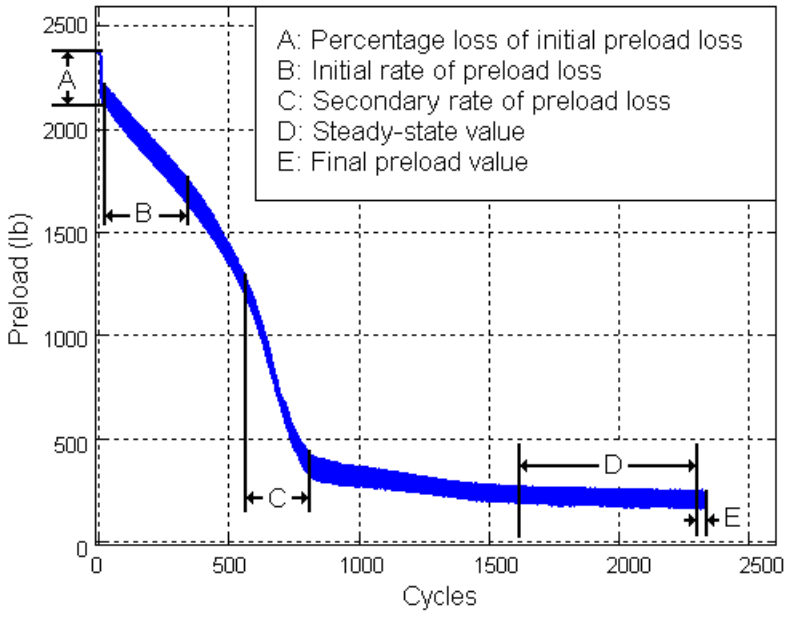

Figure 3.1 Representation of loosening parameters (run number 18).

The focus of this chapter is to extract the following parameters from the preload versus cycle data presented in Chapter 2:

1. Percentage loss of initial preload
2. Initial rate of preload loss
3. Secondary rate of preload loss
4. Steady-state value
5. Final preload value

Since there is variation in these parameters, statistical analysis is used to quantify them.

3.2 Percentage loss of initial preload parameter

3.2.1 Data extraction

An initial loss of preload occurred almost immediately after the shear loading was applied. To assess this preload loss, data needed to be extracted. Matlab v 7.3 plotting tool was used to display the data. Figure 3.2 clearly shows an initial preload loss starting almost immediately after zero cycles. In order to quantify the percentage loss, we zoomed on the graph as shown in Figure 3.3 where two data points were extracted, as displayed with black squares on the plot. The first data point was located at zero cycles before the shear load was applied and the second data point was taken at the first minimum value. All data points are presented in Table 3.1. Note that all zoomed plots for this section are shown in the appendix B.

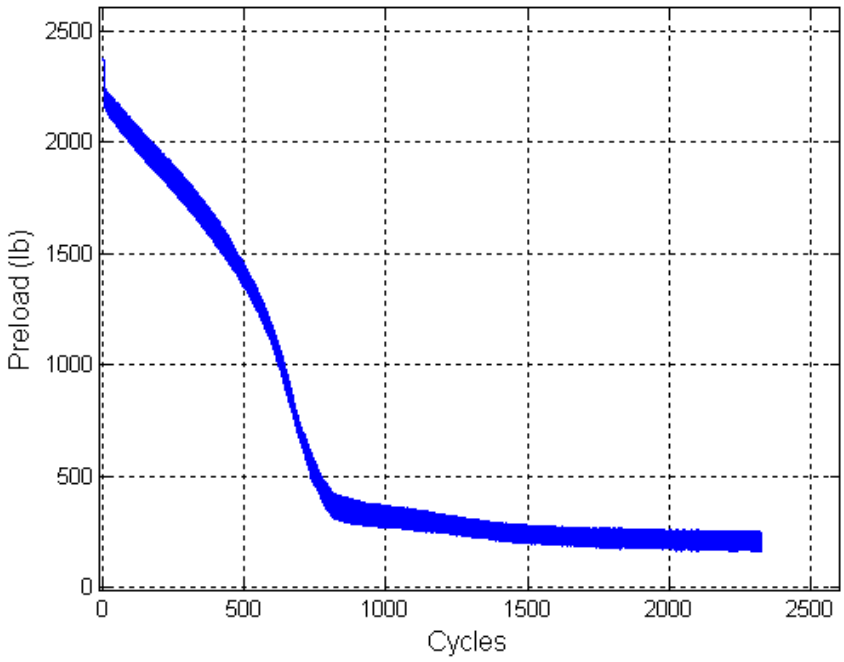

Figure 3.2 Loosening curve for "Locking Heli-Coil with Braycote" run number 18.

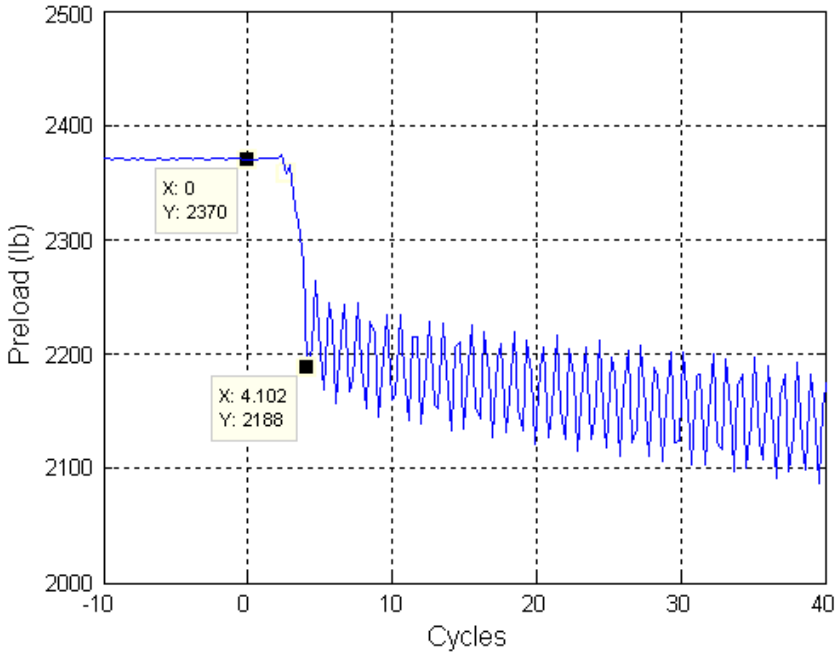

Figure 3.3 Zoomed loosening curve for "Locking Heli-Coil with Braycote" run number 18.

Table 3.1 Data extracted for all locking levels.

Run Number	Initial preload (lb)	Preload after initial drop (lb)	Cycles after initial drop
1	2365	2192	4.4
2	2375	2166	4.1
3	2375	2253	4.4
4	2370	2184	4.4
5	2360	2207	4.4
6	2360	2190	4.1
7	2350	2216	4.1
8	2365	2215	4.4
9	2370	2185	4.4
10	2365	2236	4.1
11	2370	2226	4.4
12	2370	2209	4.4
13	2370	2261	4.4
14	2375	2187	4.4
15	2375	2214	4.1
16	2360	2151	4.4
17	2370	2192	4.4
18	2370	2188	4.1
19	2385	2173	4.4
20	2370	2153	4.4
21	2365	2199	4.4
22	2380	2187	4.4
23	2365	2198	4.4
24	2365	2223	4.1
25	2350	2029	4.4
26	2330	1995	4.4
27	2345	2094	4.1
28	2335	2073	4.4
29	2345	2161	4.1
30	2315	2037	4.4
31	2355	2053	4.1
32	2345	2097	4.4
33	2340	2109	4.4
34	2340	2076	4.1
35	2340	2133	4.1
36	2340	2104	5.3

To extract the percentage loss of initial preload the following equation (3.1) was used:

$$\text{Percentage loss} = \left(\frac{(P_0 - P_r)}{P_0} \right) \cdot 100 \tag{3.1}$$

where P_0 is the initial preload at zero cycles and P_r is the preload after the initial drop. Table 3.2 presents the percentage loss of initial preload for all locking levels along with the statistical mean, median, variance and range.

Table 3.2 Percentage loss of initial preload.

Observations	Std Heli-Coil w/ Braycote	Locking Heli-Coil w/ Braycote	Std Heli-Coil w/ Loctite
1	7.3	4.6	13.7
2	8.8	8.0	14.4
3	5.1	6.8	10.7
4	7.9	8.9	11.2
5	6.5	7.5	7.9
6	7.2	7.7	12.0
7	5.7	8.9	12.8
8	6.3	9.2	10.6
9	7.8	7.0	9.9
10	5.5	8.1	11.3
11	6.1	7.1	8.9
12	6.8	6.0	10.1
Mean	6.7	7.5	11.1
Median	6.6	7.6	11.0
Variance	1.2	1.7	3.6
Range	5.1 - 8.8	4.6 - 9.2	7.9 - 14.4

3.2.2 Statistical analysis

The resulting response data (percentage loss of initial preload) from the 36 test are presented in Table 3.2. There are twelve observations for each locking level. The basic statistic mean, median, variance and range for each sample were included. It can be noted that the means and the medians for "Standard Heli-Coil with Braycote" and "Locking Heli-Coil with Braycote" are congruent whereas "Standard Heli-Coil with Loctite" is different.

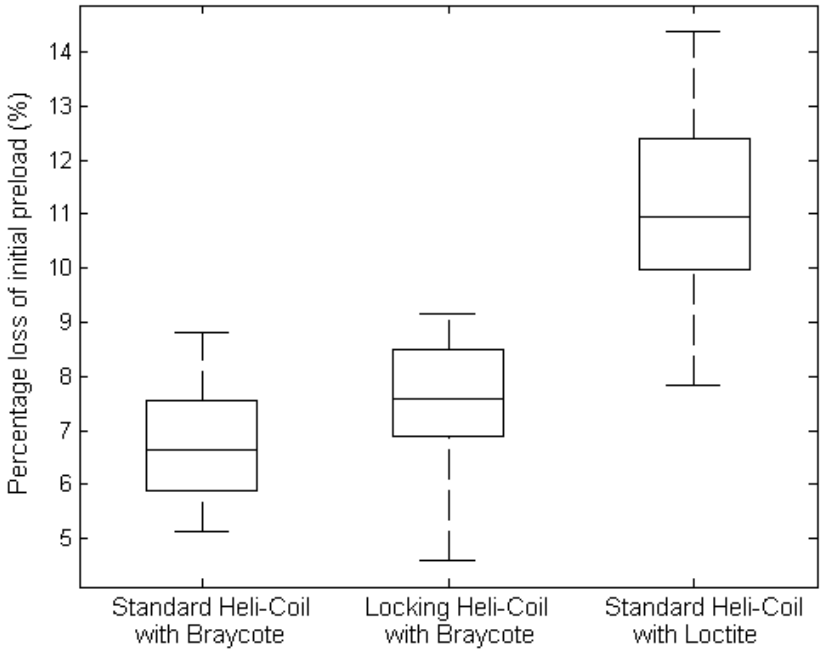

Figure 3.4 Box plot for the percentage loss of initial preload.

Figure 3.4 shows a box plot for the three levels of locking. The sample median, for each treatment, is represented by the center line of the rectangular box. The ends of the rectangles represent the upper and lower quartile of each sample and the black

whiskers extend to indicate their extent. This graphical analysis, suggests that the initial preload loss is dependent on secondary locking features. Furthermore, a statistical analysis is performed to be more objective in this result. The analysis of variance (ANOVA) will compare the means of these levels by measuring the overall variability in the data [20]. However, in order to use ANOVA, the sample population should be normally distributed, and the population sample should have equal variance. However, modest violations of these assumptions can be allowed without affecting the results [20].

In order to asses the dependency of the secondary locking features on the initial preload loss, two hypotheses are developed: 1. All population means are equal ($H_0 : \mu_1 = \mu_2 = \mu_3$), or 2. At least one mean is different. Where μ_1 is "Standard Heli-Coil with Braycote", μ_2 is "Locking Heli-Coil with Braycote" and μ_3 is "Standard Heli-Coil with Loctite". Before any analysis could be performed, the assumption of normality needs to be tested [20].

Plotting the residuals (observation values minus sample mean) on a normal probability plot helps check normality between the sample populations. This is shown in Figure 3.5 where the data points show the empirical probability versus the value for each residual sample for both levels. The solid linear fit shows that the distribution is approximately normal. Note that for this data set, modest variations from normality and equal sample variances are found, yet this is acceptable since the analysis of variance allow minor violations of these assumptions.

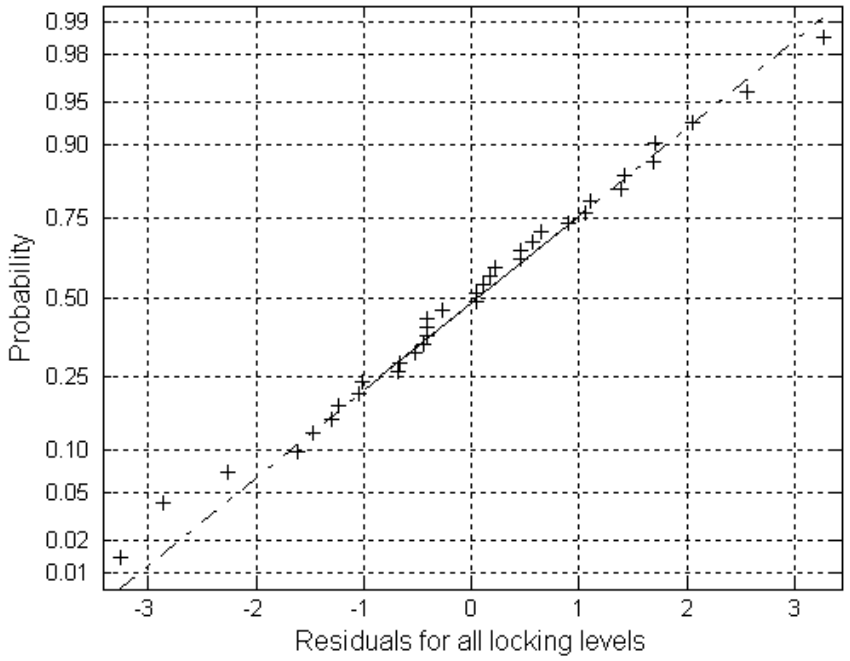

Figure 3.5 Normal probability plot of residuals for the percentage loss of initial preload.

Table 3.3 ANOVA table for the percentage loss of initial preload.

Source of Variation	Sum of Squares	Degrees of Freedom	Mean Square	Fo	P-value	F crit
Between Levels	131.3	2	65.6	30.3	< 0.01	3.3
Error (within levels)	71.6	33	2.2			
Total	202.9	35				

Table (3.3) summarized the ANOVA calculations. Note that the mean square value is larger than the value of the error which suggests that the treatments means may be different. The ratio of the mean square and the error is referred as the testing value or F_0 , (F_0 = 30.3). This value is compared to an appropriate upper-tail percentage point of the F distribution with an alpha error of 0.05. Moreover, the critical value is

$F_{0.05,2,33}$ = 3.3. Since the critical value is less than testing value ($F_0 > F_{0.05,2,33}$), H_0 is rejected. Therefore, there is dependency of initial preload loss due to a secondary locking feature.

Figure 3.6 shows a graphical interpretation of these results where the multcompare function of Matlab v 7.3 was used. The multcompare function displays a graph with each group mean represented by a symbol and an interval around the symbol [21]. The interval is approximated by following formula:

$$\text{int} = \bar{y}_i \pm t_{\alpha,N-a}\sqrt{\frac{MS_e}{2(n-1)}} \tag{3.2}$$

Where $\bar{y}_i$ is the mean of each locking level, $t_{\alpha,N-a}$ is the t-critical value, MS_e is the mean square of the error and n is the number of samples.

Two means are significantly different if their intervals are disjoint, and are not significantly different if their intervals overlap [21]. This figure suggests that the mean for the "Standard Heli-Coil with Loctite" is significantly different when compared with the other two locking levels. Also, the comparison intervals of the "Standard Heli-Coil with Braycote" and the "Locking Heli-Coil with Braycote" overlap which suggests that these means may be statistically similar. To quantify these findings, the Fisher Method of least significant difference (LSD) is be used.

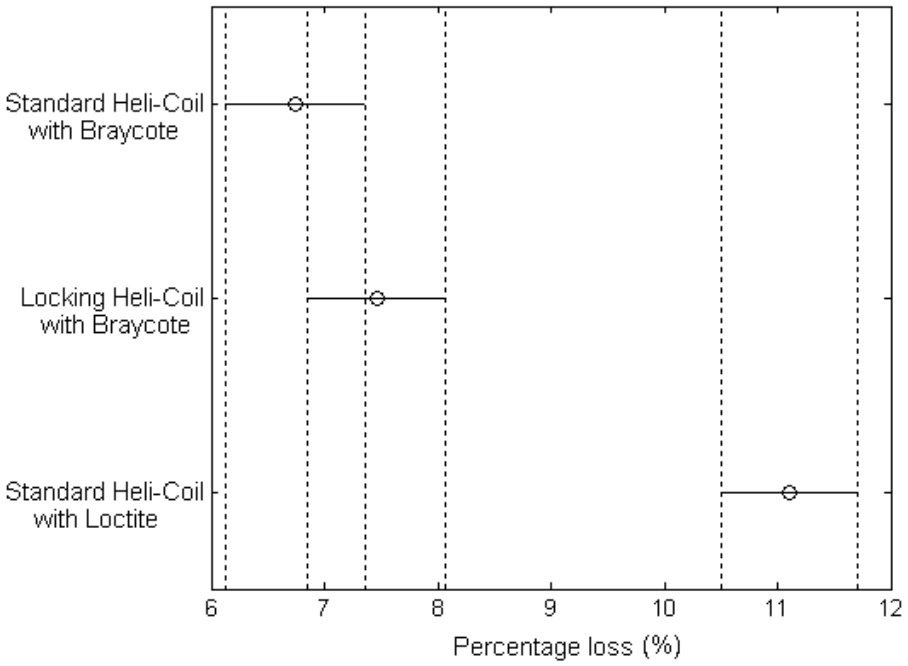

Figure 3.6 Multiple comparisons of means for the percentage loss of initial preload.

The Fisher Method of least significant difference (LSD) is used for comparing all pairs of means where the t-test statistic distribution is used for testing a hypothesis [20]. In order to use this method, a new hypothesis is created: the population means for pairs are equal ($H_0 = \mu_i = \mu_j$). Where μ_i and μ_j are the population means for each locking level.

The pairs of means are considered significantly different if the following condition is met:

$$\left|y_i - y_j\right| \geq t_{\alpha,N-a}\sqrt{\frac{2(MS_E)}{n}} \tag{3.3}$$

where y_i and y_j are the sample means of the locking levels to be compared. $t_{\alpha,N-1}$ is the t-value of the Student's t-distribution as a function of the probability and the degrees

of freedom of the error. MS_E is the mean square of the error. n is the number of samples. Table 3.4 summarizes the results of this analysis.

Table 3.4 LSD method table for the percentage loss of initial preload.

Locking Levels		Sample mean
Standard Heli-Coil with Braycote		A
Locking Heli-Coil with Braycote		B
Standard Heli-Coil with Loctite		C
Comparison		
A - B	A - C	B - C
0.71 < 1.22	4.49 > 1.22	3.78 > 1.22
Not significantly different	Significantly different	Significantly different

Table 3.4 agrees with the ANOVA analysis aforementioned. This time, however, it can be said that the initial drop of preload loss for "Standard Heli-Coil with Braycote" and "Locking Heli-Coil with Braycote" are not significantly different.

Finally, a 95 percent confidence intervals on each locking level mean is computed. Thus, showing that the population mean of each treatment (percent loss of initial preload) will lie between these intervals. This is shown in Table 3.5.

Table 3.5 95 percent confidence intervals for the percentage loss of initial preload.

Population mean
$5.9 \leq \mu_1 \geq 7.6$
$6.6 \leq \mu_2 \geq 8.3$
$10.2 \leq \mu_3 \geq 12.0$

In this section the dependency of initial preload loss parameter on secondary locking features are studied. On this basis, the results in this section reveal the following:

1. Loss of initial preload is dependent on secondary locking features.
2. The mean loss of initial preload of "Standard Heli-Coil with Braycote" and the mean loss of initial preload of "Locking Heli-Coil with Braycote" are not significantly different.
3. The mean loss of initial preload of "Standard Heli-Coil with Braycote" and the mean loss of initial preload of "Standard Heli-Coil with Loctite" are significantly different.
4. The mean loss of initial preload of "Standard Heli-Coil with Loctite" and the mean loss of initial preload of "Locking Heli-Coil with Braycote" are significantly different.

3.3 Initial rate of preload loss parameter

3.3.1 Data extraction

After the initial drop of preload occurs, the bolt begins to loosen following the criteria described by Pai and Hess [3, 4] where the loosening in the fastener is due to the accumulation of localized slip at the contact surfaces denoted, in this thesis, as the initial rate of preload loss.

To quantify the initial rate of preload loss, each preload versus cycles plot was zoomed in as shown in Figure 3.8 (all zoomed plots for this section are shown in appendix C). Then, two data points were extracted, shown with a square, along a tangent line that was manually fitted at the lower bound of the envelope graph (this location was

chosen to provide a worse-case scenario of loosening). The data extracted is documented in tables (A.1), (A.2) and (A.3) in appendix A. With the set of two data point the initial rate of preload loss was calculated using the following formula [22]:

$$m = \frac{\Delta y}{\Delta x} \tag{3.4}$$

Where m is the initial rate of preload loss, Δy is the change in the y coordinate or preload and Δx is the change in the x coordinate or cycles. These values are documented in Table 3.6. Note that the equation above will result in a negative number which implies a loss.

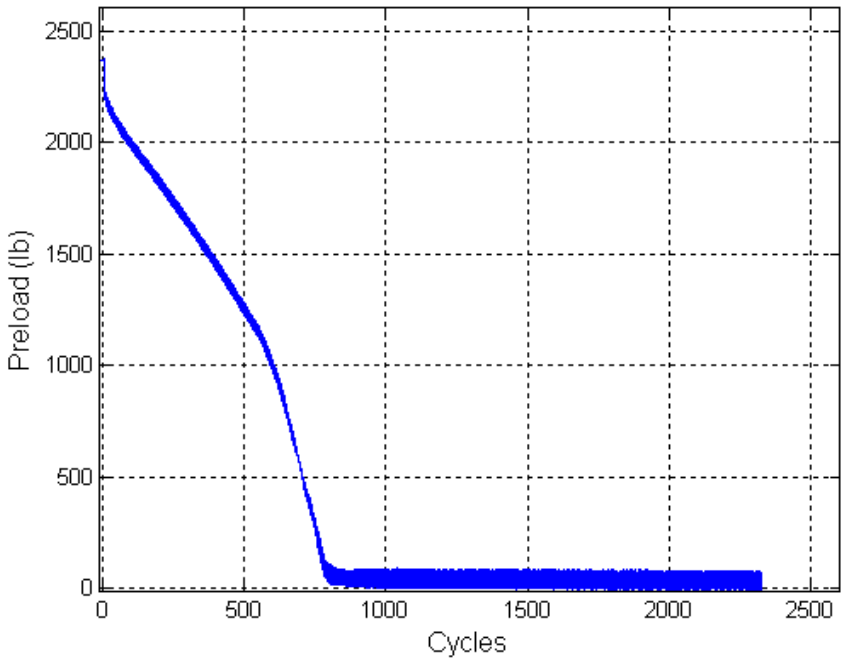

Figure 3.7 Loosening curve for "Standard Heli-Coil with Braycote" run number 11.

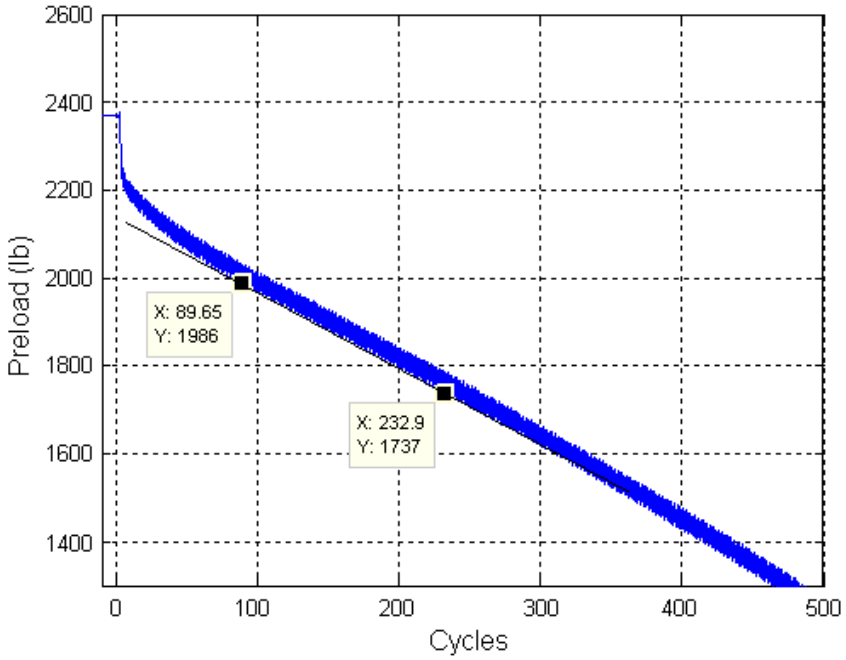

Figure 3.8 Zoomed loosening curve for "Standard Heli-Coil with Braycote" run number 11.

Table 3.6 Initial rate of preload loss for all locking levels (lb/cycle).

Observations	Std Heli-Coil w/ Braycote	Locking Heli-coil w/ Braycote	Std Heli-Coil w/Loctite
1	1.4	1.3	0.7
2	2.1	2.2	0.7
3	1.7	1.5	0.2
4	1.7	1.2	0.3
5	1.0	1.1	0.1
6	1.0	1.5	0.2
7	2.8	1.5	0.8
8	1.4	1.8	0.1
9	2.2	1.9	0.1
10	1.7	1.3	0.9
11	1.7	1.3	0.3
12	2.0	1.6	0.6
Mean	1.7	1.5	0.4
Median	1.7	1.5	0.3
Variance	0.3	0.1	0.1
Range	1.0 to 2.8	1.1 to 2.2	0.1 to 0.9

The tangent lines are then calculated using the point-slope formula [22] shown as:

$$y = m(x - x_0) + y_0 \tag{3.5}$$

Where y is the unknown preload, x is the unknown cycles, m is the initial rate of preload loss and (x_0, y_0) are coordinates of a point of the line (data points). The tangent lines are plotted in Figure 3.9, 3.10 and 3.11 for "Standard Heli-Coil with Braycote", "Locking Heli-Coil with Braycote" and "Standard Heli-Coil with Loctite" respectively.

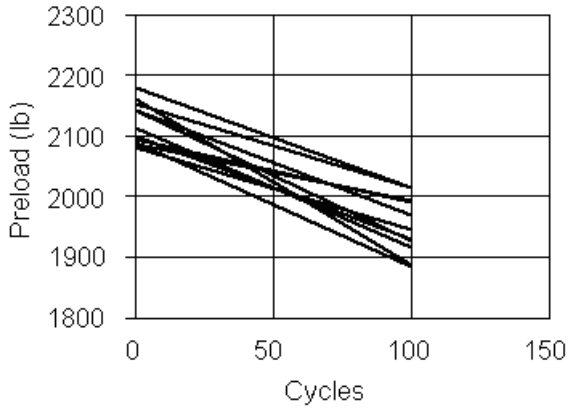

Figure 3.9 Composite tangent lines for "Standard Heli-Coil with Braycote".

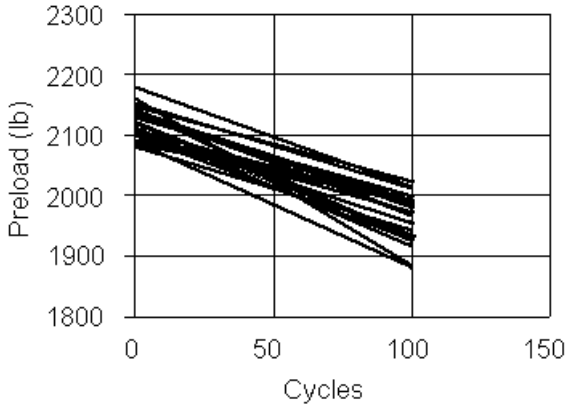

Figure 3.10 Composite tangent lines for "Locking Heli-Coil with Braycote".

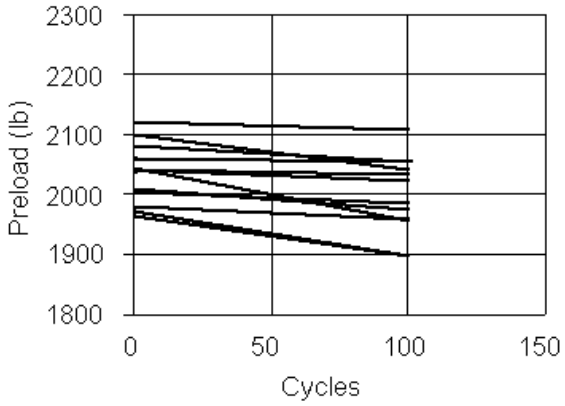

Figure 3.11 Composite tangent lines for "Standard Heli-Coil with Loctite".

It can be noted that the lines in Figure 3.9 and 3.10 appear similar whereas the lines in Figure 3.11 looked different which lead us to suspect dependencies of secondary locking features in the initial rate of preload loss. Thus, statistical tools are used to quantify any dependency.

3.3.2 Statistical analysis

The initial rates of preload loss from the 36 runs are presented in Table 3.6. There are twelve observations for each locking levels. The statistical sample mean, median, variance and range are included for the sample. There are similarities in the means of "Standard Heli-Coil with Braycote" and "Locking Heli-Coil with Braycote" while the mean of the "Standard Heli-Coil with Loctite" is different.

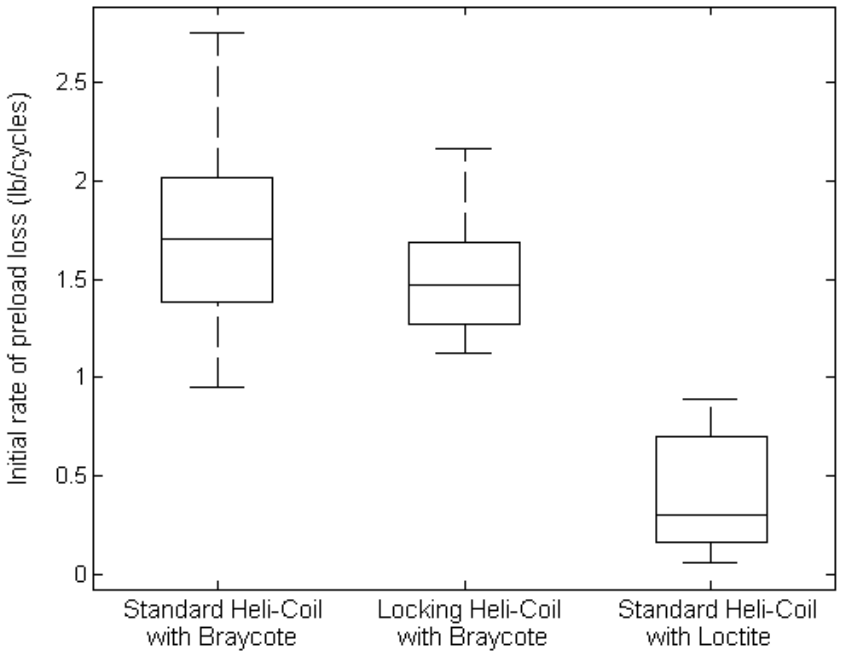

Figure 3.12 Box plot for the initial rate of preload loss.

Figure 3.12 shows a box plot for the three levels of locking. The sample median is represented by the center line of the rectangular box for each locking level. The ends of the rectangles represent the upper and lower quartile and the black whiskers extend to indicate the extent of the sample. This graphical analysis suggests, as expected, that the initial mean rate of preload loss decreases with the use of a secondary locking feature. An additional statistical analysis is performed on the groups to better quantify any difference in means. Principally, since there is variation in the observations for these two levels samples, the analysis of variance (ANOVA) compares the means of these levels by measuring the overall variability in the data [20]. In order to use ANOVA, the sample population should be normally distributed and the population sample should have equal variance, yet modest departures from these assumptions will not significantly alter the results [20].

In order to determine the dependency of the secondary locking feature on the initial rate of preload loss, two hypotheses are created: 1. All population means are equal ($H_0: \mu_1 = \mu_2 = \mu_3$), 2. At least one mean is different, where μ_1 is "Standard Heli-Coil with Braycote", μ_2 is "Locking Heli-Coil with Braycote" and μ_3 is "Standard Heli-Coil with Loctite". Before any analysis could be performed, the assumption of normality needed to be ensured.

Plotting the residuals (observation values minus sample mean) on a normal probability plot helps check normality between the sample populations. This is shown in Figure 3.13 where the data points show the empirical probability versus the value for each residual sample for both levels. The solid linear fit shows that the distribution is approximately normal. Note that for this data set, modest variations from normality and equal sample variances are found, yet this is acceptable since the analysis of variance allow minor violations of these assumptions [20].

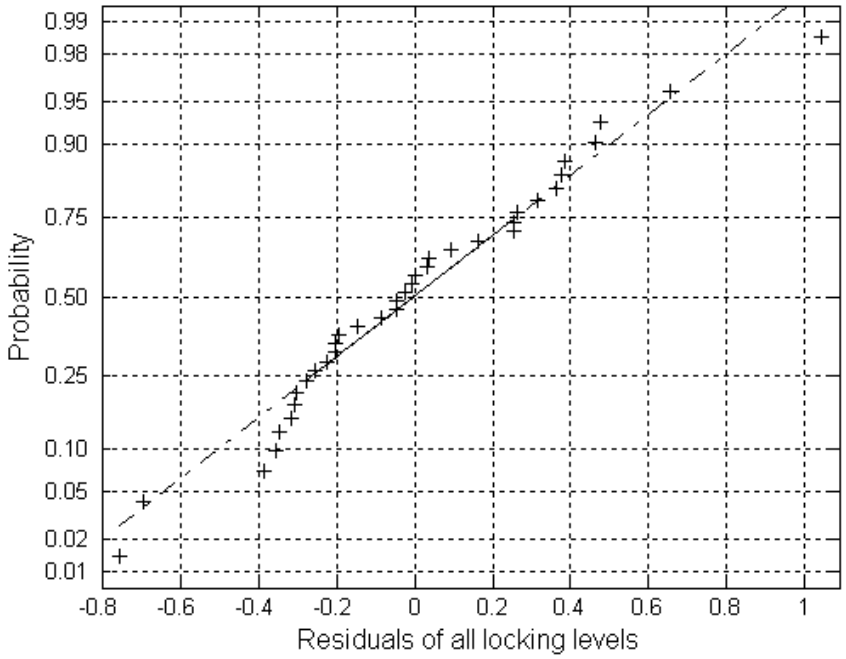

Figure 3.13 Normal probability plot of residuals for the initial rate of preload loss.

Table 3.7 ANOVA table for the initial rate of preload loss.

Source of Variation	Sum of Squares	Degrees of Freedom	Mean Square	Fo	P-value	F crit
Between Levels	11.6	2	5.8	39.8	< 0.01	3.3
Error (within levels)	4.8	33	0.1			
Total	16.4	35				

Table 3.7 summarized the ANOVA calculations. Note that the mean square value is larger than the value of the error which suggests that the treatments means may be different. The ratio of the mean square and the error is referred as the testing value or F_0 (F_0 = 44.4). This value is compared to an appropriate upper-tail percentage point of the F distribution with an alpha error of 0.05. Moreover, the critical value is $F_{0.05,2,33}$ = 3.3.

Since the critical value is less than testing value ($F_0 > F_{0.05,2,33}$), H_0 is rejected. Therefore, at least one mean is different which implies that there is a dependency on the initial preload loss due to a secondary locking feature.

Figure 3.14 shows a graphical interpretation of these results where the multcompare function of Matlab v 7.3 was used. The multcompare function displays a graph with each group mean represented by a symbol and an interval around the symbol [21]. The interval is approximated by the following formula:

$$\text{int} = \bar{y}_i \pm t_{\alpha,N-a}\sqrt{\frac{MS_e}{2(n-1)}} \tag{3.6}$$

Where $\bar{y}_i$ is the mean of each locking level, $t_{\alpha,N-a}$ is the t-critical value, MS_e is the mean square of the error and n is the number of samples.

Two means are significantly different if their intervals are disjoint, and are not significantly different if their intervals overlap [21]. This figure suggests that the mean for the "Standard Heli-Coil with Loctite" is significantly different when compared with the other two locking levels. Also, the comparison intervals of the "Standard Heli-Coil with Braycote" and the "Locking Heli-Coil with Braycote" overlap which suggests that these means may be statistically similar. To quantify these findings, the Fisher Method of least significant difference (LSD) is used.

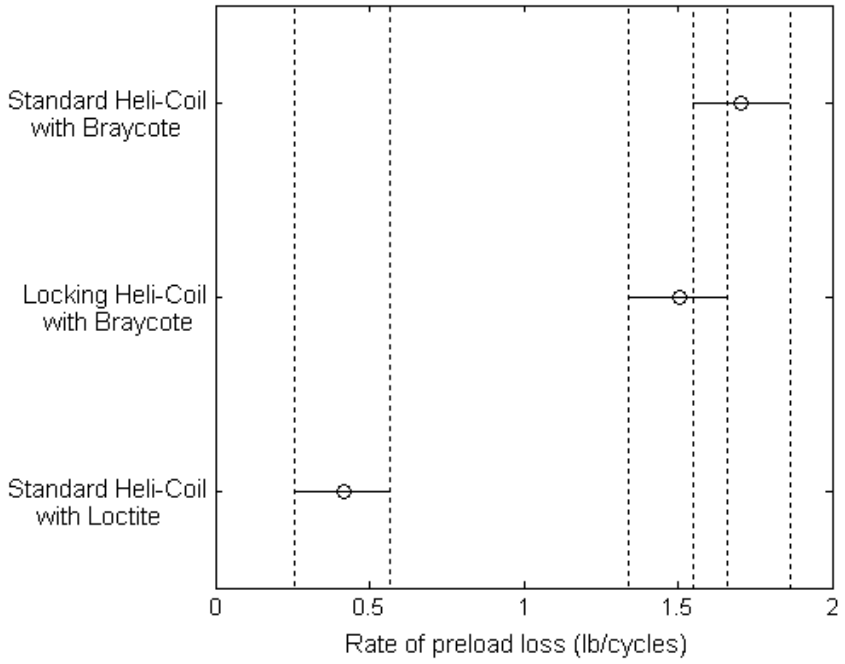

Figure 3.14 Multiple comparisons of means for the initial rate of preload loss.

The Fisher Method of least significant difference (LSD) is used for comparing all pairs of means where the student's t distribution is used for testing a hypothesis [20]. Therefore, in order to use this method, a new hypothesis is created: the population means for pairs are equal ($H_0 = \mu_i = \mu_j$). Where μ_i and μ_j are the population means for each locking level. The pairs of means will be considered significantly different if the following condition [20] is met:

$$\left|y_i - y_j\right| \geq t_{\alpha/2,N-a}\sqrt{\frac{2(MS_E)}{n}} \tag{3.7}$$

Where y_i and y_j are the sample means of the treatments to be compared. $t_{\alpha,N-1}$ is the t-value of the Student's t-distribution as a function of the probability and the degrees of

freedom of the error. MS_E is the mean square value of the error and n is the number of samples. Table 3.8 summarizes the results of this analysis.

Table 3.8 LSD method table for the initial rate of preload loss.

Locking Levels		Sample mean
Standard Heli-Coil with Braycote		A
Locking Heli-Coil with Braycote		B
Standard Heli-Coil with Loctite		C
Comparison		
A-B	A-C	B-C
0.2 < 0.3	1.4 > 0.3	1.1 > 0.3
Not significantly different	Significantly different	Significantly different

Table 3.8 agrees with the analysis of variance where there is a dependency of secondary locking feature on the initial rate of preload loss. However, statistically, it can be said that the initial drop of preload loss for "Standard Heli-Coil with Braycote" and "Locking Heli-Coil with Braycote" are not significantly different.

Lastly, a 95 percent confidence interval on each locking level mean is computed. Thus, showing that the population mean of each treatment (initial rate of preload loss) will lie between these intervals. This is shown in Table 3.9.

Table 3.9 95 percent confidence intervals for the initial rate of preload loss.

Population mean
$1.5 \leq \mu_1 \geq 1.9$
$1.3 \leq \mu_2 \geq 1.7$
$0.2 \leq \mu_3 \geq 0.6$

In this section, the parameter of the initial rate of preload loss with secondary locking features was analyzed. The low rate values mean less loosening. On this basis, the results in this section reveal the following:

1. Initial rate of preload loss is dependent on secondary locking features.
2. The initial mean rate of preload loss of "Standard Heli-Coil with Braycote" and the initial mean rate of preload loss of "Locking Heli-Coil with Braycote" are not significantly different.
3. The initial mean rate of preload loss of "Standard Heli-Coil with Braycote" and the initial mean rate of preload loss of "Standard Heli-Coil with Loctite" are significantly different.
4. The initial mean rate of preload loss of "Standard Heli-Coil with Loctite" and the initial mean rate of preload loss of "Locking Heli-Coil with Braycote" are significantly different.

3.4 Secondary rate of preload loss parameter

3.4.1 Data extraction

After the initial rate of preload loss, the bolt undergoes the loosening criteria described by Junker, Pai and Hess [1, 3, 4] where the loosening in the fastener is due to complete slip at the contact surfaces. In this thesis, this is referred to as the secondary rate of preload loss. This parameter was only extracted to "Standard Heli-Coil with Braycote" and "Locking Heli-Coil with Braycote" as a mean to quantify any difference between

them. Note that "Standard Heli-Coil with Loctite" did not exhibit this loosening parameter and is therefore not included in this section.

To quantify the secondary rate of preload loss, each preload versus cycles plot was zoomed in as shown in Figure 3.16 (all zoomed plots are shown in appendix D). Then, two data points were extracted, shown with a square, along a tangent line that was manually fitted at the lower bound of the envelope graph (this location was chosen to provide a worse-case scenario of loosening). The data extracted is documented in Table A.7 in appendix A. With the set of two data points the secondary rate of preload loss was calculated using the following formula [22].

$$m = \frac{\Delta y}{\Delta x} \tag{3.8}$$

Where m is the secondary rate of preload loss, Δy is the change in the y coordinate or preload and Δx is the change in the x coordinate or cycles. These values are documented in table 3.10. The equation above will result in a negative number which implies a loss.

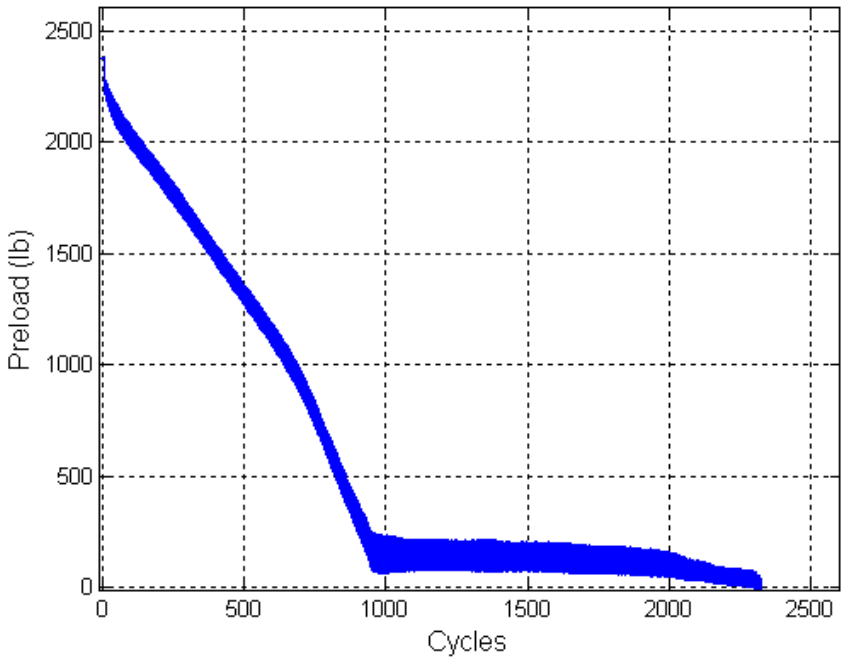

Figure 3.15 Loosening curve for "Standard Heli-Coil with Braycote" run number 3.

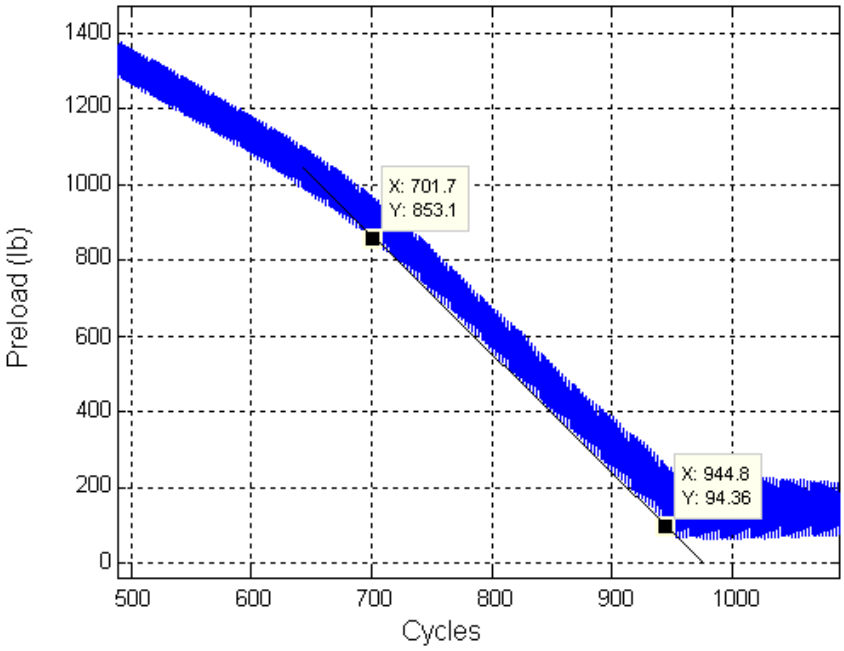

Figure 3.16 Zoomed loosening curve for "Standard Heli-Coil with Braycote" run number 3.

Table 3.10 Secondary rate of preload loss for all locking levels (lb/cycle).

Observations	Std Heli-Coil w/ Braycote	Locking Heli-Coil w/ Braycote
1	8.7	2.0
2	6.7	4.9
3	3.1	2.0
4	10.8	1.8
5	6.3	1.6
6	5.7	4.3
7	11.0	1.8
8	8.1	0.4
9	8.7	4.4
10	7.1	2.4
11	5.4	1.6
12	7.5	3.6
Mean	7.4	2.6
Median	7.3	2.0
Variance	5.1	1.9
Range	3.1 - 11.0	0.4 - 4.9

The tangent lines are then calculated using the point-slope formula [22] shown as

$$y = m(x - x_0) + y_0 \tag{3.9}$$

Where y is the unknown preload, x is the unknown cycles, m is the secondary rate of preload loss and (x_0, y_0) are coordinates of a point of the line (data points). Table 3.10 shows a difference in the mean rate for each locking level. Thus, as it was expected, the "Standard Heli-Coil with Braycote" loosens more rapidly than the "Locking Heli-Coil with Braycote". A statistical analysis will determine any dependencies of the secondary locking feature in the "Locking Heli-Coil with Braycote".

3.4.2 Statistical analysis

The Secondary rates of preload loss from the 24 runs are presented in Table 3.10. There are twelve observations for each locking levels. The statistical sample mean, median, variance and range are included for the sample. There are differences in the means of "Standard Heli-Coil with Braycote" and "Locking Heli-Coil with Braycote".

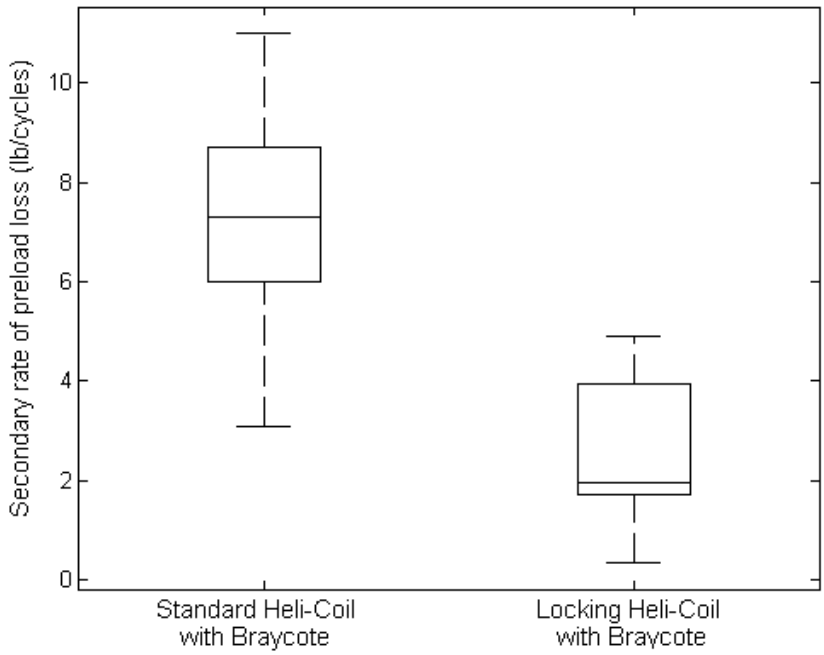

Figure 3.17 Box plot for the secondary rate of preload loss.

Figure 3.17 shows a box plot for the three levels of locking. The sample median is represented by the center line of the rectangular box for each locking level. The ends of the rectangles represent the upper and lower quartile and the black whiskers extend to indicate the extent of the sample. This graphical analysis suggests, as expected, that the secondary mean rate of preload loss decreases with the use of a secondary locking feature.

An additional statistical analysis is performed on the groups to better quantify any difference in means. Principally, since there is variation in the observations for these two levels samples, the analysis of variance (ANOVA) will compare the means of these levels by measuring the overall variability in the data [20]. In order to use ANOVA, the sample population should be normally distributed and the population sample should have equal variance, yet modest departures from these assumptions will not significantly alter the results [20].

In order to determine the dependency of the secondary locking feature on the secondary rate of preload loss, two hypotheses are created: 1. All population means are equal ($H_0 : \mu_1 = \mu_2$), 2. The means are different ($H_1 : \mu_1 \neq \mu_2$), where μ_1 is "Standard Heli-Coil with Braycote" and μ_2 is "Locking Heli-Coil with Braycote". Before any analysis could be performed, the assumption of normality needed to be ensured.

Plotting the residuals (observation values minus sample mean) on a normal probability plot helps check normality between the sample populations. This is shown in Figure 3.18 where the data points show the empirical probability versus the value for each residual sample for both levels. The solid linear fit shows that the distribution is approximately normal. Note that for this data set, modest variations from normality and equal sample variances are found, yet this is acceptable since the analysis of variance allow minor violations of these assumptions [20].

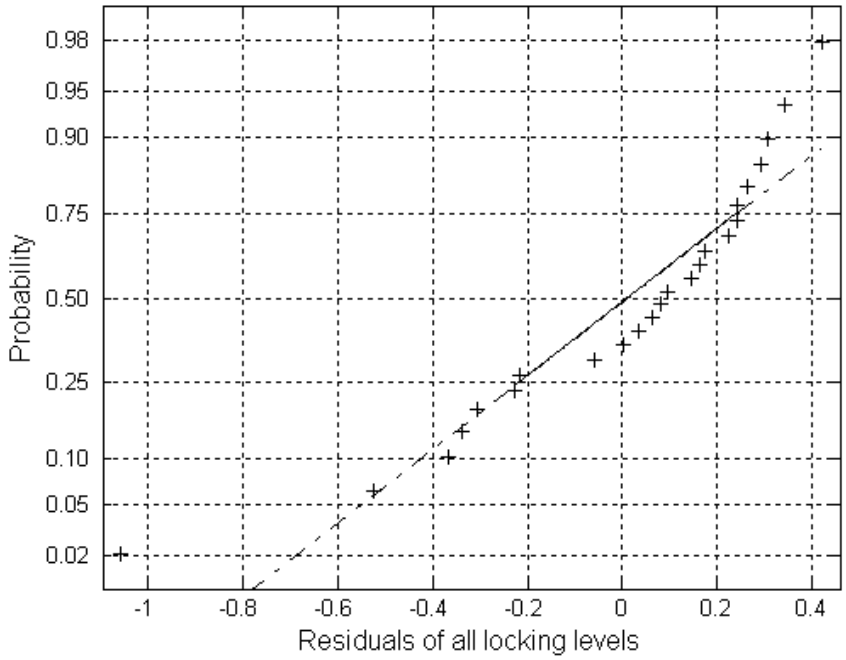

Figure 3.18 Normal probability plot for the secondary rate of preload loss.

Table 3.11 ANOVA table for the secondary rate of preload loss.

Source of Variation	Sum of Squares	Degrees of Freedom	Mean Square	Fo	P-value	F crit
Between Levels	141.9	1	141.9	40.6	< 0.01	4.3
Error (within levels)	76.9	22	3.5			
Total	218.8	23				

Table 3.11 summarized the ANOVA calculations. Note that the mean square value is larger than the value of the error which suggests that the treatments means may be different. The ratio of the mean square and the error is referred as the testing value or F_0 (F_0 = 40.6). This value is compared to an appropriate upper-tail percentage point of the F distribution with an alpha error of 0.05. Moreover, the critical value is $F_{0.05,1,22}$ = 4.3. Since the critical value is less than testing value ($F_0 > F_{0.05,1,22}$),

H_0 is rejected. Therefore, the means are different which implies that there is a dependency on the initial preload loss due to a secondary locking feature.

Figure 3.19 shows a graphical interpretation of these results where the multcompare function of Matlab v 7.3 was used. The multcompare function displays a graph with each group mean represented by a symbol and an interval around the symbol [21]. The interval is approximated by following formula:

$$\text{int} = \bar{y}_i \pm t_{\alpha,N-a}\sqrt{\frac{MS_e}{2(n-1)}} \tag{3.10}$$

Where $\bar{y}_i$ is the mean of each locking level, $t_{\alpha,N-a}$ is the t-critical value, MS_e is the mean square of the error and n is the number of samples.

Two means are significantly different if their intervals are disjoint, and are not significantly different if their intervals overlap [21]. This figure suggests that the mean for the "Standard Heli-Coil with Braycote" is significantly different when compared with the "Locking Heli-Coil with Braycote".

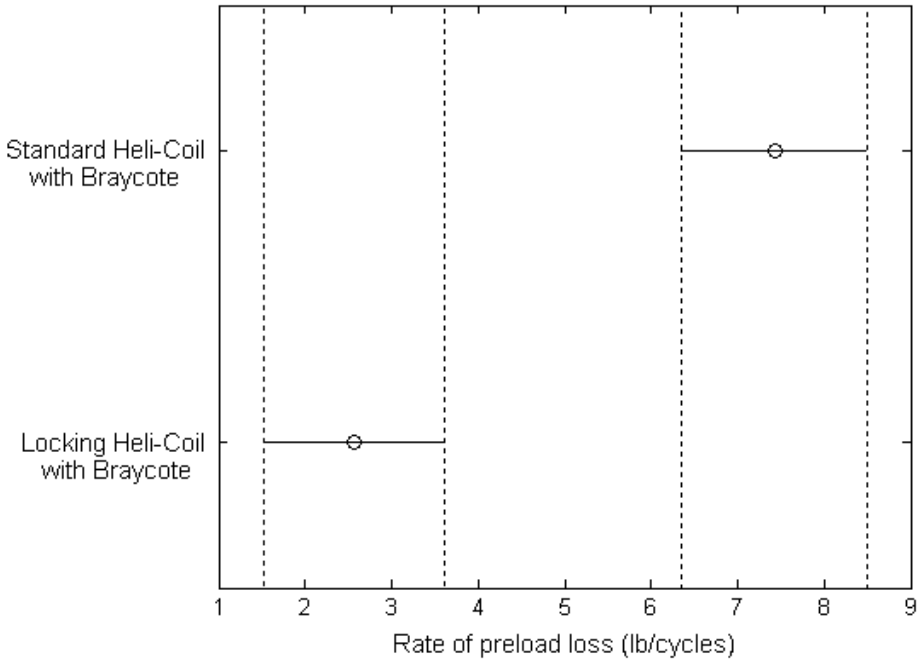

Figure 3.19 Multiple comparisons of means for the secondary rate of preload loss.

Lastly, a 95 percent confidence interval on each locking level mean is computed. Thus, showing that the population mean of each treatment (secondary rate of preload loss) will lie between these intervals. This is shown in Table 3.12.

Table 3.12 95 percent confidence intervals for the secondary rate of preload loss.

Population mean
$6.2 \leq \mu_1 \geq 8.7$
$1.3 \leq \mu_2 \geq 3.8$

In this section, the dependency of secondary rate of preload loss parameter on secondary locking features was analyzed. “Standard Heli-Coil with Loctite” did not exhibit this parameter and therefore is not included in this analysis. The Low rate values

mean more resistance to loosening. On this basis, the results in this section reveal the following:

1. Secondary rate of preload loss is dependent on secondary locking features.
2. The secondary mean rate of preload loss of "Standard Heli-Coil with Braycote" and the secondary mean rate of preload loss of "Locking Heli-Coil with Braycote" are significantly different.

3.5 Steady-state value parameter

3.5.1 Data extraction

The effect of prevailing torque on preload loss is to self-lock the fastener by generating frictional resistance to rotation between engaged treads [11] the Screwlock feature found in the Locking Heli-Coil consists of a grip coil that when it is bent outwards creates high pressures on the bolt [14]. Therefore, the prevailing torque counteracts the loosening torque reducing and can even stopping preload loss [11].

Anaerobic thread lockers are design to reduce loosening due to vibration by filling the gaps between the engaged threads. When the thread locker dries, it becomes a hard polymer [15]. Therefore, it increases the friction forces that opposes to the loosening moments. The purpose of this section is to quantify the steady-state value, which consists of a value such that preload is constant because loosening due to transverse vibration has stopped, resulting the use of the secondary locking feature found in the Locking Heli-Coil as well as the secondary locking feature created by the Loctite Threadlocker®.

To quantify a steady-state condition, data needed to be extracted. Figure 3.20 is a representative example of a steady-state condition reached after 1000 cycles. In order to

extract the data, we zoomed into the graph as shown in Figure 3.21 where two data points, shown with the squares, were extracted along a horizontal line fitted into the lower bound of the envelope graph where signs of a steady-state characteristic were present. Note that all the zoomed graphs are presented in the appendix E. The data was documented in table 3.13.

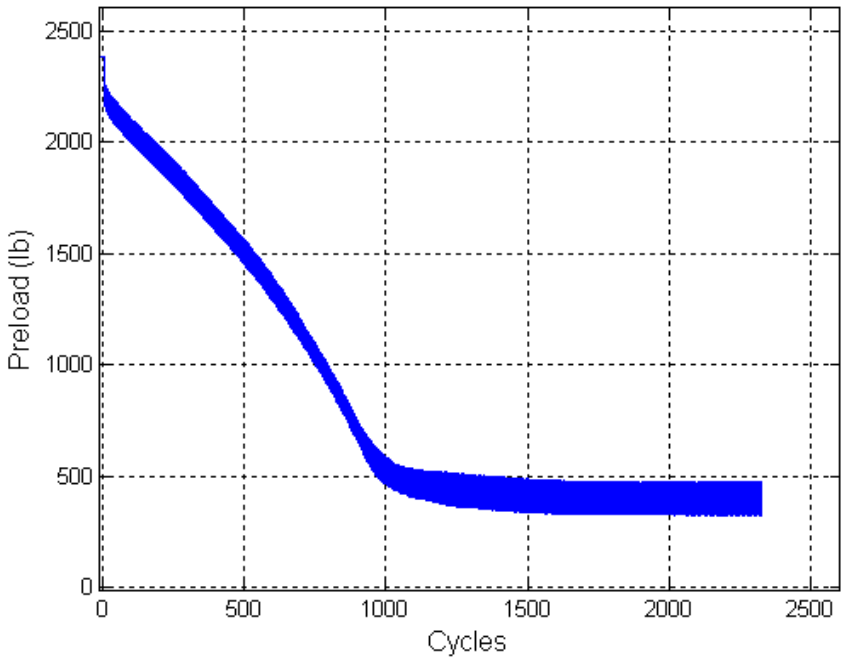

Figure 3.20 Loosening curve for "Locking Heli-Coil with Braycote" run number 22.

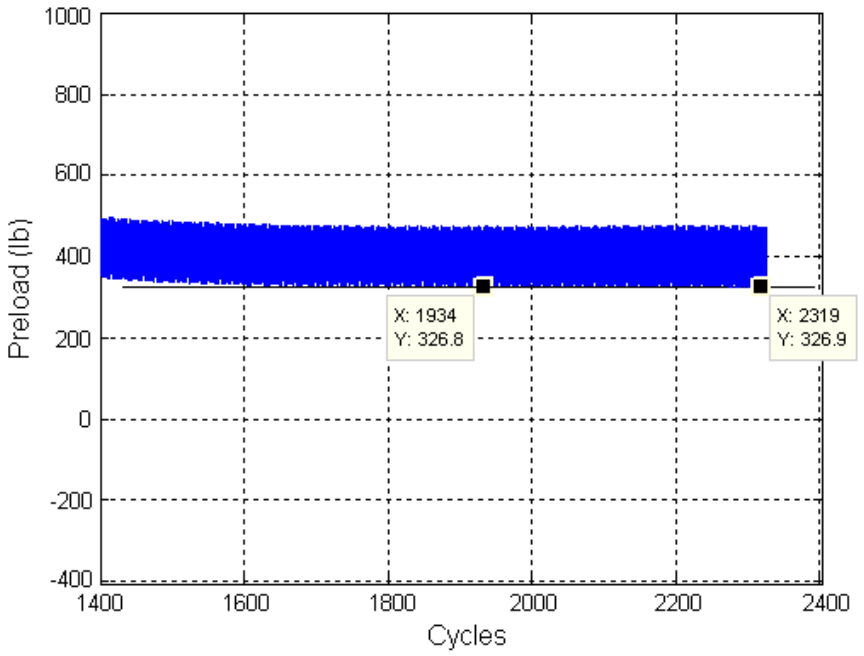

Figure 3.21 Zoomed loosening curve for "Locking Heli-Coil with Braycote" run number 22.

Table 3.13 Steady-state values for all locking levels (lb), (nr: never reached).

Observations	Std Heli-Coil w/ Braycote	Locking Heli-Coil w/ Braycote	Std Heli-Coil w/ Loctite
1	0.0	118	nr
2	0.0	21	253
3	0.0	248	nr
4	0.0	nr	nr
5	0.0	237	nr
6	0.0	163	nr
7	0.0	141	nr
8	0.0	nr	1989
9	0.0	110	nr
10	0.0	325	nr
11	0.0	417	nr
12	0.0	44	nr
Mean	0.0	182	1121
Median	0.0	152.0	1121.0
Variance	0.0	15482	1506848
Range	0.0	21 to 417	253 to 1989

Table 3.13 shows that "Locking Heli-Coil with Braycote" reaches steady-state more often than "Standard Heli-Coil with Loctite" and since there was complete loosening on the bolt for "Standard Heli-Coil with Braycote", the value is represented by a zero. Figures 3.22 and 3.23 portray all the steady-state values for all locking levels.

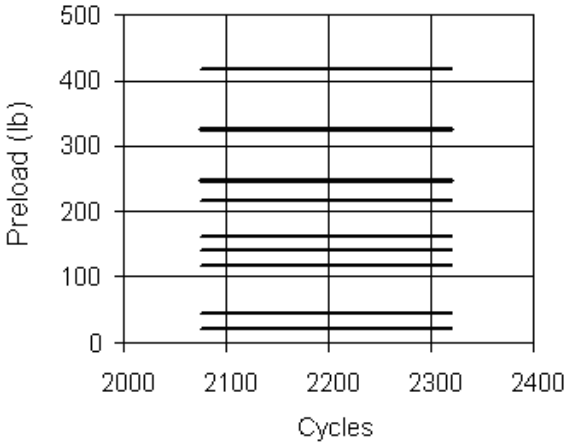

Figure 3.22 All steady-state value plots for "Locking Heli-Coil with Braycote".

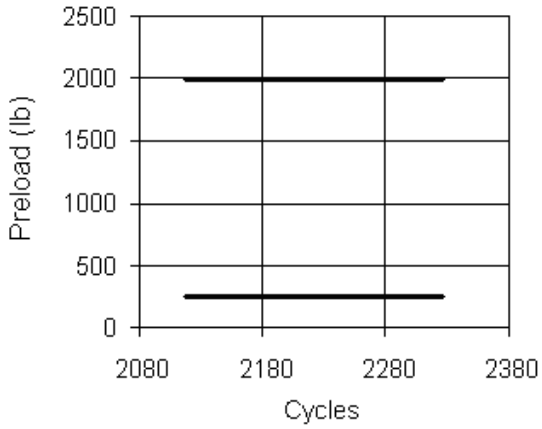

Figure 3.23 All steady-state value plots for "Locking Heli-Coil with Loctite".

3.5.2 Statistical analysis

Note that a statistical comparative analysis can not be performed on the steady-state parameter since the population's sample size was not consistent between any locking levels and the variance between the groups a significantly different. However, since "Standard Heli-Coil with Braycote" always lost its entire preload, it is strongly suspected that the steady-state parameter is dependent on secondary locking features.

Based on the data and the figures aforementioned in this section, it can be concluded that:

1. "Standard Heli-Coil with Braycote" loosened completely.
2. 83.3% of "Locking Heli-Coil with Braycote" reached steady-state.
3. 16.7% of "Standard Heli-Coil with Loctite" reached steady-state.
4. The steady-state condition is dependent on the secondary locking feature.
5. There is not enough data to perform a statistical analysis comparing all locking levels.

3.6 Final preload value parameter

3.6.1 Data extraction

Since a comparative statistical analysis was not performed on the steady-state value, the final preload value was extracted in order to asses not only any loosening dependency due to secondary locking features, but also to quantify the secondary locking feature with the best locking performance. Note that the comparative assessment is only on the final preload value of the "Standard Heli-Coil with Loctite" against the final preload values reached by the "Locking Heli-Coil with Braycote".

"Standard Heli-Coil with Braycote" will not be considered in this assessment since it has already been determined that there was complete loosening and it was denoted by the number zero. Hence, the only meaningful statistical representation "Standard Heli-Coil with Braycote" has for this section is to state that there exists a dependency on secondary locking features in resisting preload loss.

To quantify the final preload value, data needed to be extracted. The data was extracted by zooming into the figure and the final recorded value was extracted shown with the square. Figure 3.25 shows a representative example of a final preload value extracted for "Standard Heli-Coil with Braycote". Note that all the zoomed graphs are presented in the appendix E. The data was documented in Table 3.14.

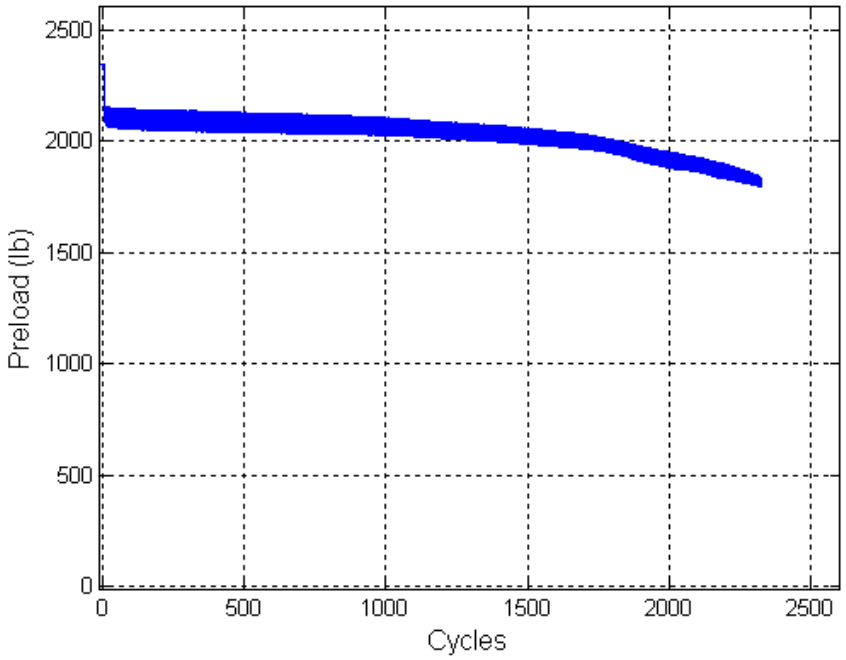

Figure 3.24 Loosening curve for "Standard Heli-Coil with Loctite" run number 33.

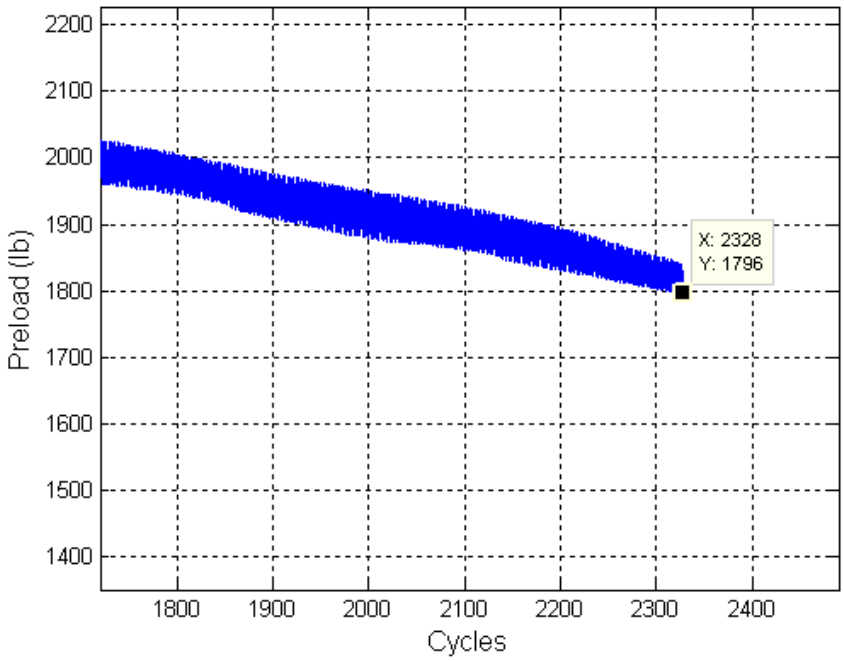

Figure 3.25 Zoomed loosening curve for "Standard Heli-Coil with Loctite" run number 33.

Table 3.14 Final preload values for all locking levels (lb), (** bolt broke).

Observations	Std Heli-Coil w/ Braycote	Locking Heli-Coil w/ Braycote	Std Heli-Coil w/ Loctite
1	0.0	118	205
2	0.0	21	253
3	0.0	248	1814
4	0.0	217	1422
5	0.0	237	**
6	0.0	163	1759
7	0.0	141	1840
8	0.0	1135	1989
9	0.0	110	1795
10	0.0	325	448
11	0.0	417	1680
12	0.0	44	1819
Mean	0.0	265	1366
Median	0.0	190.0	1121.0
Variance	0.0	87888	489020
Range	0.0	21 to 417	253 to 1989

Table 3.14 shows a mean of "Standard Heli-Coil with Loctite" to be higher than the "Locking Heli-Coil with Braycote"; suggesting that Loctite Threadlocker is a better secondary locking feature in resisting bolt loosening. Note that run number 29 broke and there is not a final preload value recorded for this plot. Note that for "Standard Heli-Coil with Braycote" complete loosening of the bolt occurred at this stage represented in the table with a zero.

3.6.2 Statistical analysis

The final preload values from the 36 runs are presented in Table 3.14. There are twelve observations for each locking levels. The statistical sample mean, median, variance and range are included for the sample. Note that since "Standard Heli-Coil with Braycote" loosened completely, it will not be considered for this statistical analysis. However, based on Table 3.14, it can be concluded that there is a significant dependency of secondary locking feature in resisting loosening since neither "Locking Heli-Coil with Braycote" or "Standard Heli-Coil with Loctite" lost its entire preload at this stage. Nonetheless, there is one question that prevails. Which of the secondary locking features is best? To answer this question a statistical analysis will be perform on the final preload values.

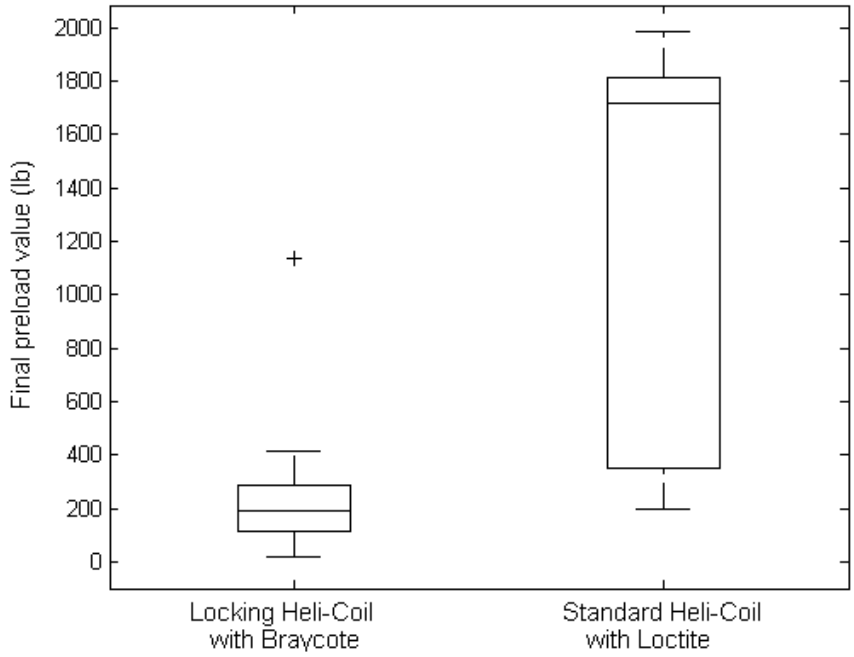

Figure 3.26 Box plot for the final preload value.

Figure 3.26 shows a box plot for "Locking Heli-Coil with Braycote" and "Standard Heli-Coil with Loctite". The sample median is represented by the center line of the rectangular box for each locking level. The ends of the rectangles represent the upper and lower quartile and the black whiskers extend to indicate the extent of the sample. This graphical analysis suggests that with the use of Loctite preload is maintained at higher values. However, the variability of these values is quite high.

An additional statistical analysis is performed on the groups to better quantify any difference in means. The t-test statistic will compare the means of these levels even though the variances and the sample size are not equal. In order to use t-test statistic, the sample population should be normally distributed, yet modest departures from these assumptions will not significantly alter the results [20].

In order to determine the best locking performance of the secondary locking feature on the final preload value, two hypotheses are created: 1. All population means are equal ($H_0 : \mu_1 = \mu_2$). 2. The means are different ($H_1 : \mu_1 \leq \mu_2$), where μ_1 is "Locking Heli-Coil with Braycote" and μ_2 is "Standard Heli-Coil with Loctite". Before any analysis could be performed, the assumption of normality needed to be ensured.

Plotting the residuals (observation values minus sample mean) on a normal probability plot helps check normality between the sample populations. This is shown in Figure 3.27 where the data points show the empirical probability versus the value for each residual sample for both levels. The solid linear fit shows that the distribution is approximately normal. Note that for this data set, variations from normality are found, but they are at the end points. Nonetheless, this is acceptable since the t-test statistic allows minor violations of these assumptions [20].

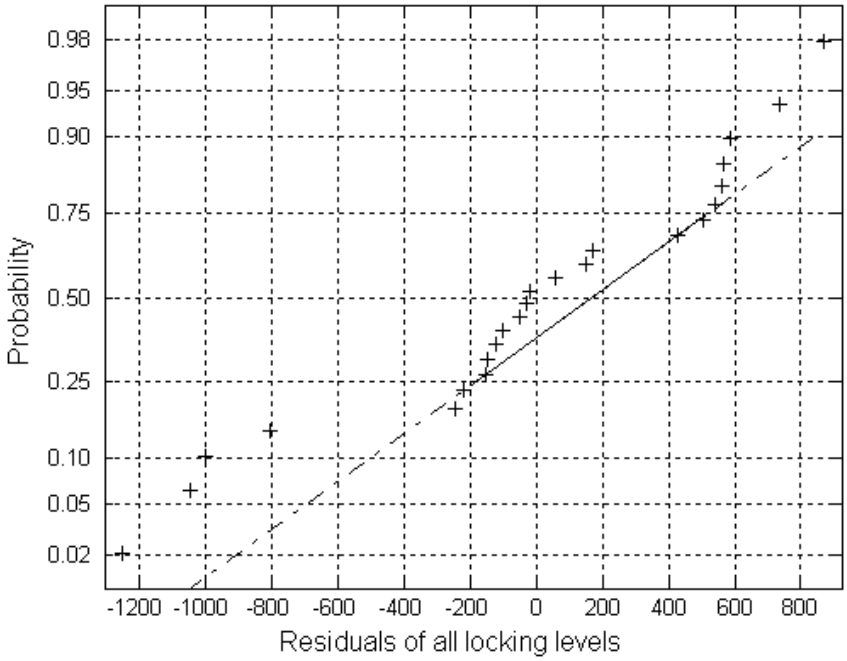

Figure 3.27 Normal probability plot of residuals for the final preload value.

Table 3.15 t-test statistic table for the final preload value.

t_o	t-critical	degress of freedom	P-value
-4.8	2.16	21	<0.01

Table 3.15 shows a summary of the result of t-test mean comparison of the "Locking Heli-Coil with Braycote" and "Standard Heli-Coil with Loctite". To test the hypothesis t_0 is calculated by the following equation [20]:

$$t_0 = \frac{\bar{y}_1 - \bar{y}_2}{\sqrt{\frac{S_1^2}{n_1} + \frac{S_2^2}{n_2}}} \tag{3.11}$$

Where $\bar{y}_i$ is the mean of each locking levels, S_i^2 is the sample variance of each group

and n_i is the sample size of each locking levels. Thus, t_0 is compared to an appropriate one-tail percentage point of $t_{\alpha,\upsilon}$, which is an approximation of the t distribution, where υ is calculated by [20]:

$$\upsilon = \frac{\left(\frac{S_1^2}{n_1} + \frac{S_2^2}{n_2}\right)}{\frac{\left(\frac{S_1^2}{n_1}\right)^2}{n_1 - 1} + \frac{\left(\frac{S_2^2}{n_2}\right)^2}{n_2 - 1}} \tag{3.12}$$

Since t_0 is less than $-t_{0.05,13.5}$ (-4.8 < 2.6), H_0 is rejected. Thus, concluding that not only the means of the groups are significantly different, but also that the means of "Standard Heli-Coil with Loctite" is higher than "Locking Heli-Coil with Braycote".

Figure 3.28 shows a graphical interpretation of these results where the multcompare function of Matlab v 7.3 was used. The multcompare function displays a graph with each group mean represented by a symbol and an interval around the symbol [21]. The interval is approximated by following formula:

$$\text{int} = \bar{y}_i \pm t_{\alpha,N-a}\sqrt{\frac{MS_e}{2(n-1)}} \tag{3.13}$$

Where $\bar{y}_i$ is the mean of each locking level, $t_{\alpha,N-a}$ is the t-critical value, MS_e is the mean square of the error and n is the number of samples.

Two means are significantly different if their intervals are disjoint, and are not significantly different if their intervals overlap [21]. This figure suggests that the mean for the "Locking Heli-Coil with Braycote" is significantly different when compared with the "Standard Heli-Coil with Loctite".

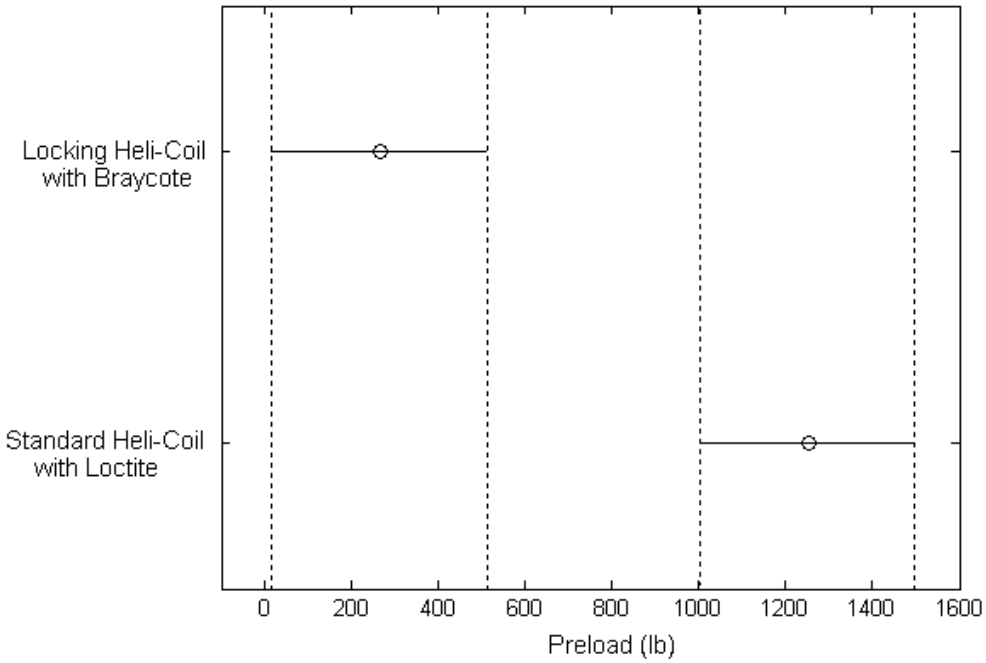

Figure 3.28 Multiple comparisons of means for the final preload value.

Lastly, a 95 percent confidence interval on each locking level mean is computed. Thus, showing that the population mean of each treatment (final preload value) will lie between these intervals. This is shown in Table 3.16.

Table 3.16 95 percent confidence intervals for the final preload value.

Population mean		
79.8 ≤	μ_1	≥ 449.6
929.6 ≤	μ_2	≥ 1801.9

This section focused on quantifying the dependency of the final preload value parameter on secondary locking features. Based on the calculations and the figures aforementioned in this section we can conclude the following:

1. “Standard Heli-Coil with Braycote” loosened completely.
2. Final preload value parameter is dependent on secondary locking features.
3. “Standard Heli-Coil with Loctite” has, statistically, the best locking performance of the group.
4. “Locking Heli-Coil with Braycote” reaches steady-state more often than any other group.

Chapter 4

Interpretation of Results

4.1 Introduction

This thesis has quantified the dependencies of loosening parameters on secondary locking features. To better understand the loosening process, it is important to understand, first, the forces that act on the bolt at the moment of assembly are not only friction forces at the head and threads that act against the input torque, but also elastic components and even prevailing torque will contribute against it [7].

Figure 4.1 shows the reaction forces on a bolt. Figure 4.1a represents a bolt at the moment of assembly where T_{in} is the input torque, M_h is the reaction moment created by the friction between the head of the bolt and the washer or joint, M_t is the reaction moment created by the threads of the nut and the Heli-Coil threads, M_θ is the a reaction moment due to the torsional stress stored in the bolt, M_p is the reaction moment created due to the stretch of the bolt by the interaction of the incline plane of the threads of the bolt and the Heli-Coil threads, T_P is the prevailing torque due to secondary locking features.

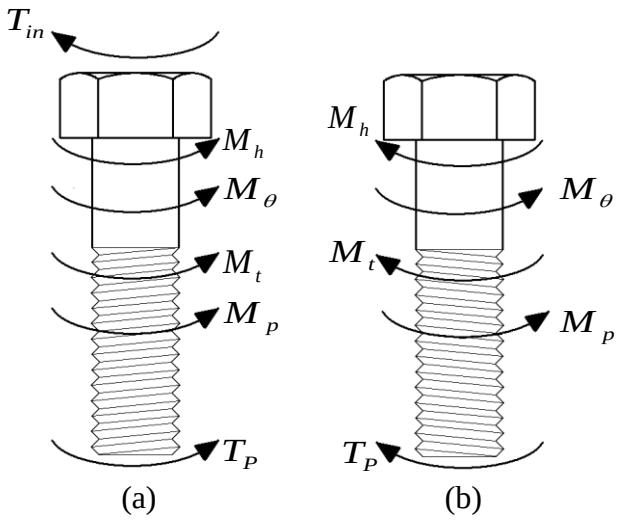

Figure 4.1 Reaction forces on bolts.

Figure 4.1a shows the reaction moments as the torque is applied. The bolt is being stretched and some of the applied torque is stored as torsion due to the difference of the frictional moments of the head and threads [3, 4]. Once the desired torque is achieved, the wrench is taken off the bolt. Figure 4.1b shows the bolt after assembly; here the bolt has stretched; also, axial and torsional relaxation takes place [7]. Note that friction and the prevailing torque are responsible to maintain the preload. The instant transverse vibration is induced to the joint, the friction forces might be overcome and the loosening process starts [1, 2].

The following is the analysis of the results at every parameter studied in this thesis. The Motosh [10] equation was modified and it is used in this section to explain the behavior of the secondary locking features. The modified torque equation proposed by Bickford [7] is:

$$T_{OFF} = F_P\left(\frac{-P}{2\pi} + \frac{\mu_t r_t}{\cos(\beta)} + \mu_h r_h\right) + T_P \qquad (4.1)$$

Where T_{OFF} is the breakaway torque or torque require for removal, F_P is the Preload created in the fastener, P is the pitch of the threads, μ_t is the coefficient of friction between Heli-Coil and bolt threads, r_t is the effective contact radius of the threads, μ_h is the coefficient of friction between the face of the bolt's head and the lower surface of the joint, r_h is the effective radius of contact between the bolt's head and the joint surface, β is the half-angle of the threads, T_P is the Prevailing torque (if applicable).

In order to represent a condition for maintaining preload if no external moments are present, the torque-preload equation was modified as follow:

$$\frac{P}{2\pi} < \frac{\mu_t r_t}{\cos(\beta)} + \mu_h r + \frac{T_P}{F_P} \tag{4.2}$$

The term at the left side of the equation is the reaction created by the elongation of the bolt and the incline plane of the threads, the term at the right hand side are the reactions created by the friction of the thread and head respectively and the reaction created by the prevailing torque. Note that this equation does not include dynamic effects from external sources.

4.2 Percentage loss of initial preload parameter

Initial preload loss is observed almost immediately after the tests begins, which suggest that the two requirements for loosening explained by Pai and Hess [3, 4] are satisfied. The first requirement would be the torsional moments at the head at the onset of loosening, the second requirement, including its factors, is achieved the moment the shear loading begins [3, 4]. Thus, the friction is reduced enough to allow the moment due to the

stored torsion to be released. This explains the initial drop of preload experienced by the three different locking levels.

Also, the bolt was tightened through the head of the bolt which increases torsion in the bolt. It was noted that the percentage loss of preload for "Standard Heli-Coil with Loctite" was statistically higher that any of the two other locking levels (2% higher). This is expected since, only Loctite was applied at the thread instead of Braycote for the other two cases. This increases the friction coefficient in the engaged threads, creating a greater moment at the head. Hence, more preload was stored in torsional deformation.

The average angle of twist along with the minimum, maximum angle of twist was calculated. Assuming that the bolt is a simple circular bar and the bar is in pure torsion, the angle of twist (ϕ_{twist}) can be calculated by the following equation [23]:

$$\phi_{twist} = \frac{TL_e}{GI_P} \tag{4.3}$$

Where T is the torque applied to the bolt. L_e is the effective length of the bolt; G is the shear modulus of elasticity, and I_P moment of inertia. Thus, the angle of twist is are shown in table 4.1.

Table 4.1 Minimum, mean and maximum angle of twist.

	Torque (lbs)	Effective length of bolt (in)	Shear modulus of elasticity (lb/in^2)	Moment of inertia (in^4)	Angle of twist
Minimum	100	1.884	1.12E+07	3.73E-04	2.6
Average	110	1.884	1.12E+07	3.73E-04	2.8
Maximum	125	1.884	1.12E+07	3.73E-04	3.2

In order to correlate the angle of twist to a preload value, the following expression was used [7]:

$$F_p = K_B \cdot \Delta L \tag{4.4}$$

where K_B is the stiffness of the bolt and ΔL is the bolt stretch. In order to find the stiffness of the bolt the following equation was used [7]:

$$K_B = \frac{EA_S}{L_e} \tag{4.5}$$

where E is the modulus of elasticity ($E = 30x10^6\ psi$); A_s is the tensile stress area ($A_s = 3.58x10^{-2}\ in^2$) and L_e is effective length of the bolt ($L_e = 1.883in$). Therefore $K_b = 569888.5\ ^{lb}/_{in}$.

The tensile stress area is calculated using the following expression [7]:

$$A_s = \frac{\pi}{4}\left(D_b - \frac{0.9743}{n} \right)^2 \tag{4.6}$$

where D_b is the diameter of the bolt ($D_b = 0.24825in$) and n is the number of threads per inch ($n = 28\ ^{thread}/_{in}$).

To calculate the bolt stretch, ΔL the "lead screw equation" [7] was used:

$$\Delta L = P\frac{\theta_R}{360} \tag{4.7}$$

In which θ_R is the nut rotation in degrees and P is the pitch in inches. Thus, a nut rotation of would be the angle of twist (in degrees) in order to simulate the stretch of the bolt if the bolt twisted. From using all of the above information the minimum mean and maximum preload is documented in table 4.2.

Table 4.2 Preload due to angle of twist.

ΔL (in)	Kв (lb/in)	Preload (lb)
0.00026	569888.5	146.1
0.00028	569888.5	160.7
0.00032	569888.5	182.6

Moreover, Table 4.2 summarizes the preload calculation if the bolt in this study experienced the aforementioned angles of twists. In terms of preload loss, this preload calculation would represent a range of 6.1% to 7.6% of preload loss. The data, in chapter 2, gave a range of percentage of preload loss of 4.9% to 14.4%. Note that the calculated angle of twist is only for a bar in pure torsion whereas a bolt would not only experience torsional stress but also longitudinal stress. Thus, the angle of twist is an approximate calculation. However, it still falls within the range of the values obtained by the data.

4.3 Initial rate of preload loss parameter

The initial rate of preload loss occurs after the release of torsional energy and only localized slips occurs at the contact surfaces that accumulates over the loading cycles and causes loosening slips over the entire contact. [3, 4]

Chapter 3 shows that there was a loosening dependency on the secondary locking feature. However, the difference was only for the “Standard Heli-Coil with Loctite” while the other two cases remained statistically similar. This suggests that the Loctite actually reduced the rate of loosening significantly. However, the Screwlock found at the “Locking Heli-Coil with Braycote” seemed to be almost ineffective in this period since the rate of loosening was not significantly different to the “Standard Heli-Coil with

Braycote". This situation can be explained using the modified torque-preload equation [7]:

$$\frac{P}{2\pi} < \frac{\mu_t r_t}{\cos(\beta)} + \mu_h r + \frac{T_P}{F_P} \tag{4.8}$$

For the case of "Locking Heli-Coil with Braycote", it can be noticed that a third term on the right hand side, which is the term related to the prevailing torque caused by the "Locking Heli-Coil with Braycote", depends on the amount of preload. Thus, when the preload is high, the prevailing torque is not dominant and almost ineffective. The prevailing torque would only become dominant when the amount of preload decreases. By doing so, the amount of prevailing torque would be divided by a smaller value of preload and therefore resulting in a more dominant term.

For the case of "Standard Heli-Coil with Loctite" the equation is as follow

$$\frac{P}{2\pi} < \frac{\mu_t r_t}{\cos(\beta)} + \mu_h r \tag{4.9}$$

Loctite fills the gap between the engaged thread. Hence, increasing the friction coefficient in the first component at the right hand side ($\frac{\mu_t r_t}{\cos(\beta)}$).

4.4 Secondary rate of preload loss parameter

The secondary rate of preload loss occurs when complete head and thread slip occurs at the contact surfaces previously explained by Junker [1]. Chapter 3 quantified this loss only for the "Standard Heli-Coil with Braycote" and the "Locking Heli-Coil with Braycote" since "Standard Heli-Coil with Loctite" shows a different loosening process quantified in the Initial rate of preload loss section.

Chapter 3 shows a significant dependency of the secondary locking featured in the loosening process. It shows that the two locking levels are significantly different where "Locking Heli-Coil with Braycote" resisted loosening better than the "Standard Heli-Coil with Braycote" suggesting that the Screwlock shows a good performance because the preload has decreased enough to counteract with the prevailing torque making this term significant. Equation (4.10) shows again that as the preload decreases the prevailing torque becomes more significant.

$$\frac{P}{2\pi} < \frac{\mu_t r_t}{\cos(\beta)} + \mu_h r + \frac{T_P}{F_P} \tag{4.10}$$

4.5 Steady-state / final preload value parameter

The effect of prevailing torque on preload loss is to self-lock the fastener by generating frictional resistance to rotation between engaged treads [11] the Locking Heli-Coil insert consists of a grip coil that when it is bent outwards creates high pressures on the bolt [14]. Therefore, the prevailing torque counteracts the loosening torque that can reduce and can even stop preload loss [11].

Anaerobic thread lockers are design to reduce loosening due to vibration by filling the gaps between the engaged threads. When the thread locker dries, it becomes a hard polymer [15]; therefore, increasing the friction force that opposes the loosening moments.

Chapter 3 quantified the dependencies and found a steady-state that is dependent on secondary locking feature for the "Locking Heli-Coil with Braycote" suggesting that the Screwlock is dominant when in average 80% of the initial preload is lost. Equation (4.10) will demonstrate that as the preload decreases to about 80% of initial preload, the

prevailing torque is dominant. Thus, the preload loss is contained. “Standard Heli-Coil with Loctite” did not reach steady-state as frequently as the “Locking Heli-Coil with Braycote”. However, the final preload values were statistically analyzed and showed that even though it didn’t reached steady-state, “Standard Heli-Coil with Loctite” had a better locking performance because the Threadlocker filled the gap and increased the friction coefficient.

Chapter 5

Conclusions

In order to study the dependency of the loosening parameter on secondary locking features of threaded fasteners, the loosening process was divided in five parameters: Initial preload loss, initial rate of preload loss, secondary rate of preload loss, steady-state value and final preload value. Statistical analysis was used to quantify the dependencies concluding the following:

For the dependency of the initial preload loss parameter on secondary locking features it can be concluded that:

1. Loss of initial preload is dependent on secondary locking features.
2. The mean loss of initial preload of "Standard Heli-Coil with Braycote" and the mean loss of initial preload of "Locking Heli-Coil with Braycote" are not significantly different.
3. The mean loss of initial preload of "Standard Heli-Coil with Braycote" and the mean loss of initial preload of "Standard Heli-Coil with Loctite" are significantly different.
4. The mean loss of initial preload of "Standard Heli-Coil with Loctite" and the mean loss of initial preload of "Locking Heli-Coil with Braycote" are significantly different.

For the parameter of the initial rate of preload loss with secondary locking features the following can be concluded:

1. Initial rate of preload loss is dependent on secondary locking features.
2. The initial mean rate of preload loss of "Standard Heli-Coil with Braycote" and the initial mean rate of preload loss of "Locking Heli-Coil with Braycote" are not significantly different.
3. The initial mean rate of preload loss of "Standard Heli-Coil with Braycote" and the initial mean rate of preload loss of "Standard Heli-Coil with Loctite" are significantly different.
4. The initial mean rate of preload loss of "Standard Heli-Coil with Loctite" and the initial mean rate of preload loss of "Locking Heli-Coil with Braycote" are significantly different.

For the dependency of secondary rate of preload loss parameter on secondary locking features the following can be concluded:

1. "Standard Heli-Coil with Loctite" did not exhibit this parameter and therefore is not included in this analysis
2. Secondary rate of preload loss is dependent on secondary locking features.
3. The secondary mean rate of preload loss of "Standard Heli-Coil with Braycote" and the secondary mean rate of preload loss of "Locking Heli-Coil with Braycote" are significantly different.

For the dependency of the steady-state value parameter on secondary locking features it can be concluded that:

1. "Standard Heli-Coil with Braycote" loosened completely.

2. 83.3% of “Locking Heli-Coil with Braycote” reached steady-state.
3. 16.7% of “Standard Heli-Coil with Loctite” reached steady-state.
4. The steady-state condition is dependent on the secondary locking feature.
5. There is not enough data to perform a statistical analysis comparing all locking levels.

For the dependency of the final preload value parameter on secondary locking features it can be concluded that:

1. “Standard Heli-Coil with Braycote” loosened completely.
2. Final preload value parameter is dependent on secondary locking features.
3. “Standard Heli-Coil with Loctite” has, statistically, the best locking performance of the group.
4. “Locking Heli-Coil with Braycote” reaches steady-state more often than any other group.

Table 5.1 Dependency of loosening parameters on secondary locking features.

Loosening parameters	Secondary locking features	
	Locking Heli-Coil with Braycote	Standard Heli-Coil with Loctite
Percentage loss of initial preload	Does not depend	Depends
Initial rate of preload loss	Does not depend	Depends
Secondary rate of preload loss	Depends	Depends
Steady-state value	Depends	Depends
Final preload value	Depends	Depends

In short, there is a clear dependency on the loosening parameter on secondary locking features. Table 5.1 summarizes the dependencies of loosening parameters on the individual secondary locking features provided by the prevailing torque and Loctite. Note that two loosening parameters (Percentage loss of initial preload and initial rate of preload loss) were independent on the secondary locking feature in the "Locking Heli-Coil with Braycote", but were dependent on the "Standard Heli-Coil with Loctite".

References

1. Junker, G. H. (1969). New Criteria for Self-Loosening of Fasteners Under Vibration, *Society of Automotive Engineers Transactions*, Vol. 78, pp. 314-335.

2. Hess, D. P. (1998). Vibration- and Shock- Induced Loosening, Chapter 40 in *Handbook of Bolts and Bolted Joints*, New York: Marcel Dekker Inc., pp. 757-824.

3. Pai, N.P. and Hess, D.P. (1997). Experimental Study of Loosening of Threaded Fasteners Due to Dynamic Shear Load, *Journal of Sound and Vibration*, Vol. 253, pp. 585-692.

4. Pai, N.P. and Hess, D.P. (2002). Three-Dimensional Finite Element analysis of threaded fastener loosening due to dynamic shear load, *Engineering Failure Analysis*, Vol. 9, pp. 383-402.

5. Bolt Science, (1999-02). Vibration Loosening of Bolts and Threaded Fasteners, www.boltscience.com/pages/vibloose.

6. Sanclemente, J.A. and Hess, D.P. (2006). Parametric Study of Threaded Fastener Loosening Due to Cyclic Transverse Load, *Engineering Failure Analysis*, Vol. 14, pp. 239-249, 2006.

7. Bickford, J.H. (1995). *An Introduction to the Design and Behavior of Bolted Joints*, 3rd ed., Marcel Dekker Inc.

8. Fisher, J. W., and Struik, J. H. A. (1974), Guide to Design Criteria for Bolted and Riveted Joints, Wiley, New York, pp. 57-58.

9. Ibrahim, R. A., and Pettit, C. L. (2003). "Uncertainties and Dynamic Problems of Bolted Joints and Other Fasteners," *Journal of sound and vibration*, pp. 872-873.

10. Motosh, N. (1976). Development of Design Charts for Bolts Preloaded up to the Plastic Range, Eng. Ind.

11. Finkelston, R. F. (1972). "How Much Shake Can Bolted Joints Take," *Machine Design*, pp. 122-125.

12. Eccles, W. (1984). Bolted Joint Design, *Engineering Design* Vol. 10, pp. 10-14.

13. Wolfe, P. E. (1954). "Functions Performed by Thread Inserts," pp. 120-122.

14. Hillcliff tools ltd. (2007). "Helicoil Wire Thread Inserts," http://www.hillcliff-tools.com/helicoil.html.

15. Henkel Technologies. (2007) *The Adhesive Sourcebook*, Vol. 7, http://www.henkelna.com.

16. Bardon, A. (2004). Thread Locking Technologies, *Plant Engineering*, Vol. 58. Barrington, Iss. 8; pp. 56-59.

17. NAS 1003 thru 1020, (1991). National Aerospace Standard, pp. 1-3.

18. NAS 1149, (1994). National Aerospace Standard, pp. 1-6.

19. Emhart Teknologies, 2003. Heli-Coil Bulletin, www.emhart.com.

20. Montgomery, D. C., *Design and Analysis of Experiments*, 6th ed., New Jersey: John Wiley & Sons, Inc., 2005.

21. The Mathworks Inc. (2007) Matlab v 7.3 Technical Support, http://www.mathworks.com.

22. Smith, R. T. and Minton, R. B. (2002). *Calculus*, 2nd ed. New York: McGraw-Hill, Inc., pp. 13-14.

23. Gere, J. M. (2004). *Mechanics of Materials*, 6th ed., California: Thomson Learning, Inc., pp. 185-219.

Appendices

Appendix A: Data extracted for all locking levels

This appendix depicts the points obtained during the extraction of data for the initial rate of preload loss, secondary rate of preload loss and for the steady-state value of all locking levels. Also, the points extracted for secondary rate of preload loss and final preload value.

Table A.1 Extracted data from "Standard Heli-Coil with Braycote".

Standard heli-coil w/ Braycote				
Test number	Rate of preload loss		Steady state	
	Preload (lb)	Cycles	Preload (lb)	Cycles
1	1711.00	272.20	0	N/R
	1944.00	100.50	0	N/R
2	1730.00	174.00	0	N/R
	1939.00	72.95	0	N/R
3	1723.00	243.70	0	N/R
	1998.00	82.91	0	N/R
4	1705.00	232.00	0	N/R
	1972.00	75.00	0	N/R
5	1795.00	293.80	0	N/R
	1989.00	102.50	0	N/R
6	1810.00	292.70	0	N/R
	1991.00	101.40	0	N/R
7	1645.00	187.80	0	N/R
	2023.00	50.39	0	N/R
8	1871.00	200.70	0	N/R
	2083.00	49.51	0	N/R
9	1777.00	176.10	0	N/R
	1995.00	64.16	0	N/R
10	1860.00	192.50	0	N/R
	2094.00	51.27	0	N/R
11	1737.00	232.90	0	N/R
	1986.00	89.65	0	N/R
12	1720.00	200.70	0	N/R
	1984.00	66.21	0	N/R
Mean	1878.42	150.23		

Appendix A (continued)

Table A.2 Extracted data from "Locking Heli-Coil with Braycote".

Locking heli-coil w/ Braycote				
Test number	Rate of preload loss		Steady state	
	Preload (lb)	Cycles	Preload (lb)	Cycles
13	1680.00	374.40	118.5	2320
	1996.00	122.20	118.5	2168
14	1795.00	161.40	21.69	2327
	2060.00	38.67	21.85	2193
15	1882.00	174.00	248.8	2318
	2025.00	75.88	248.6	1824
16	1576.00	280.10	217.2	2315
	1918.00	83.79	216.6	1735
17	1792.00	274.20	238.7	2324
	1931.00	150.60	239.7	2252
18	1845.00	199.50	163.8	2317
	2052.00	59.18	163.8	2023
19	1868.00	155.60	141.9	2324
	2001.00	69.14	141.6	2248
20	1946.00	144.70	N/R	N/R
	2054.00	49.51	N/R	N/R
21	1648.00	251.70	109.7	2326
	1953.00	89.65	112.6	2225
22	1739.00	298.80	325.8	2314
	2032.00	74.12	325.8	2001
23	1803.00	232.00	417.4	2328
	1999.00	80.86	417.7	2082
24	1690.00	281.00	44.67	2327
	1985.00	96.39	44.67	2069
Mean	1886.25	159.06	186.34	2198.18

Appendix A (continued)

Table A.3 Extracted data from "Standard Heli-Coil with Loctite".

Standart heli-coil w/ Loctite				
Test number	Rate of preload loss		Steady state values	
	Preload (lb)	Cycles	Preload (lb)	Cycles
25	1764.00	295.90	N/R	N/R
	1907.00	83.79	N/R	N/R
26	1751.00	300.00	253.6	2326
	1944.00	34.86	253	2182
27	1980.00	325.20	N/R	N/R
	2018.00	123.00	N/R	N/R
28	1908.00	306.70	N/R	N/R
	1991.00	52.44	N/R	N/R
29	2097.00	177.00	N/R	N/R
	2116.00	37.50	N/R	N/R
30	1893.00	399.90	N/R	N/R
	1950.00	138.90	N/R	N/R
31	1959.00	230.90	N/R	N/R
	1991.00	67.97	N/R	N/R
32	2026.00	171.10	1989	2327
	2038.00	50.39	1991	2052
33	2046.00	230.00	N/R	N/R
	2057.00	58.30	N/R	N/R
34	1764.00	314.40	N/R	N/R
	2003.00	45.41	N/R	N/R
35	2004.00	280.10	N/R	N/R
	2058.00	81.74	N/R	N/R
36	2076.00	38.67	N/R	N/R
	2092.00	11.13	N/R	N/R
Mean	1976.38	160.64	1121.65	2221.75

Appendix A (continued)

The following tables were calculated using the slope-point equation used in chapter 3. These data points are used for the plotting of the rates of preload loss and the steady-state values.

Table A.4 Refined data points from "Standard Heli-Coil with Braycote".

Std heli-coil w/ brycote				
Test Number	Initial loss		Steady state	
	Preload (lb)	Cycles	Preload (lb)	Cycles
1	2080.38	0	N/R	N/R
	1944.67	100	N/R	N/R
2	2089.88	0	N/R	N/R
	1883.05	100	N/R	N/R
3	2139.8	0	N/R	N/R
	1968.77	100	N/R	N/R
4	2099.54	0	N/R	N/R
	1929.48	100	N/R	N/R
5	2092.94	0	N/R	N/R
	1991.53	100	N/R	N/R
6	2086.94	0	N/R	N/R
	1992.32	100	N/R	N/R
7	2161.61	0	N/R	N/R
	1886.52	100	N/R	N/R
8	2152.42	0	N/R	N/R
	2012.2	100	N/R	N/R
9	2141.83	0	N/R	N/R
	1925.2	100	N/R	N/R
10	2178.94	0	N/R	N/R
	2013.26	100	N/R	N/R
11	2141.83	0	N/R	N/R
	1968	100	N/R	N/R
12	2113.96	0	N/R	N/R
	1917.67	100	N/R	N/R
Mean	2136.65	0	N/R	N/R
	1967.86	100	N/R	N/R

Appendix A (continued)

Table A.5 Refined data points from "Locking Heli-Coil with Braycote".

Locking heli-coil w/ brycote				
Test Number	Initial loss		Steady state	
	Preload (lb)	Cycles	Preload (lb)	Cycles
13	2149.11	0	118	2075
	2023.8	100	118	2320
14	2143.5	0	21	2075
	1927.6	100	21	2320
15	2135.6	0	248	2075
	1989.9	100	248	2320
16	2109.3	0	217	2075
	1989.8	100	217	2320
17	2100.4	0	239	2075
	1987.9	100	239	2320
18	2139.3	0	163	2075
	1991.8	100	163	2320
19	2107.4	0	141	2075
	1953.5	100	141	2320
20	2110.2	0	N/R	N/R
	1933.5	100	N/R	N/R
21	2121.7	0	110	2075
	1933.5	100	110	2320
22	2128.7	0	325	2075
	1998.3	100	325	2320
23	2103.9	0	417	2075
	1974.2	100	417	2320
24	2139.0	0	44	2075
	1979.2	100	44	2320
Mean	2037.90	0.00	185.73	2075.00
	1889.12	100	186.20	2320.00

Appendix A (continued)

Table A.6 Refined data points from "Standard Heli-Coil with Loctite".

Standart heli-coil w/ Loctite				
Test Number	Initial		Steady	
	Preload (lb)	Cycles	Preload (lb)	Cycles
25	1963.5	0	N/R	N/R
	1896.1	100	N/R	N/R
26	1969.4	0	253	2117
	1896.6	100	253	2326
27	2041.1	0	N/R	N/R
	2022.3	100	N/R	N/R
28	2008.1	0	N/R	N/R
	1975.5	100	N/R	N/R
29	2121.1	0	N/R	N/R
	2107.5	100	N/R	N/R
30	1980.3	0	N/R	N/R
	1958.5	100	N/R	N/R
31	2004.3	0	N/R	N/R
	1984.7	100	N/R	N/R
32	2043.0	0	1989	2117
	2033.1	100	1989	2326
33	2060.7	0	N/R	N/R
	2054.3	100	N/R	N/R
34	2043.3	0	N/R	N/R
	1954.5	100	N/R	N/R
35	2080.3	0	N/R	N/R
	2053.0	100	N/R	N/R
36	2098.5	0	N/R	N/R
	2040.4	100	N/R	N/R
Mean	2011.0	0	N/R	N/R
	1974.5	100	N/R	N/R

Appendix A (continued)

The following data points were extracted to quantify the secondary rate of preload loss.

Table A.7 Extracted data from "Standard Heli-Coil with Braycote" and "Locking Heli-Coil with Braycote".

Std heli-coil w/ brycote		
Run number	secundary loss	
	Preload (lb)	Cycles
1	250.70	739.20
	765.90	680.30
2	287.00	522.40
	949.90	423.30
3	94.36	944.80
	853.10	701.70
4	193.10	961.40
	554.20	658.00
5	272.20	1028.00
	616.30	973.80
6	139.50	1415.00
	464.30	1358.00
7	317.10	389.10
	1000.00	327.20
8	342.60	635.40
	813.00	577.40
9	167.70	1020.00
	493.50	982.60
10	493.30	607.30
	939.40	544.60
11	84.00	776.40
	746.00	652.70
12	262.20	543.20
	980.50	447.90
Mean	503.33	746.24

Locking heli-coil w/ brycote		
Run number	Initial loss	
	Preload (lb)	Cycles
13	354.30	1301.00
	949.40	997.60
14	620.70	501.90
	1243.00	375.30
15	582.50	998.10
	1201.00	685.30
16	506.10	862.80
	1110.00	536.10
17	693.40	1166.00
	1116.00	904.10
18	493.50	735.40
	1081.00	597.90
19	667.80	1095.00
	942.90	943.70
20	1138.00	2317.00
	1293.00	1877.00
21	600.10	665.00
	959.40	582.70
22	567.00	932.80
	967.70	767.00
23	744.30	986.40
	1091.00	769.60
24	324.20	803.90
	897.80	643.90
Mean	607.66	1030.44

Appendix B: Zoomed data plots for the percentage loss of initial preload parameter

These plots were used in order to extract the values used in Chapter 3 under the percentage loss of preload loss section

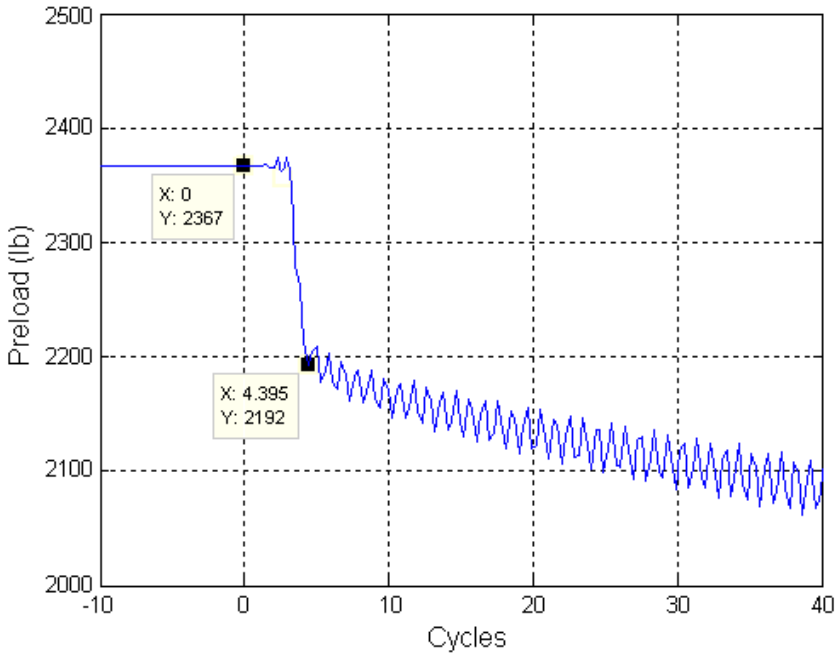

Figure B.1 Loss of initial preload for "Standard Heli-Coil with Braycote" run number 1.

Appendix B (continued)

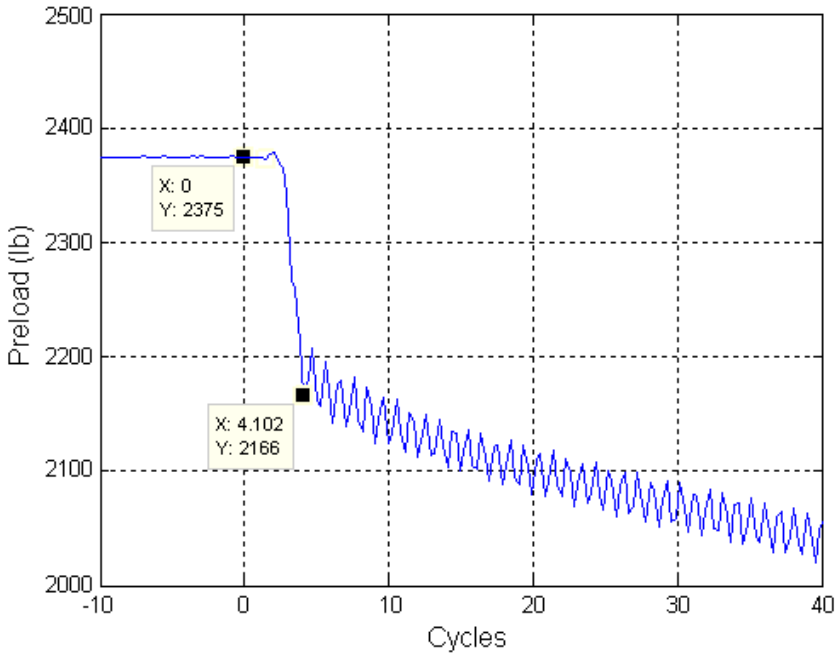

Figure B.2 Loss of initial preload for "Standard Heli-Coil with Braycote" run number 2.

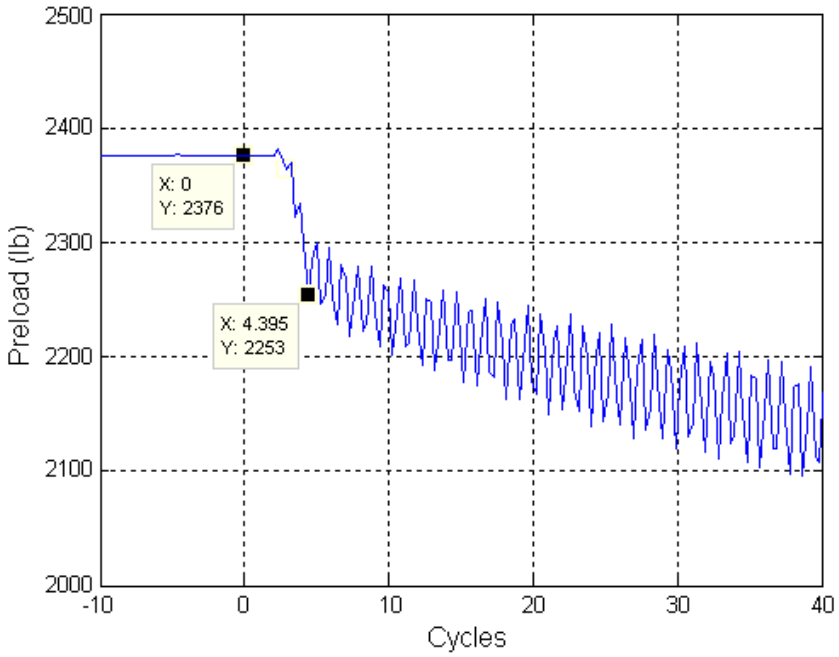

Figure B.3 Loss of initial preload for "Standard Heli-Coil with Braycote" run number 3.

Appendix B (continued)

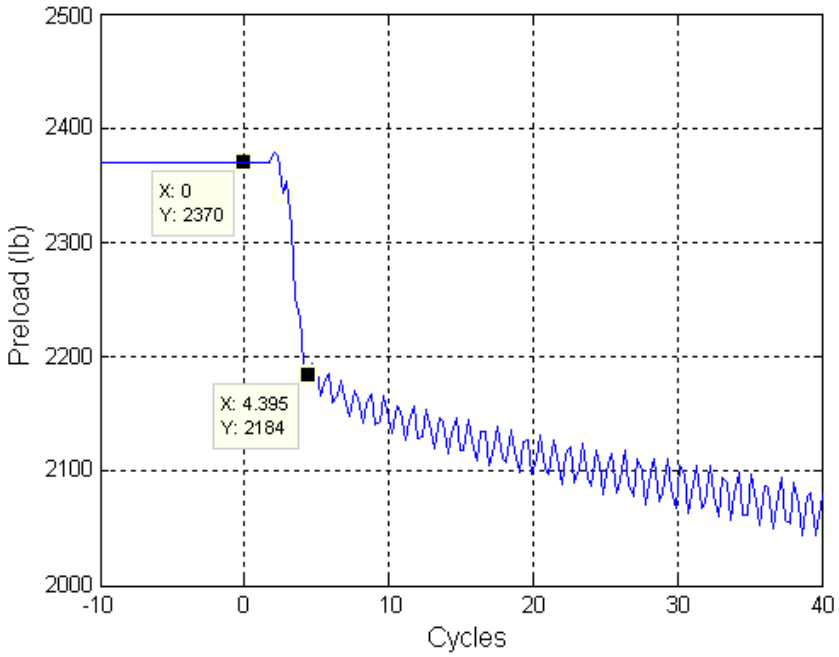

Figure B.4 Loss of initial preload for "Standard Heli-Coil with Braycote" run number 4.

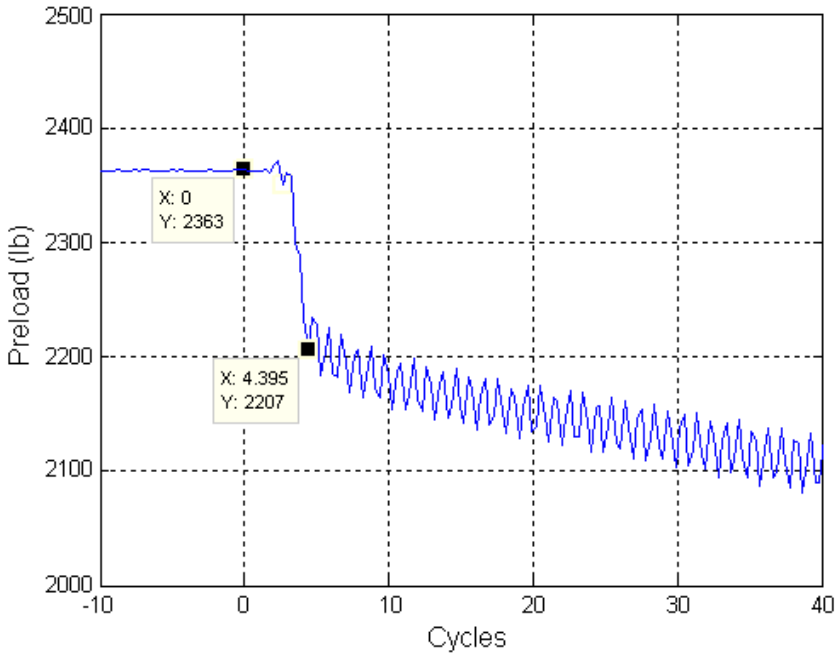

Figure B.5 Loss of initial preload for "Standard Heli-Coil with Braycote" run number 5.

Appendix B (continued)

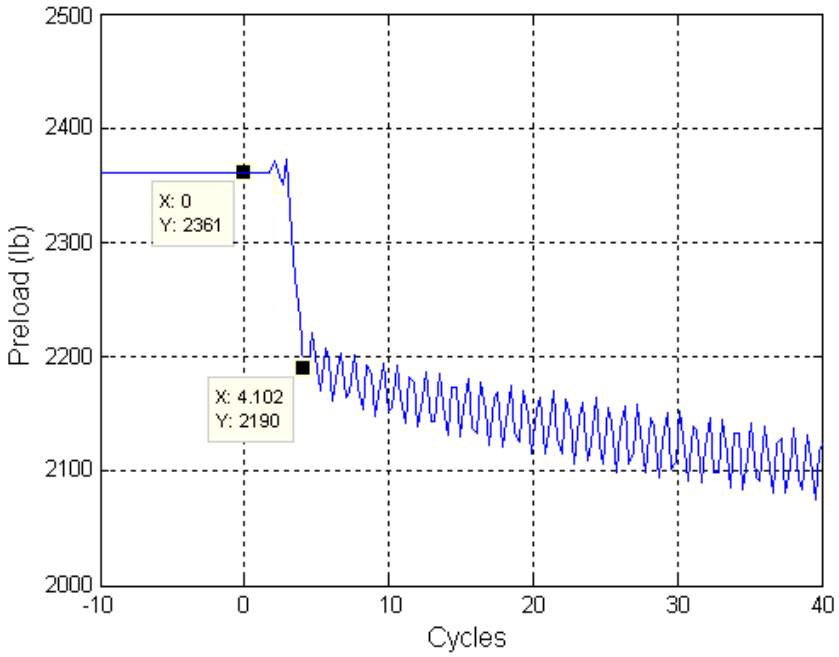

Figure B.6 Loss of initial preload for "Standard Heli-Coil with Braycote" run number 6.

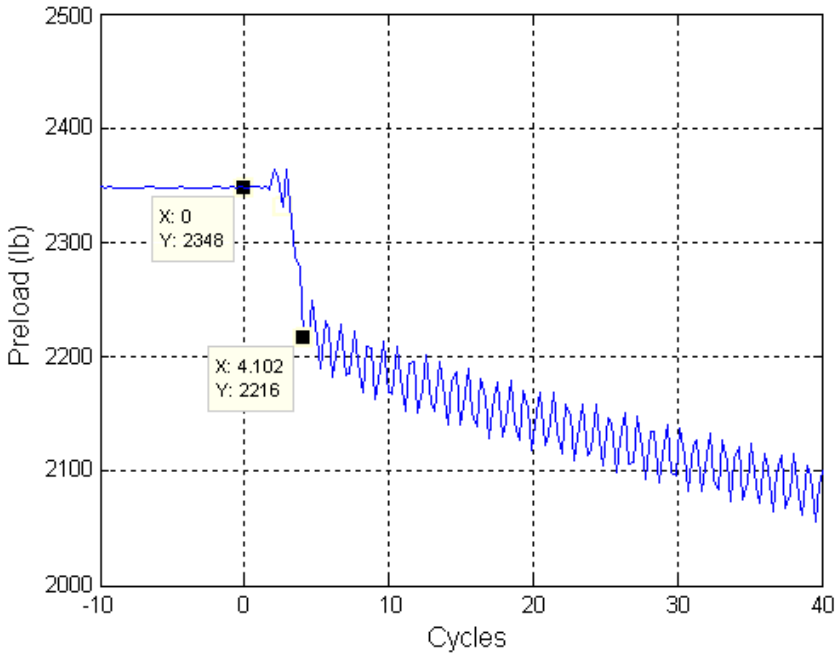

Figure B.7 Loss of initial preload for "Standard Heli-Coil with Braycote" run number 7.

Appendix B (continued)

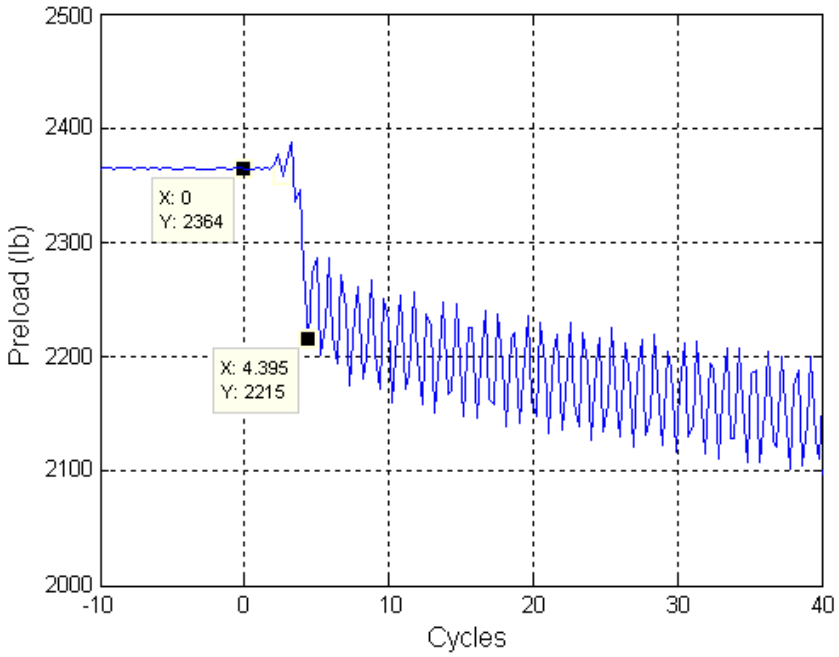

Figure B.8 Loss of initial preload for "Standard Heli-Coil with Braycote" run number 8.

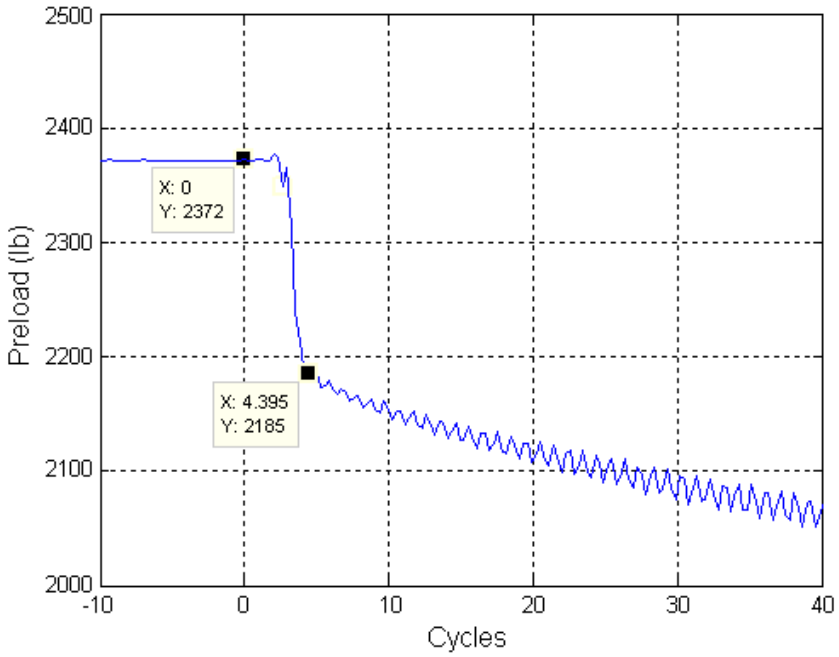

Figure B.9 Loss of initial preload for "Standard Heli-Coil with Braycote" run number 9.

Appendix B (continued)

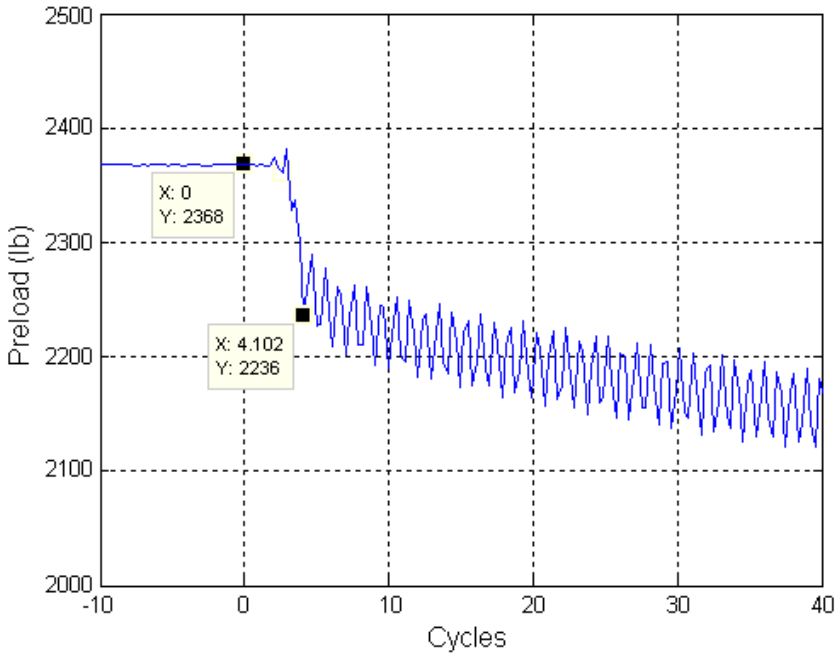

Figure B.10 Loss of initial preload for "Standard Heli-Coil with Braycote" run number 10.

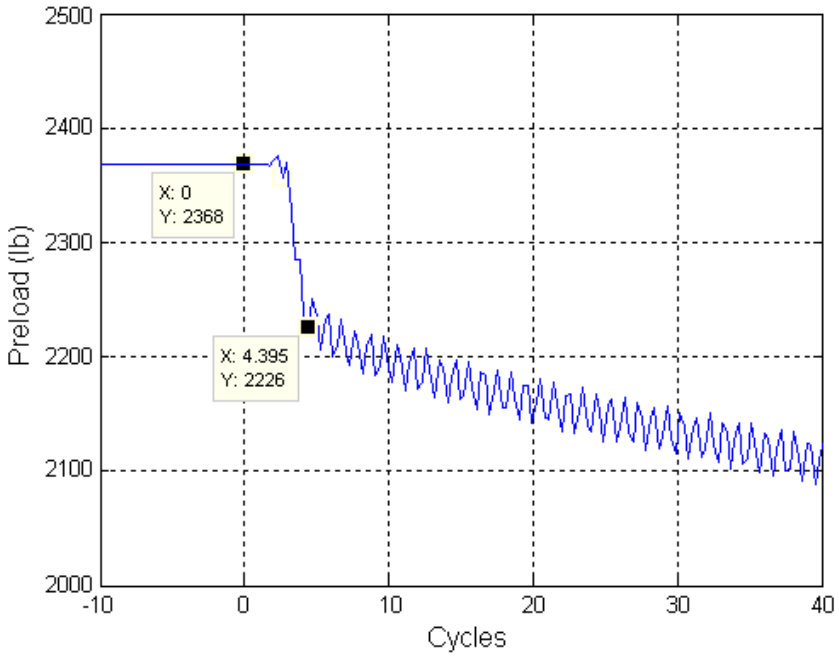

Figure B.11 Loss of initial preload for "Standard Heli-Coil with Braycote" run number 11.

Appendix B (continued)

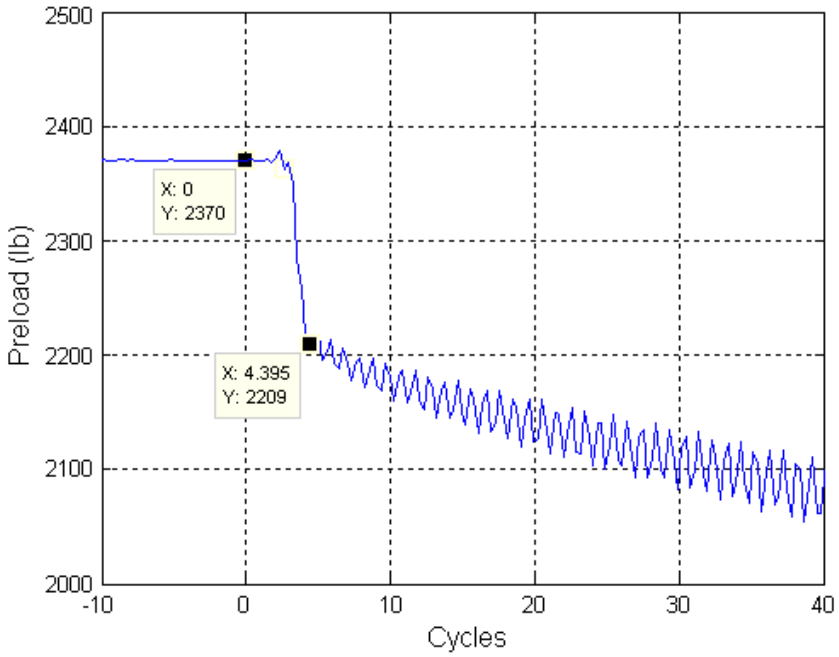

Figure B.12 Loss of initial preload for "Standard Heli-Coil with Braycote" run number 12.

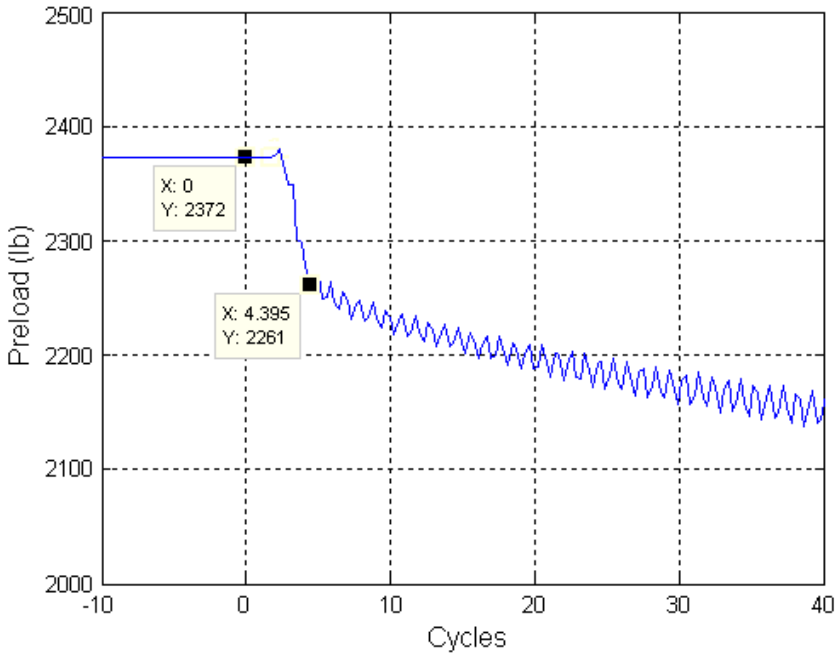

Figure B.13 Loss of initial preload for "Locking Heli-Coil with Braycote" run number 13.

Appendix B (continued)

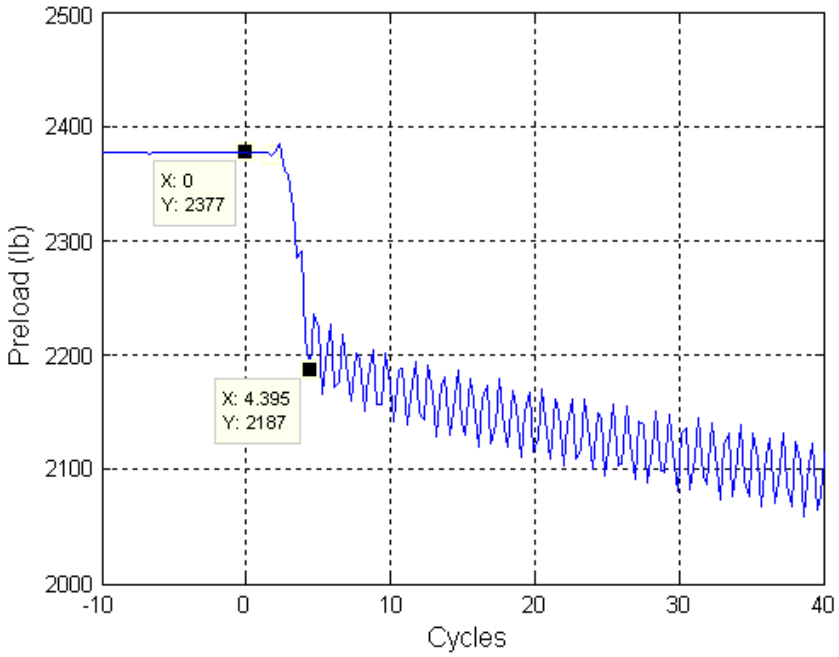

Figure B.14 Loss of initial preload for "Locking Heli-Coil with Braycote" run number 14.

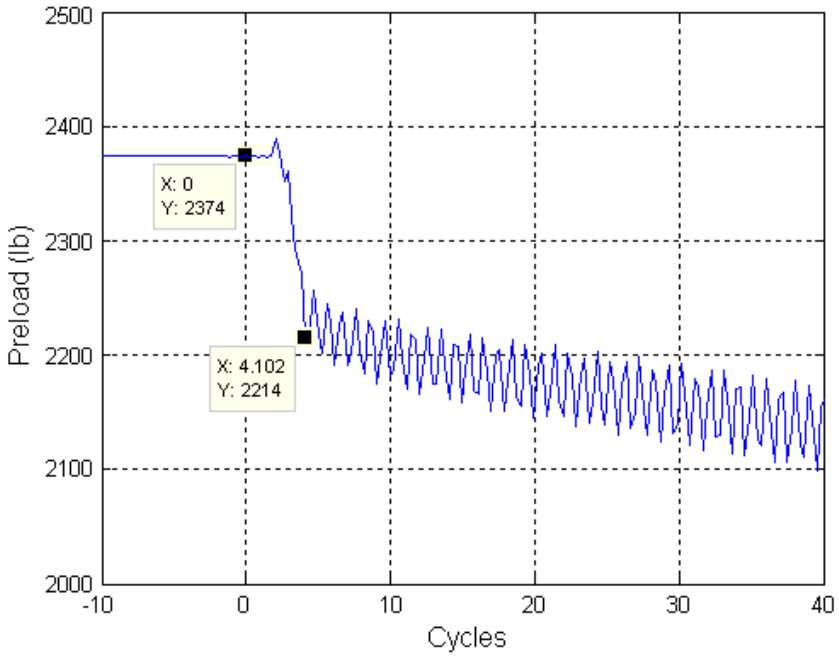

Figure B.15 Loss of initial preload for "Locking Heli-Coil with Braycote" run number 15.

Appendix B (continued)

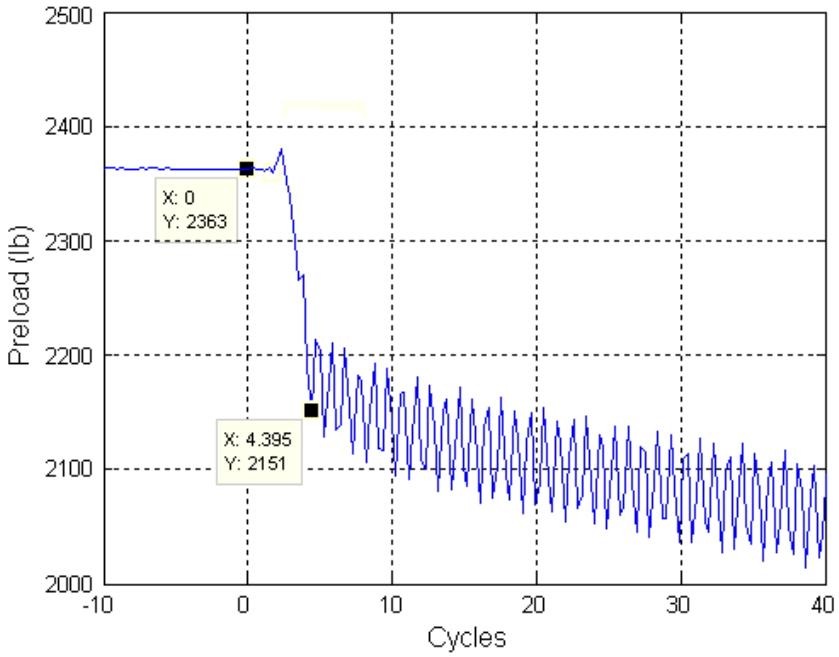

Figure B.16 Loss of initial preload for "Locking Heli-Coil with Braycote" run number 16.

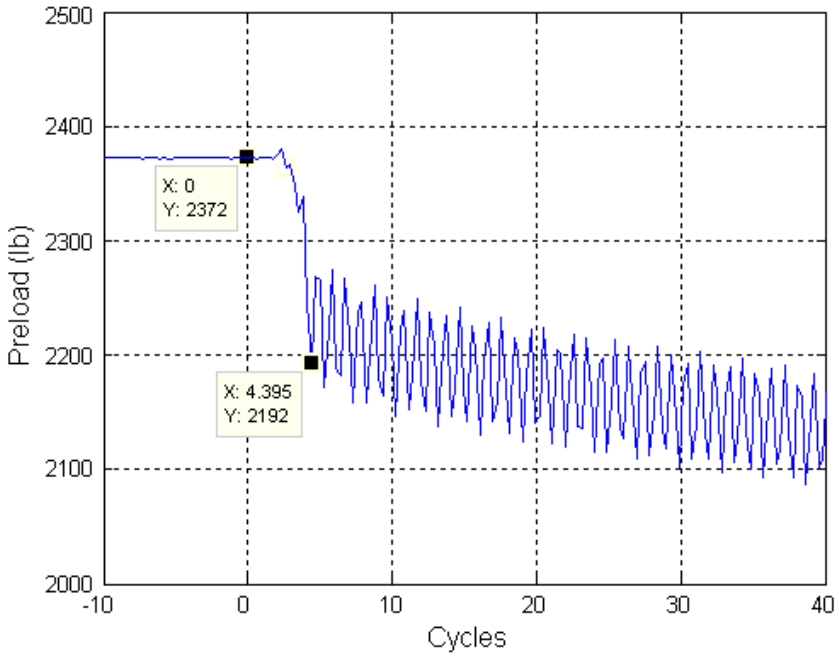

Figure B.17 Loss of initial preload for "Locking Heli-Coil with Braycote" run number 17.

Appendix B (continued)

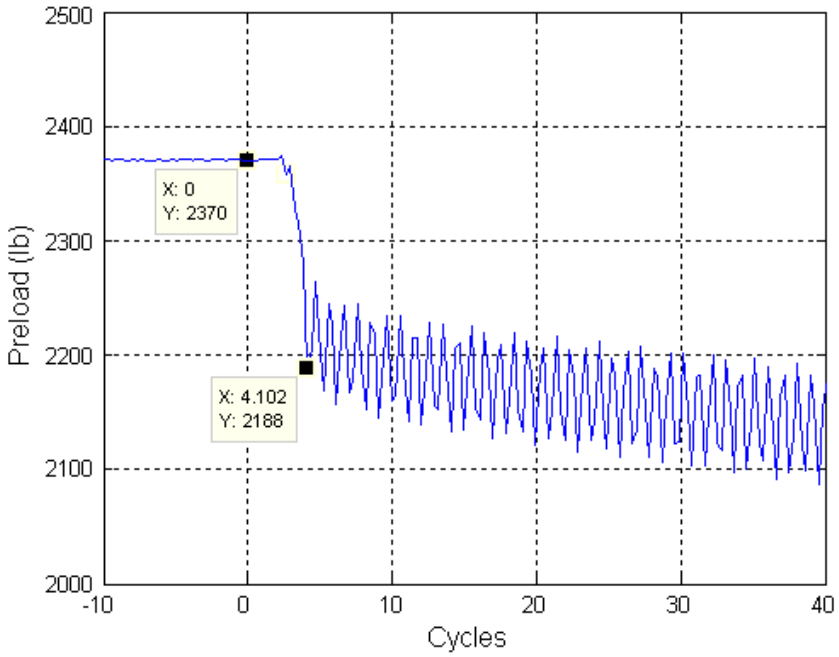

Figure B.18 Loss of initial preload for "Locking Heli-Coil with Braycote" run number 18.

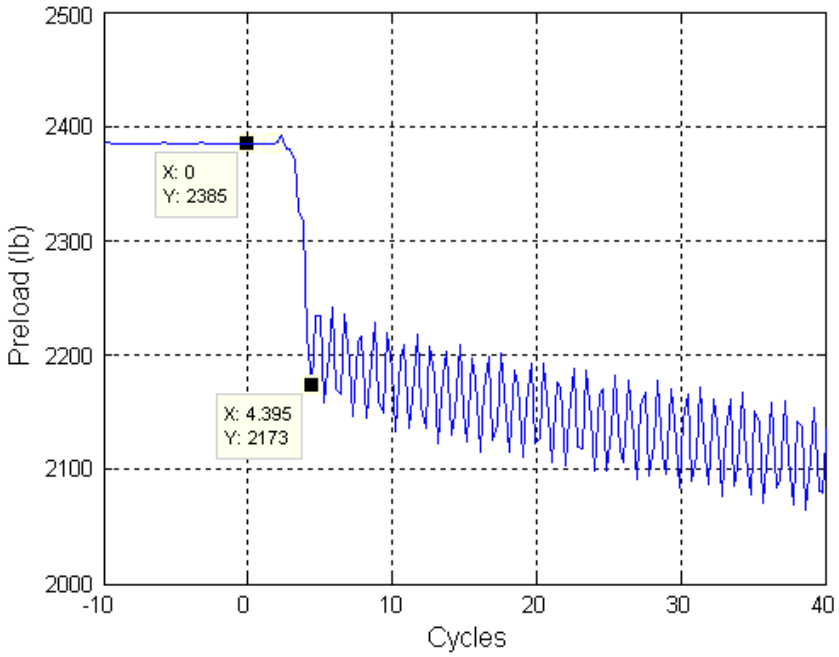

Figure B.19 Loss of initial preload for "Locking Heli-Coil with Braycote" run number 19.

Appendix B (continued)

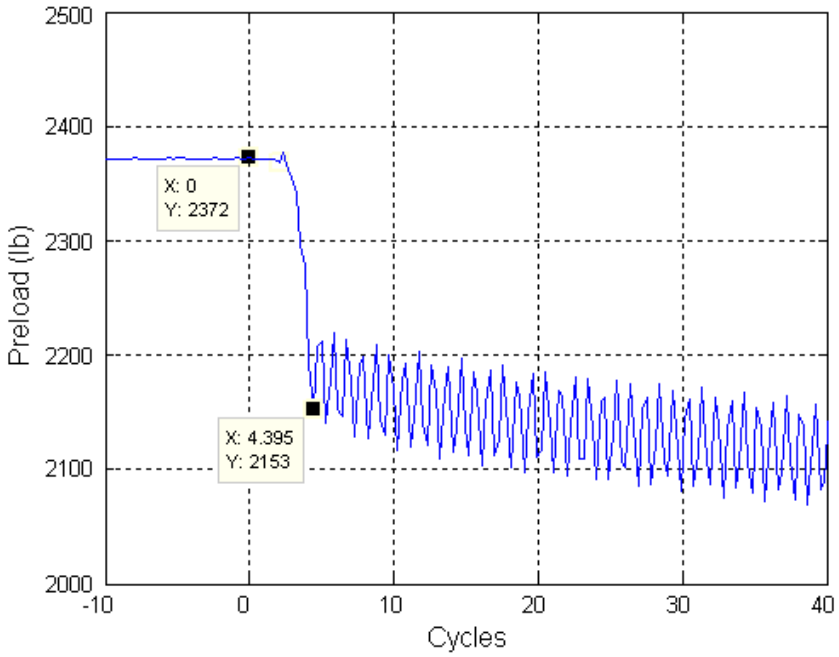

Figure B.20 Loss of initial preload for "Locking Heli-Coil with Braycote" run number 20.

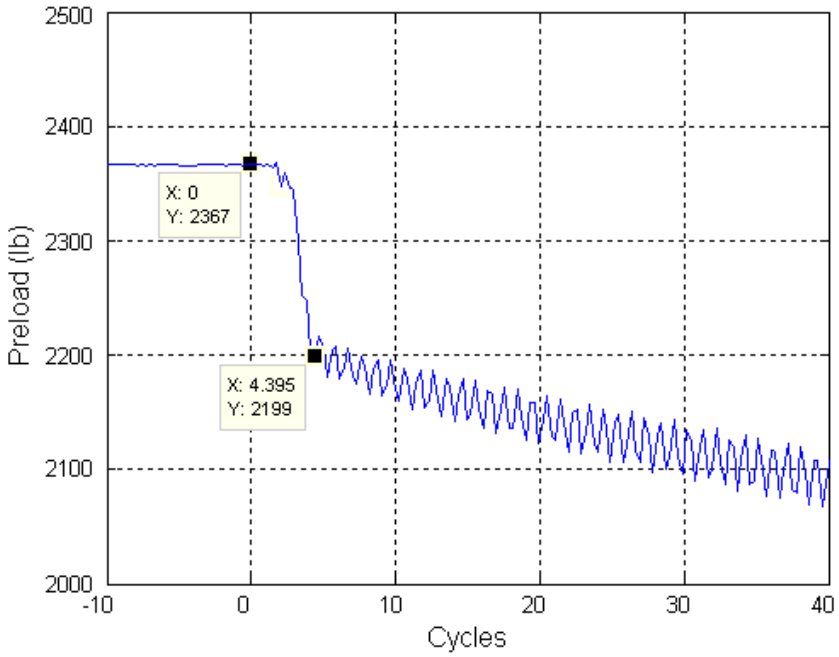

Figure B.21 Loss of initial preload for "Locking Heli-Coil with Braycote" run number 21.

Appendix B (continued)

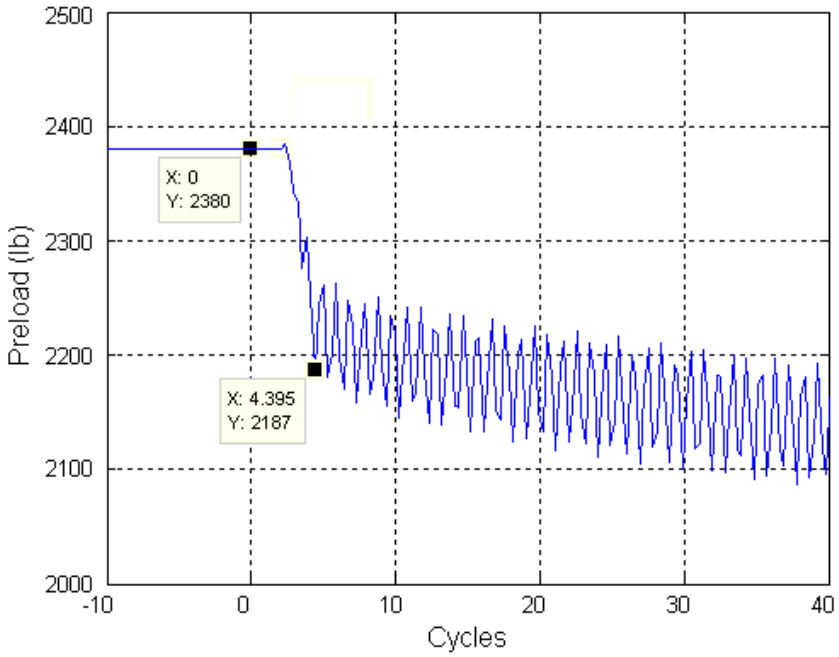

Figure B.22 Loss of initial preload for "Locking Heli-Coil with Braycote" run number 22.

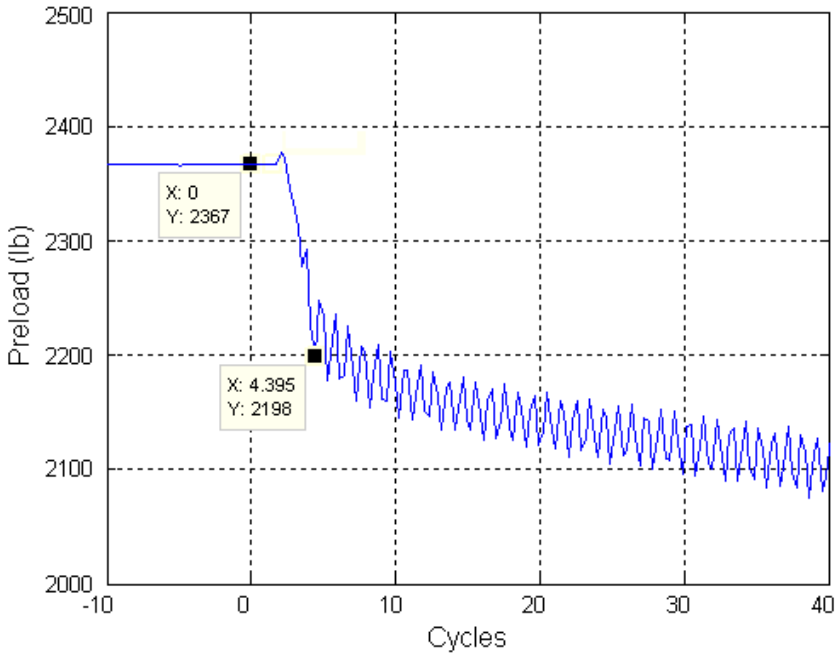

Figure B.23 Loss of initial preload for "Locking Heli-Coil with Braycote" run number 23.

Appendix B (continued)

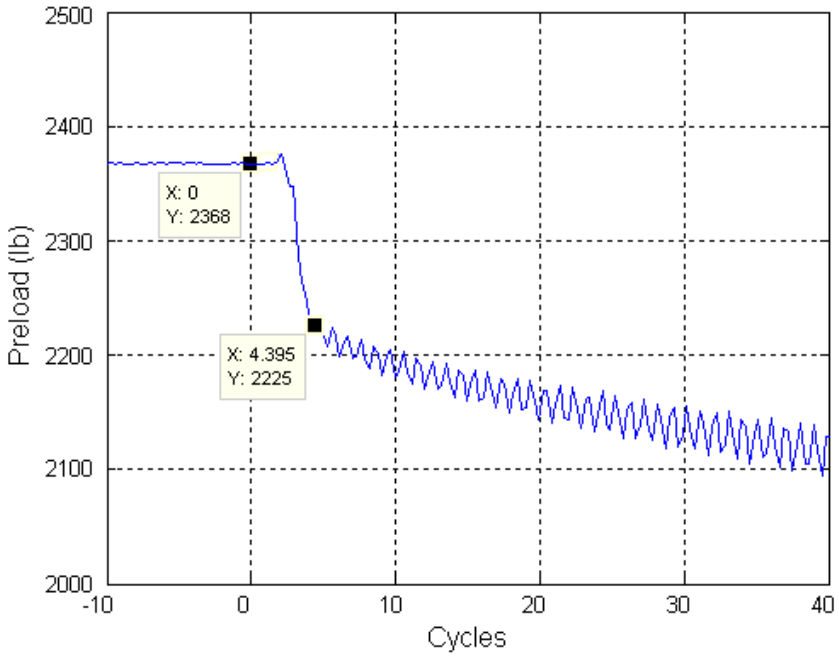

Figure B.24 Loss of initial preload for "Locking Heli-Coil with Braycote" run number 24.

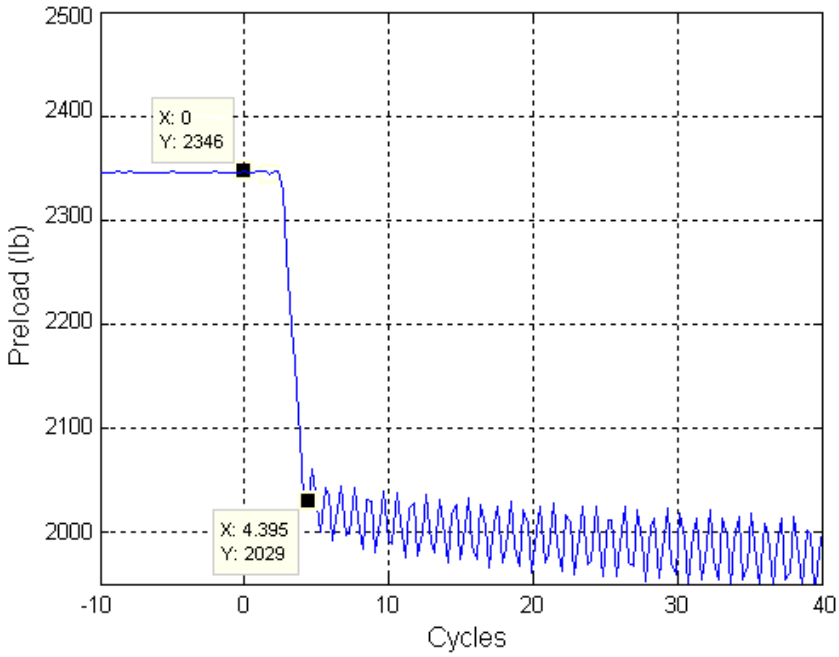

Figure B.25 Loss of initial preload for "Standard Heli-Coil with Loctite" run number 25.

Appendix B (continued)

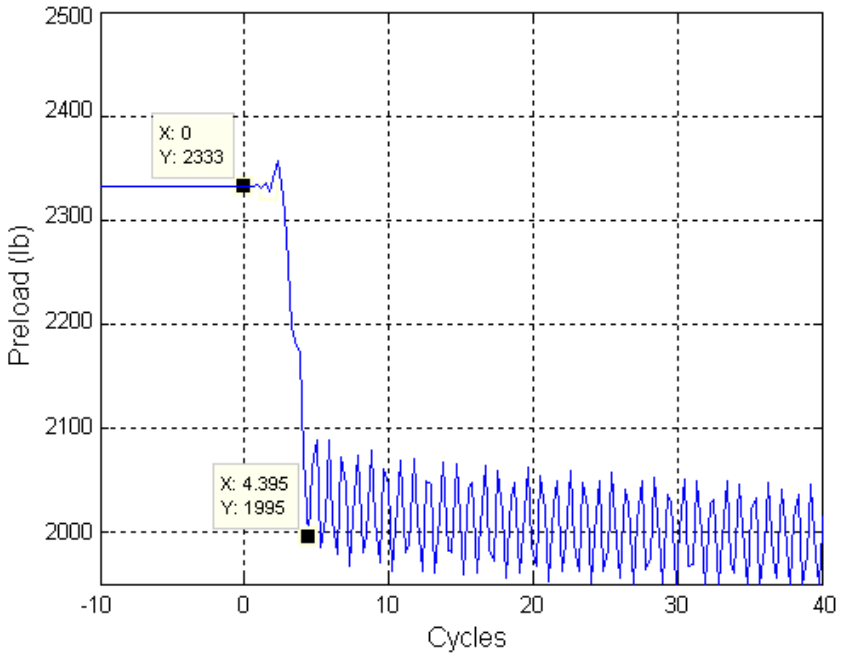

Figure B.26 Loss of initial preload for "Standard Heli-Coil with Loctite" run number 26.

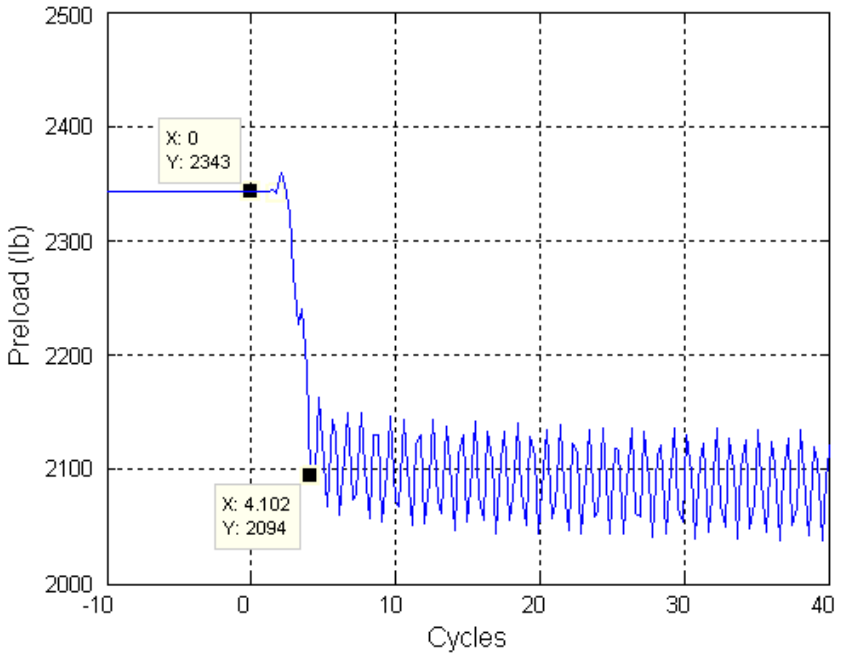

Figure B.27 Loss of initial preload for "Standard Heli-Coil with Loctite" run number 27.

Appendix B (continued)

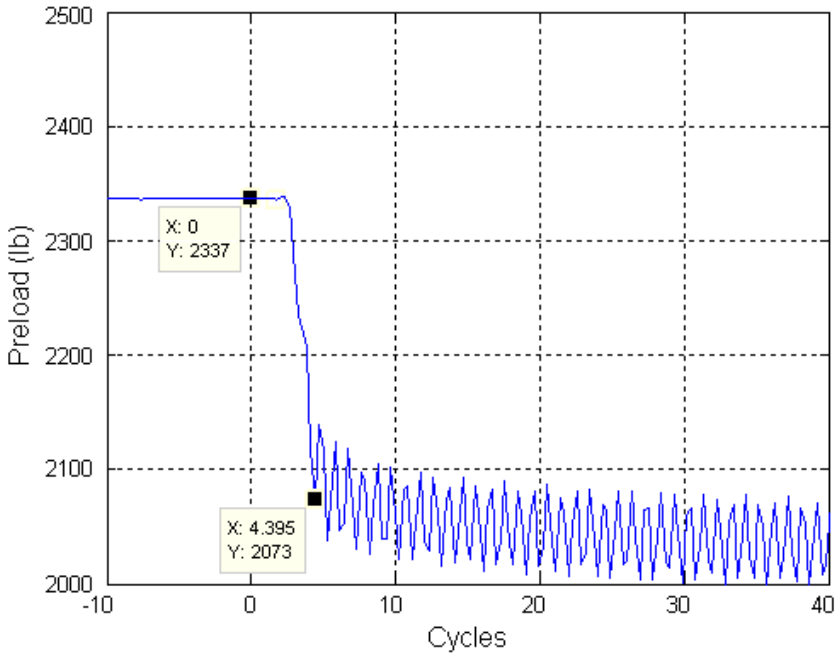

Figure B.28 Loss of initial preload for "Standard Heli-Coil with Loctite" run number 28.

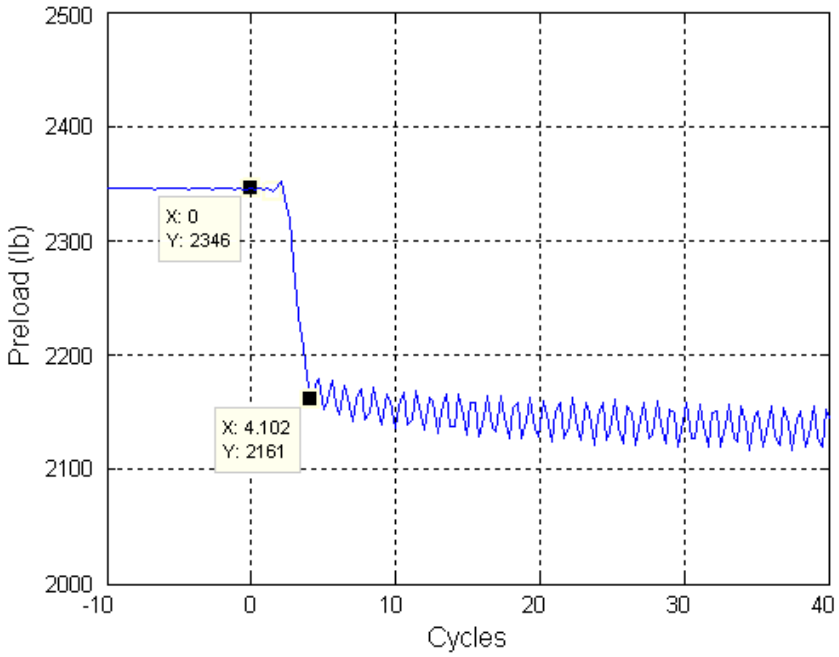

Figure B.29 Loss of initial preload for "Standard Heli-Coil with Loctite" run number 29.

Appendix B (continued)

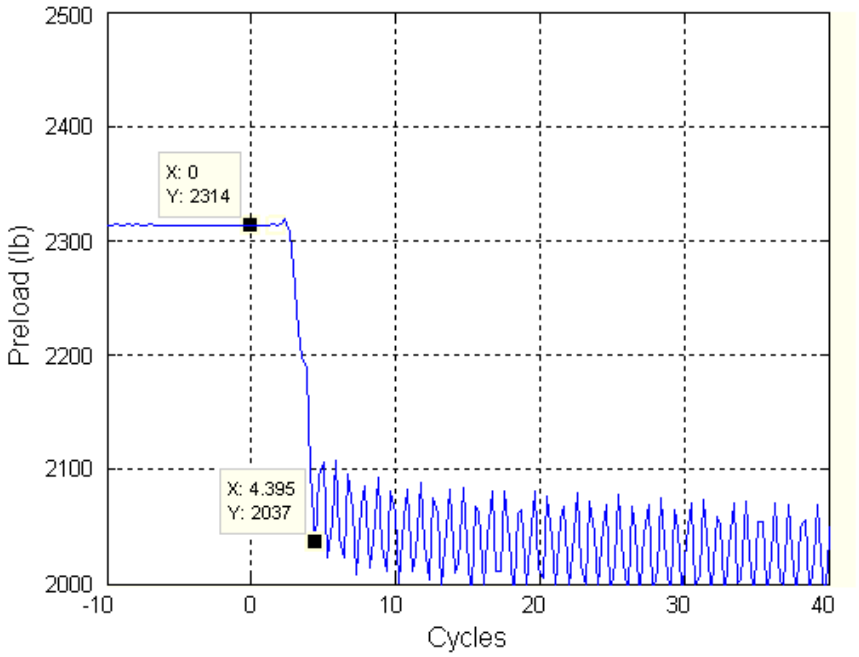

Figure B.30 Loss of initial preload for "Standard Heli-Coil with Loctite" run number 30.

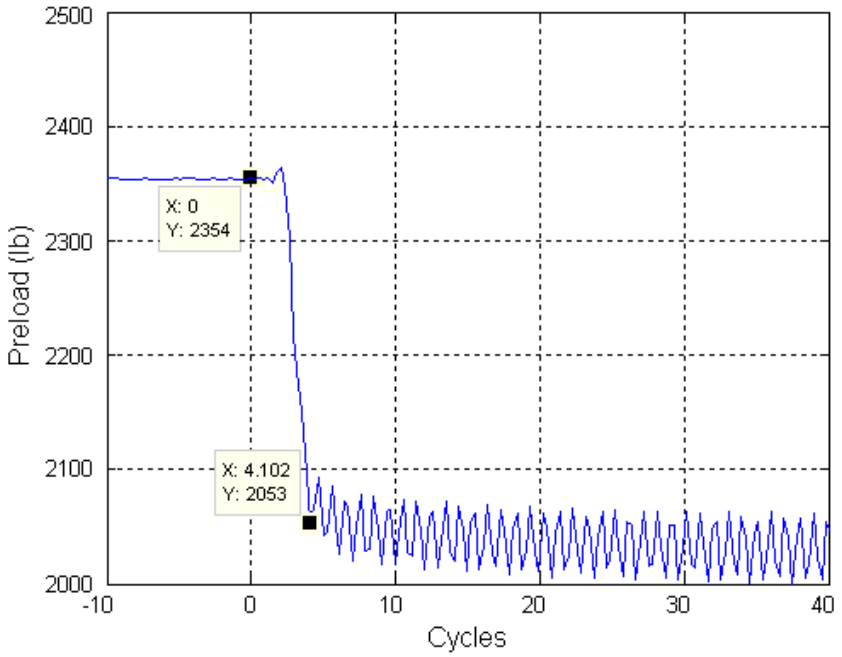

Figure B.31 Loss of initial preload for "Standard Heli-Coil with Loctite" run number 31.

Appendix B (continued)

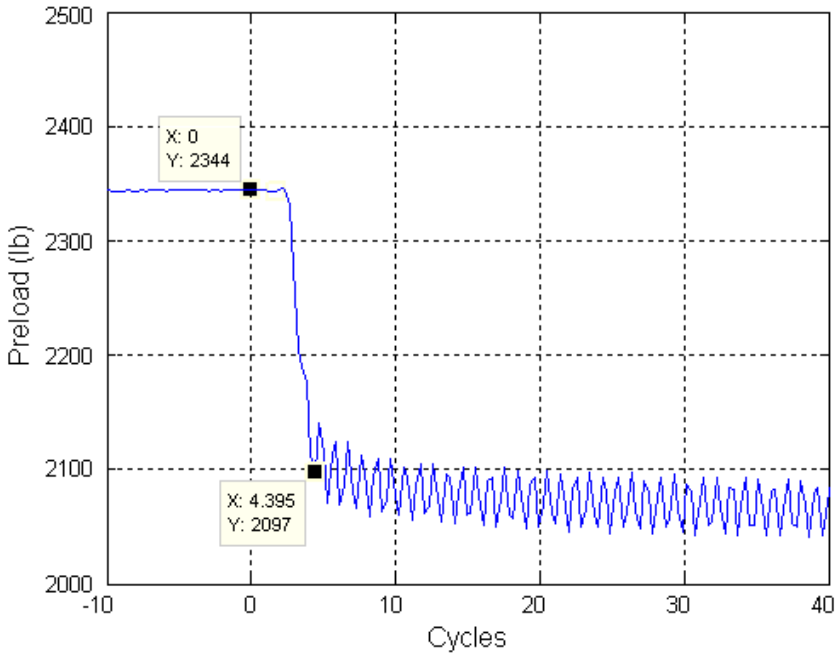

Figure B.32 Loss of initial preload for "Standard Heli-Coil with Loctite" run number 32.

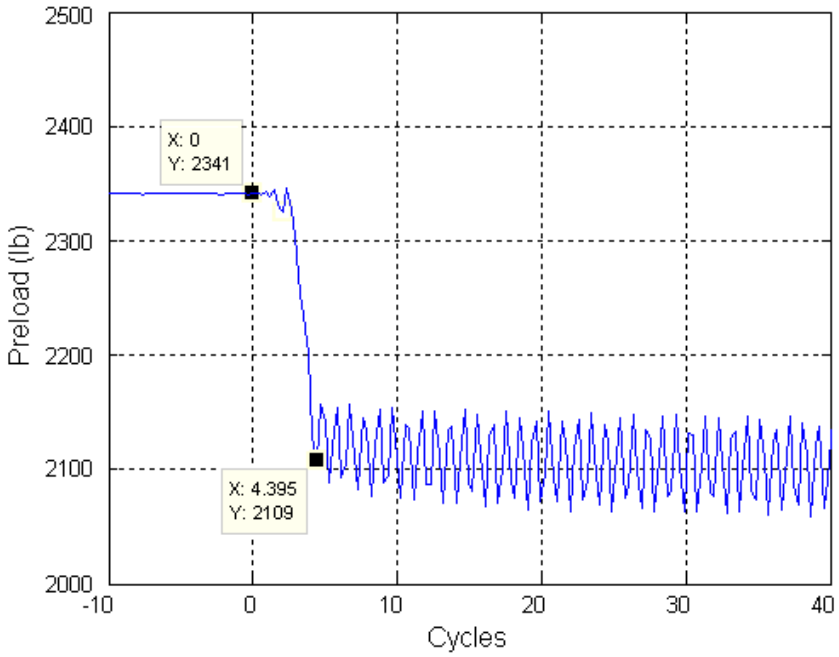

Figure B.33 Loss of initial preload for "Standard Heli-Coil with Loctite" run number 33.

Appendix B (continued)

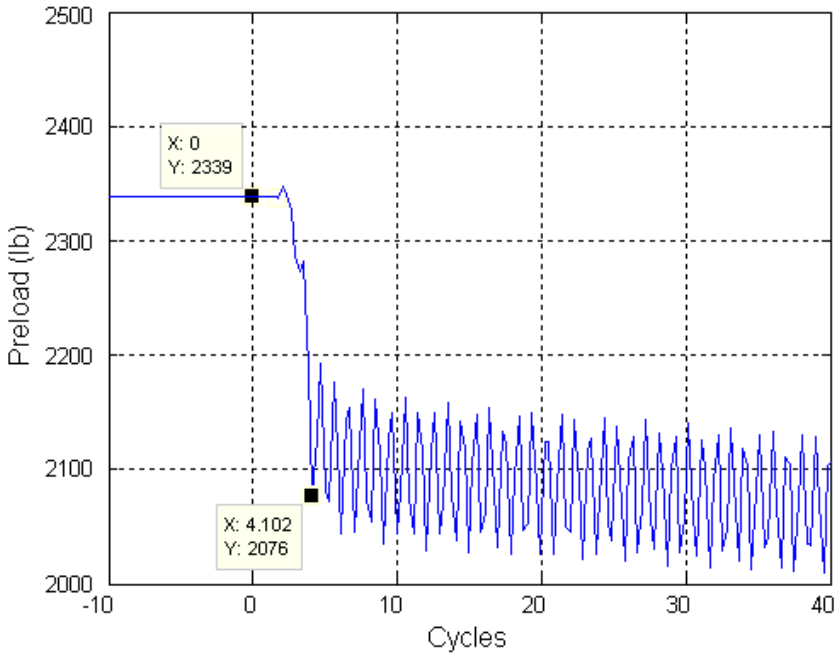

Figure B.34 Loss of initial preload for "Standard Heli-Coil with Loctite" run number 34.

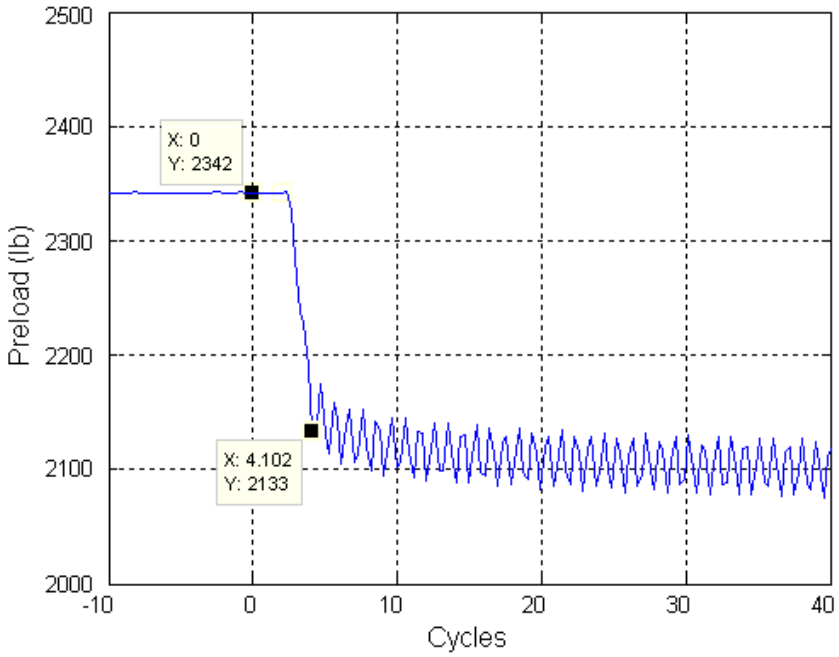

Figure B.35 Loss of initial preload for "Standard Heli-Coil with Loctite" run number 35.

Appendix B (continued)

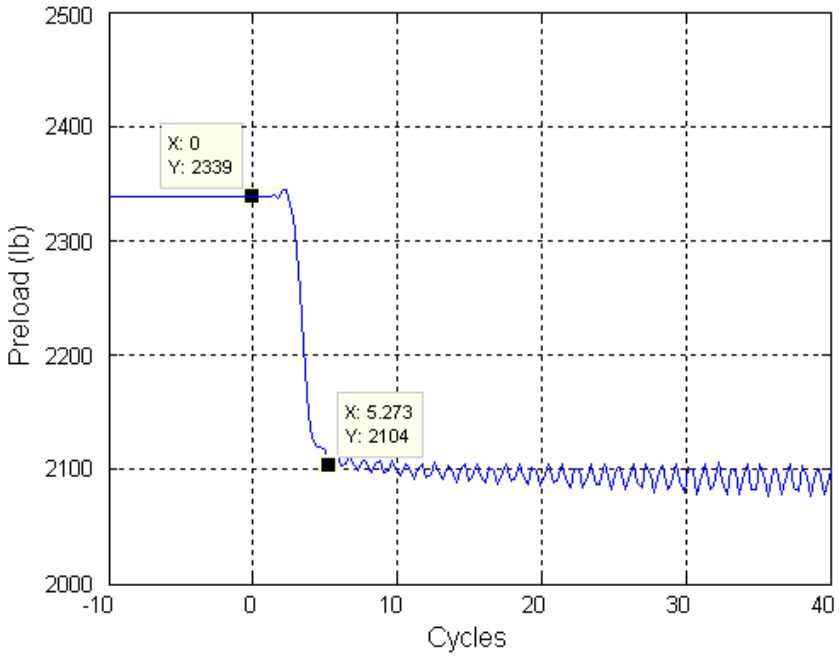

Figure B.36 Loss of initial preload for "Standard Heli-Coil with Loctite" run number 36.

Appendix C: Zoomed data plots for the initial rate of preload loss parameter

These plots were used in order to obtain the initial rate of preload loss used in Chapter 3.

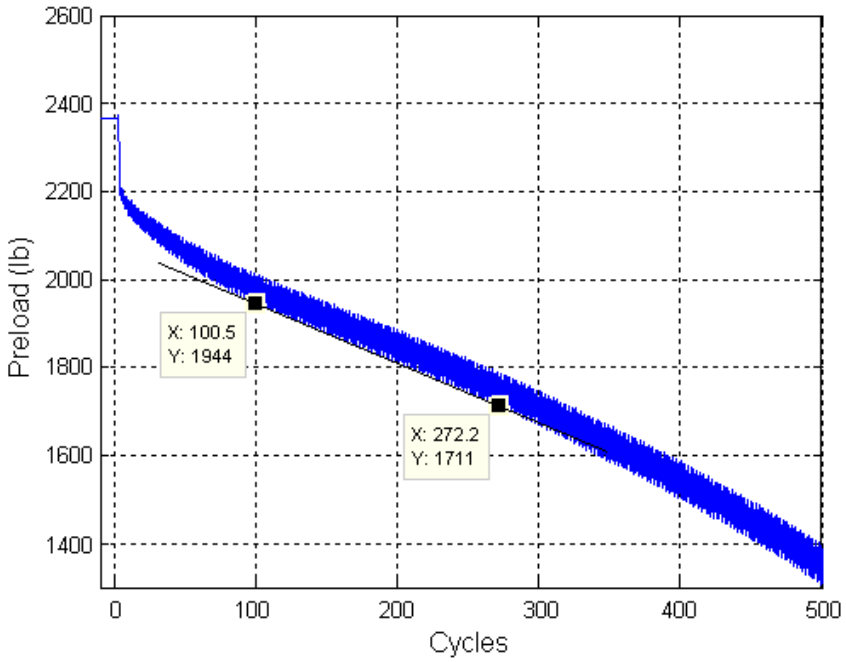

Figure C.1 Initial rate of preload loss for "Standard Heli-Coil with Braycote" run number 1.

Appendix C (continued)

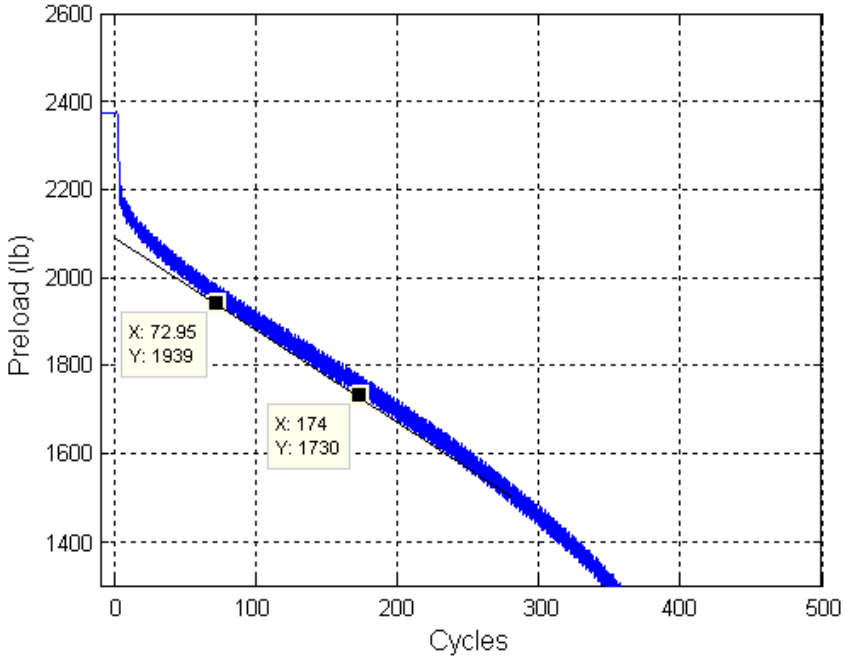

Figure C.2 Initial rate of preload loss for "Standard Heli-Coil with Braycote" run number 2.

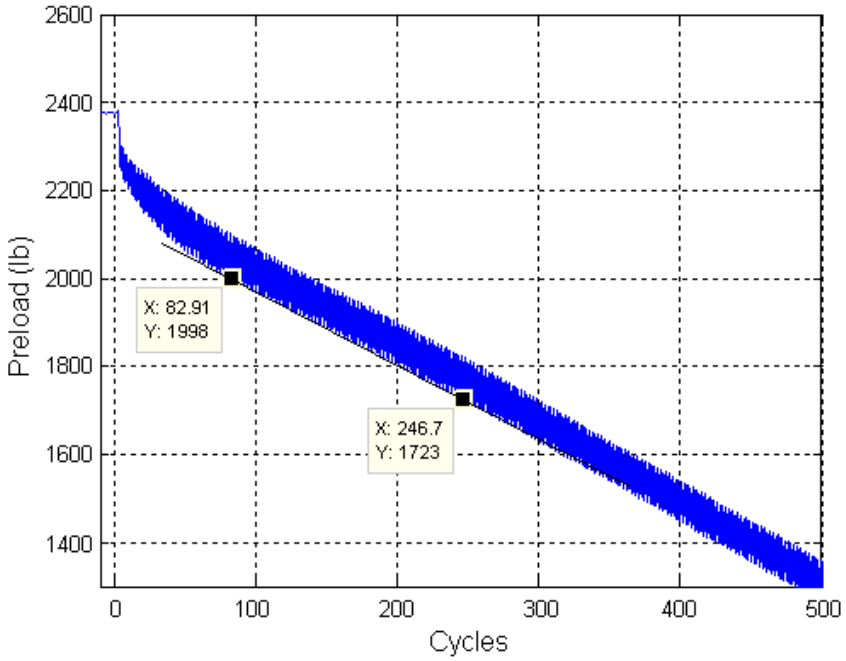

Figure C.3 Initial rate of preload loss for "Standard Heli-Coil with Braycote" run number 3.

Appendix C (continued)

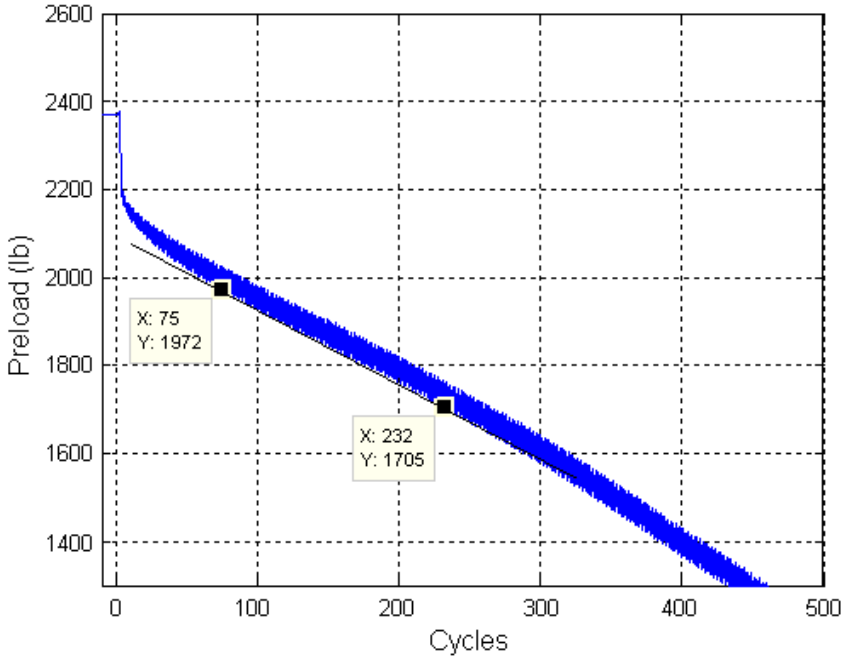

Figure C.4 Initial rate of preload loss for "Standard Heli-Coil with Braycote" run number 4.

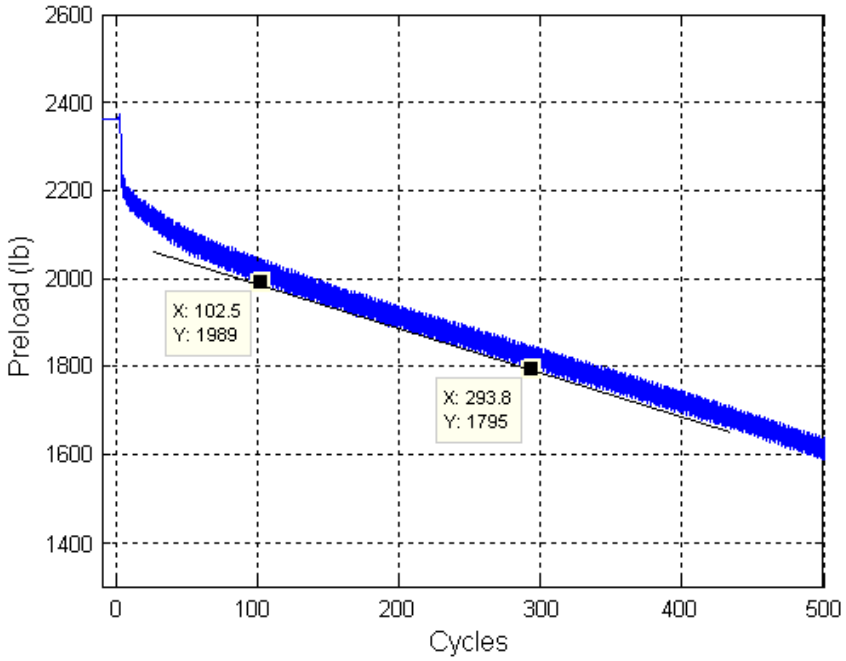

Figure C.5 Initial rate of preload loss for "Standard Heli-Coil with Braycote" run number 5.

Appendix C (continued)

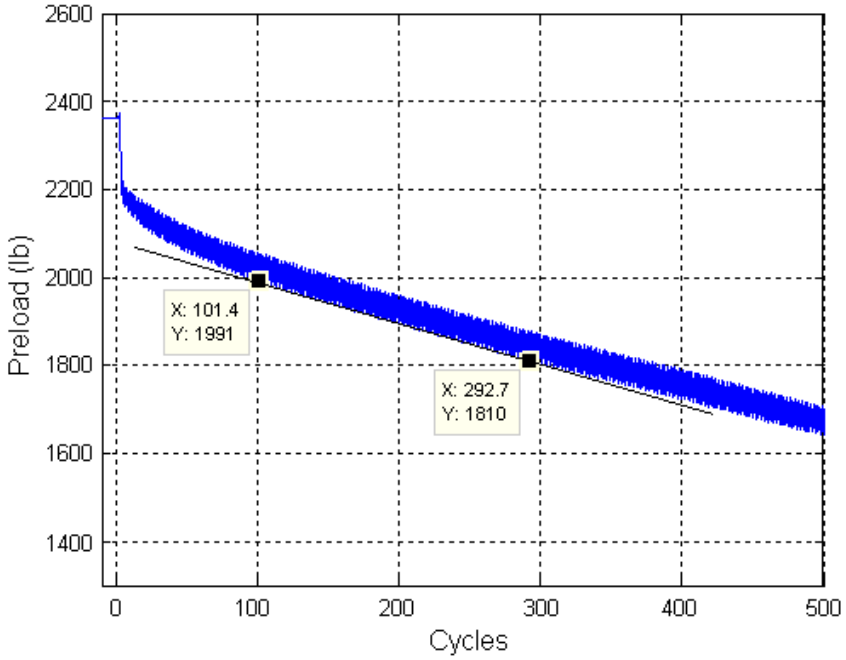

Figure C.6 Initial rate of preload loss for "Standard Heli-Coil with Braycote" run number 6.

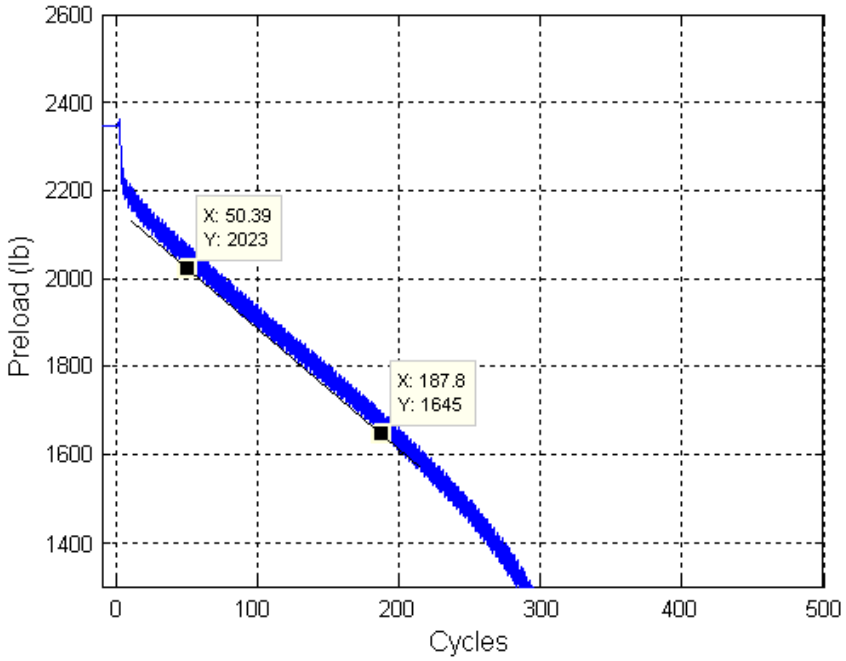

Figure C.7 Initial rate of preload loss for "Standard Heli-Coil with Braycote" run number 7.

Appendix C (continued)

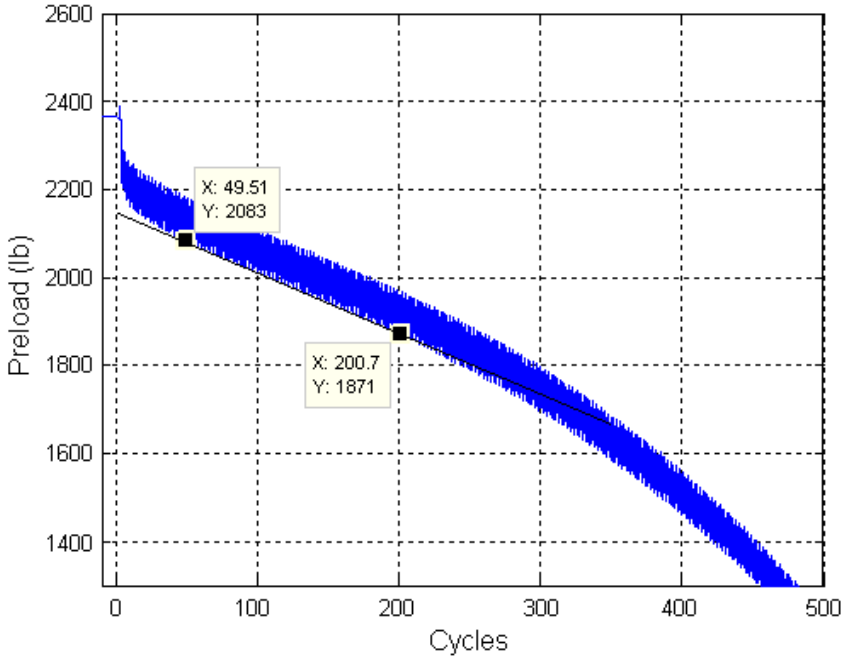

Figure C.8 Initial rate of preload loss for "Standard Heli-Coil with Braycote" run number 8.

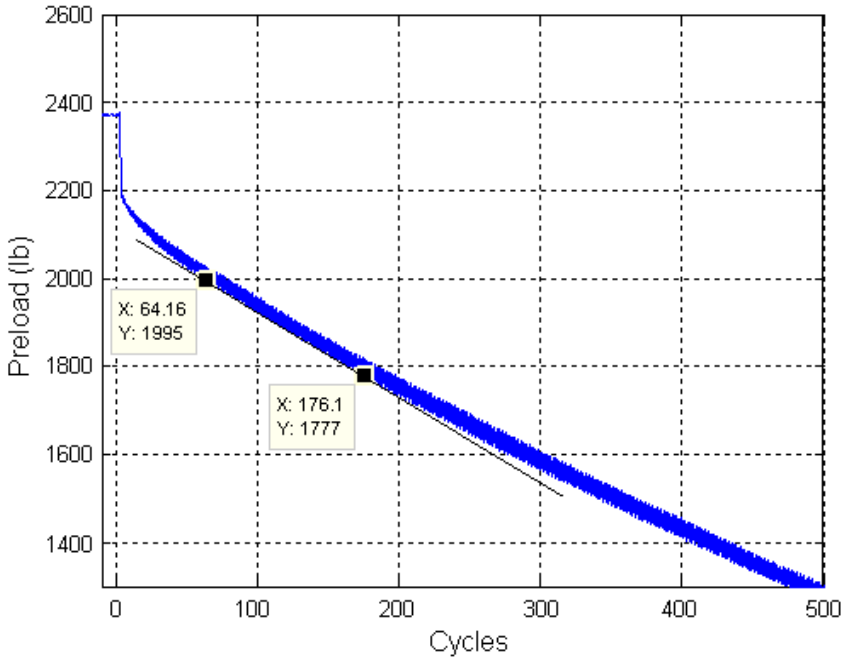

Figure C.9 Initial rate of preload loss for "Standard Heli-Coil with Braycote" run number 9.

Appendix C (continued)

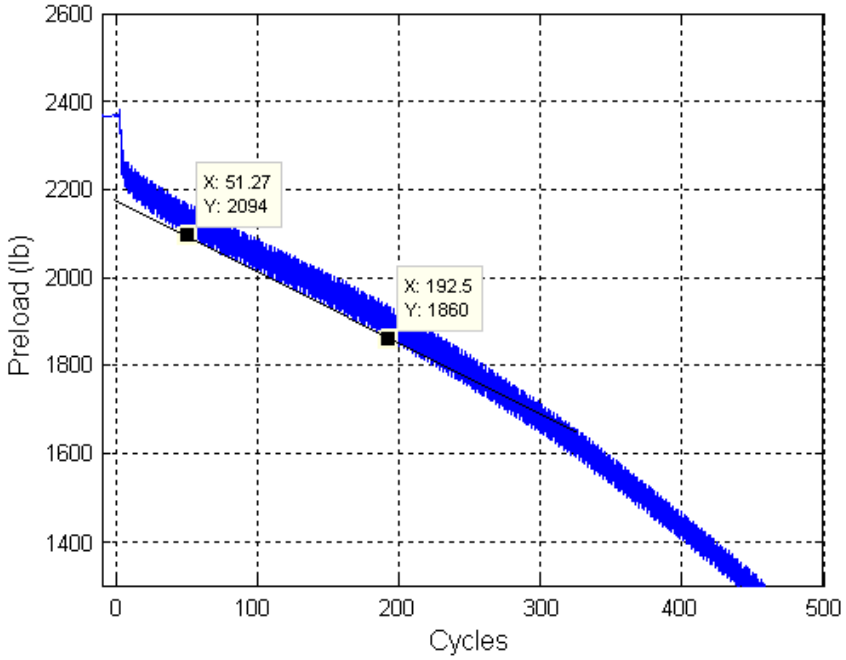

Figure C.10 Initial rate of preload loss for "Standard Heli-Coil with Braycote" run number 10.

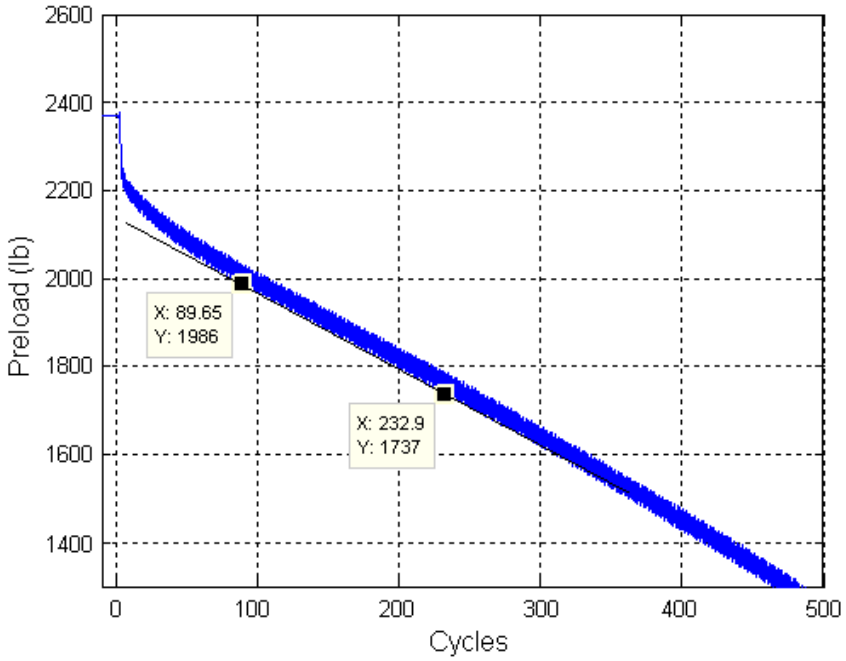

Figure C.11 Initial rate of preload loss for "Standard Heli-Coil with Braycote" run number 11.

Appendix C (continued)

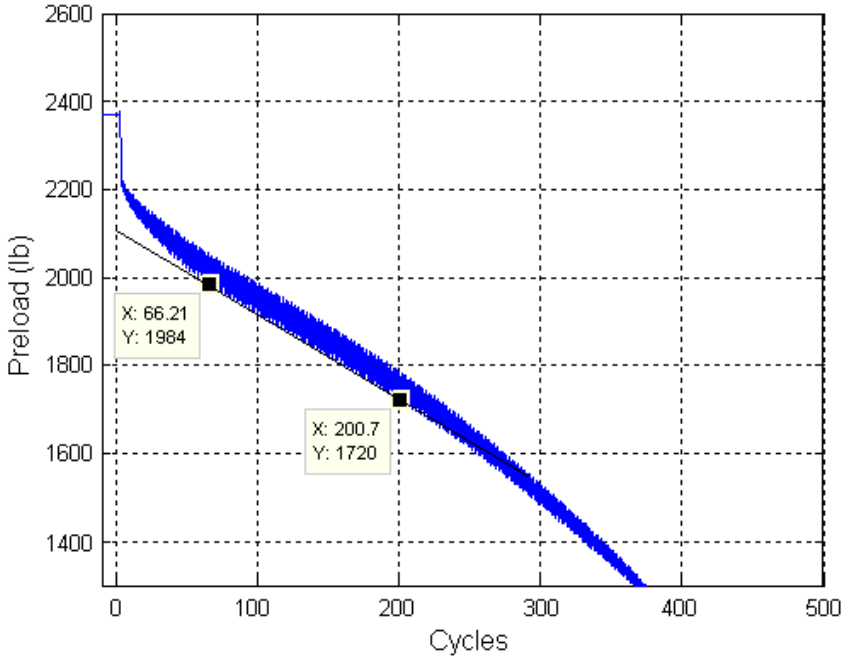

Figure C.12 Initial rate of preload loss for "Standard Heli-Coil with Braycote" run number 12.

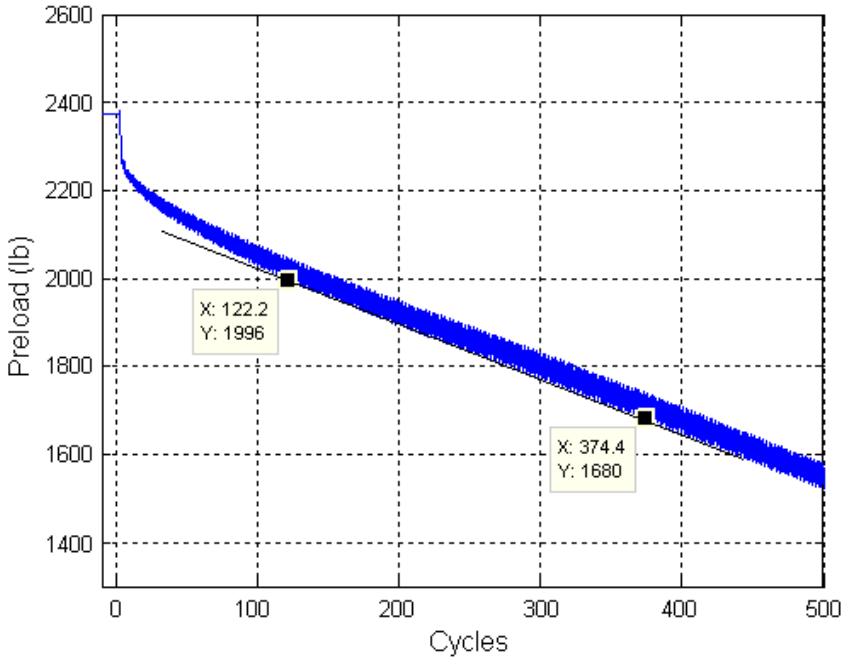

Figure C.13 Initial rate of preload loss for "Locking Heli-Coil with Braycote" run number 13.

Appendix C (continued)

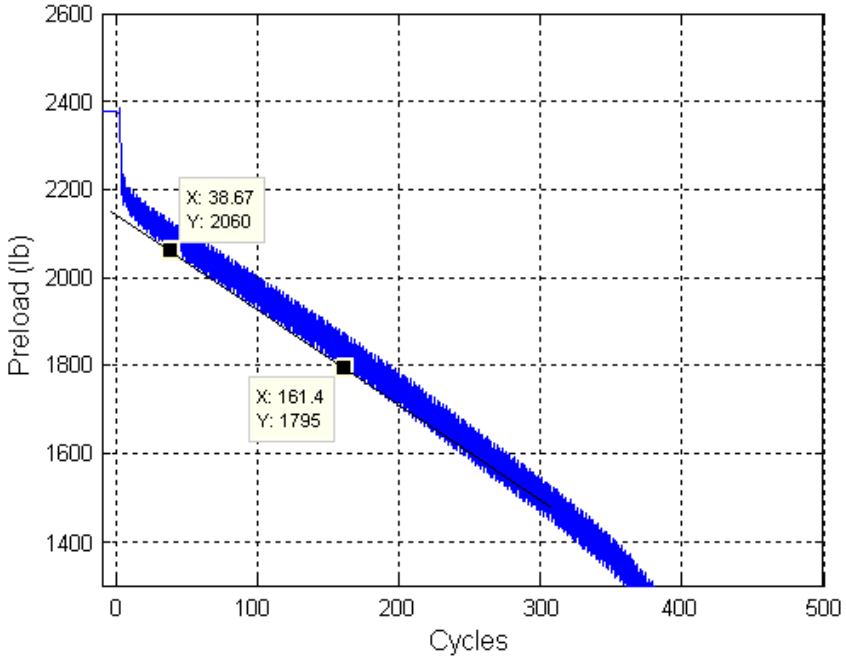

Figure C.14 Initial rate of preload loss for "Locking Heli-Coil with Braycote" run number 14.

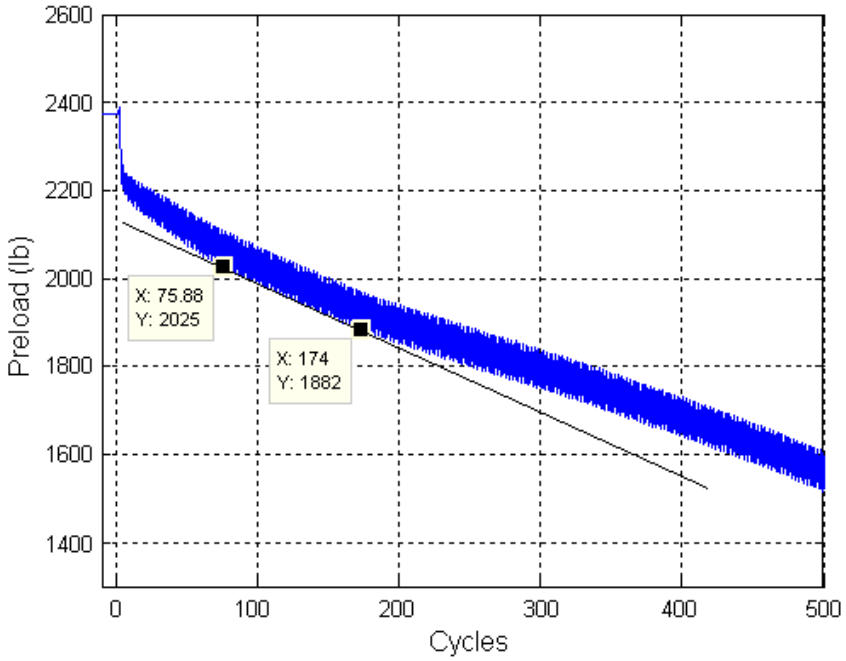

Figure C.15 Initial rate of preload loss for "Locking Heli-Coil with Braycote" run number 15.

Appendix C (continued)

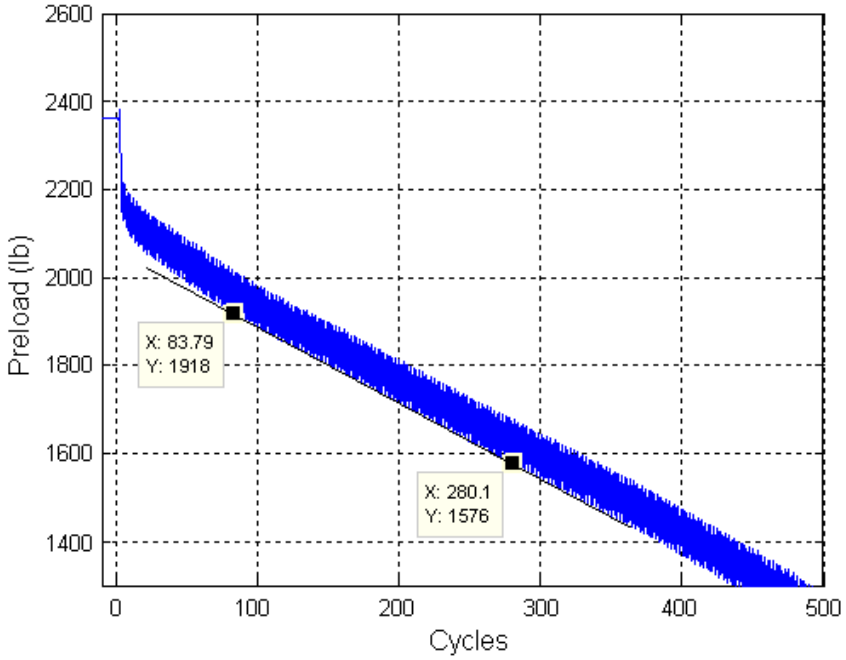

Figure C.16 Initial rate of preload loss for "Locking Heli-Coil with Braycote" run number 16.

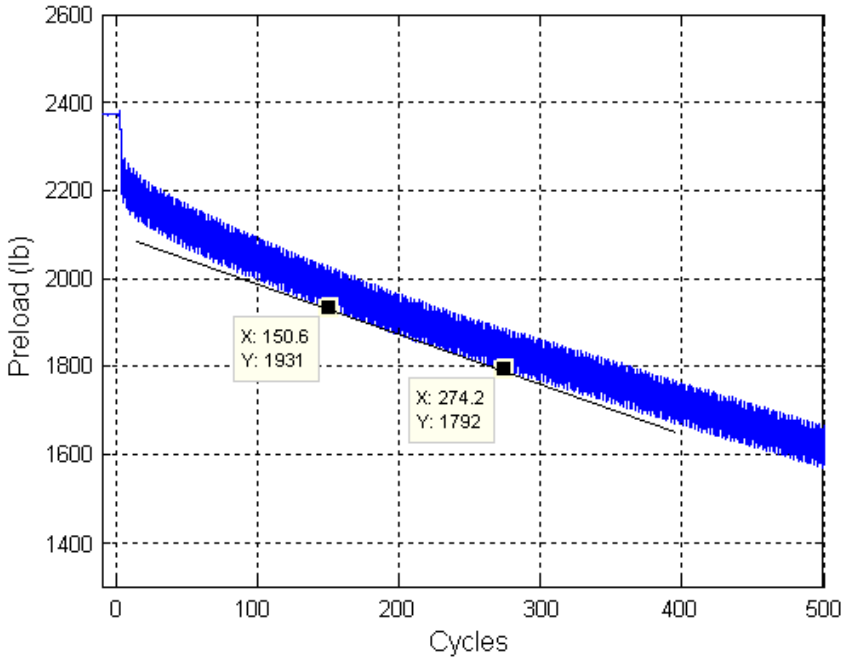

Figure C.17 Initial rate of preload loss for "Locking Heli-Coil with Braycote" run number 17.

Appendix C (continued)

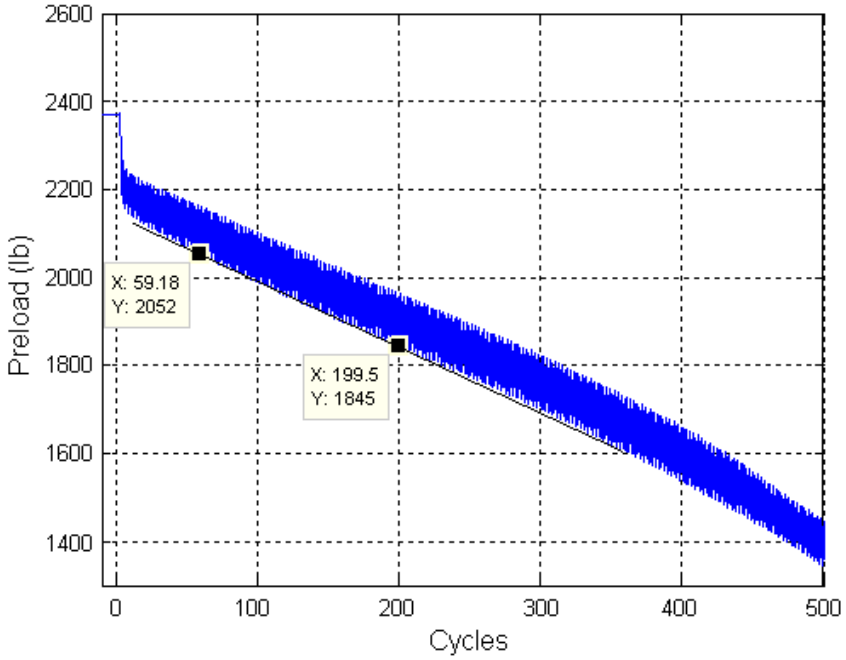

Figure C.18 Initial rate of preload loss for "Locking Heli-Coil with Braycote" run number 18.

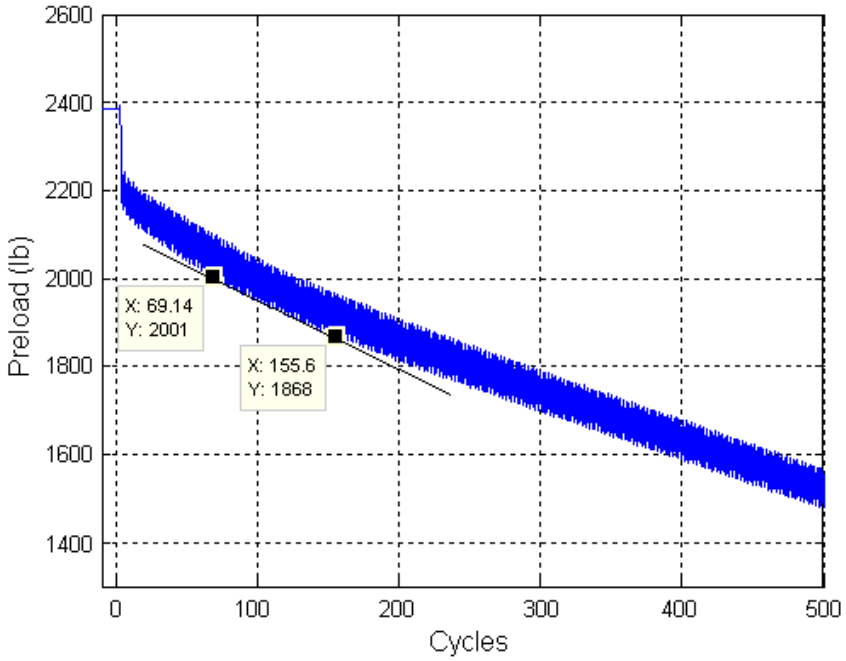

Figure C.19 Initial rate of preload loss for "Locking Heli-Coil with Braycote" run number 19.

Appendix C (continued)

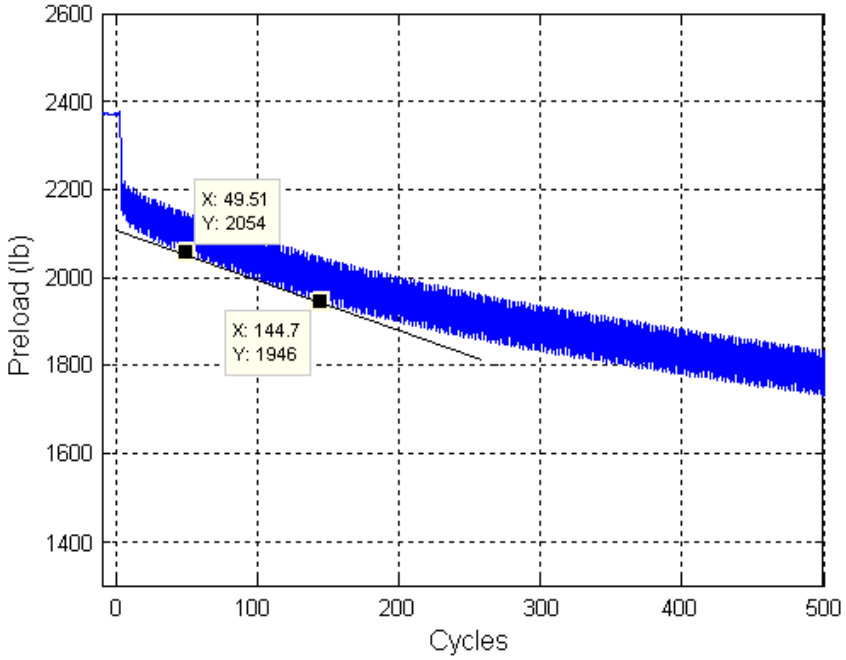

Figure C.20 Initial rate of preload loss for "Locking Heli-Coil with Braycote" run number 20.

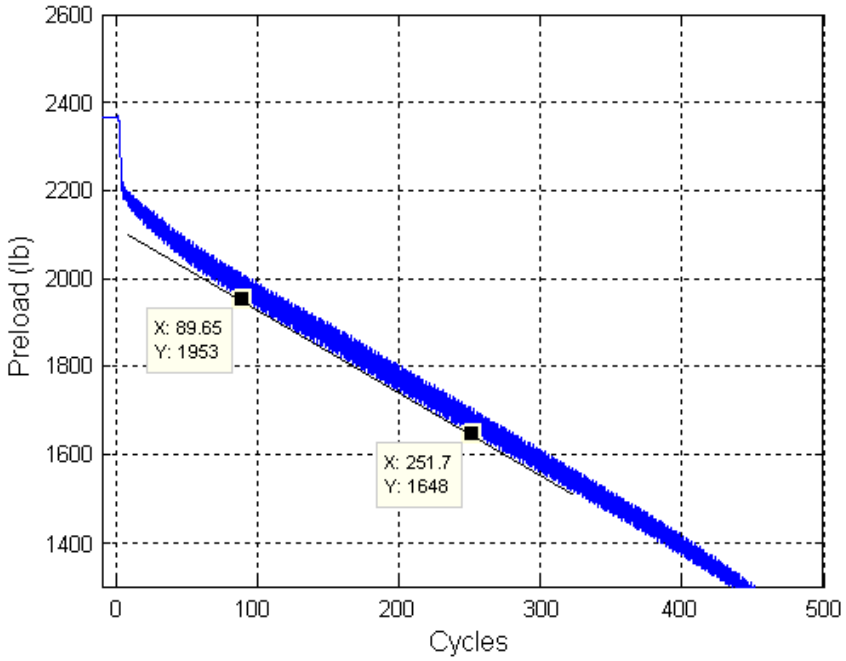

Figure C.21 Initial rate of preload loss for "Locking Heli-Coil with Braycote" run number 21.

Appendix C (continued)

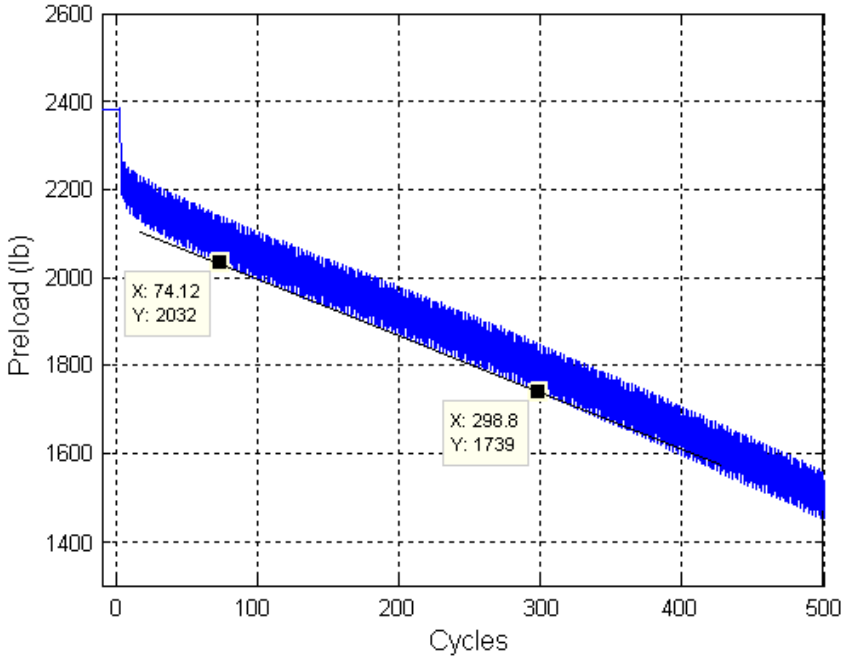

Figure C.22 Initial rate of preload loss for "Locking Heli-Coil with Braycote" run number 22.

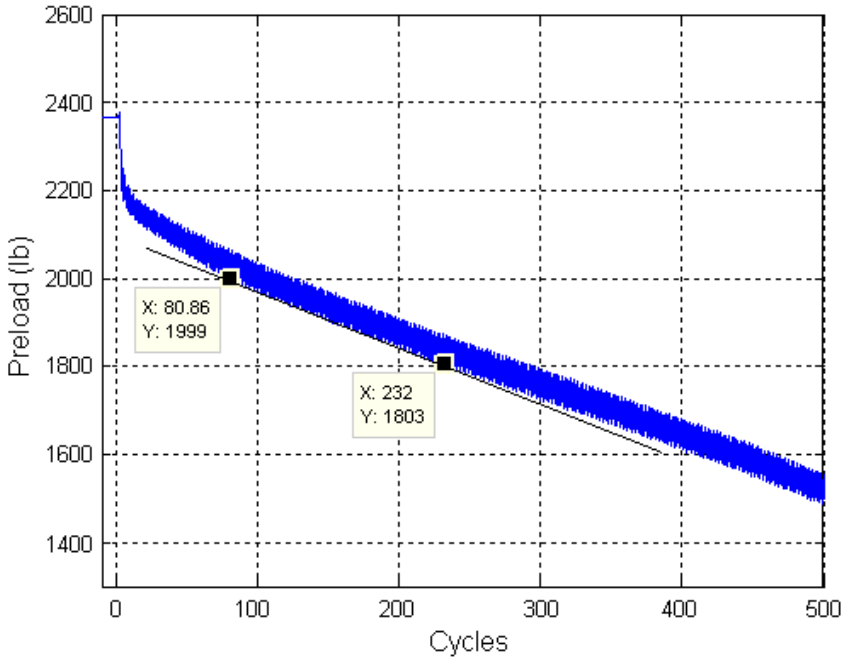

Figure C.23 Initial rate of preload loss for "Locking Heli-Coil with Braycote" run number 23.

Appendix C (continued)

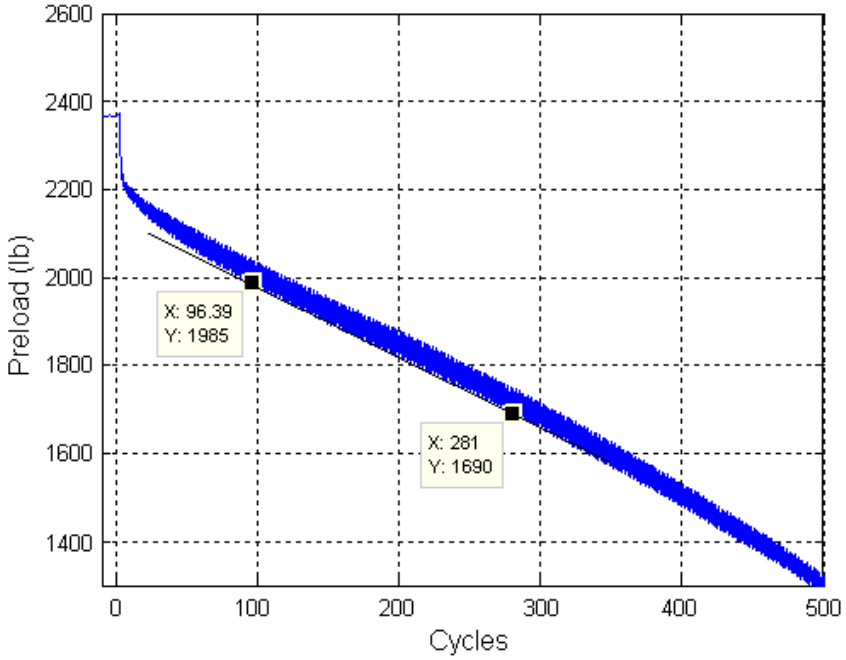

Figure C.24 Initial rate of preload loss for "Locking Heli-Coil with Braycote" run number 24.

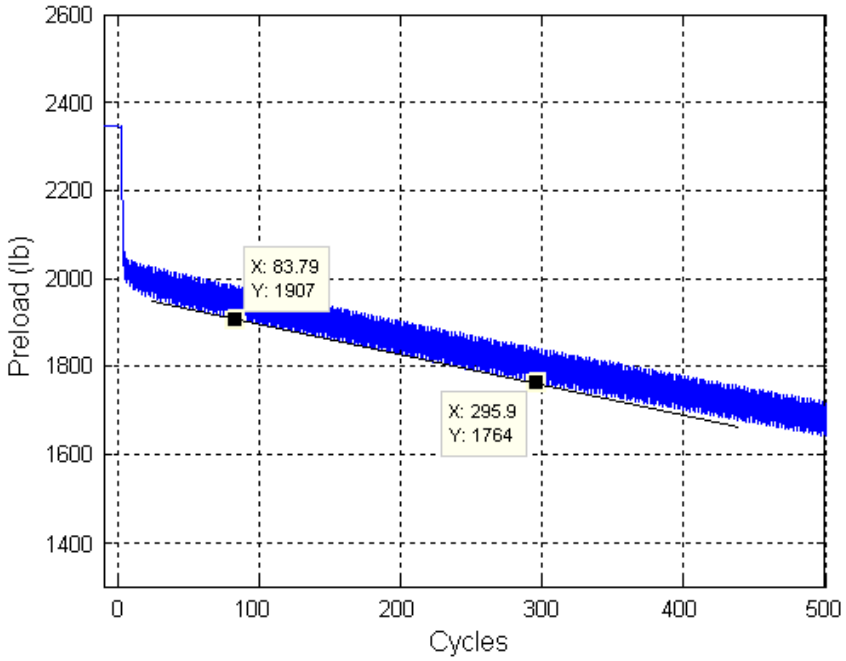

Figure C.25 Initial rate of preload loss for "Standard Heli-Coil with Loctite" run number 25.

Appendix C (continued)

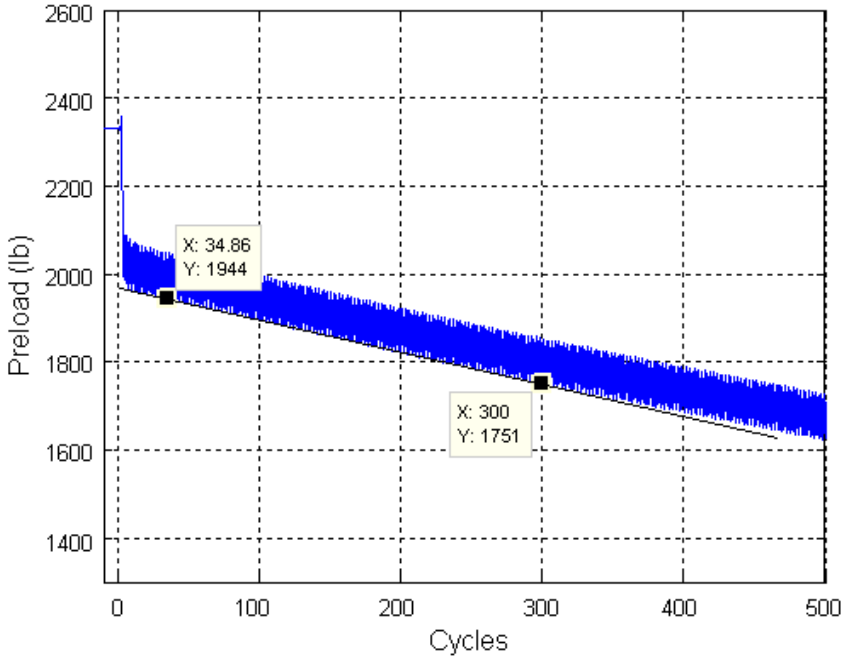

Figure C.26 Initial rate of preload loss for "Standard Heli-Coil with Loctite" run number 26.

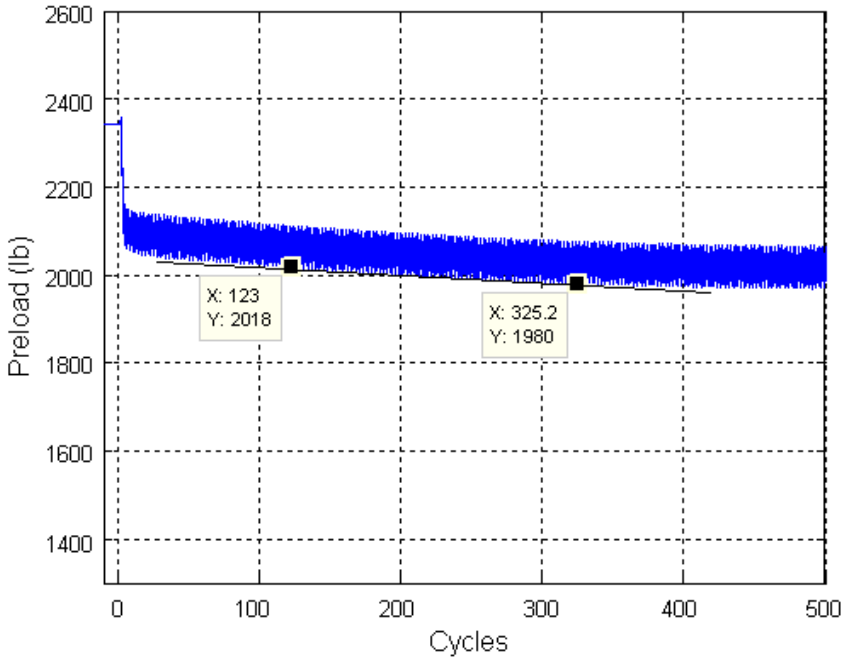

Figure C.27 Initial rate of preload loss for "Standard Heli-Coil with Loctite" run number 27.

Appendix C (continued)

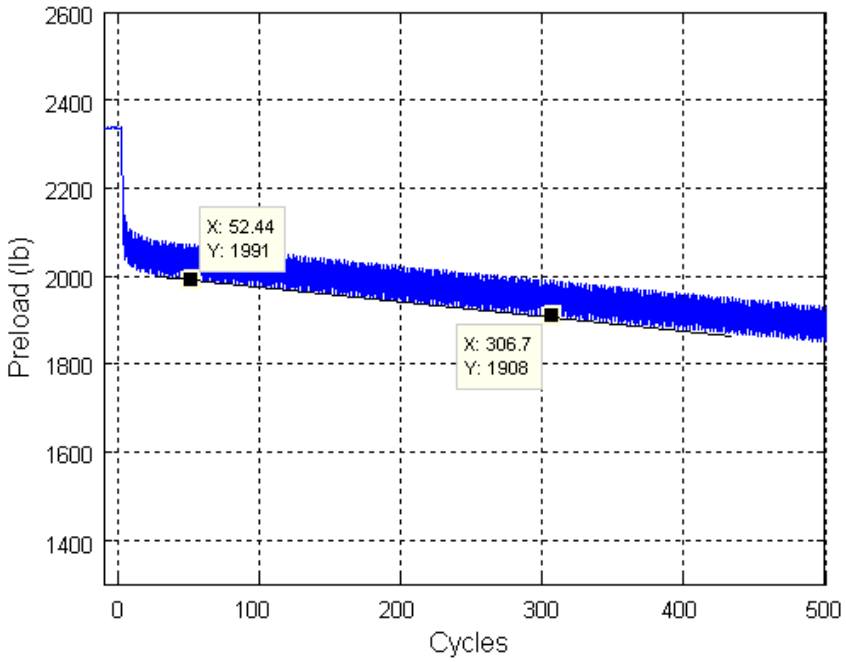

Figure C.28 Initial rate of preload loss for "Standard Heli-Coil with Loctite" run number 28.

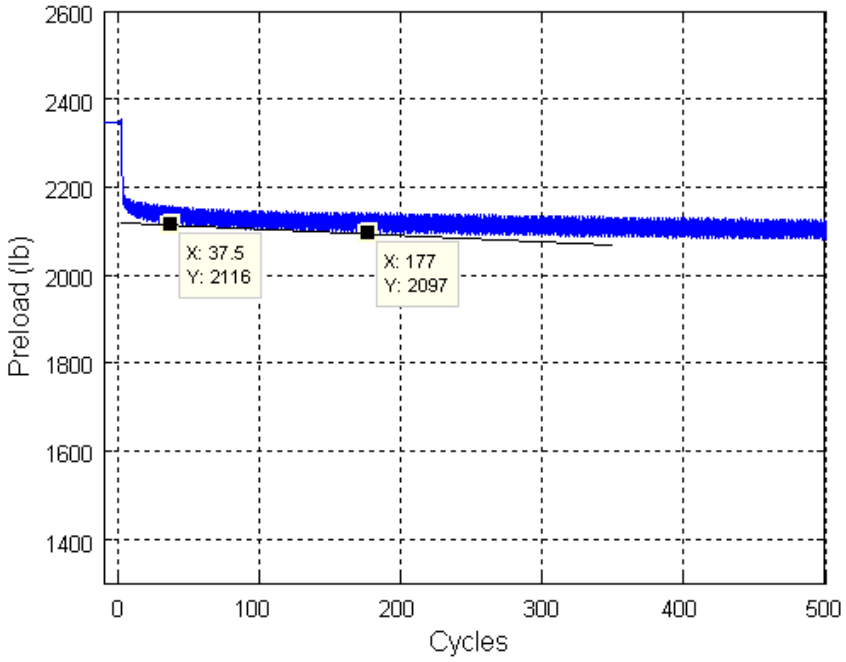

Figure C.29 Initial rate of preload loss for "Standard Heli-Coil with Loctite" run number 29.

Appendix C (continued)

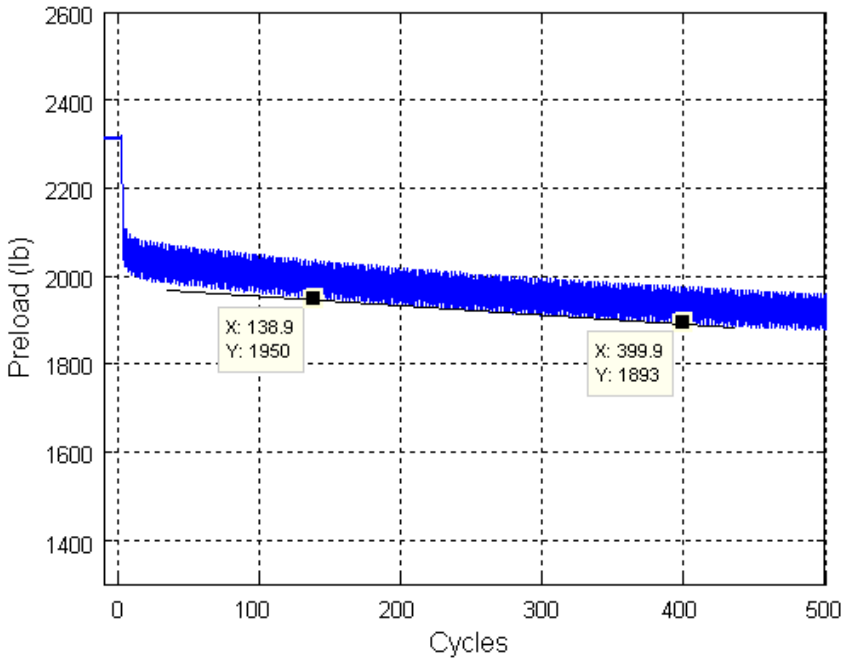

Figure C.30 Initial rate of preload loss for "Standard Heli-Coil with Loctite" run number 30.

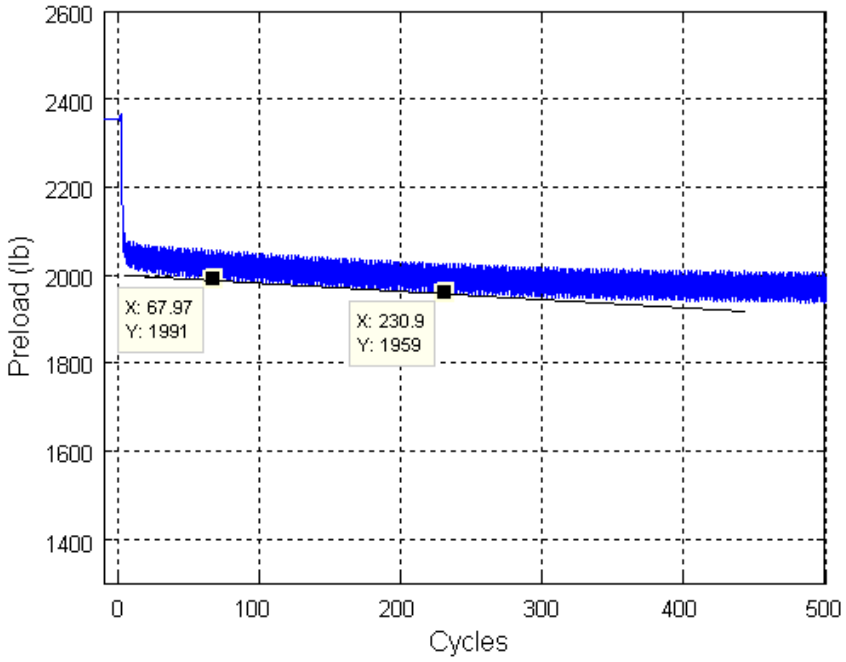

Figure C.31 Initial rate of preload loss for "Standard Heli-Coil with Loctite" run number 31.

Appendix C (continued)

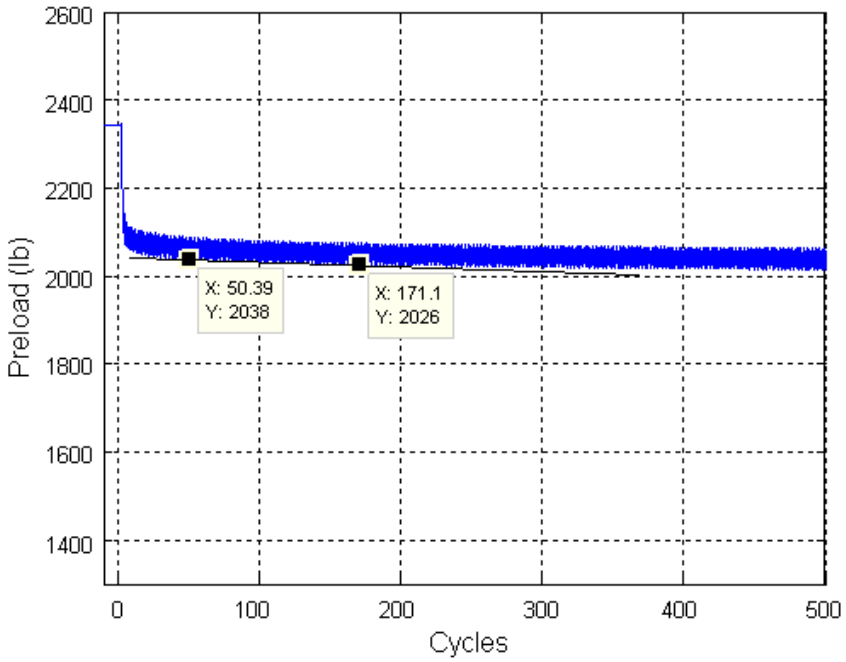

Figure C.32 Initial rate of preload loss for "Standard Heli-Coil with Loctite" run number 32.

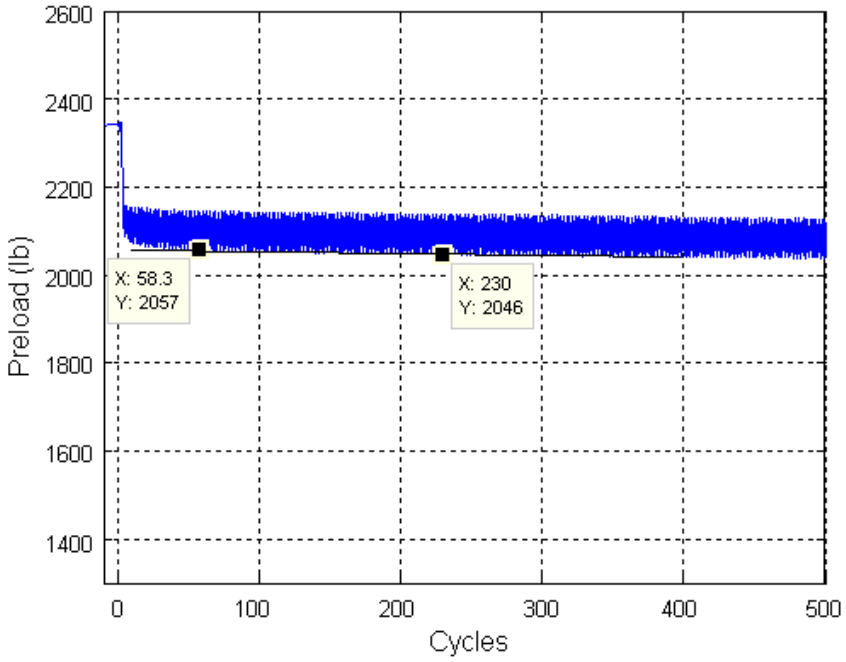

Figure C.33 Initial rate of preload loss for "Standard Heli-Coil with Loctite" run number 33.

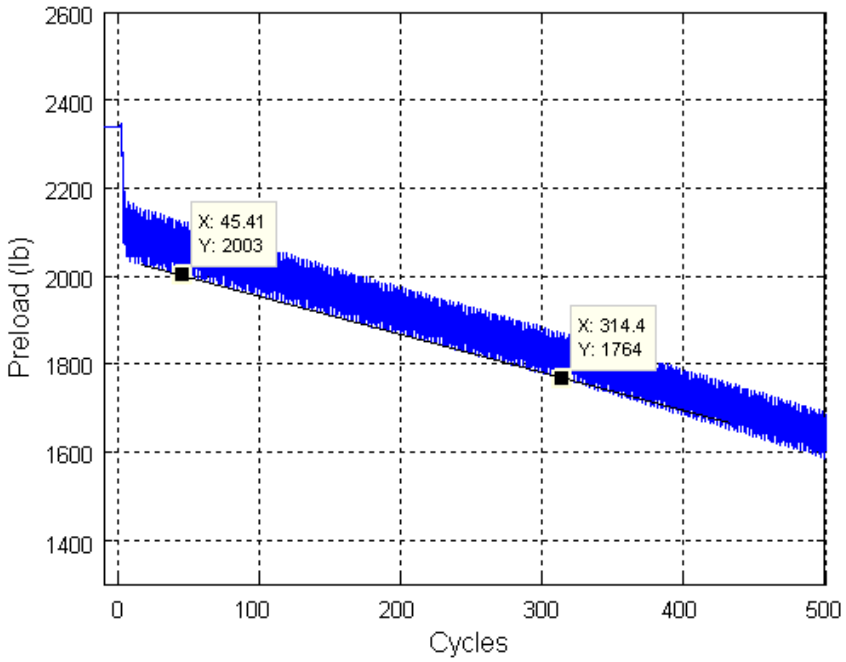

Figure C.34 Initial rate of preload loss for "Standard Heli-Coil with Loctite" run number 34.

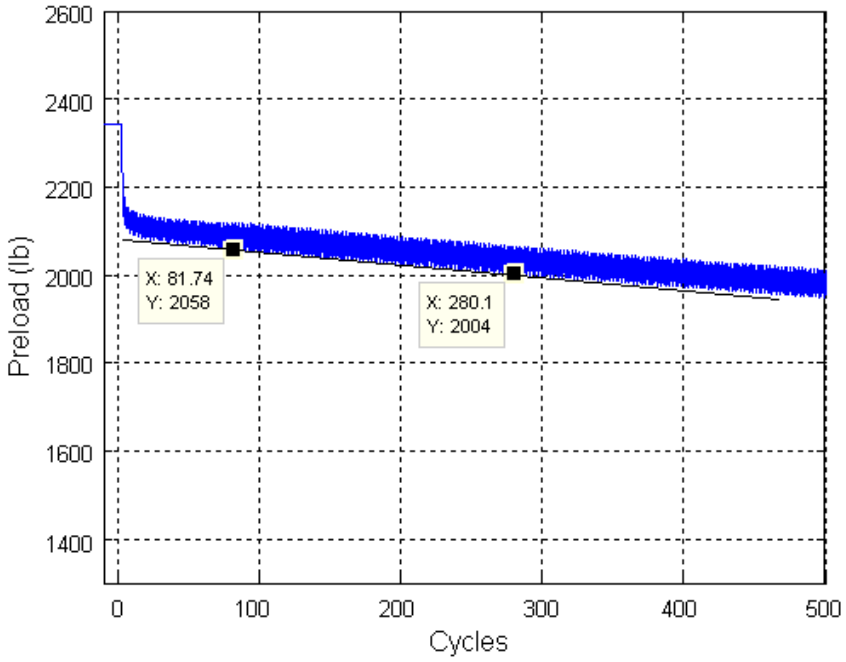

Figure C.35 Initial rate of preload loss for "Standard Heli-Coil with Loctite" run number 35.

Appendix C (continued)

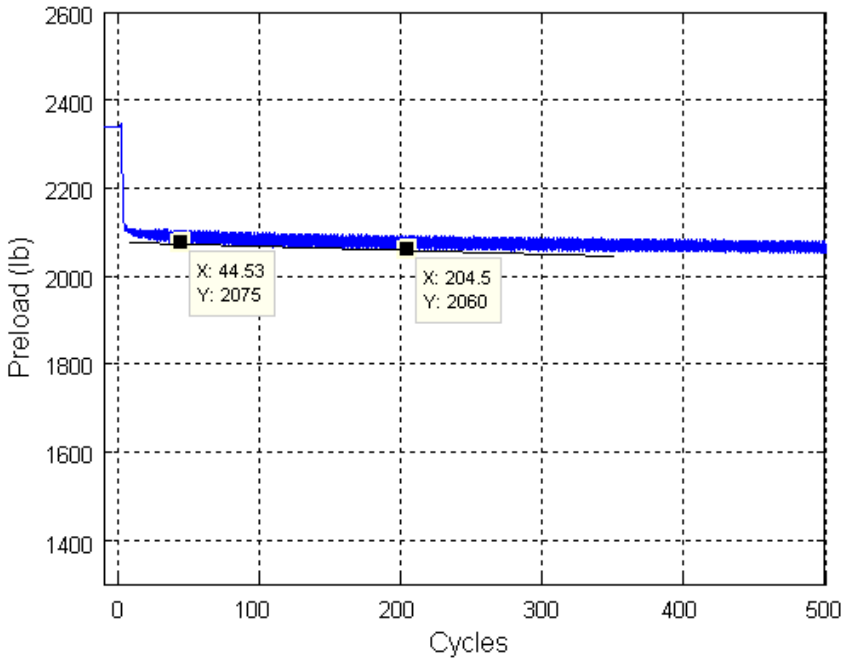

Figure C.36 Initial rate of preload loss for "Standard Heli-Coil with Loctite" run number 36.

Appendix D: Zoomed data plots for the secondary rate of preload loss parameter

These plots were used in order to obtain the secondary rate of preload loss in Chapter 3.

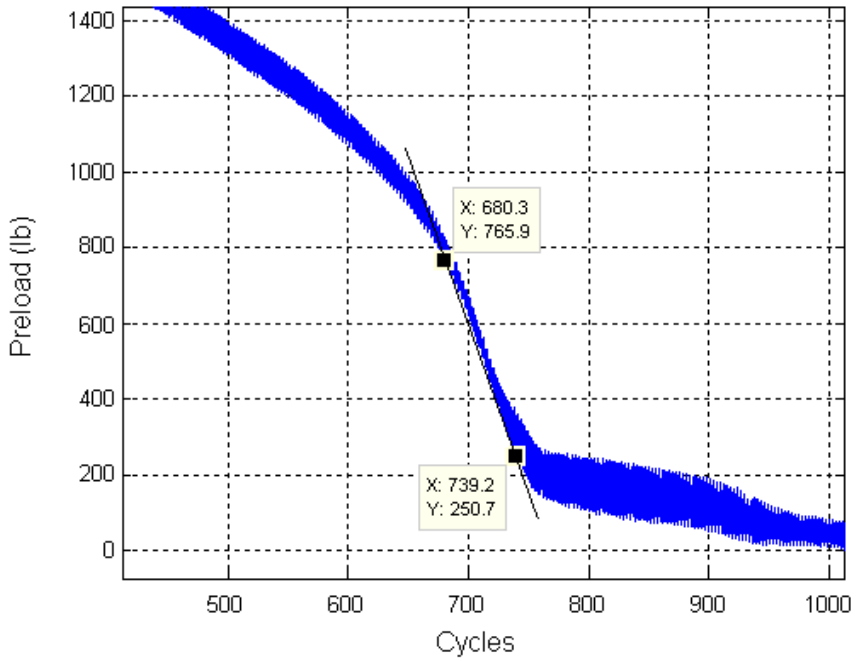

Figure D.1 Secondary rate of preload loss for "Standard Heli-Coil with Braycote" run number 1.

Appendix D (continued)

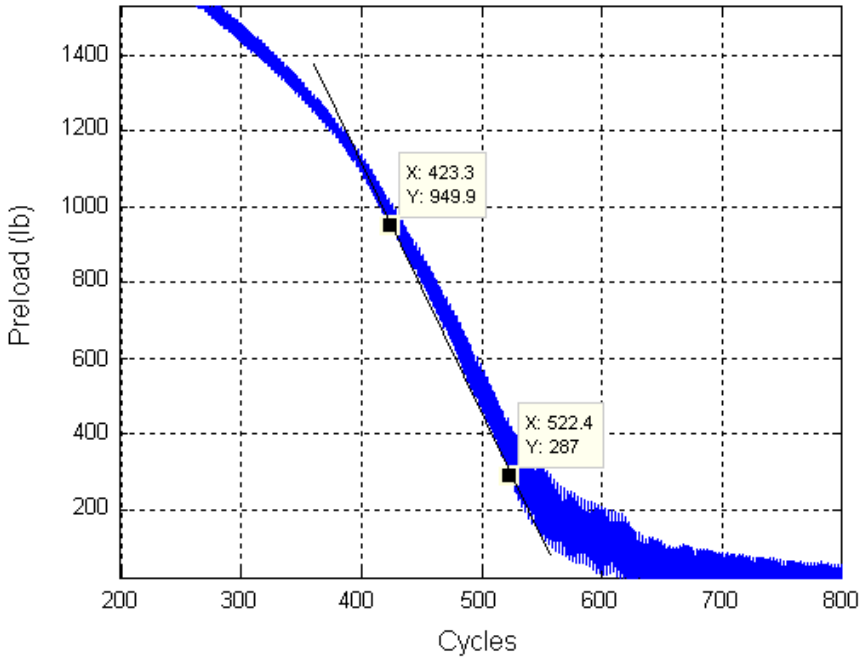

Figure D.2 Secondary rate of preload loss for "Standard Heli-Coil with Braycote" run number 2.

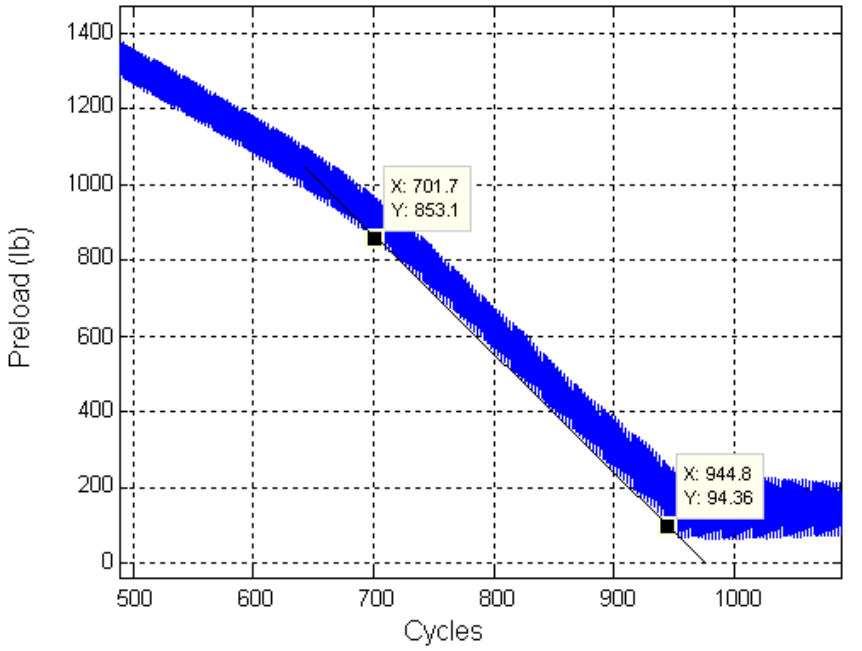

Figure D.3 Secondary rate of preload loss for "Standard Heli-Coil with Braycote" run number 3.

Appendix D (continued)

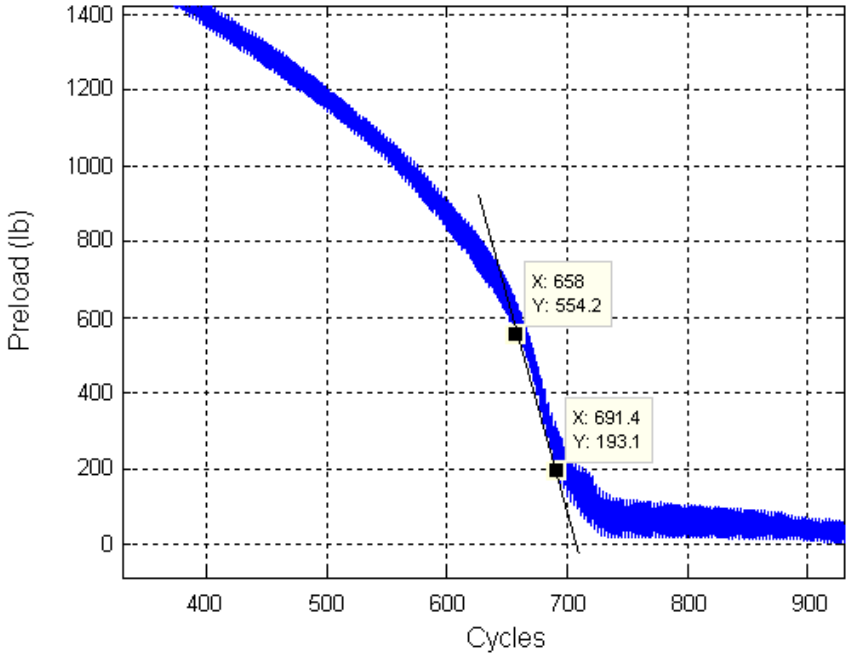

Figure D.4 Secondary rate of preload loss for "Standard Heli-Coil with Braycote" run number 4.

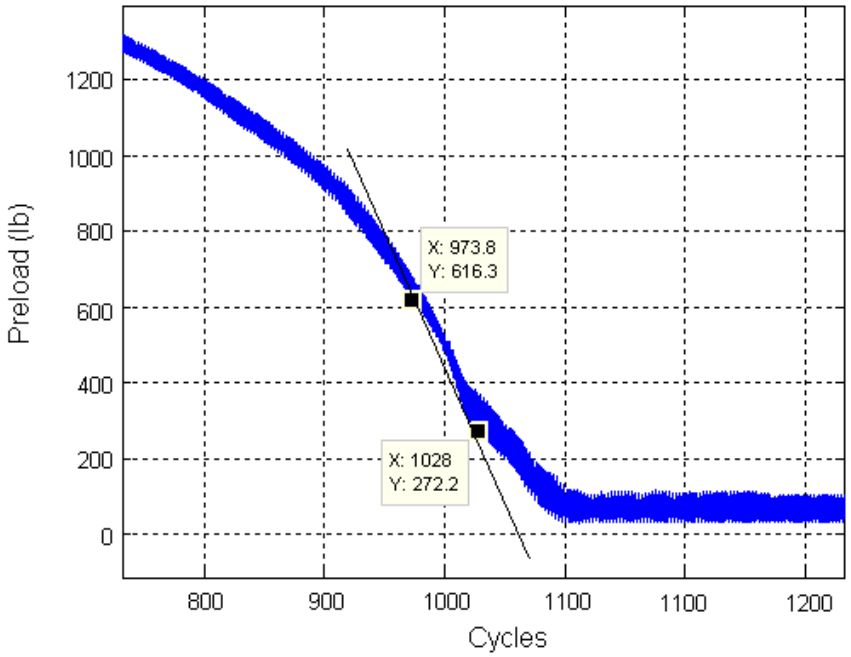

Figure D.5 Secondary rate of preload loss for "Standard Heli-Coil with Braycote" run number 5.

Appendix D (continued)

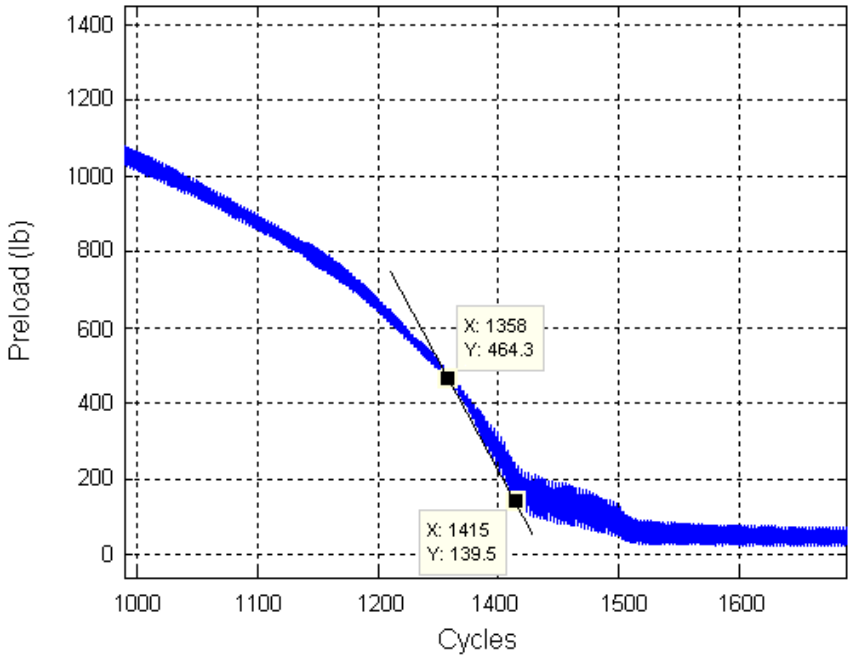

Figure D.6 Secondary rate of preload loss for "Standard Heli-Coil with Braycote" run number 6.

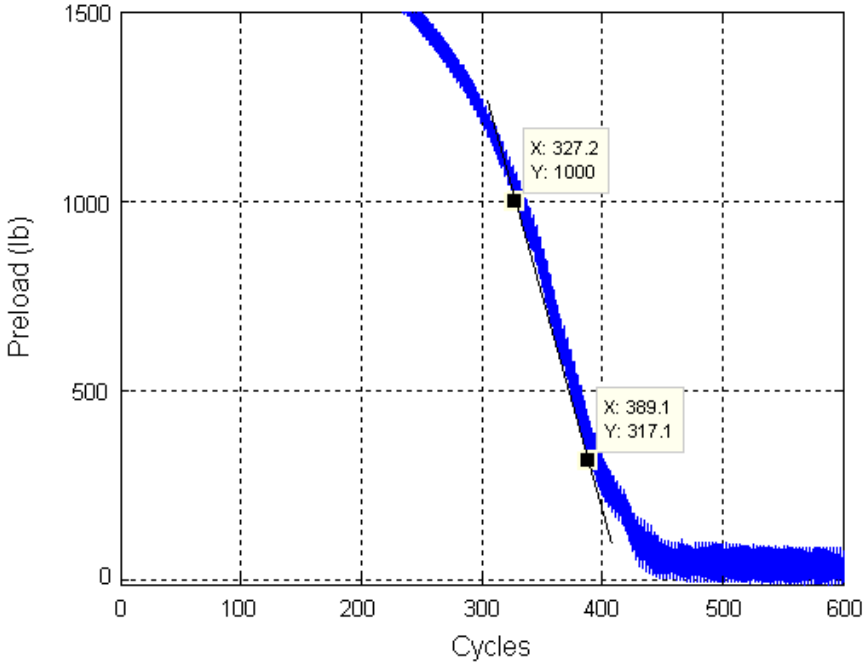

Figure D.7 Secondary rate of preload loss for "Standard Heli-Coil with Braycote" run number 7.

Appendix D (continued)

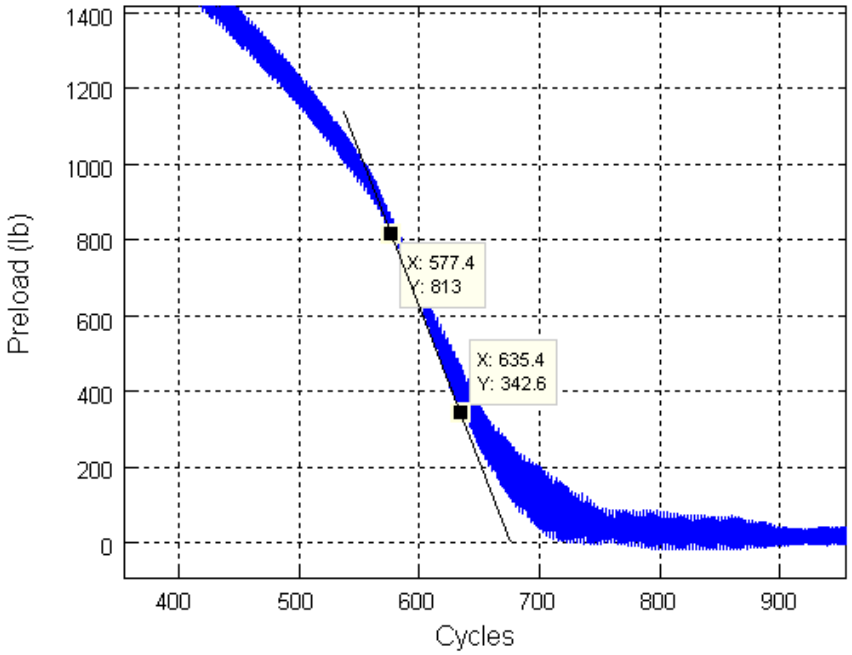

Figure D.8 Secondary rate of preload loss for "Standard Heli-Coil with Braycote" run number 8.

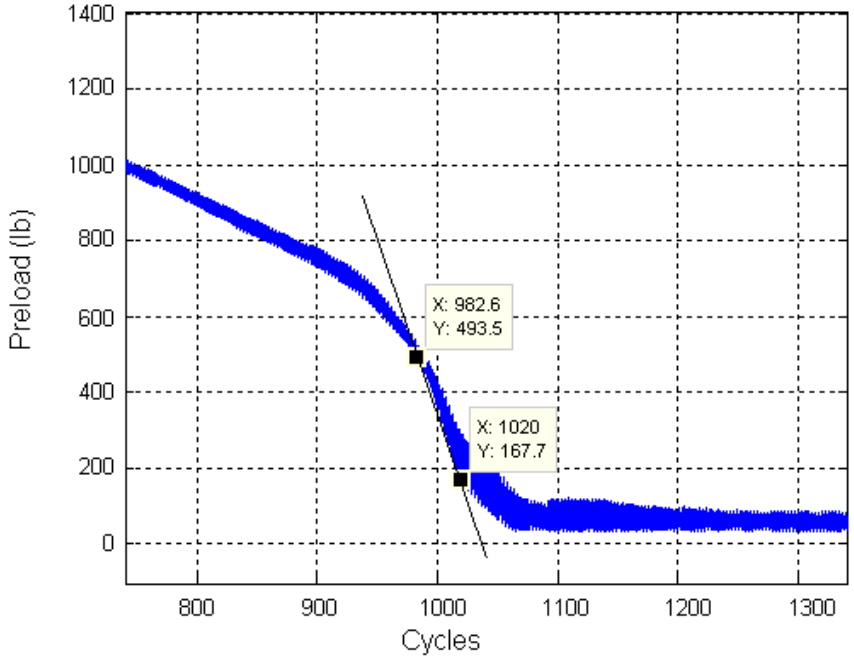

Figure D.9 Secondary rate of preload loss for "Standard Heli-Coil with Braycote" run number 9.

Appendix D (continued)

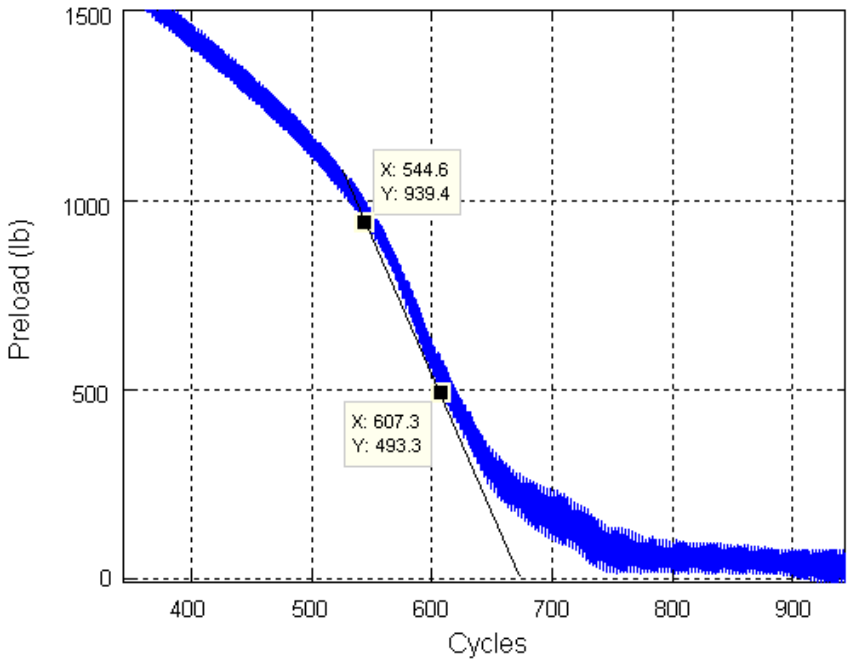

Figure D.10 Secondary rate of preload loss for "Standard Heli-Coil with Braycote" run number 10.

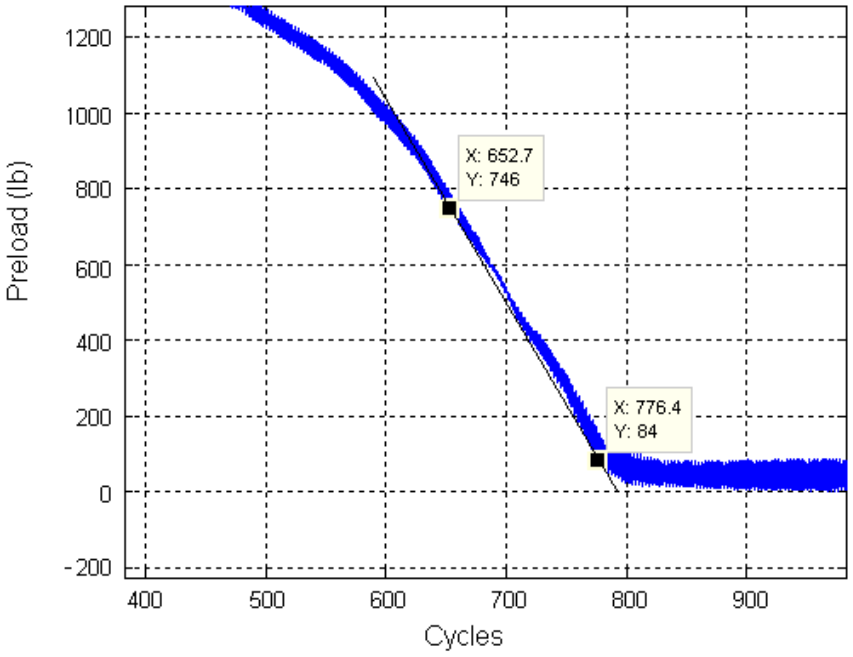

Figure D.11 Secondary rate of preload loss for "Standard Heli-Coil with Braycote" run number 11.

Appendix D (continued)

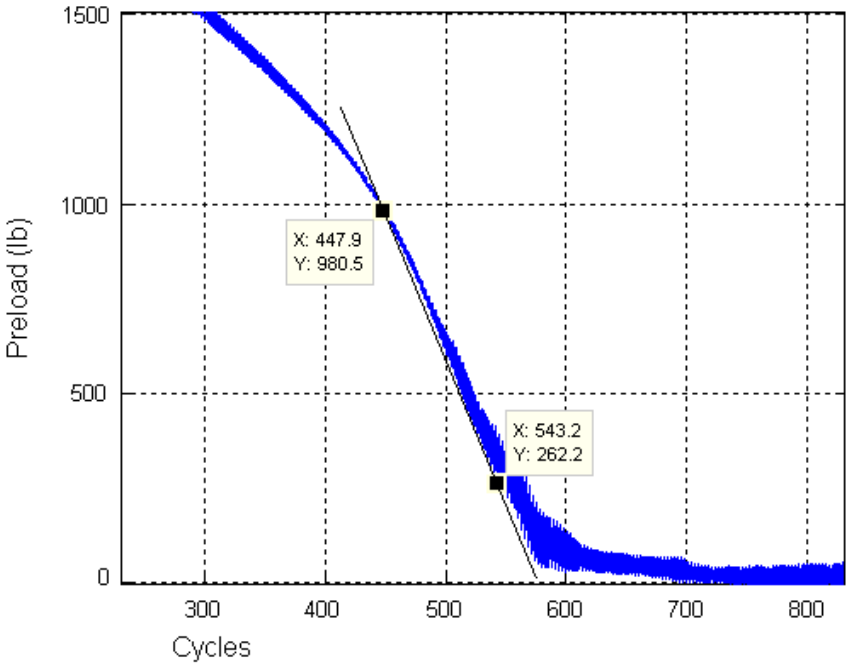

Figure D.12 Secondary rate of preload loss for "Standard Heli-Coil with Braycote" run number 12.

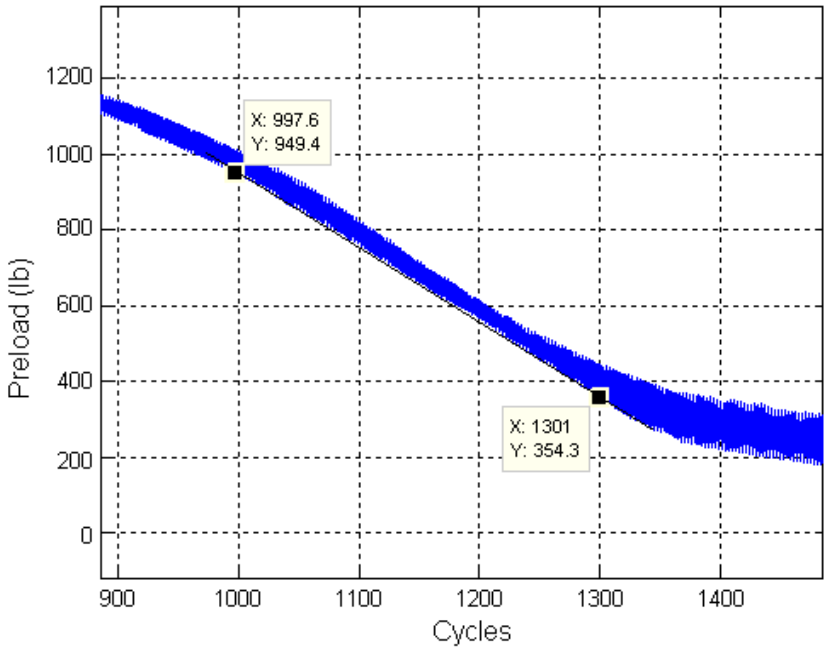

Figure D.13 Secondary rate of preload loss for "Locking Heli-Coil with Braycote" run number 13.

Appendix D (continued)

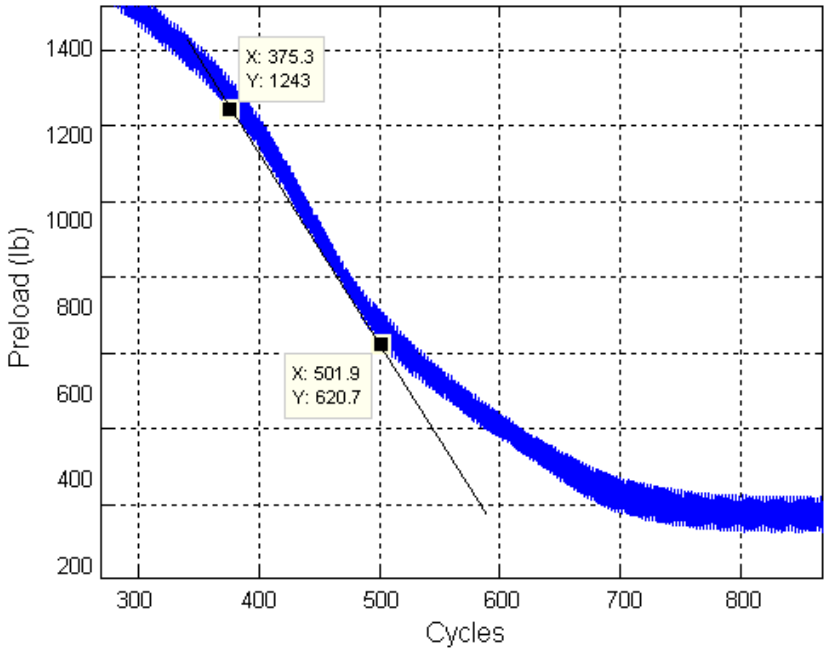

Figure D.14 Secondary rate of preload loss for "Locking Heli-Coil with Braycote" run number 14.

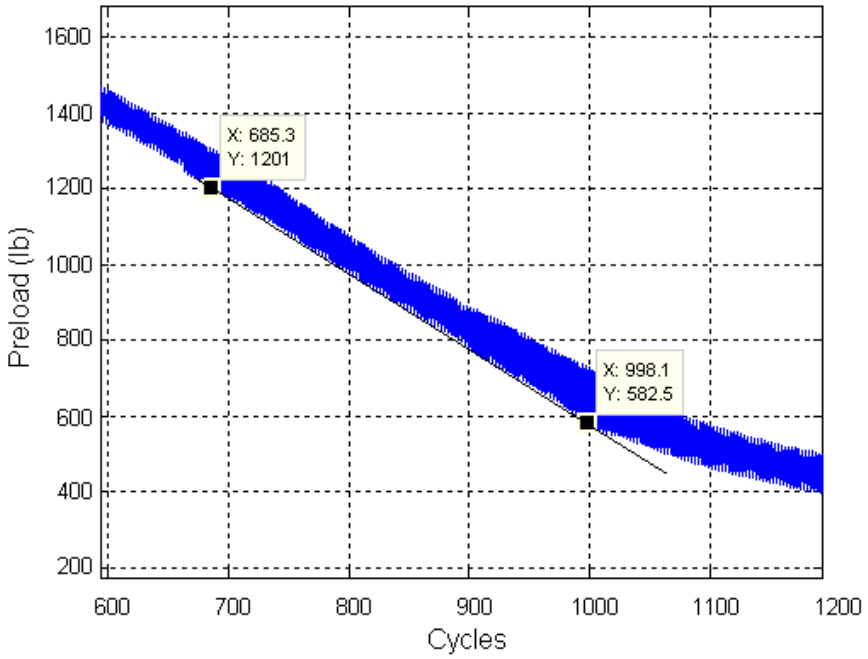

Figure D.15 Secondary rate of preload loss for "Locking Heli-Coil with Braycote" run number 15.

Appendix D (continued)

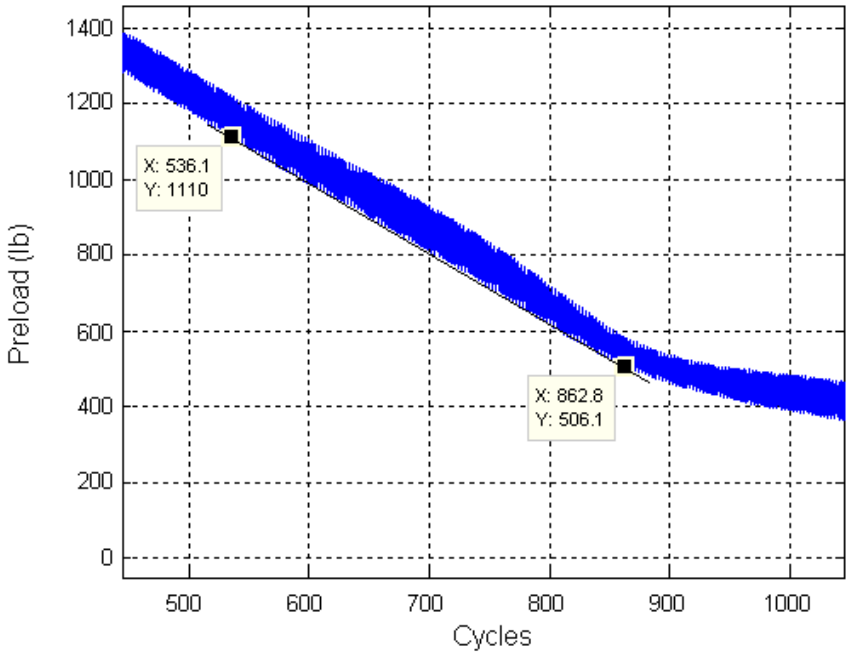

Figure D.16 Secondary rate of preload loss for "Locking Heli-Coil with Braycote" run number 16.

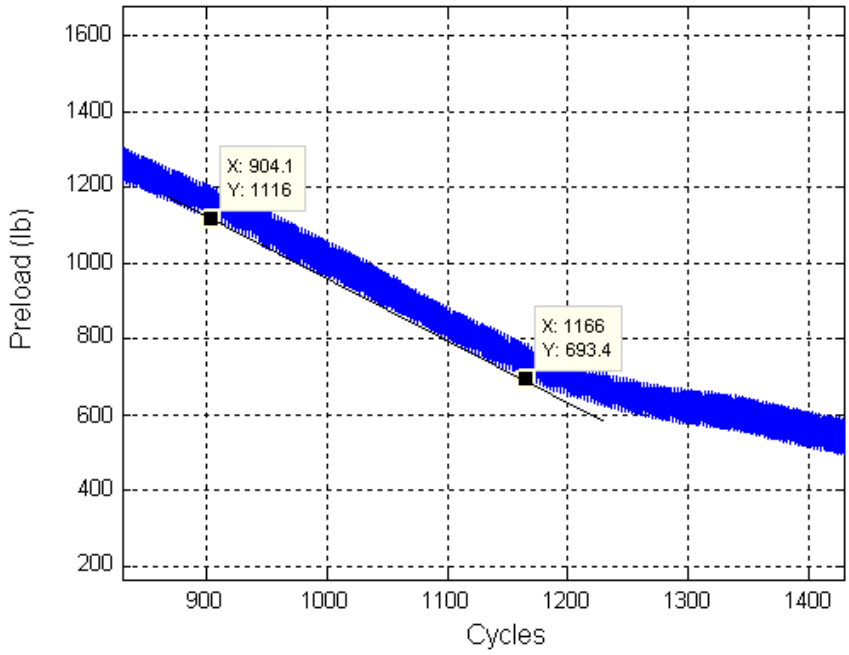

Figure D.17 Secondary rate of preload loss for "Locking Heli-Coil with Braycote" run number 17.

Appendix D (continued)

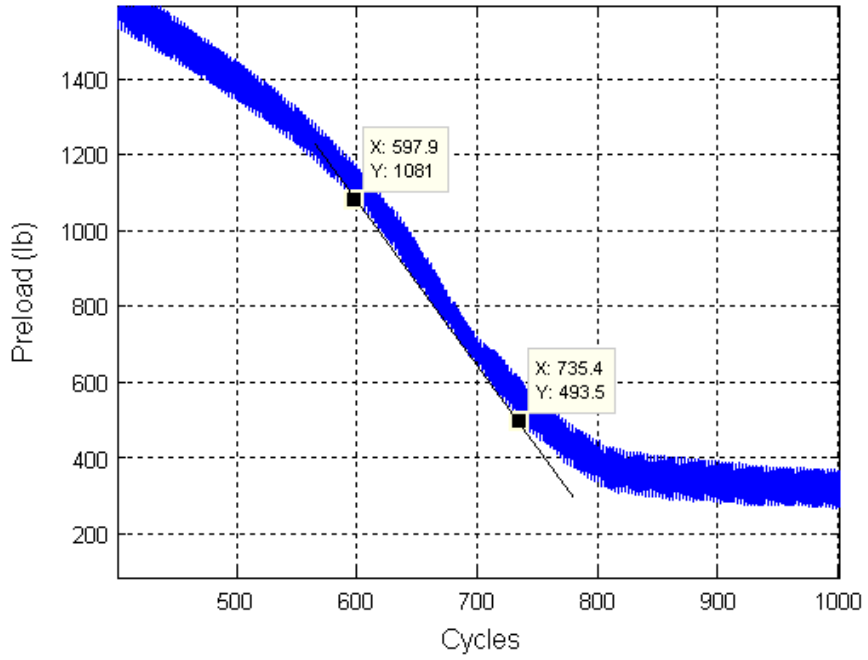

Figure D.18 Secondary rate of preload loss for "Locking Heli-Coil with Braycote" run number 18.

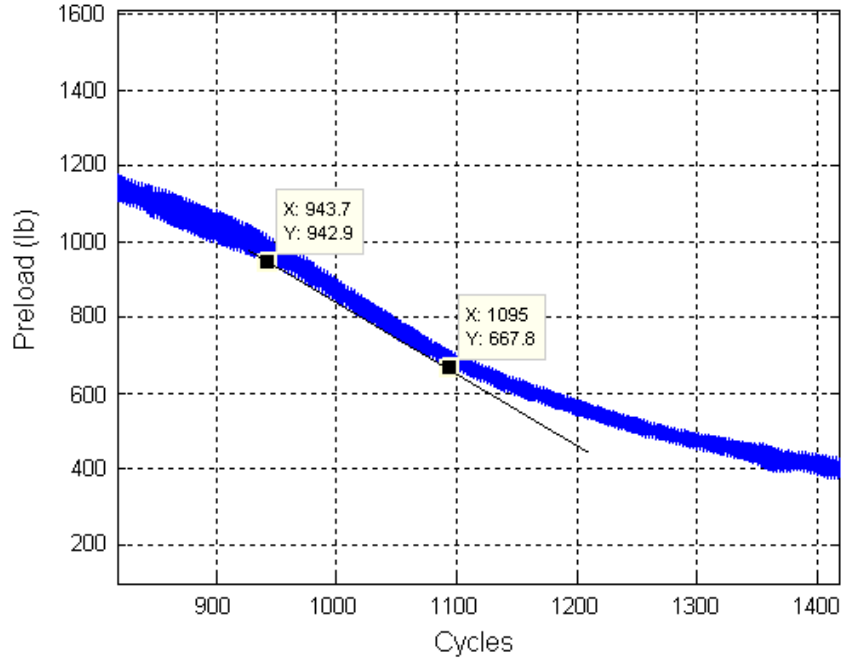

Figure D.19 Secondary rate of preload loss for "Locking Heli-Coil with Braycote" run number 19

Appendix D (continued)

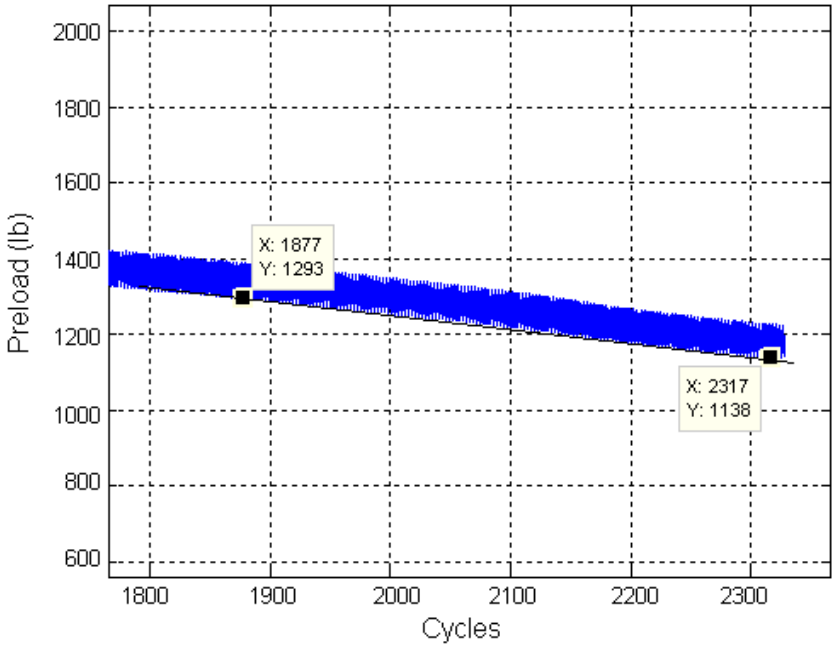

Figure D.20 Secondary rate of preload loss for "Locking Heli-Coil with Braycote" run number 20.

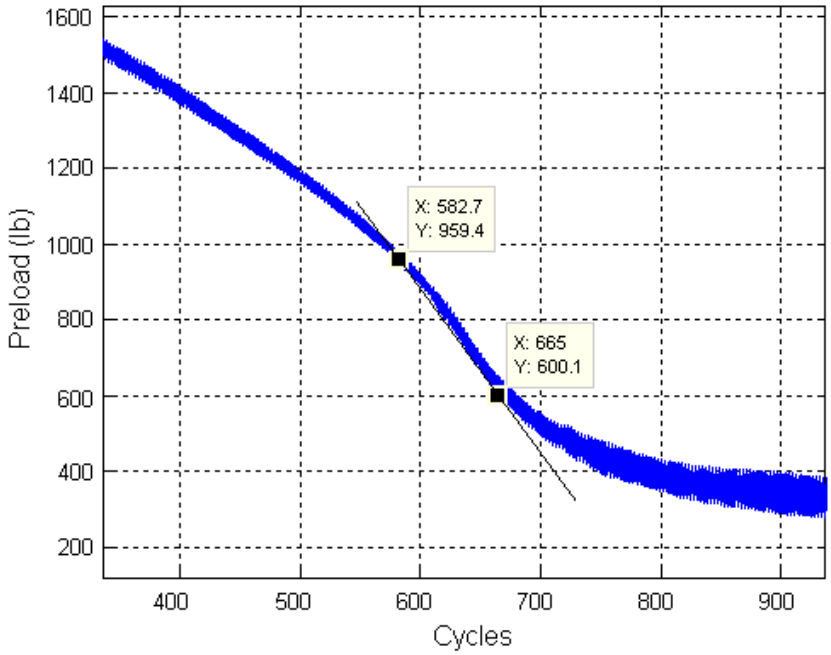

Figure D.21 Secondary rate of preload loss for "Locking Heli-Coil with Braycote" run number 21.

Appendix D (continued)

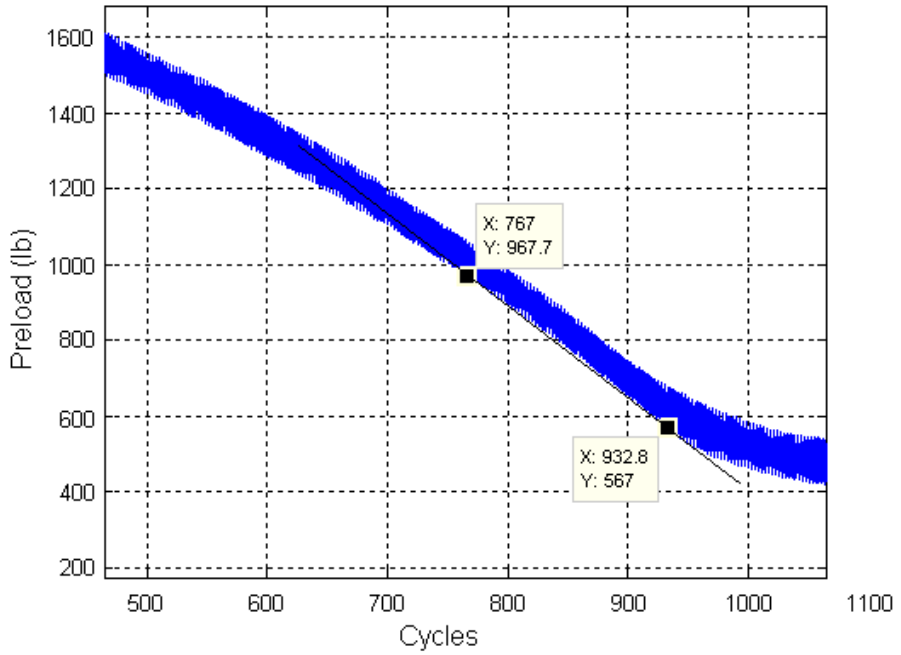

Figure D.22 Secondary rate of preload loss for "Locking Heli-Coil with Braycote" run number 22.

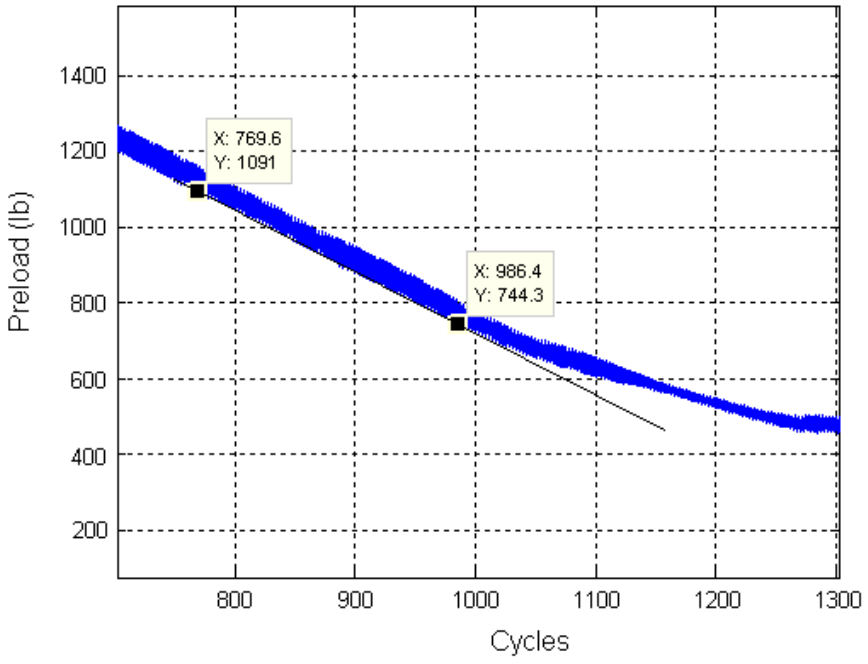

Figure D.23 Secondary rate of preload loss for "Locking Heli-Coil with Braycote" run number 23.

Appendix D (continued)

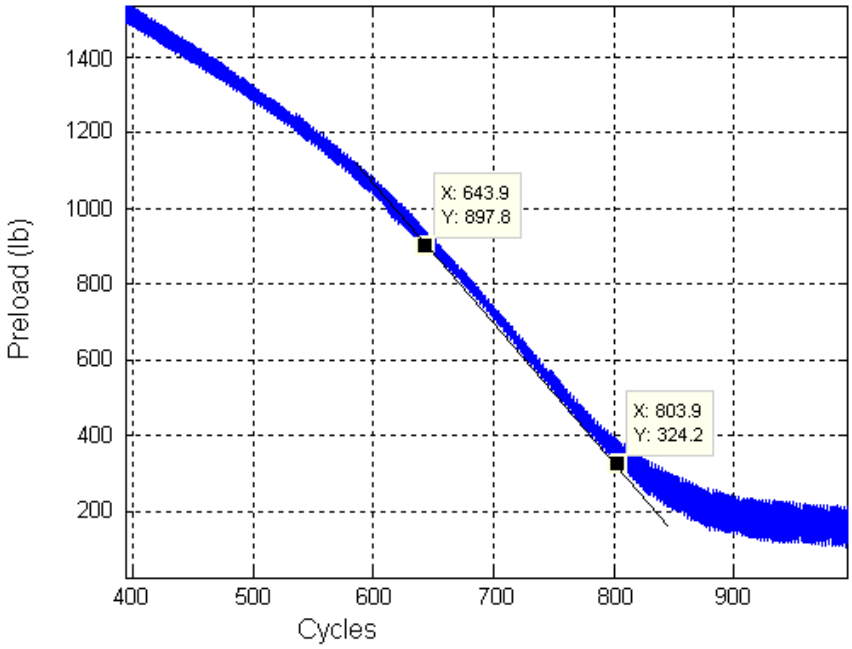

Figure D.24 Secondary rate of preload loss for "Locking Heli-Coil with Braycote" run number 24.

Appendix E: Zoomed data plots for the steady-state and the final preload value parameter

These plots were used in order to obtain the steady state value (if applicable) and also the finale preload value used in Chapter 3.

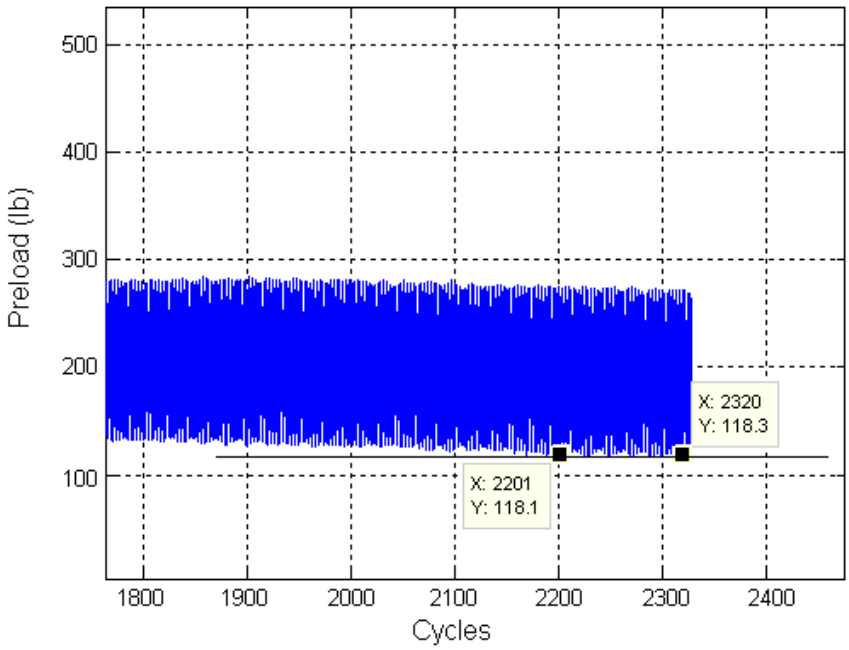

Figure E.1 Steady-state value for "Locking Heli-Coil with Braycote" run number 13.

Appendix E (continued)

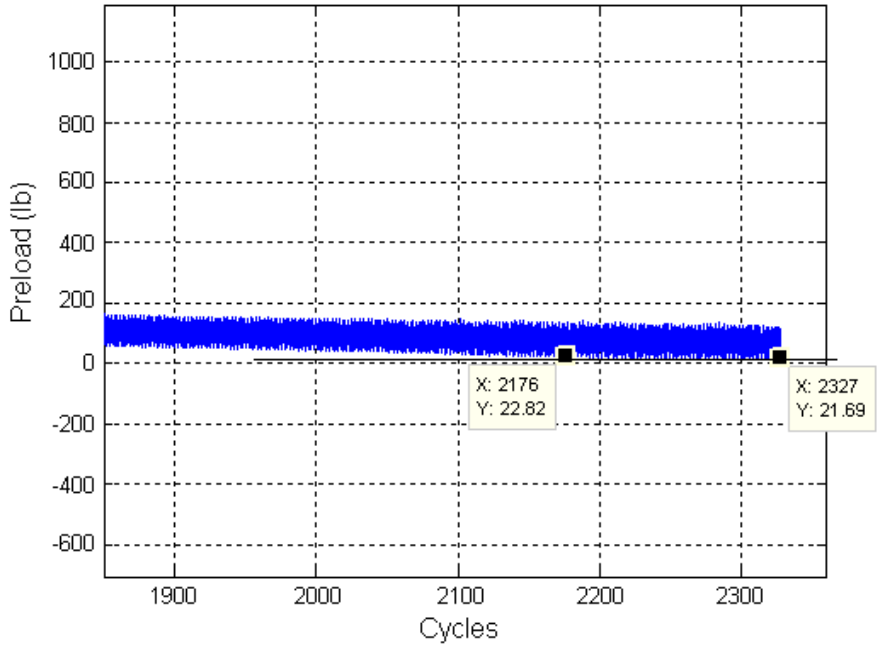

Figure E.2 Steady-state value for "Locking Heli-Coil with Braycote" run number 14.

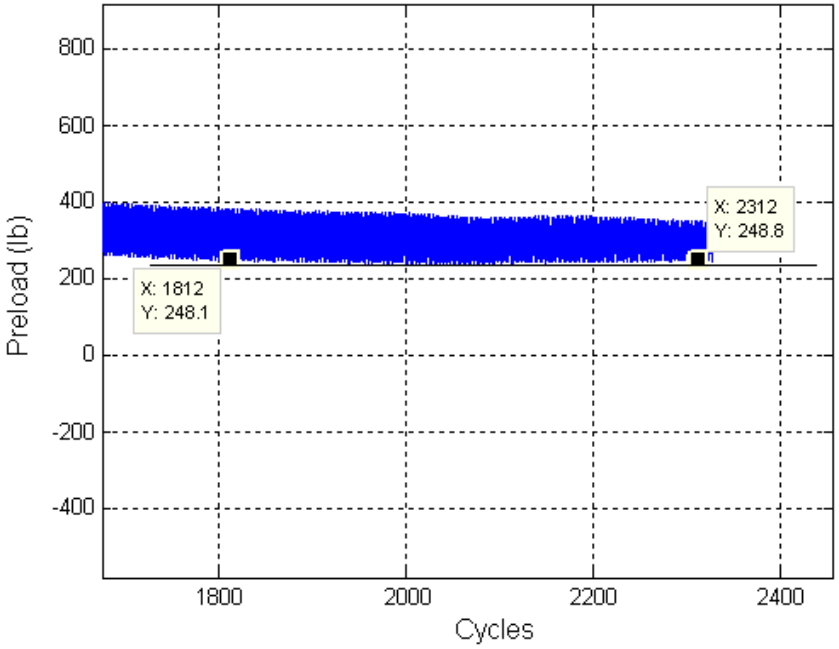

Figure E.3 Steady-state value for "Locking Heli-Coil with Braycote" run number 15.

Appendix E (continued)

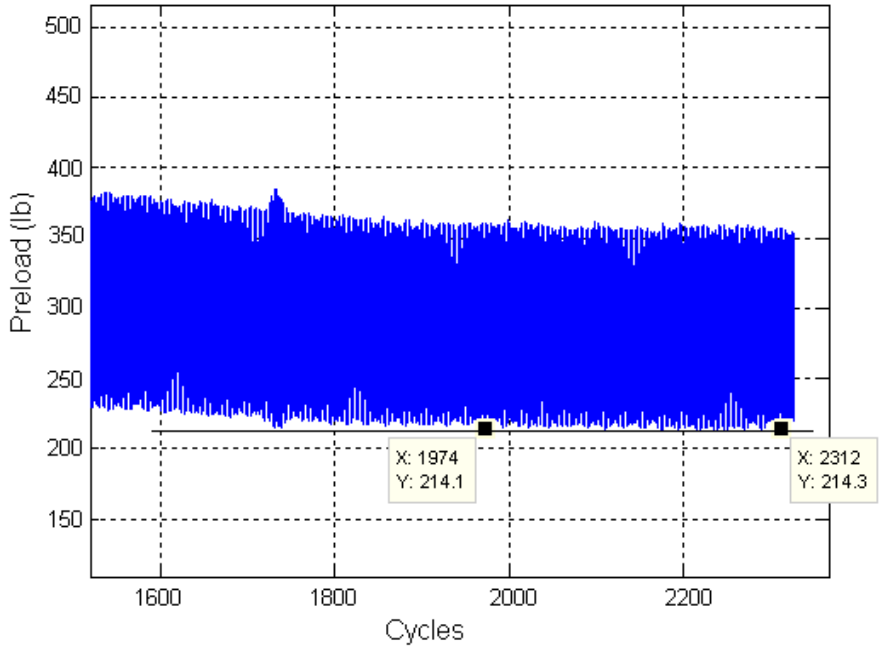

Figure E.4 Steady-state value for "Locking Heli-Coil with Braycote" run number 16.

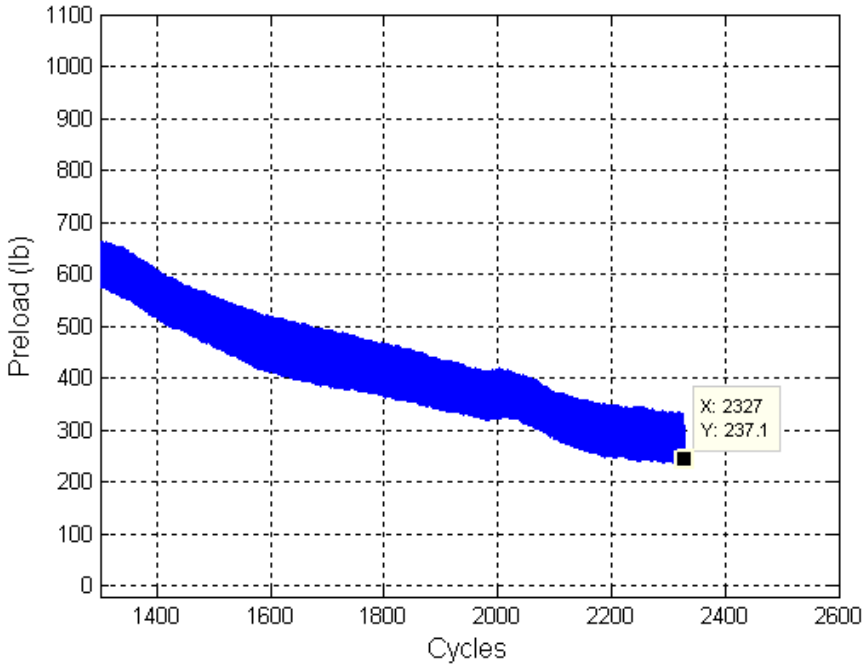

Figure E.5 Final preload value for "Locking Heli-Coil with Braycote" run number 17.

Appendix E (continued)

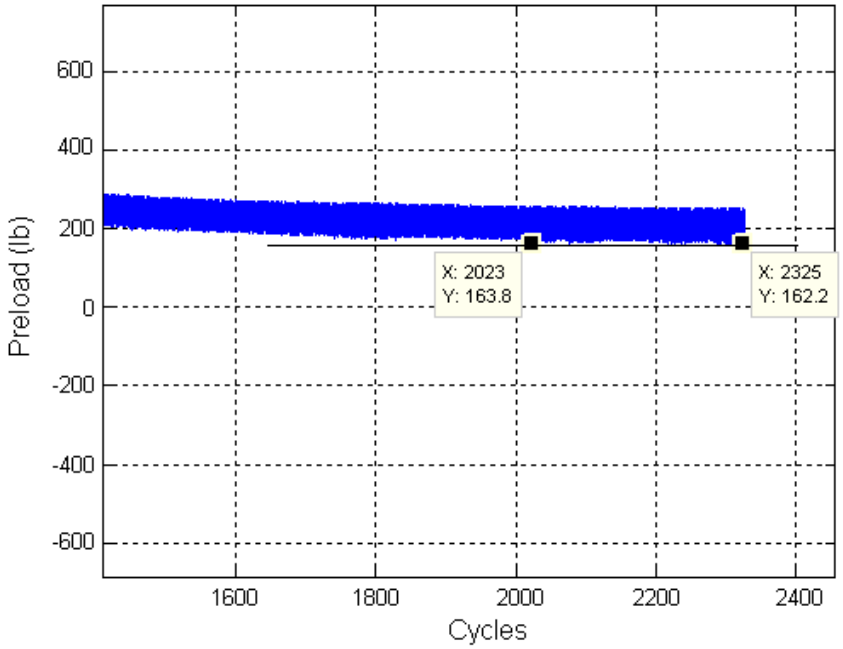

Figure E.6 Steady-state value for "Locking Heli-Coil with Braycote" run number 18.

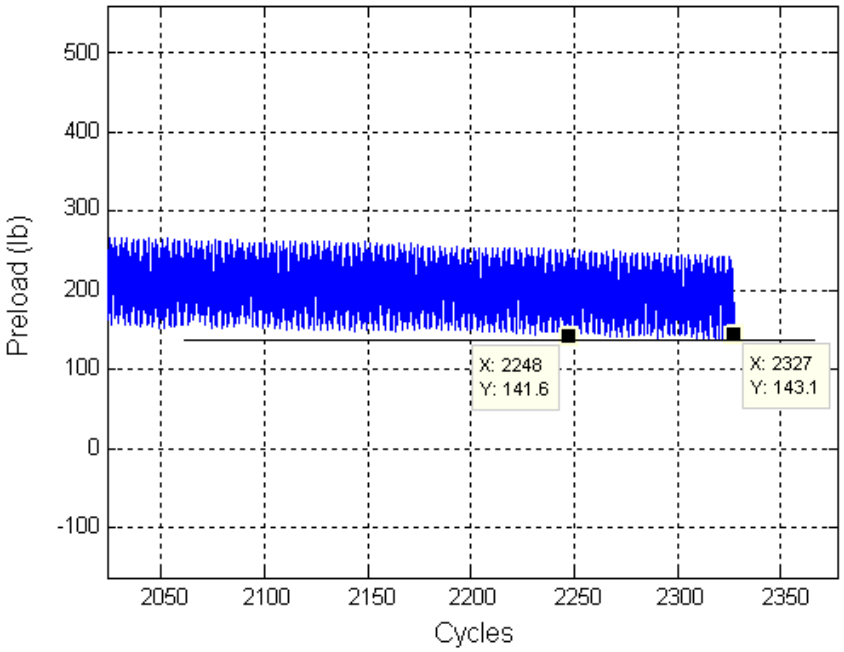

Figure E.7 Steady-state value for "Locking Heli-Coil with Braycote" run number 19.

Appendix E (continued)

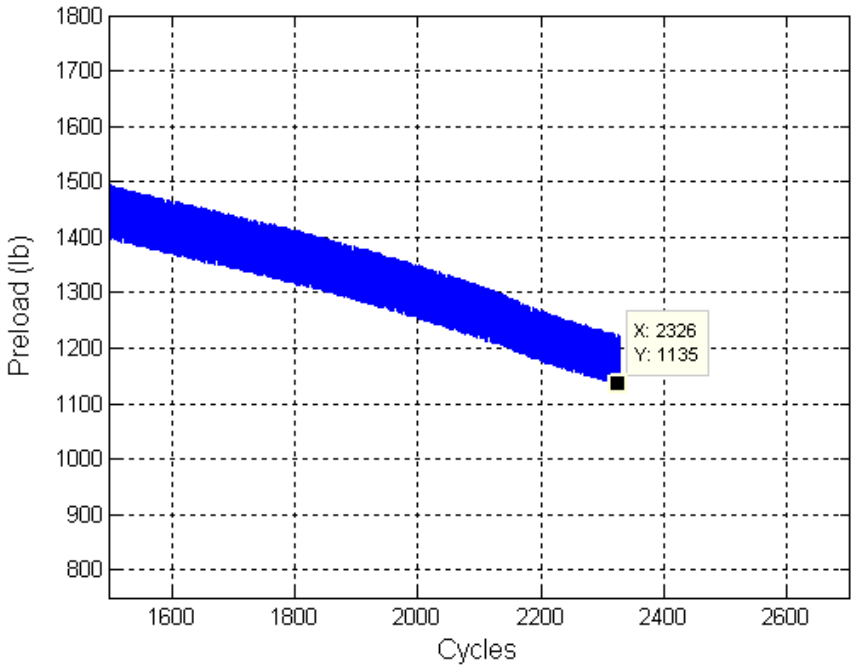

Figure E.8 Final preload value for "Locking Heli-Coil with Braycote" run number 20.

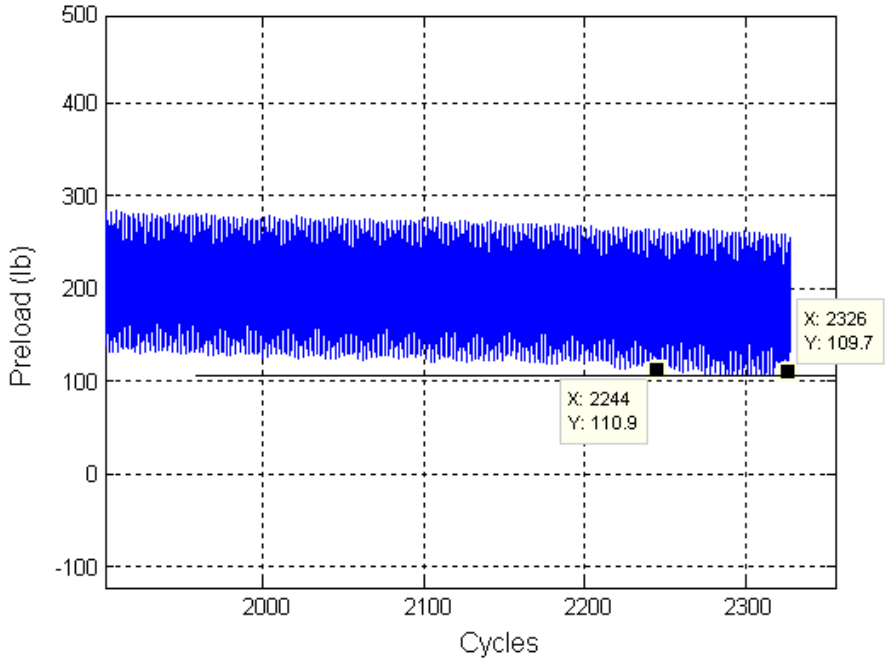

Figure E.9 Steady-state value for "Locking Heli-Coil with Braycote" run number 21.

Appendix E (continued)

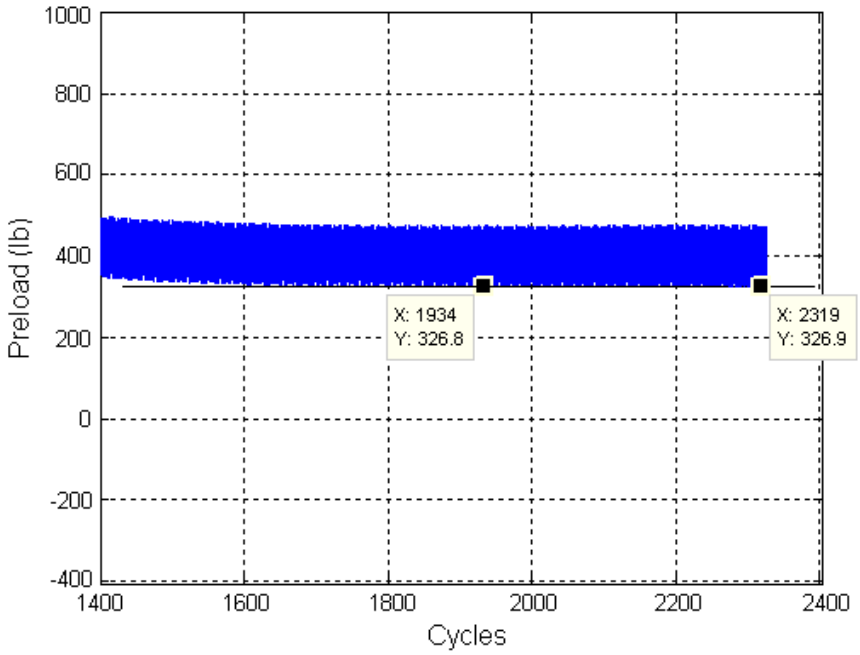

Figure E.10 Steady-state value for "Locking Heli-Coil with Braycote" run number 22.

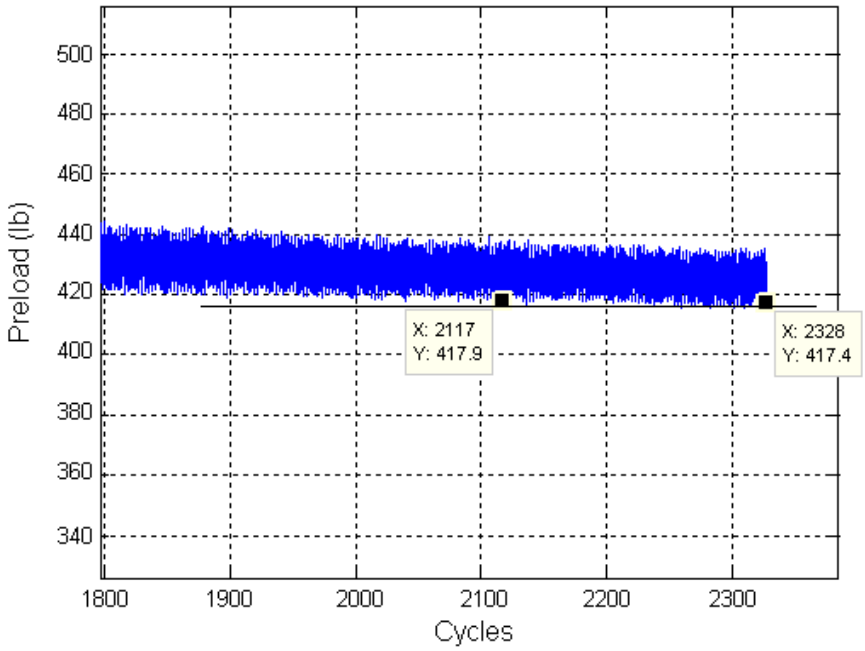

Figure E.11 Steady-state value for "Locking Heli-Coil with Braycote" run number 23.

Appendix E (continued)

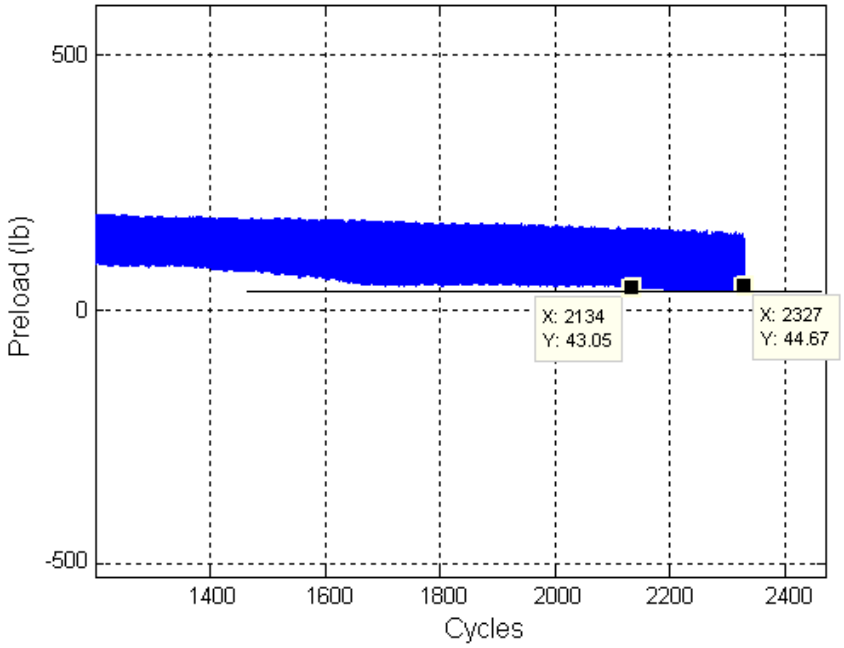

Figure E.12 Steady-state value for "Locking Heli-Coil with Braycote" run number 24.

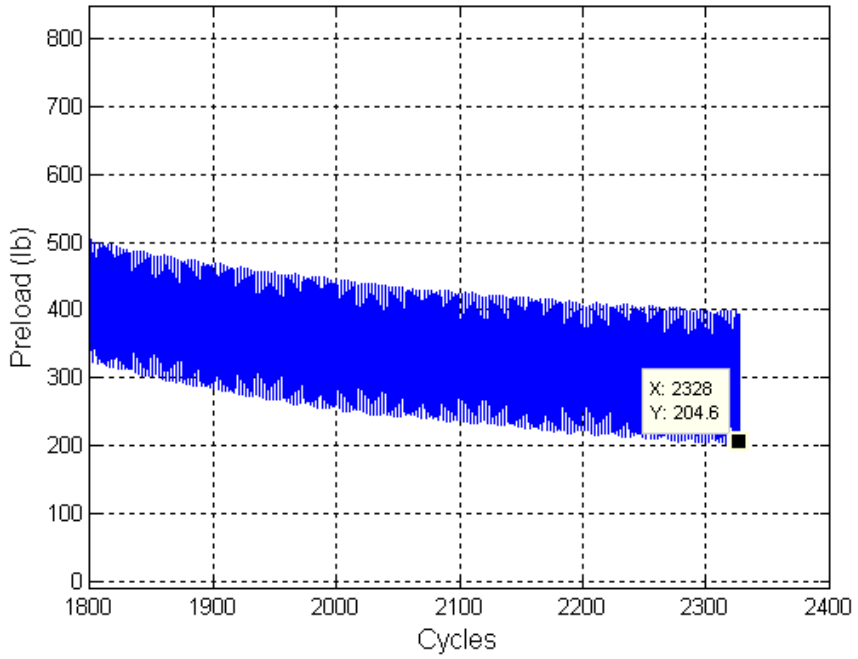

Figure E.13 Final preload value for "Standard Heli-Coil with Loctite" run number 25.

Appendix E (continued)

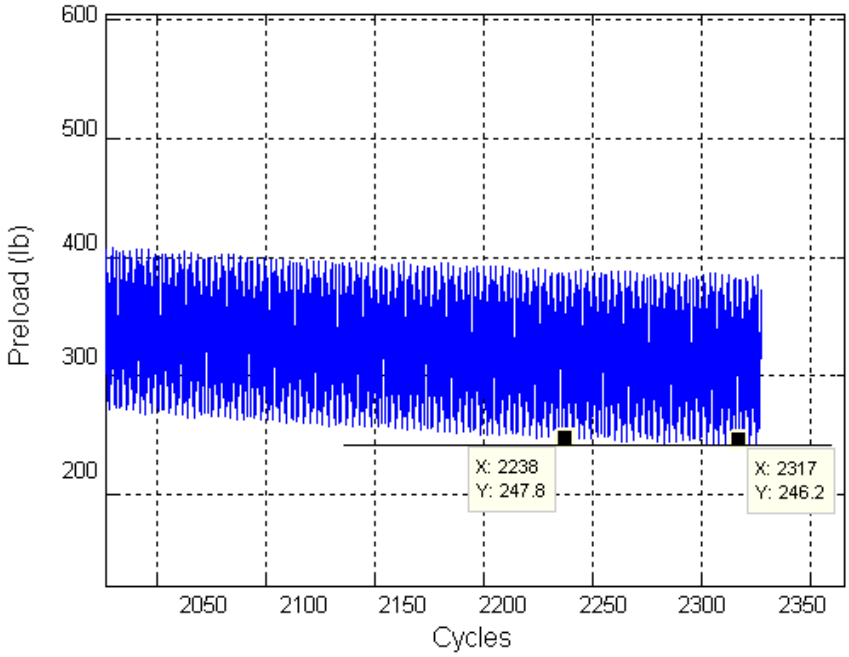

Figure E.14 Steady-state value for "Standard Heli-Coil with Loctite" run number 26.

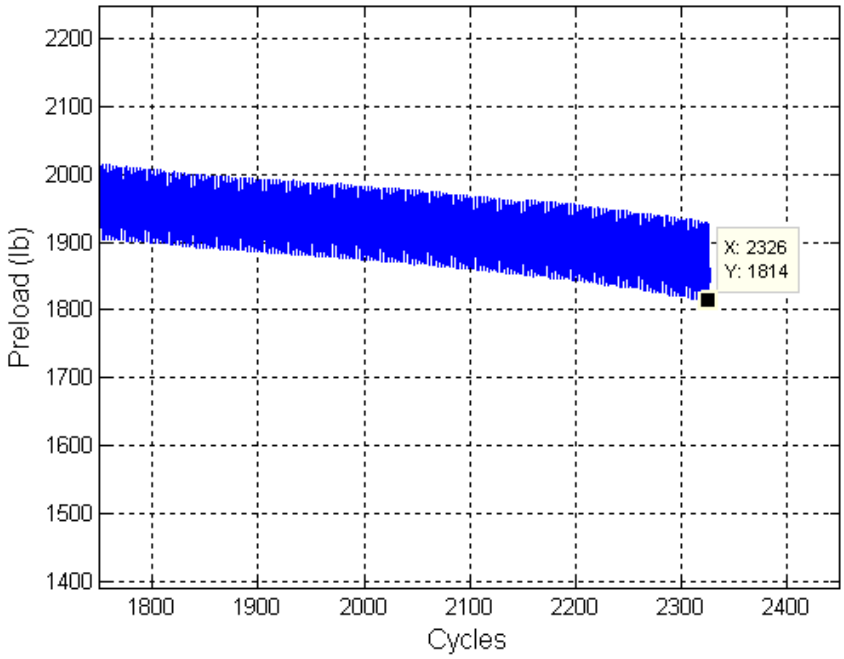

Figure E.15 Final preload value for "Standard Heli-Coil with Loctite" run number 27.

Appendix E (continued)

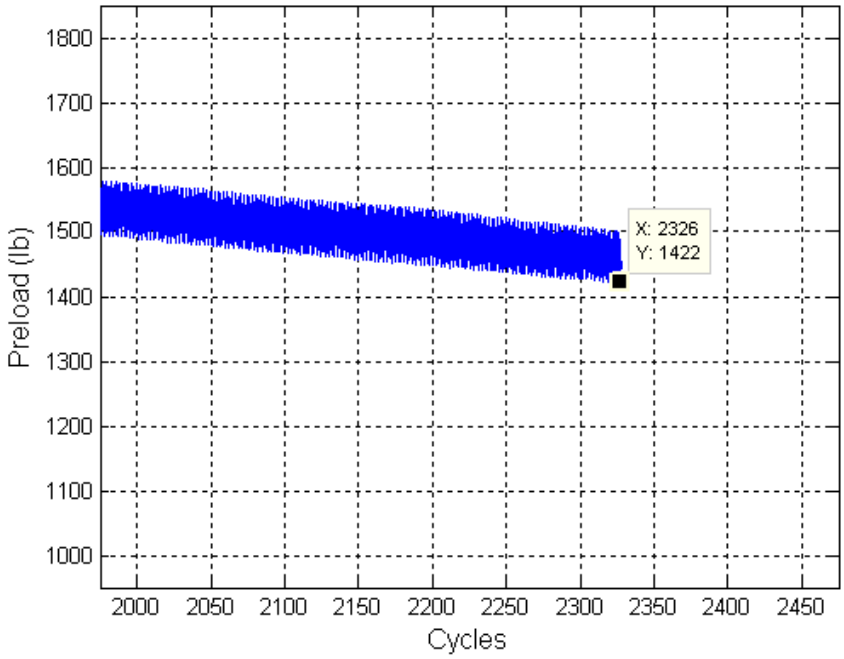

Figure E.16 Final preload value for "Standard Heli-Coil with Loctite" run number 28.

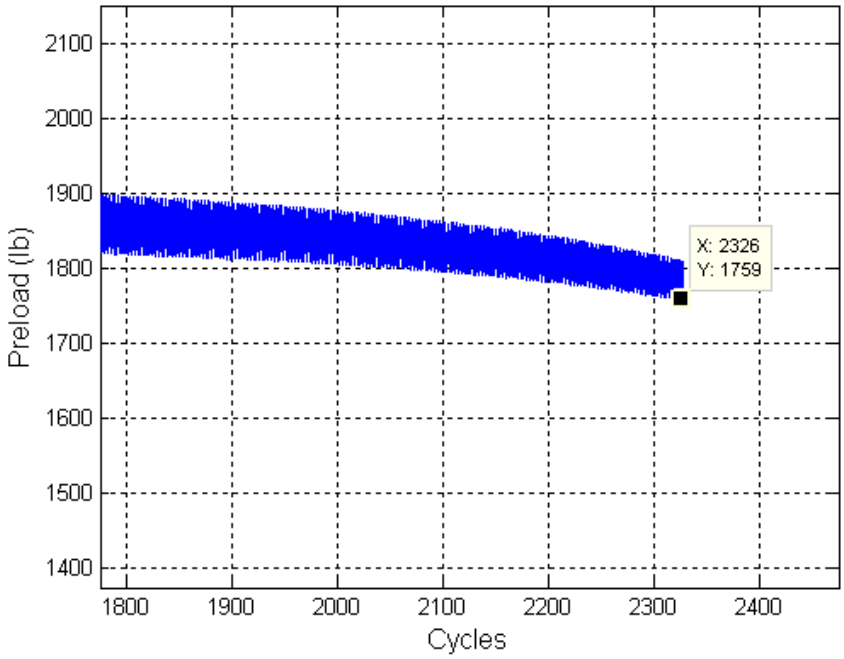

Figure E.17 Final preload value for "Standard Heli-Coil with Loctite" run number 30.

Appendix E (continued)

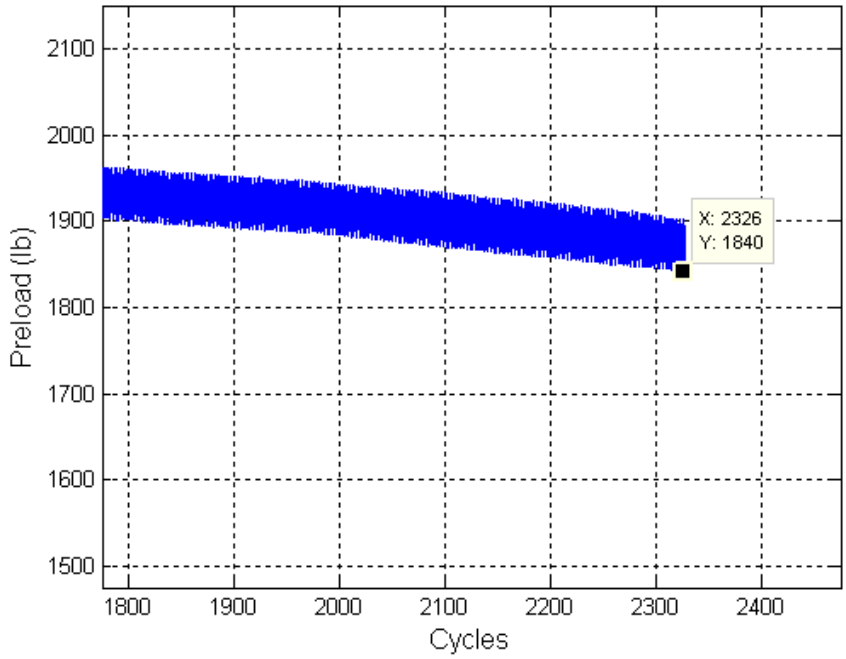

Figure E.18 Final preload value for "Standard Heli-Coil with Loctite" run number 31.

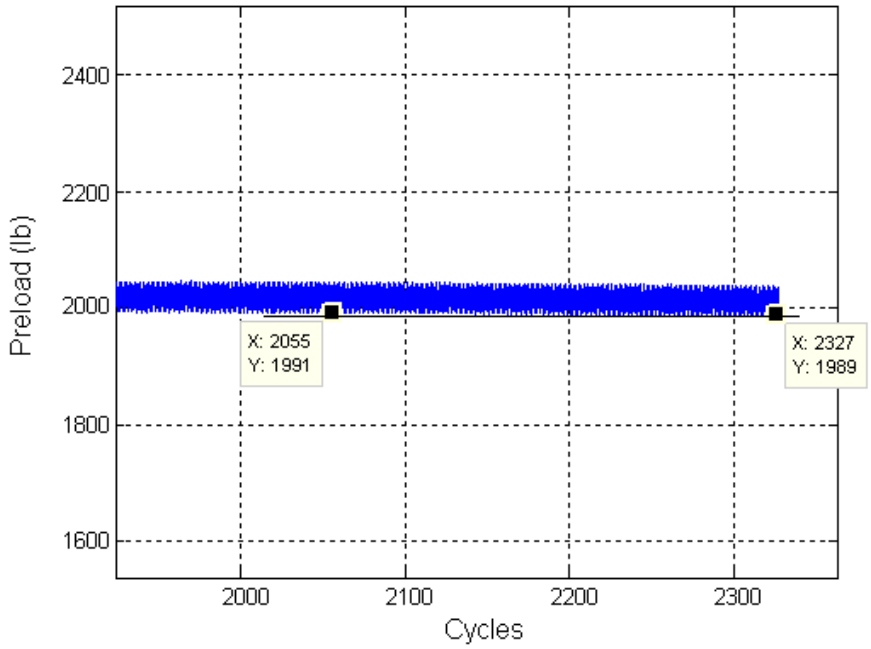

Figure E.19 Steady-state value for "Standard Heli-Coil with Loctite" run number 32.

Appendix E (continued)

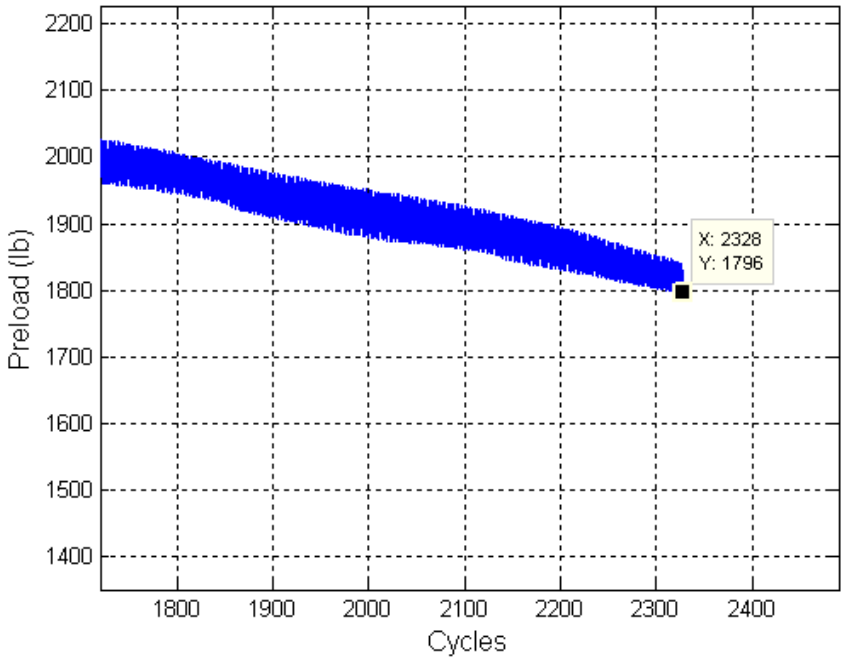

Figure E.20 Final preload value for "Standard Heli-Coil with Loctite" run number 33.

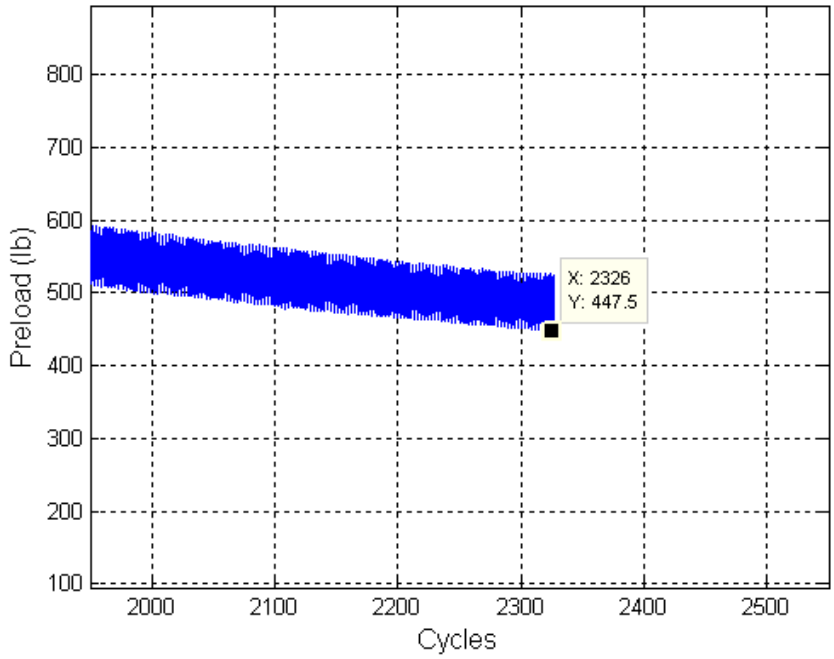

Figure E.21 Final preload value for "Standard Heli-Coil with Loctite" run number 34.

Appendix E (continued)

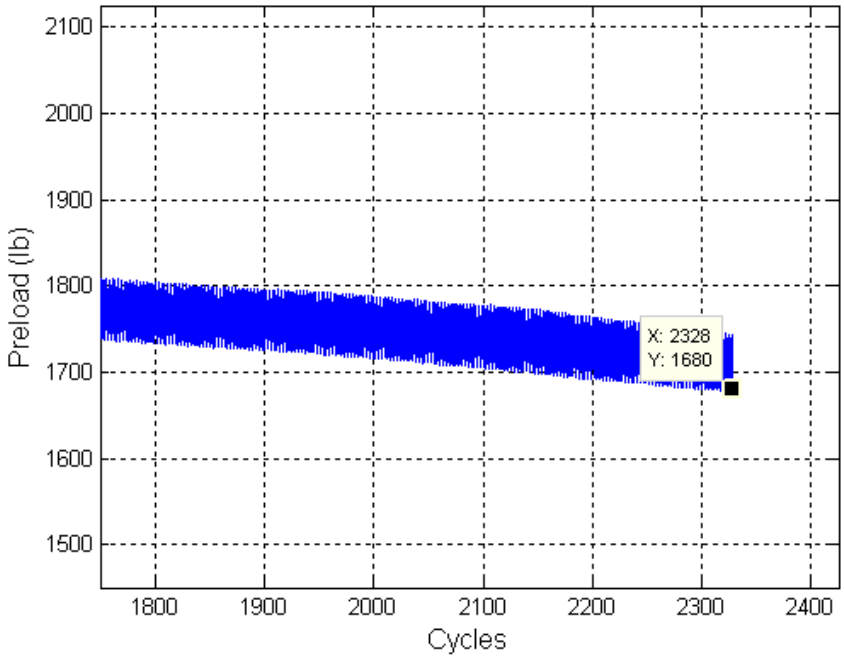

Figure E.22 Final preload value for "Standard Heli-Coil with Loctite" run number 35.

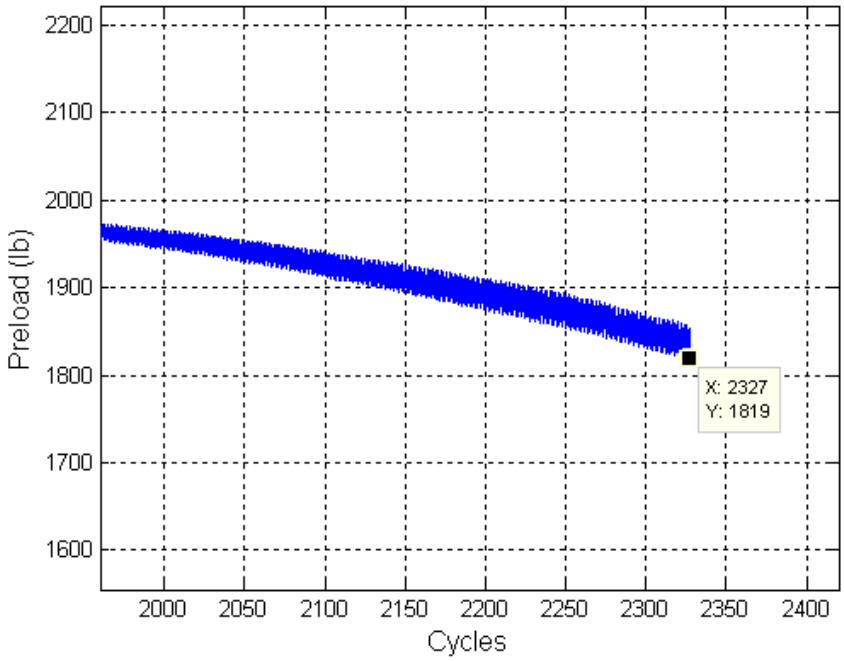

Figure E.23 Final preload value for "Standard Heli-Coil with Loctite" run number 36.